Studies on Bidentate E,N (E = S, Se, Te), N,N (Redox Active) and Tridentate N,N,N Ligands: Complexes with Lanthanoids, Tin and Transition Metals

Submitted in partial fulfillment of the requirements

of the degree of

Doctor of Philosophy

of the
Indian Institute of Technology, Bombay, India
and
Monash University, Australia

by

Rajesh Deka

Supervisors:

Prof. H. B. Singh (IIT Bombay)

Prof. Glen B. Deacon (Monash University)

Dr. David Turner (Monash University)

The course of study for this award was developed jointly by
Monash University, Australia and the Indian Institute of Technology, Bombay
and was given academic recognition by each of them.
The programme was administered by The IITB-Monash Research Academy

(2018)

Dedicated to My Sister in Heaven,

whom I lost in July, 2013, when I started for my PhD

Approval Sheet

The thesis entitled "**Studies on Bidentate E,N (E = S, Se, Te), N,N (Redox Active) and Tridentate N,N,N Ligands: Complexes with Lanthanoids, Tin and Transition Metals**" by Rajesh Deka (IITB Roll No.: 134034001; Monash ID: 25557165) is approved for the degree of Doctor of Philosophy
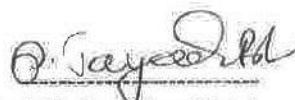
(Prof. Ajai K. Singh)
External Examiner

(Prof. R. Murugavel)
Internal Examiner

(Prof. H. B. Singh)
IITB Supervisor

(Prof. Glen B. Deacon)
Monash Supervisor

(Prof. P. Jayadeva Bhat)
Chairperson

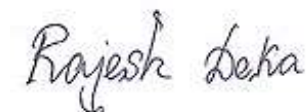Date: 06-11-2019
Place: Mumbai, India

Declaration

I declare that this written submission represents my ideas in my own words and where others' ideas or words have been included, I have adequately cited and referenced the original sources. I also declare that I have adhered to all principles of academic honesty and integrity and have not misrepresented or fabricated or falsified any idea/data/fact/source in my submission. I understand that any violation of the above will be cause for disciplinary action by the Institute and can also evoke penal action from the sources which have thus not been properly cited or from whom proper permission has not been taken when needed.

Notice 1

Under the Copyright Act 1968, this thesis must be used only under the normal conditions of scholarly fair dealing. In particular no results or conclusions should be extracted from it, nor should it be copied or closely paraphrased in whole or in part without the written consent of the author. Proper written acknowledgement should be made for any assistance obtained from this thesis.

Notice 2

I certify that I have made all reasonable efforts to secure copyright permissions for third-party content included in this thesis and have not knowingly added copyright content to my work without the owner's permission.

Student Name: Rajesh Deka
IITB ID: 134034001
Monash ID: 25557165

Date: 04-12-2018
Mumbai

IIITB-Monash Research Academy

Certificate of Course Work

I, Rajesh Deka, hereby declare that I was admitted to the candidacy of the Ph.D. degree dated on 12-07-2013 and have successfully completed the required course work during the period of July, 2013-June, 2014. The details of the course work are given below:

Semester 1: July, 2013-Dec, 2013

Course code	Course Name	Grade	Credits
CH 521	Interpretative Molecular Spectroscopy	BB	6.0
CH 807	Organic Synthesis	AB	6.0
CH 821	Topics in Chemistry I	AA	6.0
CH 827	Inorganic Complexes	BB	6.0
CH 831	Advanced Laboratory Techniques	AA	8.0

Semester 2: Jan, 2014-April, 2014

Course code	Course Name	Grade	Credits
CHS802	Seminar	AB	4.0
HS 699	Communication and Presentation Skills	PP	4.0

CPI: 9.06

List of Abbreviations and Acronyms

Synthetic

DMF	Dimethylformamide
DMSO	Dimethyl sulfoxide
DCM	Methylene Dichloride
DME	1,2-Dimethoxyethane
THF	Tetrahydrofuran
TEAP	Tetraethylammonium perchlorate
h	Hours
min	Minutes
rt	Room temperature
TMS	Trimethylsilane
COD	1,5-Cyclooctadiene
n-BuLi	*n*-Butyl Lithium

Analytical/spectroscopic

Å	Angstrom
cm	Centimetre
mm	Millimetre
nm	Nanometre
ppm	Parts per million
ºC	Degree celsius
C	Concentration
M	Molar

Δ	Chemical shift
λ	Wavelength
g	Gram
IR	Infrared
K	Kelvin
Mg	Milligram
mL	Millilitre
μL	Microlitre
M.P.	Melting point
MS	Mass spectrometry
HRMS	High resolution mass spectrometry
ESI	Electron spray ionization
NMR	Nuclear magnetic resonance
EPR	Electron paramagnetic resonance
FTIR	Fourier transform infrared
ATR	Attenuated total reflection
Hz	Hertz
MHz	Megahertz
DFT	Density functional theory
NBO	Natural bond orbital
AIM	Atoms in molecules
IChB	Intramolecular chalcogen interaction

Table of Contents

Chapter 2 : Facile Synthesis of Monomeric Lanthanide Chalcogenolates from 2-(dimethylamino)methyl)phenyltellurolate and Quinoline-8-tellurolate Ligand

1

Introduction

Outline

The thesis deals with the coordination chemistry of several diverse classes of ligands with different metals. In particular, these include; lanthanoid complexes of tellurolate ligands (Chapter 2), tin complexes of thiolate ligand (Chapter 3), ruthenium and osmium complexes of redox active *N, N*-bidentate ligand (Chapter 4) and palladium, platinum, selenium and tellurium complexes of pincer type pyrrolyl ligands (Chapter 5). Hence, the introductory chapter aims to briefly review the general aspects of lanthanoid and chalcogen elements, and lanthanoid chalcogen complexes (Part A), redox active ligands (Part B) and pincer ligands and their current perspectives (Part C). The aspects, more closely related to the work carried out, are reviewed in detail in the respective chapters.

<u>Part A</u>

1.1. General Introduction of Lanthanoid Elements

Lanthanoids consist of 15 metallic elements whose atomic numbers lie between 57 (Lanthanum, La) and 71 (Lutetium, Lu) in the periodic table (Figure 1.1). These elements, together with the chemically similar elements scandium (Sc, Z = 21) and yttrium (Y, Z = 39), are often collectively known as the 'rare earth elements'. Since neither these seventeen elements are found as free metals in the earth's crust, nor pure minerals of these individual metals exist, they were termed as 'rare-earths' at the time of their discovery. However, the name 'rare earth' can be considered as misnomer as they are not 'rare' in terms of their terrestrial abundance, except promethium (Pm, Z = 61), which is radioactive and occurs only in trace amounts in nature. In fact, it is observed that lighter lanthanoids [Lanthanum (La), Cerium (Ce), Neodymium (Nd)] are quite abundant in nature, whereas the most abundant lanthanoid on earth, Ce has similar crustal abundance to nickel (Ni) or copper (Cu).[1,2] Even, the sparsest lanthanoids [Thulium (Tm) and Lutetium (Lu)] have more abundance than bismuth (Bi), silver (Ag) or platinum (Pt) metals.

^{57}La	^{58}Ce	^{59}Pr	^{60}Nd	^{61}Pm	^{62}Sm	^{63}Eu	^{64}Gd	^{65}Tb	^{66}Dy	^{67}Ho	^{68}Er	^{69}Tm	^{70}Yb	^{71}Lu

Figure 1.1. Lanthanoid elements (La-Lu).

There are three primary mineral sources from where rare-earth metals are extracted and each source contains different concentrations of individual lanthanoid oxides. For example, (i)

Bastansite $LnFCO_3$ and (ii) Monazite (Ln, Th)PO_4, both are richer in earlier lanthanoids, while (iii) Xenotime (Y, Ln)PO_4 contains higher abundance of heavier lanthanoids.[1-3] There are some other mineral ores, such as Cerite, Allanite, Euxenite and Gadolinite which contain extractable quantities of rare-earths but are not used as common commercial sources.[3] There are standard extraction procedures for extracting the lanthanoid oxides from the mineral sources.[4] In particular, acid digestion is used in case of Bastansite, while both sodium hydroxide digestion as well as acid digestion are used for the extraction of lanthanoid oxides from Monazite and Xenotime. Once the lanthanoid oxides are extracted from the ores, the lanthanoids can be separated using common separation techniques such as chemical separations, fractional crystallization, ion exchange methods and solvent extraction.[4]

1.1.1 General Properties of Lanthanoid Elements

1.1.1.1. Electronic configurations: Lanthanoid Contraction

All the lanthanoid metals, La to Lu are highly electropositive in nature and share remarkable uniformity in their chemical properties. The electronic configuration of lanthanoid elements are characterized by filling of $4f$ sub-shell. The general electronic configuration of the free lanthanoid atoms is [Xe]$4f^{n}5d^{0}6s^2$ (n=1-14), with exceptions of Ce, Gd and Lu, where the electronic configuration becomes [Xe]$4f^{n}5d^{1}6s^2$(n=1-14). Consequently, the general electronic configurations of +3 ions become [Xe]$4f^{n}$ (n=1,7 and 14 respectively). It is worth mentioning that $4f$ shell is buried inside the $5s$ and $5p$ electrons from the [Xe] core and are well-shielded by penetrated $5s$ and $5p$ orbitals. As a consequence, the deep embedded $4f$ orbitals display poor overlap with the ligand orbitals. This essentially contributes to the predominant ionic character of organolanthanoid complexes. The unavailability of $4f$ orbitals in overlap also leads to the fact that the common properties of the resulting complexes, such as spectroscopic as well as magnetic properties are not influenced by the nature of the auxiliary ligands. This is in direct contrast to the d-block metal complexes, wherein the outer d-orbitals take direct participation in overlap with ligand orbitals.

While filling up the $4f$ sub-shell along the lanthanoid series, there is a decrease in both atomic as well as ionic radii, the phenomenon is known as 'lanthanoid contraction'. On moving from left to right along the group, although each increase in nuclear charge is exactly balanced by a simultaneous increase in electronic charge, due to the 'imperfect' shielding by $4f$ orbitals, as

stated earlier, there is a net increase in attraction for the electron charge cloud and as a consequence, each ion experiences a further diminution in comparison with its predecessor. Another factor which attributes substantially to lanthanoid contraction is relativistic effect, however, this effect is more pronounced in 'actinide contraction'.[2]

1.1.1.2. Oxidation States and Coordination Number

Almost all the lanthanoid elements commonly adopt +3 oxidation state. The prevalence of the +3 oxidation state can be attributed to combination of several circumstances. The order of penetration of the orbitals through the inert core of electrons towards the nucleus is 4f >5d >6s. The same order is also followed for the stabilization effect on the orbitals for successive removal of electron from a neutral lanthanoid. As successive electrons are removed from a neutral lanthanoid atom, by the time an ionic charge of +3 has been reached, the preferential stabilization of the 4f orbitals is such that in all cases the 6s and 5d orbitals have been emptied. Again, in most cases, the 4f electrons are far embedded in the inert core and consequently they are so strongly attracted by the nucleus that as it requires huge energy to ionize them further. However, there are some anomalies, in particular, in early lanthanoids Ce and Pr where the 4f orbitals are still at a comparatively high energy and the effective nuclear charge is not so high to be able to attract the 4f electrons and therefore, they can lose further electrons. In fact, Ce(IV) acquires a noble gas configuration when it adopts +4 oxidation state. Again, in cases of Eu and Yb, +2 oxidation state is more stable which can be attributed to their half-filled ($4f^7$) and fully filled ($4f^7$) subshells respectively. The stability of the trivalent oxidation state also comes from the fact that the fourth ionization energy in most of the lanthanoids are larger than the sum of the first three ionization energies, with the exceptions of Ce, Tb, and Yb. In case of Yb, it has large third ionization energy which stabilizes the +2 oxidation state.

As the lanthanoid ions are large in size, they adopt a wide range of coordination numbers in their complexes. In fact, lanthanoid complexes with coordination number as high as 12 are well documented in literature.[1,6] However, since *f*-orbital do not have stereo-chemical influence on the resulting complex, the steric bulkiness of the ligand plays decisive role in the coordination number of the complexes.[6] In fact, the common norm for lanthanoid complexes is high coordination numbers with ligands, provided they adopt a geometry that minimizes inter-ligand repulsions.

1.1.1.3. Nature of *f*-orbitals

The associated quantum numbers for a lanthanoid *f*-orbitals are $n = 4$, $l = 3$ and $m_l = +3, +2, +1, 0, -1, -2, -3$. Consequently, a set of *f*-orbitals is 7-fold degenerate and all are 'ungerade' in nature. There are generally two ways to represent the *f*-orbitals, (i) cubic set and (ii) non-cubic set. The cubic set is related to tetrahedral, octahedral and cubic ligand filed. It comprises f_{xyz}; $f_{z(x^2-y^2)}, f_{x(y^2-z^2)}$ and $f_{y(z^2-x^2)}$ $f_{y(z^2-x^2)}$; f_{z^3}, f_{x^3} and f_{y^3}. The non-cubic set is consisted of f_{x^3}; f_{xz^2} and f_{yz^2}; f_{xyz}; $f_{z(x^2-y^2)}$, $f_{x(x^2-3y^2)}$ and $f_{y(3x^2-y^2)}$. The boundary surfaces of the *f*-orbitals in a non-cubic environment are shown in Figure 1.2.[5]
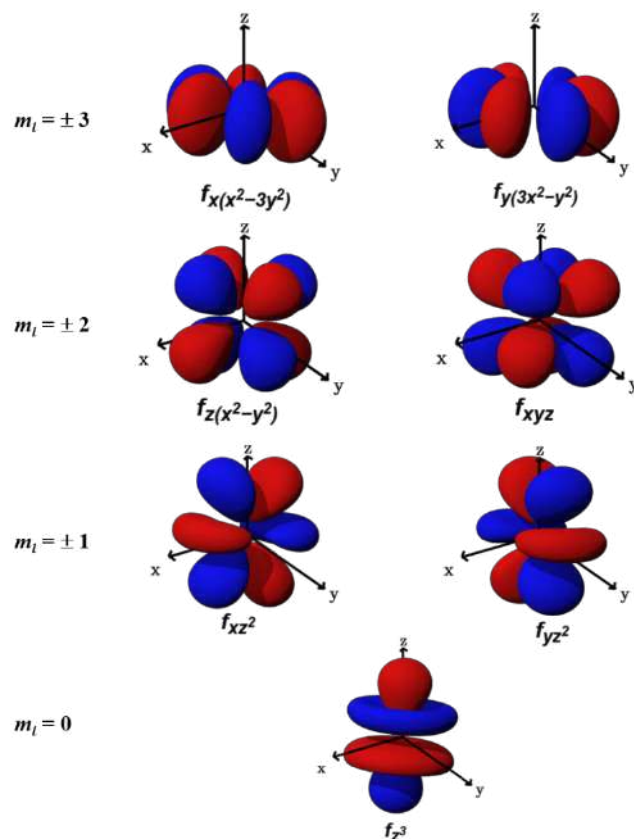
Figure 1.2. Representations of the 4*f* orbitals.[5]

As mentioned earlier, the 4*f* orbitals are spatially buried and significantly penetrated through the xenon core and do not take part appreciably in bonding with the ligand. Consequently, the *f*-orbitals experience negligible crystal-field effects, while spin-orbit coupling plays a crucial role in the electronic structure.

1.1.1.4. Spectroscopic Properties

Since *f* electrons are associated with a large number of microstates, consequently large number of transitions are possible in lanthanoid complexes. However, as there is no substantial overlap of the *f*-orbital with ligand orbitals and again due to the absence of *d-f* orbital mixing, all transitions are Laporte forbidden in lanthanoid complexes. As a consequence, the visible spectra of lanthanoid complexes usually consist of a large number of sharp, low intensity peaks with molar absorption coefficient typically in the range of 1-10 dm^3 mol^{-1} cm^{-1}.[6]

1.2. General Introduction of Chalcogen Elements

Selenium (Se, Z = 34) and tellurium (Te, Z = 52) are members of group 16 elements, which together with oxygen (O, Z = 8), sulfur (S, Z = 16), polonium (Po, Z = 84) are known as chalcogen elements. The element selenium was discovered by Swedish chemist Berzelius in 1817 and was named after the Greek goddess of moon, '*Selene*'.[7] Tellurium was discovered 35 years earlier (in 1782) than selenium by Reichenstein from gold ore called aurum album.[8] However, his finding was not well-known to the chemistry fraternity almost for a decade, until German chemist Klaporth re-assessed his finding and gave the name tellurium after the Latin word '*Tellus*' for earth.[9] Although Se and Te share the same group with oxygen (O) and sulfur (S), their chemistry remained elusive for long time even after their discovery, which might be attributed to their malodorous aroma, toxicity and instability of some of their derivatives. In fact, during the early time of its development, selenium was considered to be absolute poison for living organism and its chemistry was limited to elemental selenium as dehydrating agent and SeO_2 as oxidizing agent. However, report by Schwarz *et al.* stating the fact that selenium is important micronutrient for bacteria, mammals and birds, it has changed the age-old hesitancy towards heavier chalcogen atoms.[10] In fact, selenocysteine, the selenium analogue of cysteine can be found at various active site of enzymes (especially in glutathione peroxidase) and is considered to be the 21st amino acid.[11]

There are six naturally occurring isotopes for selenium: ^{74}Se (0.87%), ^{76}Se (9.02%), ^{77}Se (7.58%), ^{78}Se (23.52%), ^{80}Se (49.82%) and ^{82}Se (9.19%). On the other hand, although several isotopes exist for tellurium, only eight isotopes have substantial natural abundance: ^{120}Te (0.09%), ^{122}Te (2.55%), ^{123}Te (0.89%), ^{124}Te (4.74%), ^{125}Te (7.07%), ^{126}Te (18.84%), ^{128}Te (31.74%) and ^{130}Te (34.08%).[12] Due to the diverse distribution of isotopes, both Se and Te

display characteristic splitting patterns in the mass spectra of their corresponding organochalcogen compounds. Again, among the isotopes, ^{77}Se and ^{125}Te have the nuclear spin I = ½ with significant natural abundance. Consequently, both ^{77}Se and ^{125}Te nuclear magnetic resonance (NMR) spectroscopy are used as the most common and powerful tools for the characterization of organosleneium and organotellurium compounds.[13] Like sulfur, both selenium and tellurium, can adopt various oxidation states ranging from −2 (Na_2Se/Na_2Te) to +6 (SeO_4^{-2}/TeO_4^{-2}). It is noteworthy to mention that in comparison to S, the higher oxidation state are more common and stable for selenium and tellurium, which are attributed to their lower ionization energies.

1.2.1. Organotellurium Compounds: Synthesis of Diorganyl ditelluride

Organotchalcogen compounds have garnered significant interest in contemporary chemistry with respect to their interesting properties and wide spread applications, such as ligands in coordination chemistry,[14] reagents in organic synthesis,[15] precursors for nanomaterials,[16] mimics for glutathione peroxidase (GPx)[17] to name a few. The first organotellurium compound namely, diethyl ditelluride was first reported by Wöhler in 1840.[18] Subsequently, several methods have been developed for the synthesis of diorganyl ditellurides. Some common approaches for the synthesis of diorganyl ditellurides are described below:

i) S_N1 Nucleophilic Substitution Reaction

Nucleophilic substitution reaction (S_N1) of organic halide by alkali metal chalcogenide is a very effective method for the preparation of organochalcogen derivative. Generally, the synthesis of alkali metal chalcogenide of the form M_2Se_n (where M is alkali metal and n = 1, 2) is achieved by the reaction of elemental chalcogen with alkali metal in presence of reducing agents such as, Na/Liq. NH_3,[19] $NaBH_4$,[20] $LiAlH_4$,[21] $Li(C_2H_5)_3BH$,[22] $NH_2NH_2.H_2O$[23] (Scheme 1.1).

$$2M \ + \ nE \ \xrightarrow{\text{Reducing Agent}} \ M_2E_n$$

$$M = Li/Na/K; \ E = Se/Te; \ n = 1,2$$
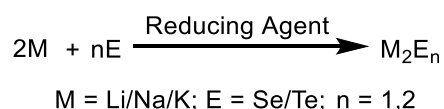
Scheme 1.1. Generation of alkali metal chalcogenides, M_2Se_n.

The subsequent reaction of chalcogenide anion with organic halides or organic tosylates afforded the desired diorganyl dichalcogenides, R_2E_2 (Scheme 1.2).[24]

$$R\text{-}X \xrightarrow{M_2E_2} R_2E_2 \ + \ MX$$

E = Se, Te
X = Cl, Br, I, OTs
M = Li, Na, K
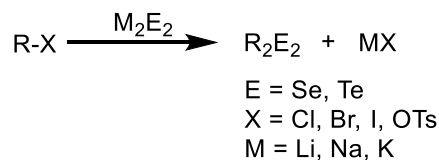
Scheme 1.2. Synthesis of diorganyl dichalcogenides, R_2E_2 by nucleophilic substitution reaction.

For example, when 2, 4-dichloropyrimidine, **1.1** was treated with Na_2Te_2, selective nucleophilic substitution took place on the C-2 carbon by the telluride anion to give ditelluride, **1.2**. Interestingly, the chlorine atom on C-4 also being reactive, underwent substitution by the N, N-dimethylamino anion derived from DMF (Scheme 1.3).[25]
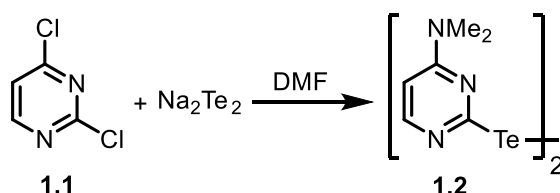
Scheme 1.3. Synthesis of ditelluride **1.2** by Na_2Te_2.

Atwood *et al.* have reported the synthesis of L-tellurocystine **1.4** by the reaction of *β*-chloro-L-alanine **1.3** with Na_2Te_2 (Scheme 1.4).[26] Recently, Satheeskumar *et al.* have reported the reactivity and antioxidant activity of **1.4** and its various derivatives.[27]
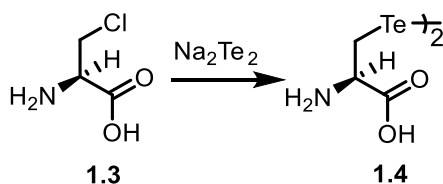
Scheme 1.4. Synthesis of L-tellurocystine **1.4** *β*-chloro-L-alanine **1.3** by Na_2Te_2.

ii) Lithiation Route

Lithiation is one of the convenient methods for the preparation of diorganyl dichalcogenide. Lithiation involves either H-abstraction from the aromatic systems or Br/Li exchange reaction with *n*-BuLi/*t*-BuLi. The aryl carbanion generated, when reacted with

elemental selenium/tellurium, followed by oxidation, results in the formation of corresponding diorganyl dichalcogenides.

For example, Engman *et al.* synthesized a series of diaryl ditellurides, **1.9-1.12** from respective aryl bromides, **1.5-1.8** following a sequence of lithiation, tellurium insertion and oxidation (Scheme 1.5). All the synthesized ditellurides were assessed for glutathione peroxidase-like activities.[28]

1.5 4-H
1.6 2-OMe
1.7 2,4,6-tri-Me
1.8 4-NMe$_2$

1.9 4-H
1.10 2-OMe
1.11 2,4,6-tri-Me
1.12 4-NMe$_2$
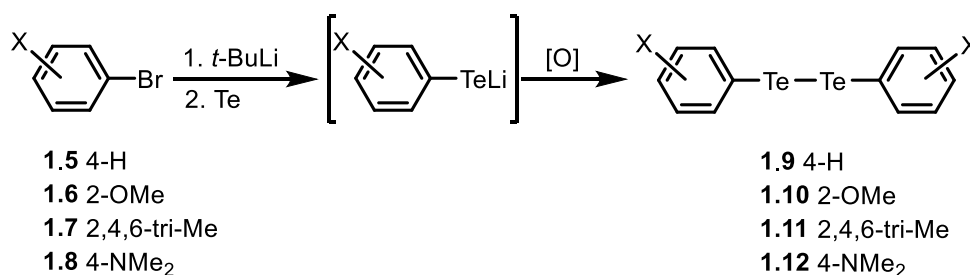
Scheme 1.5. Synthesis of ditellurides **1.9-1.12** by lithiation route.

Kaur *et al.* have reported the synthesis of bis[2-(dimethylaminomethyl)-phenyl] ditelluride **1.14** from N,N-dimethylbenzylamine **1.13** following the *ortho*-lithiation route (Scheme 1.6). Compound **1.13** was first treated with *n*-BuLi solution, which on treatment with tellurium powder gave lithium organotellurolate intermediate. Subsequent oxidative workup afforded ditelluride **1.14**. Similar heteroatom directed lithiation route was also followed by Mugesh *et al.* for the synthesis of series of diaryl ditellurides such as (*r*),(*r*)-bis[2-(4-ethyl-2-oxazolinyl)phenyl] ditelluride, diferrocenyl ditelluride, 2-methyl dinaphthyl ditelluride. All these ditellurides were found to be promising GPx-mimetics.[29]

1.13

1.14
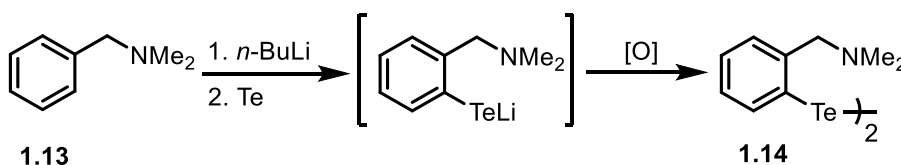
Scheme 1.6. Synthesis of ditelluride **1.14** by lithiation route.

iii) Grignard Route

Since *n*-BuLi/ *t*-BuLi are very strong bases, in some cases selective deprotonation become unsuccessful. Again, insertion of tellurium into C–Li bond in all substrates are not

successful. A milder approach for the synthesis of dichalcogenides is the Grignard route, where organyl halides such as **1.15** and **1.17** are treated with magnesium turnings to give corresponding organylmagnesium halides. Addition of tellurium powder followed by oxygen afforded the desired ditellurides **1.16** and **1.18** (Scheme 1.7).[30]
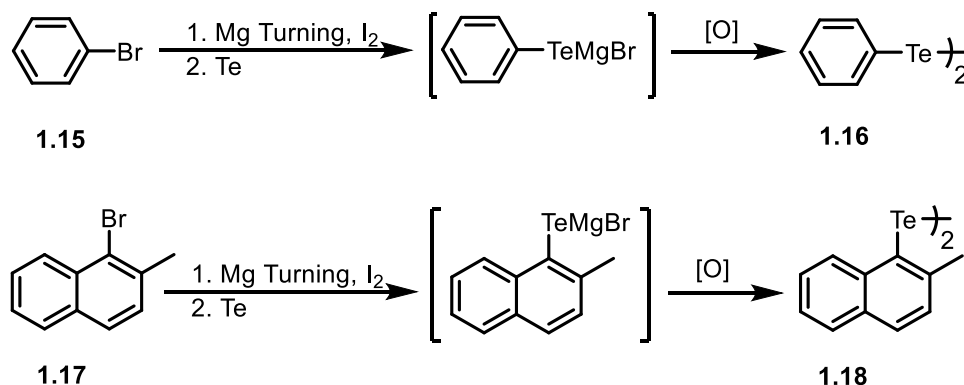
Scheme 1.7. Synthesis of ditellurides **1.16 and 1.18** by Grignard route.

iv) Other Methods

Uemura *et al.* have reported a novel method for the synthesis of unsaturated ditelurides from the reaction of tellurium dioxide (TeO_2) with non-conjugated diene. For example, when non-conjugated dienes such as 4-vinylcyclohex-1-ene **1.19** and hexa-1,5-diene **1.21** were treated with TeO_2 in acetic acid in presence of lithium bromide, it afforded bis(2-acetoxyalkenyl)ditellurides **1.20** and **1.22** respectively (Scheme 1.8).[31]
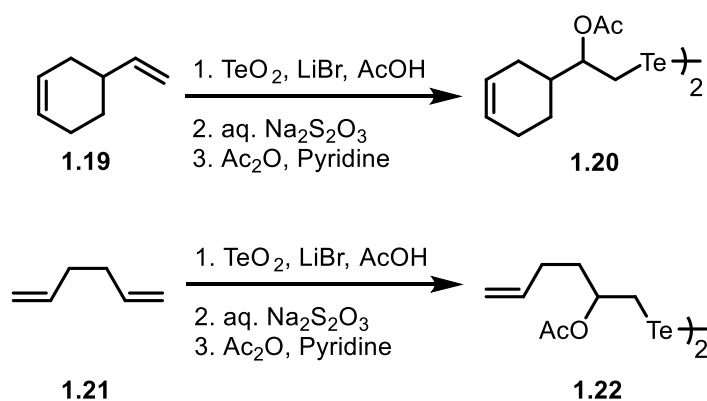
Scheme 1.8. Synthesis of ditelluride **1.20** and **1.22** from non-conjugated diene **1.19** and **1.21**.

This methodology was also successful for terminal alkenes in the sense that when **1.23**-**1.25** were treated with TeO_2 in alcoholic hydrochloric acids and sodium bisulfite ($Na_2S_2O_5$), it afforded bis(β-alkoxyalkyl) ditellurides, **1.26**-**1.28** (Scheme 1.9).[32]

1.23 R = *n*-C$_4$H$_9$
1.24 R = *i*-C$_4$H$_9$
1.25 R = *n*-C$_6$H$_{13}$

R^1 = Me
1.26 R = *n*-C$_4$H$_9$
1.27 R = *i*-C$_4$H$_9$
1.28 R = *n*-C$_6$H$_{13}$
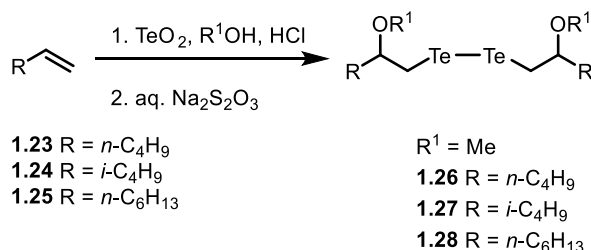
Scheme 1.9. Synthesis of ditellurides **1.26**-**1.28** from terminal alkenes **1.23**-**1.25** by tellurium dioxide (TeO_2).

Srivastava *et al.* have reported that when (2-phenylazophenyl-C, *N´*)tellurium(IV) trichloride, **1.29** was reacted with an excess of hydrazine hydrate, it afforded bis[2-phenylazophenyl-C, *N´*] ditelluride, **1.30** (Scheme 1.10). A mixed-valent chloro derivative, **1.31** was also obtained as subsidiary product during the course of the reaction.[33]

1.29   **1.30**   **1.31**
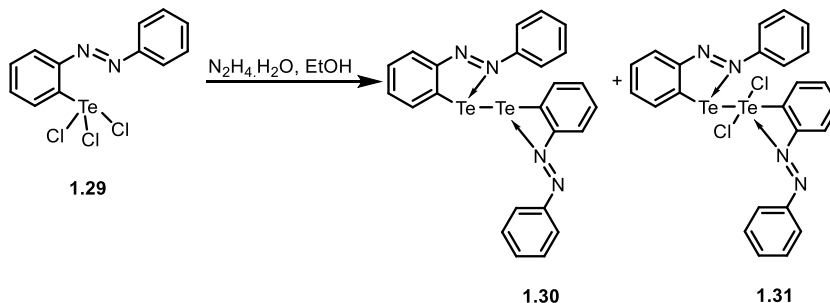
Scheme 1.10. Synthesis of ditelluride **1.30** from reduction of Te(IV) trichloride, **1.29**.

It is worth mentioning that ditellurides **1.14** and **1.30** are stabilized by Intramolecular Chalcogen Bonding (IChB) interactions. Hence, a brief general introduction of IChB is included in the following section.

1.2.2. Intramolecular Chalcogen Bonding (IChB)

Intramolecular Chalcogen Bonding (IChB), also known under the name of secondary bonding interactions or non-covalent interactions are a sub-class of σ-hole interactions, which play crucial role in stabilisation of the organochalcogen compounds.[34] By definition, IChB can be best

described as a 3c-4e, donor–acceptor interactions $n^2(Y) \rightarrow \sigma^*(E–X)$ in which the lone pair of a donor atom Y (e.g., N, O) interacts with the antibonding σ^* orbital of the heavy atom E (e.g., Se, Te) and a more electronegative atom X (e.g., Cl, Br) [Figure 1.3(a)]. Ideally, this interatomic interaction E$\cdots$Y is longer than sum of the covalent radii of the two atoms and shorter than the sum of their van der Waals radii. The origin of this interaction can be explained by accounting the concept of electrostatic effect invoking the idea of σ-hole (arising from partial charges) and dispersion distribution. The σ-hole can be described as a region of positive electrostatic potential, which is located on the opposite side of covalent bonds (R–E) and is protruded towards a negatively charged atom resulting in a non-covalent interaction. Figure 1.3(b) shows the molecular structure of 2-formylphenylselenenyl bromide and its electrostatic surface potential on the isodensity surface, $\rho(r) = 0.001$ au, showing one sigma hole on the Se atom.[34g] While moving down the group, electronegativity decrease and polarizability increases in the order of O < S < Se < Te. Consequently, the size of the σ-hole increases and the energy difference between $\sigma(E–X)$ and $\sigma^*(E–X)$ orbitals decrease in heavier chalcogen atoms in comparison to the lighter ones. As a result of these effects, Te compounds exhibit stronger IChB interactions compared to those of Se and S. Again, it is noteworthy to mention that secondary bonding interaction is directional in the sense that E$\cdots$D requires to be colinear with E–X bond as shown in Figure 1.3(c).
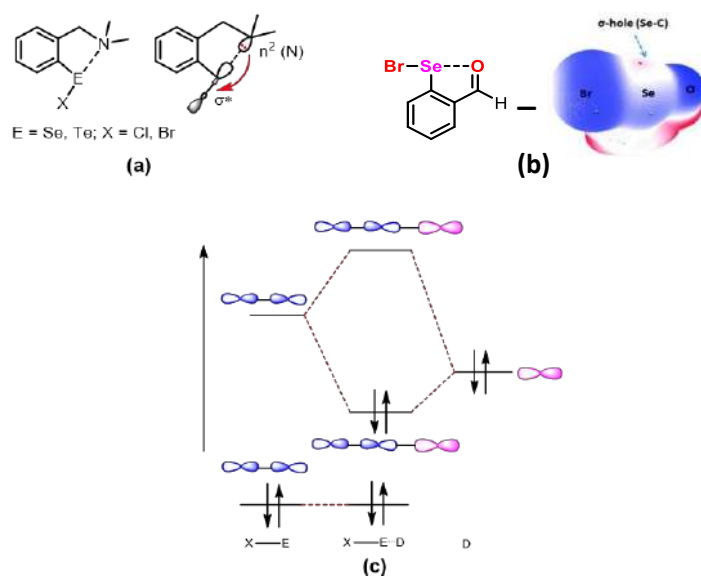
Figure 1.3. (a) Stabilization of [2-(dimethylaminomethyl)phenyl]chalcogenyl halide via a $n^2(N)$ $\rightarrow$ $\sigma*$ (E–X) (E = Se/Te, X = Cl, Br), (b) electrostatic surface potential of 2-formylphenylselenenyl bromide on the isodensity surface, $\rho(r) = 0.001$ au, showing one sigma

hole on the Se atom, (c) Molecular orbital interaction for secondary bonding, for simplicity, only *p* atomic orbitals are considered.[34g]

1.3. Lanthanoid Chalcogen Complexes

In recent times, interest in the chalcogenols (REH) and chalcogenolates (RE⁻) has immensely intensified as auxiliary ligands for the synthesis of metal chalcogenolate complexes.[35] In fact, many alkali and alkaline earth metal chalcogenolates,[36] transition metal chalcogenolates[37] and main group chalcogenolates[38] have been synthesized and found interesting applications in various aspects of contemporary chemistry. Interest in metal chalcogenolates particularly, metal selenolates, also stems from their relevance as model for the active sites of selenocysteine-containing metalloproteins.[39]

Like other metal complexes, complexes with lanthanoids have also gained profound interest, both from synthetic and application point of view. In particular, lanthanoid alkoxide complexes have been extensively investigated in literature.[40] However, lanthanoid complexes with heavier chalcogens are not much prevalent as compared to analogous species with oxygen[40] or sulfur[41]. The sluggish development of lanthanoid complexes with heavier chalcogens stems from the fact that lanthanoids are generally considered to be 'hard' metals, and they most readily form complexes with 'hard' ligands. Consequently, synthesis of complexes having bonds between hard, electropositive lanthanoid metal cations and soft, covalent chalcogen based ligands is very challenging. Again, most of the studies on lanthanoid chalcogenolates have been focused either on clusters of lanthanoid compounds or on oligomer or polymer of the same,[42] which is essentially attributed to their affinity for high and variable coordination number. Consequently, synthesis of monomeric lanthanoid chalcogenolates becomes even more challenging.

1.3.1. Synthesis of Organolanthanoid Chalcogenolate Complexes

A detailed insight in to literature of lanthanoid complexes, especially with Se and Te are given in the introductory portion of Chapter 2, where special focus has been given to monomeric complexes and the influence of metal, chalcogen and solvents on the complexes. Here, in this section, synthetic procedures commonly used for organolanthanoid chalcogenolate complexes are explained in detail.

i) Oxidation Reaction of Divalent Lanthanoid Complexes

One of the efficient approaches for the synthesis of organolanthanoid chalcogenolate complexes is by oxidation reaction of divalent lanthanoid complexes with organic dichalcogenides. For example, Evans *et al.* have reported the synthesis of trivalent organosamarium chalcogen complex $(C_5Me_5)_2Sm(SPh)(THF)$ **1.33** by reducing the S−S bond in diphenyl disulfide using $(C_5Me_5)_2Sm(THF)_2$ **1.32** (Scheme 1.11).[43] Similar Yb complexes were also reported by reacting $(C_5Me_5)Yb(NH_3)_2$ with PhEEPh (E = S, Se, Te).[44, 45] In complex **1.33**, the coordination number around Sm is sufficed by two η^5-cyclopentadienyl rings, one sulfur atom from the thiolate ligand and one oxygen atom from THF molecule.

1.32   **1.33**
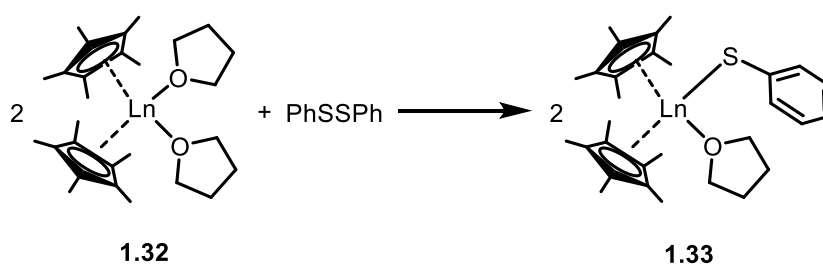
Scheme 1.11. Synthesis of lanthanoid chalcogen complex **1.33** by oxidation reaction of divalent lanthanoid complex **1.32**.

ii) Transmetallation

Transmetallation is a very effective method for synthesizing lanthanoid chalcogenolates. Brennan *et al.* have synthesized a series of lanthanoid(III) benzenefluorothiolate complexes such as $(THF)_3Ln(SC_6F_5)_3$ (Ln = Sm Er, Ho), $(DME)_2Er(SC_6F_5)_3$, $[(THF)_2Sm(SC_6F_5)_2(\mu\text{-}SC6F5)]_2$ by transmercuration of elemental lanthanoid with mercury thiolates $Hg(SC_6F_5)_2$.[46, 47] The reaction associated with formation of $(THF)_3Ho(SC_6F_5)_3$ **1.35** from $Hg(SC_6F_5)_2$ **1.34**, is shown in Scheme 1.12. Brennan *et al.* have further observed that when lanthanoid(III) benzenefluorothiolates $Ln(SC_6F_5)_3$ (Ln = Ce-Sm)) were treated with $Hg(SC_6F_5)_2$, heterometallic compounds with the general formula $[(DME)_3Ln(SC_6F_5)_2]_2[Hg_2(SC_6F_5)_6]$ (Ln = La-Gd), were obtained.[48]

2Ho + 3Hg(SC$_6$F$_5$)$_2$ $\xrightarrow{\text{THF}}$

1.34

1.35
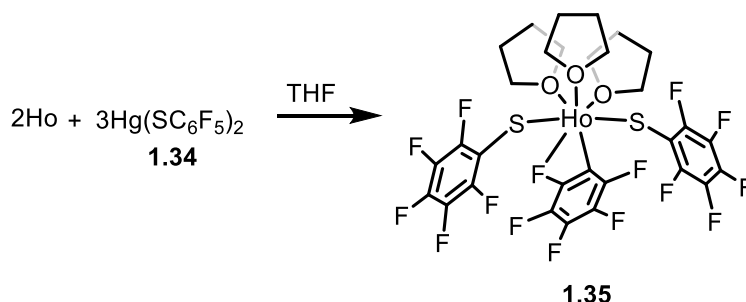
Scheme 1.12. Synthesis of lanthanoid chalcogen complex **1.35** by transmetallation.

iii) Salt-Metathesis

Salt metathesis reactions present another convenient approach for the synthesis of lanthanoid chalcogenolate complexes. In fact, various lanthanoid dithiolene complexes were reported by salt-metathesis reactions.[49-51] For example, Zheng *et al.* have reacted K$_2$dmit (dmit = 1,3-dithiole-2-thione-4, 5-dithiolate anion) with LnCl$_3$ (Ln = La, Nd, Sm, Gd, Er, Y) in presence of 1,10-phenanthroline to afford lanthanoid dithiolene complexes with the formula K$_2$[Ln(dmit)(phen)$_2$Cl$_3$]·6H$_2$0.[49] Ephritikhine *et al.* synthesized tris(dithiolene) complexes of Nd and Ce by reacting Ln(BH$_4$)$_3$(THF)$_3$ (Ln = Nd, Ce) and M$_2$dddt (M = Na, K; dddt = 5,6-dihydro-1,4-dithiine-2,3-dithiolate).[50] In another instance, when [Ln(Cp*)$_2$Cl$_2$K] **1.36** was reacted with K$_2$dddt, it afforded dimeric lanthanoid complexes [{Ln(Cp*)$_2$(dddt)K(thf)$_2$}$_2$] [**1.37 (Ce)**, **1.38** (Nd)], which on subsequent reaction with 15-crown-5 resulted [K(15-crown-5)$_2$][Ln(Cp*)$_2$(dddt)] [**1.39 (Ce)**, **1.40** (Nd)] (Scheme 1.13).[51]

[Ln(Cp*)$_2$Cl$_2$K] $\xrightarrow[\text{THF}]{\text{K}_2\text{dddt}}$ [{Ln(Cp*)$_2$(dddt)K(thf)$_2$}$_2$] $\xrightarrow[\text{THF}]{\text{15-crown-5}}$ [K(15-crown-5)$_2$]

1.36   **1.37** (Ce), **1.38** (Nd)

1.39 (Ce), **1.40** (Nd)
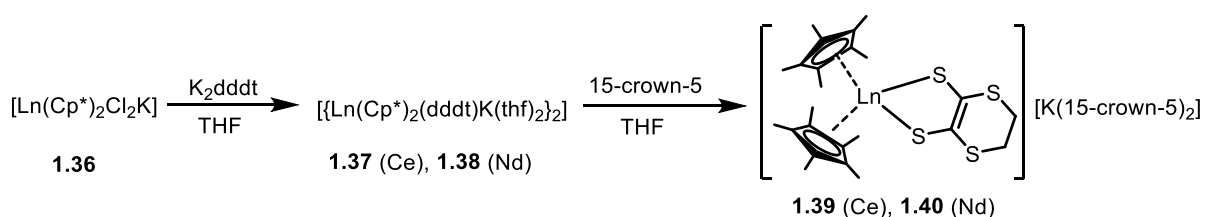
Scheme 1.13. Synthesis of lanthanoid chalcogen complexes **1.39-1.40** by salt metathesis reaction.

iv) **Reactions of Elemental Chalcogens with Lanthanoid Chalcogenolates: Synthesis of Chalcogen-rich Lanthanoid Clusters**

Brennan *et al.* reported the synthesis of chalcogen-rich lanthanoid clusters containing fluorinated thiolate ancillary ligands by following a two-step procedure. First lanthanoid fluorothiolates $Ln(SC_6F_5)$ and benzenechalcogenolates $Ln(EPh)_3$ (E = S, Se) were synthesized. In the subsequent step, the mixture of $Ln(SC_6F_5)$ (Ln = Yb) and $Ln(EPh)_3$ was treated with elemental S (or Se), which proceeded through the oxidative elimination of PhEEPh (E = S, Se) to afford tetranuclear clusters $(THF)_6Ln_4E(EE)_4(SC_6F_5)_2$ **1.41-1.43** [**1.41** (E = S, Ln = Yb); **1.42** (E = Se, Ln = Yb); **1.43** (E = Se; Ln = Tm)] (Scheme 1.14).[52] Similarly, when $Yb(SPh)_3$, synthesized by the reaction of PhSSPh with Yb/Hg in pyridine, was reacted with elemental S, it afforded a cubane cluster $(py)_{10}Yb_6S_6(SPh)_6$, **1.44**.[53,54]
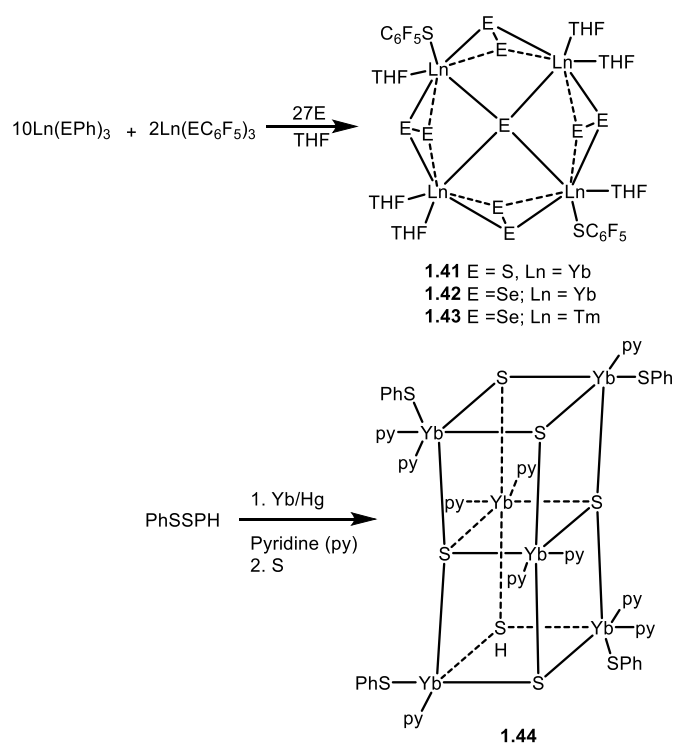
Scheme 1.14. Synthesis of lanthanoid chalcogen clusters **1.41-1.44** by salt metathesis reaction.

1.3.2. Applications of Organolanthanoid Chalcogenolate Complexes

Due to the high electrophilicity and high Lewis acid nature of of Ln–ER bond, the organolanthanoid chalcogen complexes show interesting reactivity profile. Some important reaction behavior of lanthanoid complexes are outlined below.

i) Organolanthanoid Chalcogenolates as 'Sulfenylating Reagent'

Tanigushi *et al.* have reported that the lanthanoid thiolate complex, [Yb(SR)$_3$], (where R = *p*-tolyl), can react with enones to give corresponding Michael adducts, where [Ln(SR)$_3$] acts as a sulfenylating reagent.[55]

$$\text{Yb} \ + \ 3/2\ \text{RSSR} \ \xrightarrow[\text{THF-HMPA}]{\text{Ph}_2\text{CO}} \ [\text{Yb(SR)}_3]$$

1.45 R = *p*-tolyl

1.46 R^1 = Me,
R^2 = R^3 = R^4 = H
1.47 R^1 = Me, R^2 = Me,
R^3 = H, R^4 = Me

1.48 R = p-tolyl
R^1 = Me,
R^2 = R^3 = R^4 = H
1.49 R = p-tolyl
R^1 = Me, R^2 = Me,
R^3 = H, R^4 = Me
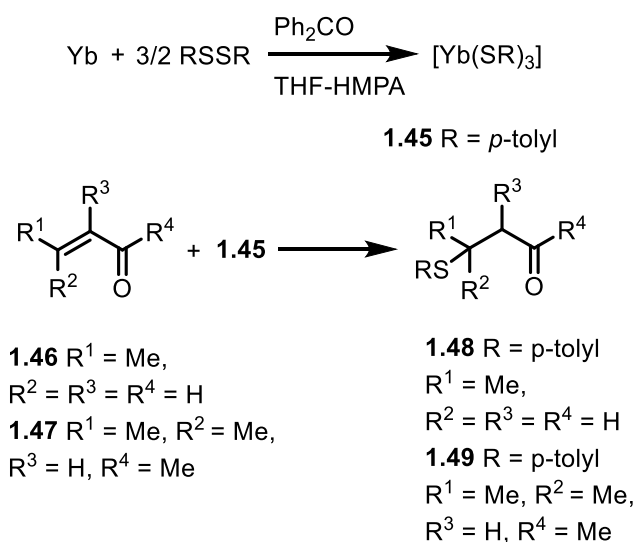
Scheme 1.15. Conjugate addition of **1.45** to enones, **1.46-1.47**.

Yb metal when reacted with bis(*p*-tolylsulfide) in the presence of benzophenone, afforded Yb(III) thiolate complex **1.45**. Complex **1.45**, when *in situ* treated with enones **1.46-1.47**, it underwent Michael addition to afford the addition complexes **1.48-1.49** as shown in Scheme 1.15.

ii) Epoxide Opening Reaction

Dowsland *et al.* have reported that ytterbium(III) chalcogenolate complexes can be efficiently used in epoxide opening reaction.[56] In particular, when Yb metal was treated with diphenyl dichalcogenide in the presence of methyl iodide, it afforded Yb(III) chalcogenolate complexes

1.50-1.52 (Scheme 1.16). The resulting complexes, when treated with epoxides **1.53-1.54**, the epoxides underwent facile ring opening reactions to give respective addition complexes **1.55-1.60**.

Yb + PhEEPh $\xrightarrow{\text{MeI}}$ [Yb(EPh)$_3$]or [{Yb(EPh)$_2$(μ-EPh)$_2$]

1.50 (E = S) , **1.51** (E = S3), **1.52** (E = Te)

1.53 R^1 = Me,
1.54 R^1 = Ph

1.55 R^1 = Me, E = S
1.56 R^1 = Me, E = Se
1.57 R^1 = Me, E = Te
1.58 R^1 = Me, E = S
1.59 R^1 = Me, E = Se
1.60 R^1 = Me, E = Te
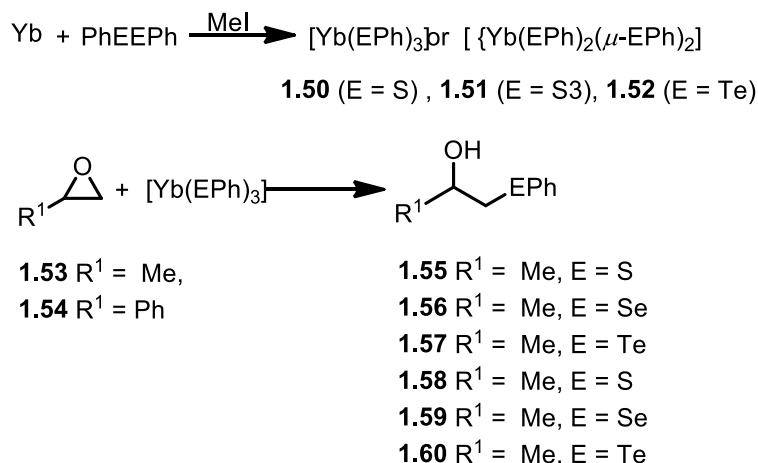
Scheme 1.16. Epoxide ring opening reactions by lanthanoid chalcogenolates **1.50-1.52**.

iii) Polymerisation of Olefin

Organolanthanoid complexes such as [Cp*$_2$LnR] (R =alkyl and hydride) have attracted significant attention as active catalysts for the polymerization of ethylene.[57] Recently, Hou *et al.* have reported that Sm(II) complexes [(C$_5$Me$_5$)Sm(THF)$_m$(ER)(μ-C$_5$Me$_5$)K(THF)$_n$]$_\infty$ (m = 0 or 1; n =1 or 2; ER = OC$_6$H$_2$ ^{t}Bu$_2$-2,6- Me-4, OC$_6$H$_3$ ^{i}Pr$_2$-2,6, SC$_6$H$_2$ ^{i}Pr$_3$-2,4,6] showed high catalytic activity for polymerization and block-copolymerization of styrene and ethylene.[58] Similarly, (Me$_5$C$_5$)$_2$LnR (Ln = Sm, Yb, Lu and Y; R = H, Me) are found to be effective catalysts for the polymerization of methyl methacrylate (MMA).[59] Similar catalytic activities were also observed for Ln(SPh)$_3$(HMPA)$_3$ (Ln = Sm, Eu, Yb), [{Ln(HMPA)$_3$}$_2$(μ-SPh)$_3$][SPh] (Ln = Sm, Yb) and [Ln(SC$_6$H$_2$Pr^i$_3$-2,4,6)(μ-SC$_6$H$_2$Pr^i$_3$-2,4,6)(THF)$_3$]$_2$ (Ln = Sm, Yb), where these complexes were used for the polymerization of MMA to give syndiotic polymers.[60] It was observed that due to the presence of highly coordinating HMPA ligands, the syndiospecificity of the polymers increases significantly.

iv) Organolanthanoid Chalcogenolates in Optoelectronics

From the recent development in organolanthanoid chalcogenolates, it is observed that these compounds possess interesting luminescence behavior, which is important for the perspective of

rational design of emissive material. However, due to the extreme air- and moisture- sensitivity of the resulting complexes, the real-time optoelectronic applications of organolanthanoid chalcogenolates are still not well explored. Recently, Brennan *et al.* have reported that the bimetallic cluster $[(py)_8Ln_4M_2Se_2(SePh)_4]$ [Ln = Er; M= Hg, Cd] exhibits promising luminescence properties with emission lifetime of 1.41 ms (Er/Cd) and 0.71 ms (Er/Hg).[61] Similarly, Nd thiolate complex $[(DME)_2Nd(SC_6F_5)]$ and oxyselenido complex $[(THF)_8Nd_8O_2Se_2(SePh)_{16}]$ are found to be highly emissive at 1077 and 925 nm respectively.[62]

Part B

1.4. General Introduction of Redox Active Ligands

In coordination chemistry, the properties of a metal complex as a whole depends on the interactions between the metal center and its surrounding ligands. In other words, the synergistic cooperation between the metal and the ligands play pivotal role in the determining the overall properties of the metal complex and eventually its applicability. Conceptually, the assignment of exact oxidation state of the metal ion is one of the foremost tasks in a metal complex. In fact, in contemporary coordination chemistry, the usefulness of oxidation state formalism has gained pronounced attention with respect to the prediction of the spectroscopic, electrochemical, magnetic properties of the complexes as well as to understand their reactivity profiles. In classical Warner type complexes, the assignment of oxidation was easy as shown in Scheme 1.17.
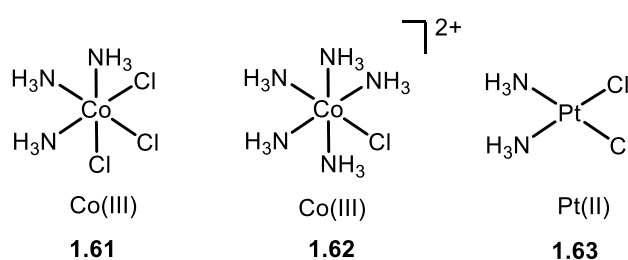
Scheme 1.17. Representative examples of classical Warner type complexes **1.61-1.63**.

However, complicacy in determining the formal oxidation state arises when the coordinated ligand has the potential to stabilize more than one oxidation states. In this context, Jørgensen introduced the concept of "non-innocence" feature of the ligand to address the apparent ambiguity in assigning the oxidation states of metal.[63] According to Jørgensen's theory, a ligand is termed as 'innocent' if it allows the unambiguous determination of the oxidation state of the central metal atom. A ligand is called non-innocent when it has several energetically accessible levels that allow redox reactions to change their charge state. For example, in Ni(gma) complex [where, gma = glyoxalbis(2-mercaptoanil)], it becomes difficult to precisely define the oxidation state of the central metal atom or the charges on the donor atoms of the ligand.[64] This is because, there are four possible ways to explain the electronic state of the complex, such as 16-electron Ni(II) complex with diiminodithiolate (**1.64a)** or di(iminothiosemiquinonate) (**1.64b**); as a 14-

electron Ni(IV) complex (**1.64c**) or, alternatively, as an 18-electron Ni(0) complex (**1.64d**). Consequently, the complex is best described by formulations (**1.64a-1.64e**) with delocalized bonds (Scheme 1.18).
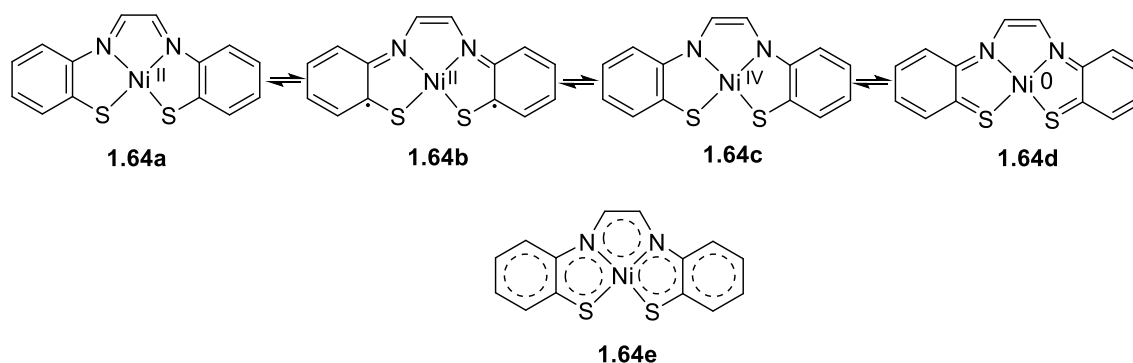
Scheme 1.18. Redox non-innocence behavior of gma = glyoxalbis(2-mercaptoanil) ligand in Ni(gma) complex, **1.64a-e** .

Another redox non-innocent ligand which has been extensively used in coordination chemistry is quinone moiety, **1.65**.[65] This can undergo two successive one-electron oxidation, thereby offering variable oxidation states to the bonded metal atom (Scheme 1.19). The redox innocence behavior is also common among the various biochemically relevant ligands, such as nitrosyl (**1.66**),[66] molecular oxygen (**1.67**)[67] and azo based ligands (**1.68**)[68]; possible redox states of these ligands are shown in Scheme 1.19.
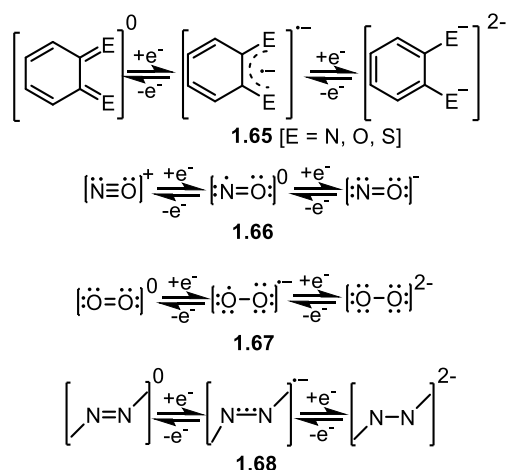
Scheme 1.19. Different redox states of some common non-innocent ligands, **1.65-1.68**.

Due to extensive and ambiguous involvement of electrons in the metal-ligand bond, it apparently becomes impossible to determine the electronic structure properties of metal complex which

incorporates non-innocent ligand by a single characterization techniques. In fact, a wide array of analytical techniques like mass spectrometry, UV-vis, IR, NMR and conductivity, X-ray diffraction studies in combination with theoretical calculations (DFT/TD-DFT) need to be deployed to get a clear perception of electronic structure properties of the complex (*vide infra*).

1.4.1. Common Techniques to Establish Electronic Structural Forms of the Metal Complexes Incorporating Non-innocent Ligands

1.4.1.1. Structural Studies

The various bond parameters obtained from the single crystal X-ray diffraction studies offer crucial information in assigning the oxidation state of the coordinated non-innocent ligands. For example, in a metal complex which contains quinone ligand or a azo ligand, the C–X, C–Y and C–C distances of coordinated quinone moiety, or the N=N bond distances of the azo-aromatics significantly vary with respect to different oxidation states of the ligands as shown in Table 1.1.[69] Consequently, comparing the respective bond distances with the literature reported values can give a clear idea about the oxidation state of the ligand.

Table 1.1. Various bond distances observed for coordinated quinone and azo moieties in different oxidation states

	Bond Distance (Å)		
	Oxidized form	Intermediate form	Reduced form
C-O	1.22	1.30	1.34
C-N	1.31	1.35	1.38
C-S	1.69	1.72	1.75
N-N	1.23-1.30	1.35	1.40-1.45

1.4.1.2. Electrochemistry and UV-vis-NIR-IR Spectroelectrochemistry

Various electrochemical techniques such as cyclic voltammetry, differential pulse voltammetry and controlled potential coulometry together with UV-vis-NIR-IR spectroelectrochemistry provide significant information in determining the electronic structures of metal complex. For example, in the case of quinone based ruthenium complex, {Ru^{II}-$Q^{\bullet}$} (Q = Quinonoid based ligand), the presence of a low energy intense band near 1000 nm corresponding to HOMO

[$d\pi$(Ru)] to LUMO [π*(Q$^\bullet$)] transition. However, this low energy band is absent in {Ru^{III}-Q$^\bullet$} or {Ru$^{II/III}$-Q} moiety.[69a, 70]

1.4.1.3. EPR Spectroscopy

EPR spectroscopy is also a useful technique to assign the specific location of unpaired spin(s), either on the metal or ligand or both. The anisotropic parameter (Δg) or $<g>$ obtained from EPR spectrum of a paramagnetic molecule can be considered as "fingerprint" for the identification. This value contains the chemical information that lies in the interaction between the electron and the electronic structure of the molecule. Consequently, it depends on the mixing of the metal/ligands orbitals. As a general statement, $<g>$/ Δg appear to be >2.0/0.25 for metal centered spin.[71] On the other hand, the value changes to ~2.0/<0.03 for the ligand centered spin.[72] However, complexity arises due to the mixing of metal-ligand orbitals (covalency).[73]

1.4.1.4. Density Functional Theory (DFT) Calculations (Computational Studies)

DFT calculations in combination with experimental observations can provide significant insights into the electronic structure of metal complexes of redox-active ligands. The calculated Mulliken spin-density plots, Time-Dependent Density Functional Theory (TD-DFT) along with molecular orbital compositions, Natural Bond Orbital (NBO) analyses also are very helpful in determining the location of unpaired spin(s), nature of the molecular orbitals, and most importantly, to verify the origin of the experimentally observed electronic transitions.

Part C

1.5. General Introduction of Pincer Ligands

The history of pincer ligand dates back to late 1970, when Moulton *et al.* reported a series of transition metal (Ni, Pd, Pt, Rh, Ir) complexes stabilised by tridentate PCP ligand.[74] The term 'pincer' was first coined by van Koten in 1989 to describe tridentate ligand capable of imposing a meridional coordination around the metal center. With the advancement of chemistry, in current time, pincer ligands have covered almost all variation of side arms as well as various ligand backbones. It is precisely the convenience in fine-tuning the flanking arms as well as the backbone as shown in Figure 1.4, that triggers the rational design of various palindromic pincers (such as PCP, PNP, CCC, CNC, NNN, NCN, OCO, SPS, SeCSe *etc.*) as well as non-palindromic pincers (such as NNP, PCN *etc.*), which eventually makes them universal ancillary ligands in metal based chemistry.[75] Some example of palindromic as well as non-palindromic pincer ligands are shown in Chart 1.1.[75]
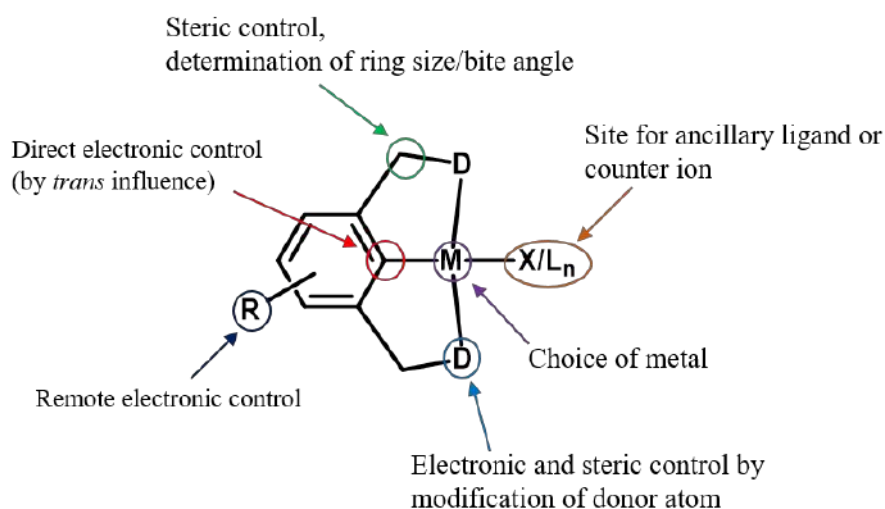
Figure 1.4. General structure motif of a pincer ligand with potential modification sites.
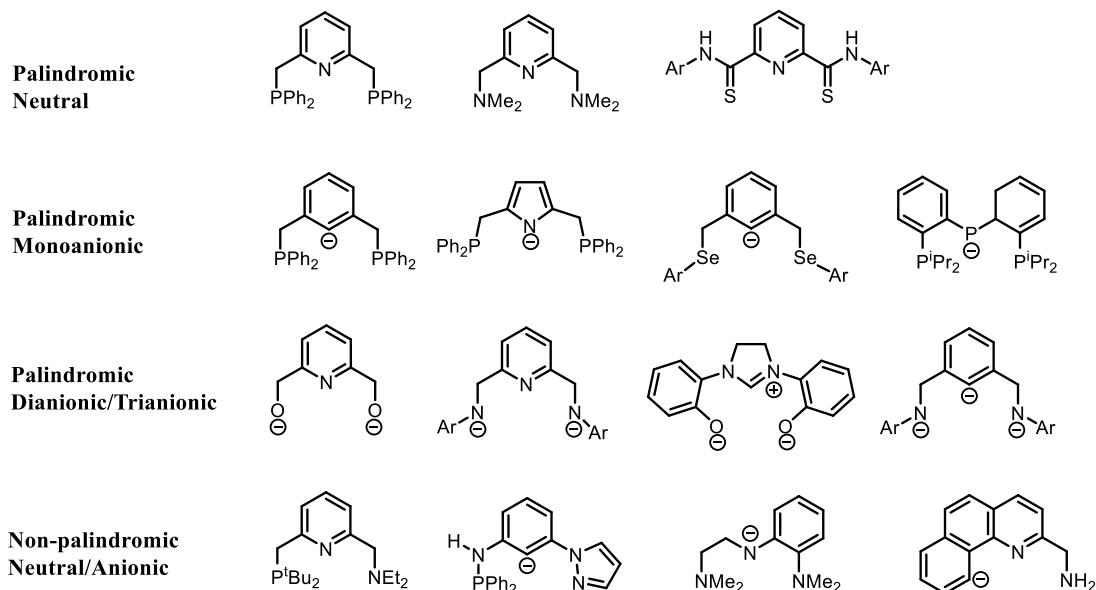
Chart 1.**1.** Some representative pincer ligands.[75]

1.5.1. Common Strategies for Synthesis of Metal Complexes of Pincer Ligands

With the advancement of chemistry of pincer ligands, various synthetic strategies have been developed and utilized for the synthesis of metal complexes of pincer ligands. However, it is noteworthy that, all the synthetic strategies are solely dependent on nature of the donor sites as well as the metal. Some common methodologies for synthesis of pincer-metal complexes are outlined below.

i) Cyclometalation

Moultan *et al.*, for the first time, introduced cyclometalation for the synthesis of metal pincer complexes. In particular, they synthesized a series of transition metal complexes, **1.70-1.74** of PCP pincer ligands, **1.69** by cyclometalation process (Scheme 1.20).[74]

1.69

1.70 M = Ni, X = Cl, n = 2
1.71 M = Pd, X = Cl, n = 2
1.72 M = Pt, X = Cl, n = 2
1.73 M = Rh, X = Cl, n = 3
1.74 M = Ir, X = Cl, n = 3
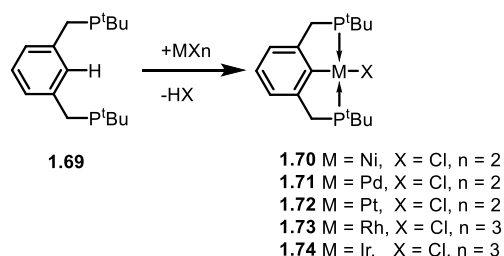
Scheme 1.20. Synthesis of pincer complexes by direct cyclometalation reaction.

After this report, the cyclometalation approach has been extensively used for the synthesis of metal complexes of various pincer scaffolds. For example, Milstein and co-workers have synthesized a series of Rh complexes of PCP pincer ligands by adopting direct cyclometalation approach.[76] Similarly, Beley *et al.* have synthesized Ru and Os complexes of NCN pincer ligands by facile cyclometalation with respective precursors.[77]

ii) Oxidative Addition

Oxidative addition by low-valent metal precursors is found to be another successful approach for synthesizing the metal complexes of pincer ligands. This process is always accompanied by increase in oxidation state and coordination number of the metal center by two unit.[78] A typical example includes the synthesis of organonickel complex **1.76** of NCN pincer ligand **1.75** where Ni(COD) (COD = 1,5-cyclooctadiene) was used as a metal precursor (Scheme 1.21).[78a]
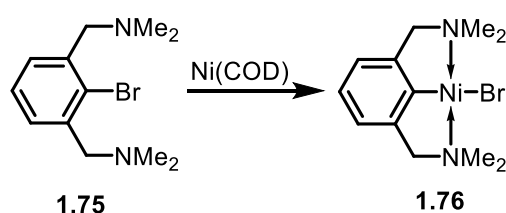
Scheme 1.21. Synthesis of pincer complex **1.76** by oxidative addition reaction.

iii) Transmetallation

Transmetallaion is one of the more conventional approaches for the synthesis of metal complexes of pincer ligands. Mostly, the synthesis of pincer complexes by transmetallation approach has been achieved by using organolithium or organomercurial reagents. However, the usage of organosilver and organocopper compounds as trasmetallating reagents is also well appreciated in literature. For example, Suárez *et al.* have synthesized Ru(II)-CNC pincer complex **1.79** by transmetallation method from corresponding Ag(I)-NHC complex **1.78** (Scheme 1.22).[79] Complex **1.78** was obtained by the reaction of bis-imidazolium salt **1.77** with Ag_2O. Similarly, Liu *et al.* reported Ag(I)-pincer complex wherein they have utilized Cu(I)-NHC complex as trasmetallating reagent.[80]
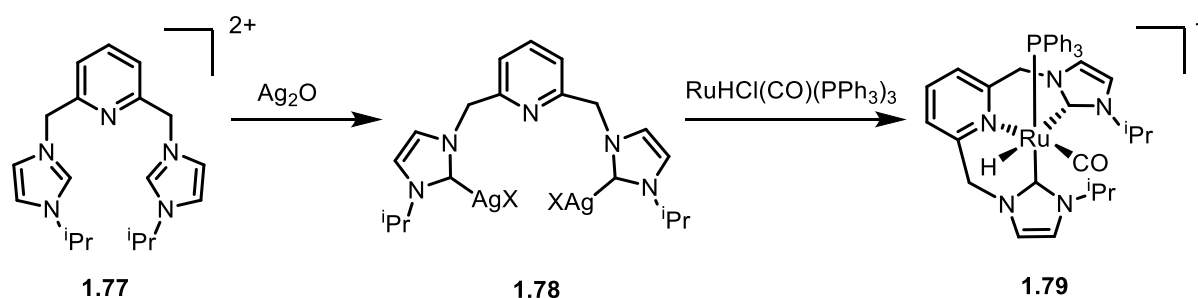
Scheme 1.22. Synthesis of pincer complex **1.79** by transmetallation of **1.78**.

1.5.2. Applications and Current Perspectives of Pincer Complexes

The robustness that the pincer ligand framework offers to the metal complexes and with their unique design, durability and versatility, the pincer ligand motifs have arguably achieved the status of privileged platform in modern organometallic and coordination chemistry. In the last 48 years since Moultan *et al.* reported the first PCP pincer complex, seminal contributions from many different groups, the coordination chemistry and reactivity of pincer complexes has achieved a multitude of applications across chemical sciences and is still continuing to find many new applications. In today's scenario, the chemistry of pincer-ligated metal complexes display extraordinarily expanded portfolio; such as starting from homogenous catalysis[81] to synthesis of novel sensor materials[82]; molecular recognition,[83] optoelectronics,[84] to supramolecular chemistry[85] to name a few. During the period of time, a number of reviews have been published describing about the scope and wide-spread applications of pincer complexes.[75[d-g], 81]

One recent area of interest where pincer complexes has gained significant attention is metallopharmaceuticals. While in some pincer ligand complexes the metal-ligand bond is labile and releases the metal from the tridentate environment quite easily, in some other pincer ligands have high stability which is quite important from the perspective of potential pharmaceutical applications. In fact, it is particularly the stability and strength of the metal-ligand bond and the ability to readily fine-tune the properties of some pincer complexes through structural alteration of the ligand, has triggered the increasing use of NHCs in metallopharmaceuticals.

1.6. Objectives and Glimpses of the Present Work

The aspects that are brought to light by the preceding discussions and the objectives of the present work are summarized below.

1. (**Chapters 2** and **3**) Due to the large atomic size and affinity for higher coordination number of the lanthanoid ions, most of the reported lanthanoid chalcogenolate complexes are either clusters or polymeric in nature. Consequently, synthesis of monomeric lanthanoid chalcogenolates is a formidable challenge. Our group has long standing interest on the stabilization of monomeric transition metal chalcogenolate complexes using hybrid, Intramolecular Chalcogen Bonding (IChB) stabilised multidentate ligands containing soft 'Te' and hard 'N' atom. The same strategy is envisaged to apply in **Chapter 2** for the synthesis of monomeric lanthanoid tellurolate complexes, wherein the donor nitrogen atoms from the auxiliary arms, which were involved in secondary bonding interaction with tellurium (N···Te) would act as chelating arms to result monomeric lanthanoid metal complexes. In this context two diorganyl ditellurides namely, bis[2-(dimethylamino)methyl)phenyl]ditelluride, and 8,8'-diquinolyl ditelluride have been considered and their reactions towards formation of lanthanoid complexes have been explored.

We further envisaged to synthesize monomeric lanthanoid thiolate complexes. For that, synthesis of quinolnie thiolate ligand was attempted by the reaction of 8-quinolinesulfonyl chloride with tin dichloride, which afforded bis(8-thiolquinolinium) hexachloridostannate(IV). It is worth noting that although bis(8-thiolquinolinium) hexachloridostannate(IV) has been extensively used in literature as reactive intermediate,[86] however, there is no structural characterization of bis(8-thiolquinolinium) hexachloridostannate(IV) available yet. Hence in **Chapter 3**, we carried out a detailed characterization of bis(8-thiolquinolinium) hexachloridostannate(IV). In addition, some interesting reaction behaviors of bis(8-thiolquinolinium) hexachloridostannate(IV) in different solvents are also explored.

2. (**Chapter 4**) In recent times, redox innocence properties of N,N′-disubstituted 1,2-diaminobenzenes have gained significant interest. It is observed that the substituents present in NH arms of 1,2-diaminobenzene play important role in the redox non-innocence of the ligand and their modification can significantly alter the electronic structural properties of the resulting metal complexes. Consequently, various substituents are incorporated to 1,2-diaminobenzene and their redox non-innocent behavior towards various metals have been extensively studied in the literature. In this context, in **Chapter 4**, two pyridine rings are incorporated as flanking arms to 1,2-diaminobenzene and it is envisaged to explore the redox innocent properties the new ligand, namely N,N′-bis(2-pyridyl)benzene-1,2-diamine with Ru and Os metal by means

spectroscopic, electrochemical, magnetic and computational investigations. It is believed that incorporation of π-acceptor group to the flanking arms would significantly alterate the redox properties of the resulting complexes. It is further planned to compare the electronic structural properties of the synthesized complexes with similar reported complexes wherein different substituents are present in the flanking arms of 1,2-diaminobenzenes.

3. (**Chapter 5**) Amidst various pincer scaffolds, NNN- pincer ligands based on pyrrole framework have recently drawn significant interest with respect to their interesting structural properties and applications.[87] However, reports on transition metal complexes and group 16 complexes of pyrrole based NNN ligands are rather scarce in literature. In **Chapter 5**, it was thought worthwhile to synthesize and explore the structural aspects of Pd, Pt, Se and Te complexes of three pyrrole based NNN-pincer ligands with different side arms, namely 2,5-bis[(dimethylamino)methyl] pyrrole, 2,5-bis[(pyrrolidino)methyl] pyrrole and 2,5-bis[(piperidino)methyl] pyrrole. To get detail insight into N–Se/Te bond, comprehensive computational study [Atoms in Molecule (AIM), Natural Bond Order (NBO)] has also been carried out.

Reference

1. Cotton, S. *Lanthanide and actinide chemistry*, John Wiley and Sons Ltd, Chichester, **2006**.

2. Housecroft C. E.; Sharpe, A. G. *Inorganic chemistry*, Pearson Education Ltd, England, *Ch. 20*, **2012**.

3. Wells, W. H.; Wells, V. L. *The lanthanides, rare earth metals* in *Patty's Toxicology* (Eds.: Bingham, E.; Cohrssen, B.), Wiley, Hoboken, *Vol. 1*, **2012**.

4. Greenwood, N.; Earnshaw, A. *Chemistry of elements*, Elsevier Butterworth-Heinemann, *Ch. 30*, **1997**.

5. Rinehart, J. D.; Long, J. R. *Chem. Sci.* **2011**, 2, 2078.

6. Atkins, P.; Overton, T.; Rourke, J.; Weller, M.; Armstrong, F.; Hangerman, M. *Inorganic chemistry,* Oxford University Press, England, *Ch. 23*, **2010**.

7. Berzelius, J. J. *Afhandl. Fys. Kemi Mineralogi* **1818**, *6*, 42.

8. von Reichenstein, F. J. M. *Phys. Arb. Freunde Wien.* **1785**, *3*, 48.

9. Klaproth, M. H. *Mem. Akad. Berlin* **1798**, *50*, 17.

10. Schwarz, K.; Foltz, C. M. *J. Am. Chem. Soc*. **1957**, *79*, 3292.

11. (a) Flohé, L.; Günzler, E. A.; Schock, H. H. *FEBS Lett*. **1973**, *32*, 132. (b) Rotruck, J. T.; Pope, A. L.; Ganther, H. E.; Swanson, A. B.; Hafeman, D. G.; Hoekstra, W. G. *Science* **1973**, *179*, 588. (c) Bhagavan, N. V; Ha, C.-E. *Essentials of Medical Biochemistry With Clinical Cases*, *2ⁿᵈ ed.*, Academic Press, Elsevier, **2015**.

12. Chivers, T.; Laitinen, R. S. *Chem. Soc. Rev.* **2015**, *44*, 1725

13. (a) Mugesh, G.; Panda, A.; Singh, H. B.; Butcher, R. J. *Chem. Eur. J.* **1999**, *5*, 1411. (b) Panda, A.; Singh, H. B. *NMR of organoselenium and organotellurium compounds* in *The Chemistry of organic Selenium and Tellurium Compounds* (Eds.: Patai, S.; Rappoport, Z.) John Wiley & Sons Inc., New York, *Ch. 3*, **2013**.

14. (a) J. Arnold, *Prog. Inorg. Chem.* **1995**, *43,* 353. (b) Jain, V. K.; Chauhan, R. S. *Coord. Chem. Rev*. **2016**, *306*, 270. (c) Kedarnath, G.; Jain, V. K. *Coord. Chem. Rev*. **2013**, *257*, 1409. (d) Mugesh, G.; Singh, H. B.; Butcher R. J. *Eur. J. Inorg. Chem.* **1999**, 1229. (e) Menon, S. C.; Panda, A.; Singh, H. B.; Butcher, R. J. *Chem. Commun*. **2000**, 143. (f) Chakraborty, T.; Sharma, S.; Singh, H. B.; Butcher, R. J. *Organometallics* **2011**, *30,* 2525. (g) Bonasia, P. J.; Arnold, J. *Inorg. Chem.* **1992**, *31*, 2508. (h) Levason, W.; Orchard, S. D.; Reid, G. *Coord. Chem. Rev*. **2002**, *225*, 159.

15. (a) Klayman, D. L.; Günther W. H. H. *Organic selenium compounds: their chemistry and biology*, John Wiley & Sons Inc., New York, **1973**. (b) Reich, H. J. *Acc. Chem. Res*. **1979**, *12*, 22. (c) Comasseto, J. V.; Piovan, L.; Wendler, E. P. in *The Chemistry of organic Selenium and Tellurium Compounds* (Eds.: Patai, S.; Rappoport, Z.) John Wiley & Sons Inc., New York, *Ch. 5*, **2013**. (d) Zade, S. S.; Singh, H. B. in *The Chemistry of organic Selenium and Tellurium Compounds* (Eds.: Patai, S.; Rappoport, Z.) John Wiley & Sons Inc., New York, *Ch. 6 &7,* **2013**.

16. (a) Mariappan, K.; Varapragasam, S. J. P.; Hansen, M. R.; Rasalingam, S.; Alaparthi, M.; Sykes, A. G. *J. Organomet. Chem*. **2018**, *866*, 251. (b) Sinha, P.; Kriegner, C. J.; Schew, W. A.; Kaczmar, S. W.; Traister, M.; Wilson, D. J. *Energy Policy* **2008**, *36*, 381. (c) Fthenakis, V. M.; Kim, H. C.; Alsema, E. *Environ. Sci. Technol*. **2008**, *42*, 2168. (d) Zweibel, K. *Science* **2010**, *328*, 699. (e) Medintz, I. L.; Uyeda, H. T.; Goldman, E. R.; Mattoussi, H. *Nat. Mater* **2005**, *4*, 435.

17. (a).Engman, L.; Stern, D.; Cotgreave, I. A.; Andersson, C. M. *J. Am. Chem. Soc*. **1992**, *114* , 9737. (b) Andersson, C.-M.; Hallberg, A.; Brattsand, R.; Cotgreave, I. A.;

Engman, L.; Persson, *J. Bioorg. Med. Chem. Lett.* **1993**, *3*, 2553. (c) Engman, L.; Stern, D.; Pelcmanl, M.; Andersson, C.-M. *J. Org. Chem.* **1994**, *59*, 1973. (d) Wieslander, E.; Engman, L.; Svensjö, E.; Erlansson, M.; Johansson, U.; Linden, M.; Andersson, C.-M.; Brattsand, R. *Biochem. Pharmacol.* **1998**, *55,* 573. (e) Mugesh, G.; Panda, A.; Kumar, S.; Apte, S. D.; Singh, H. B.; Butcher, R. J. *Organometallics* **2002**, *21*, 884. (f) McNaughton, M.; Engman, L.; Birmingham, A.; Powis, G.; Cotgreave, I. A. *J. Med. Chem*. **2004**, *47*, 233. (g) Alberto, E. E.; do Nascimento V.; Braga A. L. *J. Braz. Chem. Soc.* **2010**, *21*, 2032. (h) Yan, J.; Poon, J.-F.; Singh, V.P.; Gates, P.; Engman, L. *Org. Lett.* **2015**, *17*, 6162.

18.   Wöhler, F. *Ann. Chem*. **1840**, *35*, 11.

19.   (a) Chugaev, L; Choplin, W. Ber. **1914**, *47*, 1269; *Chem. Abstr.* **1914**, *8*, 3400. (b) Leicester, H. M. *Org. Synth.* **1943**, *2*, 238. (c) Sharp, K. W.; Koehler, W. H. *Inorg.Chem*. **1977**, *16*, 2258.

20.   Klayman, D. L.; Griffin, T. S. *J. Am. Chem. Soc*. **1973**, *95*, 197.

21.   Koketsu, M.; Nada, F.; Hiramatsu, S.; Ishihara, H. *J. Chem. Soc. Perkin Trans. I.* **2002,** 737.

22.   Gladysz, J, A.; Hornby, J. L.; Garbe, J. E. *J. Org. Chem.* **1978**, *43*, 1204.

23.   Bhasin, K. K.; Singh, J. *J. Organomet. Chem*. **2002**, *658*, 71.

24.   (a) Zingaro, R. A.; Herrera, C.; Meyers, E. A. *J. Organomet. Chem.* **1986***, 306*, C36. (b) Thompson, D. P.; Boudjouk, P. *J. Org. Chem*. **1988**, *53*, 2109. (c) Bhasin, K. K.; Gupta, V.; Gautam, A.; Sharma, R. P. *Synth. Comm.* **1990**, *20*, 2191. (d) Bhasin, K. K.; Arora, E.; Mehta, S. K.; Klapoetke, T. M. *J. Organomet. Chem.* **2011***, 696*, 835.

25.   Bhasin, K. K.; Arora, E.; Kaur, K.; Kang, S.-K.; Gobel, M.; Klapotke, T. M.; Mehta, S. K. *Tetrahedron* **2009**, *65*, 247.

26.   Alewood, P.; Muttenthaler, M.; Dekan, Z. **2011**, US WO2011/120071 A1.

27.   Satheeshkumar, K.; Raju, S.; Singh, H. B.; Butcher, R. *J. Chem. Eur. J.* **2018**, *24*, 1.

28.   Engman, L.; Stern, D.; Cotgreave, A. I.; Andersson, M. C. *J. Am. Chem. Soc*. **1992**, *114*, 9737.

29.   Kaur, R.; Singh, H. B.; Butcher, R. J. *Organometallics* **1995**, *14*, 4755.

30.   (a) Haller, W. S.; Irgolic, K. J. *J. Organomet. Chem*. **1972**, *38*, 97. (b) Mugesh, G.; Panda, A.; Kumar, S.; Apte, S. D.; Singh, H. B.; Butcher, R. J. *Organometallics* **2002,** *21*, 884. (c) Aso, Y.; Yamashita, H.; Otsubo, T.; Ogura, F. *J. Org. Chem.* **1989**, *54*, 5627.

31.   Yoshimori, Y.; Cho, C. S.; Uemura, S. *J. Organom. Chem*. **1995**, *487*, 55.

32.   Engman, L. *Organometallics* **1989**, *8*, 1997.

33.   Srivastava, K.; Shah, P.; Singh, H. B.; Butcher, R. J. *Organometallics* **2011**, *30*, 534.

34.   (a) Alcock, W. N. *Adv. Inorg. Chem. Radiochem.* **1972**, *15*, 1. (b) Bleiholder, C.; Werz, D. B.; Kölppel, H.; Gleiter, R. *J. Am. Chem. Soc.* **2006**, *128*, 2666. (c) Bleiholder, C.; Gleiter, R.; Werz, D. B.; Kölppel, H. *Inorg. Chem.* **2007**, *46*, 2249. (d) Cozzolino, A. F.; Elder, P. J. W.; Vargas-Baca, I. *Coord. Chem. Rev*. **2011**, *255*, 1426. (e) Mukherjee, A. J.; Zade, S. S.; Singh, H. B.; Sunoj, R. B. *Chem. Rev*. **2010**, *110*, 4357. (f) Pascoe, D. J.; Ling, K. B.; Cockrof, S. L. *J. Am. Chem. Soc.* **2017**, *139*, 15160. (g) Selvakumar, K.; Singh, H. B. *Chem. Sci.* **2018**, *9*, 7027.

35.   (a) Singh, A. K.; Srivastava, V. *J. Coord. Chem.* **1992**, *27*, 237. (b) Singh, A. K.; Sharma, S. *Coord. Chem. Rev.* **2000**, *209*, 49. (c) Englich, U.; Ruhlandt-Senge, K. *Coord. Chem. Rev.* **2000**, *210*, 135. (d) Briand, G. G.; Chivers, T.; Krahn, M. *Coord. Chem. Rev.* **2002**, *233-234*, 237.

36.   (a) Chadwick, S.; Englich, U.; Ruhlandt-Senge, K.; Watson, C.; Bruce, A. E.; Bruce, M. R. M. *J. Chem. Soc., Dalton Trans.* **2000**, 2167. (b) Clegg, W.; Davies, R. P.; Snaith, R.; Wheatley, A. E. H. *Eur. J. Inorg. Chem.* **2001**, 1411. (c) Englich, U.; Ruhlandt-Senge, K. *Chem. Eur. J.* **2000**, *6*, 4063 and reference therein.

37.   (a) Dabbousi, B. O.; Bonasia, P. J.; Arnold, J. *J. Am. Chem. Soc.* **1991**, *113*, 3186. (b) Ruhlandt-Senge, K.; Power P. P. *Inorg. Chem*. **1993**, *32*, 3478. (c) Tokitoh, N.; Manmaru, K.; Okazak, R.; *Organometallics* **1994**, *13*, 167. (d) Corrigan, J. F.; Fenske, D.; Power, W. P. *Angew. Chem. Int. Ed. Engl.* **1997,** 36, 1176. (e) Crespo, O.; Gimeno, M. C.; Laguna, A.; Kulcsar, M.; Silvestru, C. *Inorg. Chem.* **2009**, *48*, 4134. (f) Bhabak, K. P.; Mugesh, G. *J. Chem. Sci.* **2011**, *123*, 783. (g) Caldwell, L. M.; Hill, A. F.; Hulkes, A. G.; McQueen, C. M. A.; White, A. J. P.; Williams, D. J. *Organometallics* **2010**, *29*, 6350. (h) Lin, T. P.; Gabbaï, F. P. *Angew. Chem. Int. Ed.* **2013**, *52*, 3864. (i) Jones, J. S.; Gabbaï, F. P. *Chem. Lett.* **2016** *, 45*, 376. (j) Patel, S.; Meenakshi; Hodage, A. S.; Verma, A.; Agrawal, S.; Yadav, A.; Kumar, S. *Dalton Trans.* **2016**, *45*, 4030. (k) Cabral, B. N.; Kirsten, L.; Hagenbach, A.; Piquini, P. C.; Patzschke, M.; Lang, E. S.; Abram, U. *Dalton Trans.* **2017**, *46*, 9280.

38.   (a) Rahbarnoohi, H.; Wells, R. L.; Liable-Sands, L. M.; Yap, G. P. A.; Rheingold, A. L. *Organometallics* **1997**, *16*, 3959. (b) Grigsby, W. J.; Raston, C. L.; Tolhurst, V.-A.; Skelton, B. W.; White, A. H. *J. Chem. Soc., Dalton Trans.* **1998**, 2547. (c) DeGroot, M. W.; Corrigan, J. F.

J. Chem. Soc., Dalton Trans. **2000**, 1235. (d) Tokoro, Y.; Nagai, A.; Kokado, K.; Chujo, Y. *Macromolecules* **2009**, *42*, 2988. (e) Ding, F.; Nisbet, M. L.; Yu, H.; Zhang, W.; Chai, L.; Halasyamani, P. S.; Poeppelmeier, K. R. *Inorg. Chem.* **2018**, *57*, 7950.

39.   Stadman, T. C. *Annu. Rev. Biochem.* **1990**, *59*, 111.

40.   (a) Gulino, A.; Casarin, M.; Conticello, V. P.; Gaudiello, J. G.; Mauermann, H.; Fragalá, I.; Marks, T. J. *Organometallics* **1988**, *7*, 2361. (b) Evans, W. J.; Zucchi, Gaël.; Ziller, J. W. *J. Am. Chem. Soc.* **2003**, *125*, 10. (c) Boyle, J. T.; Ottley, M. A. L. *Chem. Rev.* **2008**, *108*, 1896. (d) Norton, K.; Kumar, G. A.; Dilks, J. L.; Emge, T. J.; Riman, R. E.; Brik, M. G.; Brennan, J. G. *Inorg. Chem.* **2009**, *48*, 3573. (e) Hou, Z.; Fujita, A.; Yoshimura, T.; Jesorka, A.; Zhang, Y.; Yamazaki, H.; Wakatsuki, Y. *Inorg. Chem.* **1996**, *35*, 7190. (f) Carpentier, J. *Organometallics* **2015**, *34*, 4175. (g) Yao, Y.; Ma, M.; Xu, X.; Zhang, Y.; Shen, Q.; Wong, W.-T. *Organometallics* **2005**, *24*, 4014. (h) Zhou, H.; Guo, H.; Yao, Y.; Zhou, L.; Sun, H.; Sheng, H.; Zhang, Y.; Shen, Q. *Inorg. Chem.* **2007**, *46*, 958. (i) Aspinall, H. C.; Tillotson, M. R. *Inorg. Chem.* **1996**, *35*, 5. (j) Annand, J.; Aspinall, H. C.; Steiner, A. *Inorg. Chem.* **1999**, *38*, 3941. (k) Blackburn, O. A.; Tropiano, M.; Natrajan, L. S.; Kenwright, A. M.; Faulkner, S. *Chem. Commun.* **2016**, *52*, 6111. (l) Artizzu, F.; Quochi, F.; Marchio, L.; Sessini, E.; Saba, M.; Serpe, A.; Mura, A.; Mercuri, M. L.; Bongiovanni, G.; Deplano, P. *J. Phys. Chem. Lett.* **2013**, *4*, 3062. (m) Thielemann, D. T.; Wagner, A. T.; Lan, Y.; Oña-Burgos, P.; Fernández , I.; Rösch, E. S.; Kölmel, D. K.; Powell, A. K.; Bräse, S.; Roesky, P. W. *Chem. Eur. J.* **2015**, *21*, 2813. (n) Chilton, N. F.; Deacon, G. B.; Gazukin, O.; Junk, P. C.; Kersting, B.; Langley, S. K.; Moubaraki, B.; Murray, K. S.; Schleife, F.; Shome, M.; Turner, D. R.; Walker, J. A. *Inorg. Chem.* **2014**, *53*, 2528. (o) Deacon, G. B.; Junk, P. C.; Leary, S. G.; Urbatsch, A. *Z. Anorg. Allg. Chem.* **2012**, *638*, 2001.

41.   (a) Mashima, K.; Nakayama, Y.; Shibahara, T.; Fukumoto, H.; Nakamura, A. *Inorg. Chem.* **1996**, *35*, 93. (b) Woodruff, D. N.; Tuna, F.; Bodensteiner, M.; Winpenny, R. E. P.; Layfield, R. A. *Organometallics* **2013**, *32*, 1224. (c) Li, H.-X.; Cheng, M.-L.; Wang, H.-M.; Yang, X.-J.; Ren, Z.-G.; Lang, J.-P. *Organometallics* ***2011, 30,*** 208. (d) Li, H.-X.; Ren, Z.-G.; Zhang, Y.; Zhang, W.-H.; Lang, J.-P.; Shen, Q. *J. Am. Chem. Soc.* **2005**, *127*, 1122. (e) Aspinall, H. C.; Bradley, D. C.; Hursthouse, M. B.; Sales, K. D.; Walker, N. P. C. *J. Chem. Soc., Chem. Commun.* **1985**, 1585. (f) Aspinall, H. C.; Cunningham, S. A. *Inorg. Chem.* **1998**, *37*, 5396. (g) Dowsland, J.; McKerlie, F.; Procter, D. J. *Tetrahedron Letters* **2000**, *41*, 4923. (h) Ma, Y.-Z.;

Bestgen, S.; Gamer, M. T.; Konchenko, S. N.; Roesky, P. W. *Angew. Chem. Int. Ed.* **2017**, *56*, 13249. (i) Konchenko, S. N.; Sanden, T.; Pushkarevsky, N. A.; Köppe, R.; Roesky, P. W. *Chem. Eur. J.* **2010**, *16*, 14278.

42.   (a) Li, H.-X.; Zhu, Y.-J.; Cheng, M.-L.; Ren, Z.-G.; Lang, J.-P.; Shen, Q. *Coord. Chem. Rev.* **2006**, *250*, 2059. (b) Kumar, G. A.; Riman, R. E.; Brennan, J. G. *Coord. Chem. Rev.* **2014**, *273-274*, 111. (c) Boncher, W.; Dalafu, H.; Rosa, N.; Stoll, S. *Coord. Chem. Rev.* **2015**, *289-290*, 279.   (d)   Nief,   F.   *Coord.   Chem.   Rev.*   **1998**,   *178-180*,   13.   (e) Freedman, D.; Melman, J.H.; Emge, T.J.; Brennan, J.G. *Inorg. Chem.* 1998, 37, 4162. (f) Lissner, F.; T. Schleid, *Z. Anorg. Allg. Chem.* **2004**, *630*, 1741. (g) Lissner, F.; Schleid, T. *Z. Anorg. Allg. Chem.* **2005**, *631*, 1119. (h) Schurz, C. M.; Talmon-Gros, P.; Lissner, F.; Schleid, T. *Solid State Sci.* **2013**, *17*, 140. (i) Lissner, F.; Schleid, T. *Z. Anorg. Allg. Chem.* **1994**, *620*, 2003.

43.   Evans, W. J.; Miller, K. A.; Lee, D. S.; Ziller, J. W. *Inorg. Chem.* **2005**, *44*, 4326.

44.   Zalkin, A.; Henly, T. J.; Andersen, R. A. *Acta Crystallogr.* **1987**, *C43*, 233.

45.   Berg, D. J.; Andersen, R. A.; Zalkin, A. *Organometallics* **1988**, *7*, 1858.

46.   Melman, J. H.; Rohde, C.; Emge, T. J.; Brennan, J. G. *Inorg. Chem.* **2002**, *41*, 28.

47.   Melman, J. H.; Emge, T. J.; Brennan, J. G. *Inorg. Chem.* **2001**, *40,* 1078.

48.   Banerjee, S.; Emge, T. J.; Brennan, J. G. *Inorg. Chem.* **2004**, *43*, 6307.

49.   Tang, Y.; Gan, X.; Tan, M.; Zheng, X. *Polyhedron* **1998**, *17*, 429.

50.   Roger, M.; Arliguie, T.; Thuéry, P.; Fourmigué, M.; Ephritikhine, M. *Inorg. Chem.* **2005**, *44*, 584.

51.   Roger, M.; Belkhiri, L.; Thuéry, P.; Arliguie, T.; Fourmigué, M.; Boucekkine, A.; Ephritikhine, M. *Organometallics* **2005,** *24,* 4940.

52.   Fitzgerald, M.; Emge, T. J.; Brennan, J. G. *Inorg. Chem.* **2002**, *41*, 3528.

53.   Freedman, D.; Emge, T. J.; Brennan, J. G. *Inorg. Chem.* **2002**, *41*, 492.

54.   Freedman, D.; Melman, J. H.; Emge, T. J.; Brennan, J. G. *Inorg. Chem.* **1998,** *37,* 4162.

55.   Taniguchi, Y.; Maruo, M.; Takaki, K.; Fujiwara, Y. *Tetrahedron Lett.* **1994**, *35*, 7789.

56.   Dowsland, J.; McKerlie, F.; Procter, D. J. *Tetrahedron Lett.* **2000**, *41*, 4923.

57.   (a) Jeske, G.; Lauke, H.; Mauermann, H.; Swepston, P. N.; Schumann, H.; Marks, T. J. *J. Am. Chem. Soc.* **1985**, *107*, 8091. (b) Watson, P. L.; Roe, D. C. *J. Am. Chem. Soc.* **1982**, *104*, 6471. (c) Watson, P. L.; Parshall, G. W. *Acc. Chem. Res.* **1985**, *18*, 51.

58.   Hou, Z.; Zhang, Y.; Tezuka, H.; Xie, P.; Tardif, O.; Koizumi, T.-a.; Yamazaki, H.; Wakatsuki, Y. *J. Am. Chem. Soc.* **2000**, *122*, 10533.

59.   Yasuda, H.; Yamamoto, H.; Yamashita, M.; Yokota, K.; Nakamura, A.; Miyake, S.; Kai, Y.; Kanehisa, N. *Macromolecules* **1993**, *26*, 713.

60.   Nakayama, Y.; Shibahara, T.; Fukumoto, H.; Nakamura, A.; Mashima, K. *Macromolecules* **1996**, *29*, 8014.

61.   Kornienko, A.; Banerjee, S.; Kumar, G. A.; Riman, R. E.; Emge, T. J.; Brennan, J. G. *J. Am. Chem. Soc.* **2005**, *127*, 14008.

62.   Kumar, G. A.; Riman, R. E.; Torres, L. A. D.; Garcia, O. B.; Banerjee, S.; Kornienko, A.; Brennan, J. G. *Chem. Mater*. **2005**, *17*, 5130.

63.   Jørgensen, C. K. *Coord. Chem. Rev*. **1966**, *1*, 164.

64.   (a) Stiefel, E. I.; Waters, J. H.; Billig, E.; Gray, H. B. *J. Am. Chem. Soc.* **1965**, *87*, 3016. (b) Holm, R.H.; Balch, A. L.; Davison, A.; Maki, A. H.; Berry, Thomas E. *J. Am. Chem. Soc.* **1967**, *89*, 2866. (c) Lalor, F.; Hawthorne, M. F.; Maki, A.t H.; Darlington, K.; Davison, A.; Gray, H. B.; Dori, Z.; Stiefel, E. I. *J. Am. Chem. Soc.* **1967**, *89*, 2278. (d) Eisenberg, R., Gray, H. B. *Inorg. Chem.* **2011**, *50*, 9741.

65.   (a) Chłopek, K.; Bothe, E.; Neese, F.; Weyhermüller, T.; Wieghardt K., *Inorg. Chem*. **2006**, *45*, 6298. (b) Khusniyarov, M. M.; Weyhermüller, T.; Bill, E.; Wieghardt, K. *Angew. Chem. Int. Ed*. **2008**, *47*, 1228. (c) Blackmore, K. J.; Joseph, N. L.; Ziller, W.; Heyduk, A. F. *J. Am. Chem. Soc.* **2008**, *130* , 2728. (d) Samanta, S.; Goswami, S. *J. Am. Chem. Soc.* **2009**, *131*, 924. (e) Janes, T.; Rawson, J. M.; Song. D. *Dalton Trans***. 2013**, *42*, 10640. (f) Munhá, R. F.; Zarkesh, R. A.; Heyduk, A. F. *Inorg. Chem.* **2013**, *52*, 11244. (g) van der Meer, M.; Manck, S.; Sobottka, S.; Plebst, S.; Sarkar, B. *Organometallics* **2015**, *34*, 5393. h) Roy, S. K.; Sengupta, D.; Rath, S. P.; Saha, T.; Samanta, S.; Goswami, S. *Inorg. Chem.* **2017**, *56*, 4966. (i) Das, A.; Ghosh, P.; Plebs, S.; Schwederski, B.; Mobin S. M.; Kaim, W.; Lahiri, G. K. *Inorg. Chem.* **2015**, *54*, 3376. (j) Ghosh, P.; Mandal, S.; Chatterjee, I.; Mondal, T. K.; Goswami, S. *Inorg. Chem.* **2015**, *54*, 6235. (k) Durgaprasad, G.; Luna, J. A.; Spielvogel, K. D.; Haas, C.; Shaw, S. K.; Daly, S.R.; *Organometallics* **2017**, *36*, 4020.

66.   Wanat, A.; Schneppensieper, T.; Stochel, G.; van Eldik, R.; Bill, E.; Wieghardt, K. *Inorg. Chem.* **2002**, *41*, 4.

67.   (a) Chen, H.; Ikeda-Saito, M.; Shaik, S. *J. Am. Chem. Soc.* **2008**, *130*, 14778. (b) Cramer, C. J.; Tolman, W. B. *Acc. Chem. Res.* **2007**, *40*, 601. (c) Schmidt, S.; Heinemann, F. W.; Grohmann, A. *Eur. J. Inorg. Chem.* **2000**, 1657. (d) Schaefer, W. P. *Inorg. Chem.* **1968**, *7*, 725. (e) Marsh, R. E.; Schaefer, W. P. *Acta Cryst.* **1968**, *B24*, 246.

68.   (a) Kaim, W.; Doslik, N.; Frantz, S.; Sixt, T.; Wanner, M.; Baumann, F.; Denninger, G.; Kümmerer, H.-J.; Duboc-Toia, C.; Fiedler, J.; Zališ, S. *J. Mol. Struct.* **2003,** *656*, 183. (b) Sarkar, B.; Patra, S.; Fiedler, J.; Sunoj, R. B. Janardanan, D.; Lahiri, G. K.; Kaim, W. *J. Am. Chem. Soc.* **2008**, *130*, 3532.

69.   (a) Bhattacharya, S.; Gupta, P.; Basuli, F.; Pierpont, C. G. *Inorg. Chem.* **2002**, *41*, 5810. (b) Kaim, W. *Coord. Chem. Rev.* **2001**, *219-221*, 463.

70.   (a) Das, D.; Mondal, T. K.; Mobin, S. M.; Lahiri, G. K. *Inorg. Chem.* **2009**, *48*, 9800. (b) Das, D.; Das, A. K.; Sarkar, B.; Mondal, T. ; Mobin, S. M.; Fiedler, J.; Zalis, S.; Urbanos, F. A.; Jimenez-Aparicio, R.; Kaim, W.; Lahiri, G. K. *Inorg. Chem.* **2009**, *48*, 11853.

71.   (a) Patra, S.; Sarkar, B.; Mobin, S. M.; Kaim, W.; Lahiri, G. K. *Inorg. Chem.* **2003**, *42*, 6469. (b) Das, D.; Sarkar, B.; Kumbhakar, D.; Mondal, T. K.; Mobin, S. M.; Fiedler, J.; Urbanos, F. A.; Jiménez-Aparicio, R.; Kaim, W.; Lahiri, G. K. *Chem. Eur. J.* **2011**, *17*, 11030. (c) DeSimone, R. E. *J. Am. Chem. Soc.* **1973**, *95*, 6238.

72.   (a) Doslik, N.; Sixt, T.; Kaim, W. *Angew. Chem., Int. Ed.* **1998**, *37*, 2403. (b) Kaim, W.; Doslik, N.; Frantz, S.; Sixt, T.; Wanner, M.; Baumann, F.; Denninger, G.; Kummerer, H. -J.; Duboc-Toia, C.; Fiedler, J.; Zalis, S. J. *Mol. Struct.* **2003**, *656*, 183.

73.   (a) Adams, H.; Morris, M. J.; Riddiough, A. E.; Yellowlees, L. J.; Lever, A. B. P. *Inorg. Chem.* **2007**, *46*, 9790. (b) Rusanova, J.; Rusanov, E.; Gorelsky, S. I.; Christendat, D.; Popescu, R.; Farah, A. A.; Beaulac, R. Reber, C.; Lever, A. B. P. *Inorg. Chem.* **2006**, *45*, 6246.

74.   Moulton, C. J.; Shaw, B. L. *J. Chem. Soc., Dalton Trans.* **1976**, 1020.

75.   (a) Morales-Morales, D.; Jensen, C. M. *The Chemistry of Pincer Compounds*; Elsevier Science B.V.: Amsterdam, Netherlands, **2007**. (b) van Koten, G.; Milstein, D. *Organometallic Pincer Chemistry*; Springer: Berlin Heidelberg, **2013**. (c) van Koten, G.; Gossage, R. A. The Privileged Pincer-Metal Platform: Coordination Chemistry & Applications; Topics in Organometallic Chemistry Series, Vol. 54; Springer: Cham, Switzerland, **2016**. (d) van Koten, G.; Gebbink, R. J. M. K. *Dalton Trans.* **2011**, *40*, 8731. (e). Zhang, H.; Lei, A. *Dalton Trans.*

2011, *40*, 8745. (f) Mazzeo, M.; Strianese, M.; Kühl, O.; Peters, J. C. *Dalton Trans*. **2011**, *40*, 9026. (g) Peris, E.; Crabtree, R. H. *Chem. Soc. Rev.* **2018**, *47*, 1959 and reference therein.

76.   (a) van der Boom, M. E.; Liou, S.-Y.; Ben- David, Y.; Shimon, L. J. W.; Milstein, D. *J. Am. Chem. Soc*. **1998**, 120, 6531. (b) van der Boom, M. E.; Liou, S.-Y.; Ben- David, Y.; Gozin, M.; Milstein, D. *J. Am. Chem. Soc.* **1998**, *120*, 13415. (c) Vigalok, A.; Milstein, D. *Organometallics* **2000**, *19*, 2341.

77.   Beley, M.; Collin, J.-P.; Sauvage, J.-P. *Inorg. Chem.* **1993**, *32*, 4539.

78.   (a) Grove, D. M.; van Koten, G.; Ubbels, H. J. C.; Zoet, R. *Organometallics* **1984**, *3*, 1003. (b) van de Kuil, L. A.; Luitjes, H.; Grove, D. M.; Zwikker, J. W.; van der Linden, J. G. M.; Roelofsen, A. M.; Jenneskens, L. W.; Drenth, W.; van Koten, G. *Organometallics* **1994**, *13*, 468.

79.   Hernández-Juárez, M.; Vaquero, M.; Álvarez, E.; Salazar, V.; Suárez, A. *Dalton Trans.* **2013**, *42*, 351.

80.   Liu, X.; Pattacini, R.; Deglmann, P.; Braunstein, P. *Organometallics* **2011**, *30*, 3302.

81.   (a) Bauer, G.; Hu, X. *Inorg. Chem. Front*. **2016**, *3*, 741; and reference therein. (b) Selander, Ni.; Szabó K. J. *Chem. Rev.* **2011**, *111*, 2048; and reference therein. (c) Gunanathan, C.; Milstein, D. *Chem. Rev.* **2014**, *114*, 12024; and reference therein. (d) Asay, M.; Morales-Morales, D. *Dalton Trans*. **2015**, *44*, 17432. (e) Urgoitia, G.; SanMartin, R.; Herrero, M. T.; Domínguez, E. *Green Chem*. **2011**, *13*, 2161. (f) Morales-Morales, D. *Rev. Soc. Quím. Méx*. **2004**, *48*, 338. (g) Benito-Garagorri, D.; Kirchner, K. *Acc. Chem. Res.* **2008**, *41*, *2*, 201; and reference therein. (h) Choi, J.; MacArthur, A. H. R.; Brookhart, M.; Goldman, A. S. *Chem. Rev.* **2011**, *111*, 1761; and reference therein.

82.   Albrecht, M.; van Koten, G. *Angew. Chem. Int. Ed.* **2001**, *40*, 3750.

83.   Tu, T.; Fang, W.; Bao, X.; Li, X.; Dötz, K. H. *Angew. Chem. Int. Ed.* **2011**, *50*, 6601

84.   Prokhorov, A. M.; Hofbeck, T.; Czerwieniec, R.; Suleymanova, A. F.; Kozhevnikov, D. N.; Yersin, H. *J. Am. Chem. Soc.* **2014**, *136*, 9637.

85.   Hall, J. R.; Loeb, S. J.; Shimizu, G. K. H.; Yap, G. P. A. *Angew. Chem., Int. Ed.* **1998**, *37*, 121.

86.   (a) Banfield, J. *J. Org. Chem.* **1960**, *25*, 300.; (b) Corsini, A.; Fernando, Q.; Freiser, H. *Anal. Chem.* **1963**, *35*, 1424.; (c) Dalziel, J. A. W.; Kealey, D. *Analyst*. **1964**, *89*, 411.; (d) Henkel, G.; Krebs, B.; Schmidt, W. *Angew. Chem. Int. Ed.* **1992**, *31*, 1366.

87.   (a) Huang, J.-H.; Kuo, P. -C.; Lee, G. -H.; Peng, S. –M.; *J. Chin. Chem. Soc.* **2000,** *47,* 1191.; (b) Kuo, P. -C.; Huang, J.-H.; Hung, C. –H.; Lee, G. -H.; Peng, S. –M. *Eur. J. Inorg. Chem.* **2003**, 1440.; (c) Banerjee, S.; Shi, Y.; Cao, C.; Odom, A. L. *J. Organomet. Chem.* **2005**, *690*, 5066.; (d) Maaß, C.; Andrada, D. M.; Mata, R. A.; Herbst-Irmer, R., Stalke, D. *Inorg. Chem.* **2013**, *52*, 9539.; (e) Vránová, I.; Jambor, R.; Růžička, A.; Hoffmann, A.; Herres-Pawlis, S.; Dostál, L. *Dalton Trans.* **2015**, *44*, 395.

2

Facile Synthesis of Monomeric Lanthanide Chalcogenolates from 2-(dimethylamino)methyl)phenyltellurolate and Quinoline-8-tellurolate Ligands

2.1 Introduction

The lanthanoid metals are regarded as hard metal centers and subsequently their chemistry has been dominated by hard donor ligands like ethers, amines, amides, *etc*. However, there have been considerable concerns in recent years for the preparation of complexes containing soft donor ligands, in particular with those of group 16. This is driven in part not only due to their promising technological interests but also from inquisitiveness to improve the understanding of such unconventional hard-soft interactions.

In fact, over the past few decades there have been a meteoric rise in the design and synthesis of lanthanoid chalcogenolates due to their appealing variety of architectures, fascinating structural chemistry and prospective applications in various aspects such as magnetism,[1] catalysis,[2-3] optics, and electronics.[4-5] However, the chemistry of this class of compounds remains somewhat dormant due to some intrinsic characteristics of lanthanoid ions; such as the high and variable coordination numbers and the extreme oxophilicity of the resulting complexes. Most often, lanthanoid chalcogenolates were prepared either by the oxidative reactions of dichalcogenides (REER) with lanthanoid(II) complexes[6] or by reaction of Ln/M amalgam with REER and trans-metallation reactions,[7-8] or by reactions of lanthanoid chalcogenolates with elemental chalcogen, E (E = S/ Se/ Te).[9-10] A detailed literature study on the synthesis of organolanthanoid chalcogenolate complexes is included in Chapter 1. It is worth mentioning that, most of the synthetic protocols for organolanthanoid chalcogenolate complexes afforded clusters or polymeric lanthanoid chalcogenolate complexes. Complexes like $[(C_5Me_5)_2Sm(\mu\text{-}EPh)]_2$ (E=S, Se, Te),[11] $(py)_8Yb_4Se_4(SePh)_4$,[12] $(THF)_8Ln_8Se_6(SePh)_{12}(Ln=Sm)$,[13] $[Sm_7S_7(SePh)_6(DME)_7][Hg_3(SePh)_7]$,[14] $[(THF)_3Eu(TeC_6H_5)_2NaTePh]_\infty$[15] are among some notable examples. Another important class of lanthanoid chalcogenolates is multinary lanthanoid chalcogen complexes. These multinary lanthanoid chalcogen complexes have gained significant attention with respect to their synthesis, diverse structural features and applications.[16] Flux method has been used for the synthesis of most of these multinary lanthanoid chalcogen complexes where all the reactants are heated at elevated temperature using a suitable flux. From structural point of view, the compounds show a wide range of structural features that can be described by the packing of metal-chalcogen polyhedra. In particular, in most of the lanthanoid nitride derivatives, the $[NLn_4]^{9+}$ unit behaves as fundamental building block, which can eventually condense in multiple ways giving rise to a variety of structures. For example, three

different crystal structures are observed in ternary compound of the form $Ln_4N_2S_3$ (Ln = La-Nd, Sm); the compound $Sm_2N_2S_3$ consists of $[NLn_4]^{9+}$ unit,[17] whereas, bitetrahedra $[N_2Ln_6]^{12+}$ is the main structural composition for the early lanthanoids (Ln = La-Nd).[18] An Additional layered arrangement of the $[NLn_4]^{9+}$ unit is observed in the case of $La_2N_2S_3$ and $Pr_2N_2S_3$.[19] Another important class of compounds which have recently attracted significant attention from the perspective of their synthesis as well as topological features is salt-inclusion solids wherein covalent metal oxide frameworks created voids which are filled by ionic salt lattice.[20-22] Compounds with such combination of both covalent and ionic sublattices are quite unconventional, which eventually makes their synthesis very challenging. Lanthanoid (III) chloride oxotellurate (IV), such as $Na_2Lu_3I_3[TeO_3]_4$,[20] $Cs_7Sm_{11}Cl_{16}[TeO_3]_{12}$, $Rb_7Nd_{11}Br_{16}[TeO_3]_{12}$[21] and $Na_2Ln_3Cl_3[TeO_3]_4$ (Ln = Sm, Eu, Gd, Tb, Dy, and Ho)[22] are some examples, wherein the molecular structures of the compounds contain cavities created by the Ln−O and M−(O, Cl) (M=Na, Cs, Rb) bonds, which are eventually filled by Te^{4+} cation.

Synthesis of monomeric organolanthanoid chalcogenolate complexes is always a challenging topic for the researchers especially due to the high affinity of Ln metals towards higher coordination number. Generally, the synthesis of monomeric lanthanoid chalcogenolates is achieved by using two approaches: using sterically demanding auxiliary ligands and by incorporating chelating ligands. For example, mononuclear bis(cyclopentadienyl)lanthanoid alkoxide complexes, $(C_5H_5)_2Ln(THF)(OR)$ [Ln =Nd, Sm, Yb; R=2,4,6-tris(trifluoromethyl)phenyl] **2.1-2.3** were prepared by reacting sterically bulky ligand, namely 2,4,6-tris(trifluoromethyl)phenol with $(C_5H_5)_3Ln$ (Ln=Nd, Sm, Yb) (Figure 2.1).[23] Similarly, reaction of elemental Sm with 1,3,5,7-cyclooctatetraene, HMPA and a bulky disulfide ligand afforded monomeric samarium(III) complex **2.4** with formula $(\eta^8\text{-}C_8H_8)Sm(SR)L_x$, where R= 2,4,6-triisopropylphenyl and L=HMPA, hexamethylphosphoramide.[24] Here, HMPA and the bulky thiolate groups play a decisive role in acquiring the mono-nuclearity of resulting complex. Similarly, treatment of $Yb[N(SiMe_3)_2]_2$ with bulky thiol, HSAr*, Ar*= 2,6-$Trip_2C_6H_3$ (Trip = 2,4,6-$^iPr_3C_6H_2$) yielded the monomeric ytterbium(II) thiolate complex $Yb(SAr^*)_2$, **2.5**. Here, steric saturation of the ytterbium center is achieved by $\eta^6\text{-}\pi$-coordinations of two flanking arene rings.[25] Similar π-encapsulated Nd or Pr selenolate complexes, **2.6-2.7** of the same ligand have also been reported.[26] The unique structural features in those complexes are Yb$\cdots\eta^6$-π-interactions between Yb and two *ortho*-2,4-6-triisopropylphenyl rings of the terphenyl groups,

wherein both terphenyl selenolate ligands are orientated in such a way that the most favorable η^6-π-arene interactions are obtained.

2.1 Ln = Nd
2.2 Ln = Sm
2.3 Ln = Yb

2.4

2.5

2.6 Ln = Nd
2.7 Ln = Pr
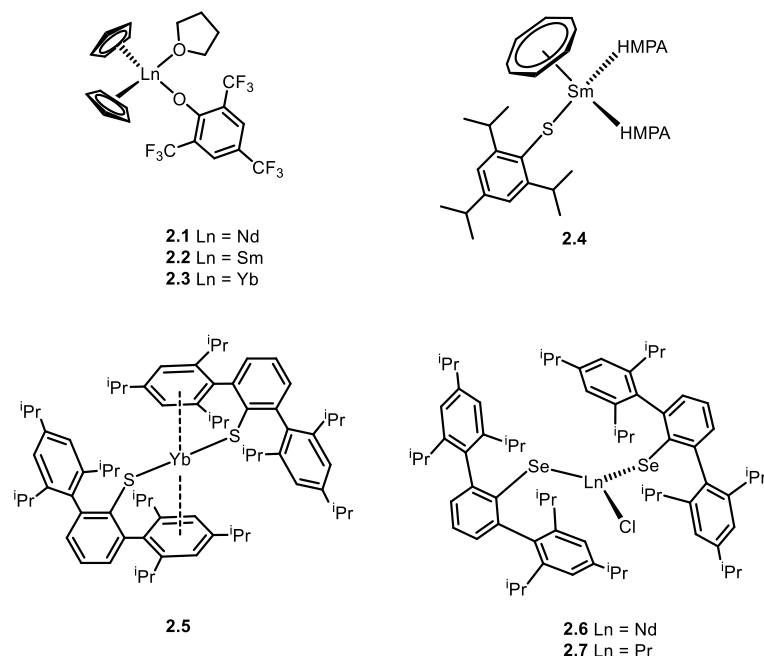
Figure 2.1. Representative monomeric lanthanoid chalcogenolates **2.1**-**2.7** using sterically demanding ligands approach.

Another successful approach for the synthesis of monomeric lanthanoid chalcogenolates is achieved by featuring chelating ligands. One such example is imidodiphosphinochalcogenido anion, $[N(EPPh_2)_2]^-$ where E =S, Se can offer two different coordination modes [η^3 or η^2; Figure 2.2(a) and 2.2(b) respectively] to bind to tris(cyclopentadienyl)lanthanoid, Cp_3Ln (Ln = La, Gd, Yb), thereby affording mononuclear lanthanoid complexes of the form $Cp_2Ln[N(EPPh_2)_2]$, **2.8**-**2.12** [Figure 2.2(c)].[27] From the solid-state structures of the complexes it is observed that early and middle lanthanoids (La, Gd) accommodated η^3-coordination from the ligand, whereas the ligand provided η^2-coordination to the late and smaller Yb centre.
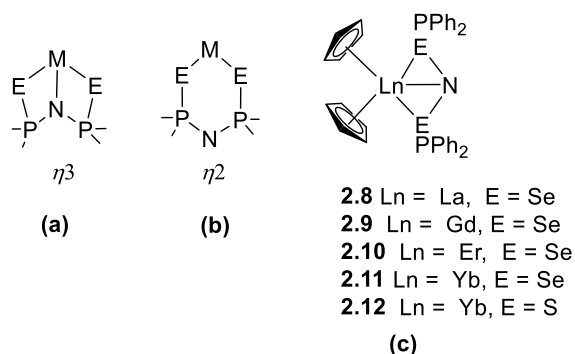
Figure 2.2: (a) η^3 coordination mode of [N(EPPh$_2$)$_2$]$^-$ ligand (b) η^2 coordination mode of [N(EPPh$_2$)$_2$]$^-$ and (c) monomeric lanthanoid chalcogenolate complexes, **2.8-2.12.**

It is worth noting that the early work in monomeric lanthanoid chalcogenolate was mostly dominated by complexes supported by cyclopentadienyl type donors of varying substitutions and modifications. However, there have been consistent attempts to design some other ancillary ligands as alternatives to the ubiquitous cyclopentadienyl ligands. For example, considerable steric congestion offered by heteroallylic ligands *viz*. benzamidinate anion, [RPhC(NSiMe$_3$)$_2$]$^-$ or Tp^{Me,Me} = tris-3,5-dimethylpyrazolylborate proved to be successful in attaining the mono-nuclearity of the resulting lanthanoid chalcogenolate complexes. For example reaction of YbI$_2$(thf)$_2$ with *N,N'*-bis-(trimethylsilyl)benzamidinates afforded ytterbium(II)benzamidinate, [PhC(NSiMe$_3$)$_2$]$_3$Yb. Subsequent reaction of [PhC(NSiMe$_3$)$_2$]$_3$Yb with diphenyldiselenide resulted in reductive cleavage of Se−Se bond to afford complex [PhC(NSiMe$_3$)$_2$]$_2$Yb(SePh)(THF), **2.13** [Figure 2.3(a)].[28] Similarly, when [Sm(Tp^{Me,Me})$_2$] was treated with diphenyldichalcogenide, the reductive cleavage of chalcogen-chalcogen bond afforded monomeric isoleptic complexes [Sm(Tp^{Me,Me})$_2$ER], E = S/Se/Te, R=Ph, **2.14-2.16** [Figure 2.3(b)].[29] Here, the coordination environment around the heptacoordinated Sm centre is occupied by one chalcogenolate ligand and two pyrazolylborates ancillary ligands in η^3-fashion. From the molecular structures of the complexes, it was observed that there was a significant distortion of pyrazolylborate ligands away from C_3 symmetry. This arises from the twisting of individual pyrazolylborate ligand around the B−N bond. The twisting played crucial role in obtaining an effective π-stacking of the phenyl group with one pyrazolyl ring. It is noteworthy that the π-stacking suffices the coordination environment of the samarium chalcogenolate complexes to attain their mono-nuclearity.
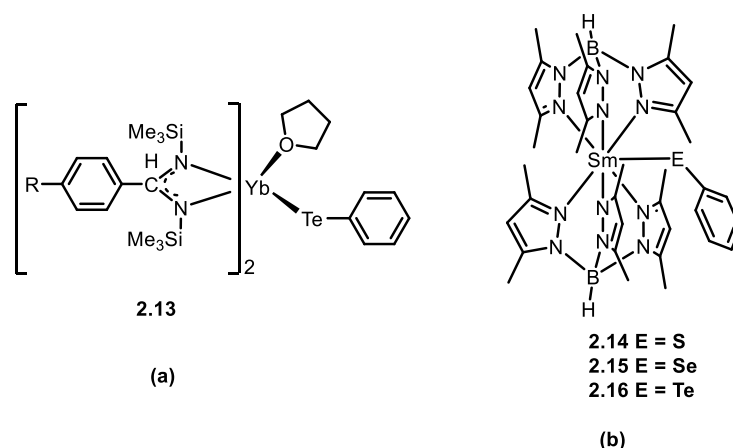
Figure 2.3. Representative examples of monomeric lanthanoid complexes **2.13**-**2.14** using alternatives of Cp ancillary ligands.

2.1.1 Influence of metal, chalcogen and solvents on nuclearity of lanthanoid chalcogenolates

Although steric demands of the ancillary ligands or the chelation play an imperative role in determining the mono-nuclearity of lanthanoid complexes, the roles of ionic radii of the metal and of E and R of the chalcogenolate ligand and nature of the solvent molecules also have significant influence on it. Brennan and co-workers have systemically investigated the role of metal on the nuclearity of the complexes and found that in case of lanthanoid benzenethiolates and selenolates, the possibility of oligomerization increases with the increase in size of the metal.[30] This trend is best illustrated in the case of benzeneselenolate compounds, where the small metal Er gives mononuclear complexes of the type $(THF)_3Er(SePh)_3$, **2.17** (Figure 2.4). On the other hand, Sm affords dimeric complexes $[(py)_3Sm(SePh)_3]_2$, **2.18** (Figure 2.4) and early lanthanoid Nd affords polymeric $[(THF)_4Nd_3(SePh)_9]_n$, **2.19** (Figure 2.4).
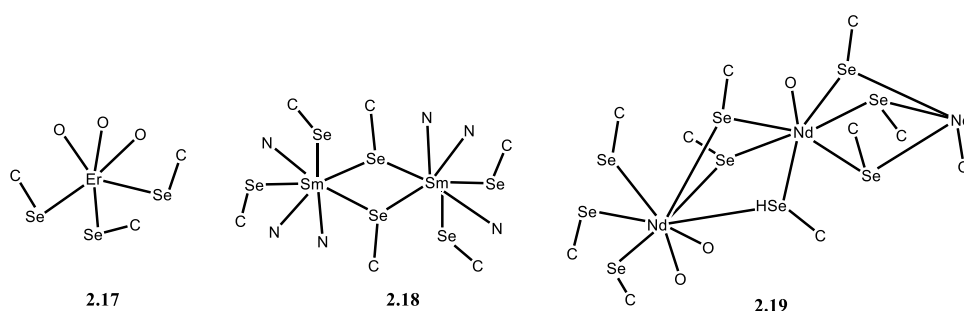
Figure 2.4. Effect of the metal size on nuclearity of lanthanoid complexes; smaller metal (Er) prefers mono-nuclearity while larger Nd tends to form polymer.

Like lanthanoid metals, the nature of chalcogen elements clearly has influences on the aggregation. For instance, the smaller and more electronegative SPh ligand is a stronger donor towards Ln ions in comparison to the larger and less electronegative SePh ligand. Consequently S has greater tendency for bridging than the higher congeners. This can be best observed in case of trivalent lanthanide chalcogenolate complexes, where $Ln(SPh)_3$ complexes are sparingly soluble in THF while $Ln(SePh)_3$ complexes are considerably more soluble. Steric properties of chalcogenolates also have prominent influences on the structure of the lanthanoid chalcogenolates, especially in terms of secondary coordination sphere interactions. In case of benzenethiolate and benzeneselenolate, it is apparent from the acute Ln-E-C(Ph) angles (Figure 2.5) that the ligand-ligand repulsion will be significantly reduced with the increase in chalcogen size. Consequently, the possibility of higher coordination number of the complexes increases with the increase in chalcogen size. This effect can be best illustrated taking divalent $Ln(EPh)_2$ as examples, where, smaller chalcogens (S, Se) resulted in octahedral complexes $(py)_4Yb(EPh)_2$ (E=S, Se), **2.20-2.21**; whereas with Te a pentagonal bipyramidal complex $(py)_5Yb(TePh)_2$, **2.22** was obtained.

2.20 E = S
2.21 E = Se

2.22
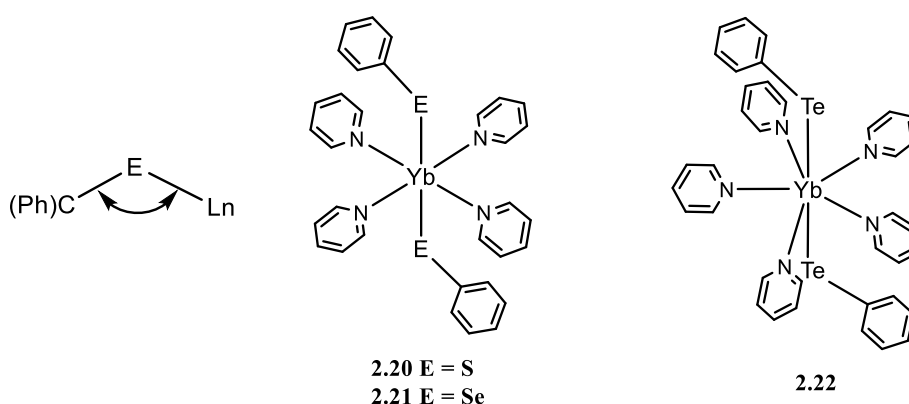
Figure 2.5. Effect of chalcogen size on the coordination number and geometry, where EPh (E = S, Se) afforded hexacoordianted complex and TePh afforded heptacoordianted complex.

Similarly, the nature of solvent also plays important role on nuclearity of the resulting lanthanoid complexes. In comparison to THF, the more basic pyridine displaces the bridging chalcogenolates more efficiently to form less extended structures. For example, while comparing the molecular structures of $[(THF)_4Sm_3(SePh)_9]_n$ and $[(py)_3Sm(SePh)_3]_2$, it is observed that in

case of weaker THF donor, Sm(SePh)$_3$ crystallizes as a one-dimensional polymer [(THF)$_4$Sm$_3$(SePh)$_9$]$_n$ with six bridging selenolates per one Sm(III) ion. On the other hand, the bridging interactions was significantly disrupted by stronger pyridine donor and a structure with only two bridging benzeneselenolates per one Sm metal is observed in [(py)$_3$Sm(SePh)$_3$]$_2$.[31] This effect also becomes apparent from the greater solubility of Ln(SPh)$_3$ in pyridine relative to THF.

2.2 Objectives

As discussed in Chapter 1, Intramolecular Chalcogen Bonding (IChB) interactions or simply secondary bonding interactions play significant roles in stabilising organochalcogen derivatives. These intramolecular interactions have found usage in the literature for the isolation of monomeric metal chalcogenolates.[32] For example, Brennan and co-workers have reported the synthesis of a series of metal selenolates/thiolates complexes using the pyridineselenolate ligand where the coordination from the pyridine nitrogen atoms played significant role in the stability of the complexes.[32f] More recently, Mugesh *et al.* have reported the isolation of monomeric group 12 metal (Zn, Cd, Hg) chalcogenolates (S, Se, Te) with the help of intramolecular secondary bonding interactions, which otherwise have tendency to form polymers through bridging by the chalcogenolate ligands.[32g-i] In particular, they have reported the synthesis of homoleptic Zn(II), Cd(II) and Hg(II) chalcogenolates incorporating the intramolecularly chelating oxazoline ligands by the metathesis reaction of OxE$^-$Li [Ox = 2-(4,4-dimethyl-2-oxazolinyl)benzene; E = S/Se/Te] with corresponding metal salts. In the complexes, the oxazoline rings from the side arms offered chelation to the metal centre, thereby resulting in mono-nuclearity of the complexes. However, to best of our knowledge, such kind of hybrid, IChB stabilized multidentate ligands containing 'soft' chalcogen atom and 'hard' N atom have not been used for the isolation of monomeric lanthanoid complexes. Hence, in the present chapter, it was envisaged to explore the reaction of IChB stabilised ditellurides namely, bis[2-(dimethylamino)methyl]phenyl]ditelluride, and 8,8'-diquinolyl ditelluride with lanthanoids. It is believed that the donor nitrogen atoms from the auxiliary arms, which were involved in secondary bonding interactions with tellurium (N···Te), would act as chelating arms to the metal centres, thereby resulting in the formation of monomeric lanthanoid metal complexes. It was further planned to get a detailed insight into the structural aspects of the complexes, especially with respect to the bonding between the hard Ln centres and the soft Te atoms.

2.3 Results and discussion

The ditelluride, bis[2-((dimethyl1amino)methyl)phenyl] ditelluride, **2.23** was synthesized following the reported procedure.[33a] Treatment of *N,N*-dimethylbenzylamine with *^{n}*BuLi followed by the addition of tellurium powder and subsequent oxidative workup afforded bis[2-((dimethyl1amino)methyl)phenyl] ditelluride, **2.23** (Scheme 2.1).

2.23
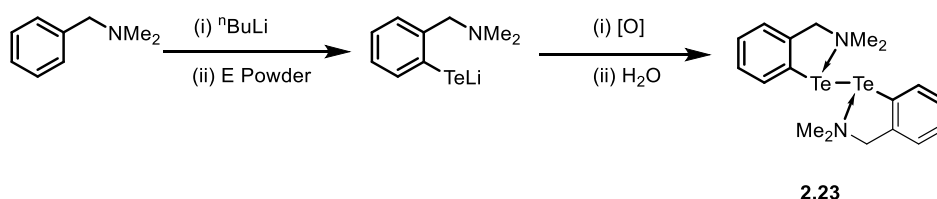
Scheme 2.1. Synthesis of bis[2-(dimethylamino)methyl)phenyl]ditelluride, **2.23**.

8,8'-Diquinolyl ditelluride, **2.24** was synthesized by reacting 8-bromoquinoline with disodium ditelluride, Na_2Te_2. 8-Bromoquinoline was first synthesizes by modified Skraup reaction wherein 2-bromoaniline was treated with glycerol and *meta*-nitrobenzenesulfonic acid sodium salt in the presence of methanesulfonic acid and ferrous sulphate hexahydrate.[33b] When 8-bromoquinoline was treated with *in situ* generated Na_2Te_2, it afforded 8,8'-diquinolyl ditelluride, **2.24** (Scheme 2.2).

1.24
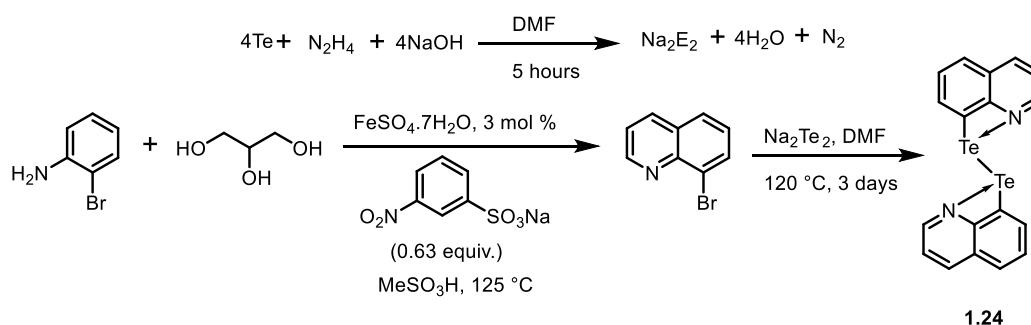
Scheme 2.2. Synthetic route for 8,8'-diquinolyl ditelluride, **2.24**.

Both ditellurides **2.23** and **2.24** were characterized by ^1H, ^{13}C and ^{125}Te NMR spectroscopy, where the NMR spectra of **2.23** matched well with the literature values.[33a] In particular, in the ^1H spectrum of **2.23**, the chemical shifts in the region 6.9-8.0 ppm correspond to the aromatic protons. The NMR resonance at 3.5 and 2.3 ppm were assigned to 'methine' and 'methyl' protons respectively. In the ^{125}Te NMR spectrum of **2.23**, a single peak was observed at

353.2 ppm. In the ^{1}H spectrum of **2.24**, six discrete resonances were observed in the aromatic region (7.3 – 9.0 ppm) corresponding to six protons of the quinoline ring. The ^{125}Te chemical shift was observed at 220 ppm, which is significantly shielded with respect to **2.23**. The upfield shift of ^{125}Te in **2.23** might be attributed to weaker Te···N interaction as compared to **2.24**.

When bis[2-(dimethylamino)methyl)phenyl]ditelluride, **2.23** was reacted with Eu metal in acetonitrile or THF, reduction of the Te-Te bond took place and the reaction afforded monomeric lanthanoid complexes of the form Eu(TeR)$_2$(Solv)$_2$ [R=2-(Me$_2$NCH$_2$)C$_6$H$_4$] (Solv=THF/acetonitrile) , **2.25-2.26** (Scheme 2.3). Similarly, the reaction of Yb metal with **2.23** in THF/pyridine afforded the isostructural complexes Yb(TeR)$_2$(Solv)$_2$ (Solv=THF/pyridine), **2.27-2.28.** It is worth mentioning that the surfaces of Yb metal needed to be activated by a drop of Hg^0 prior to the reaction with ditellurides. However, Eu being more reactive does not require activation by Hg^0.
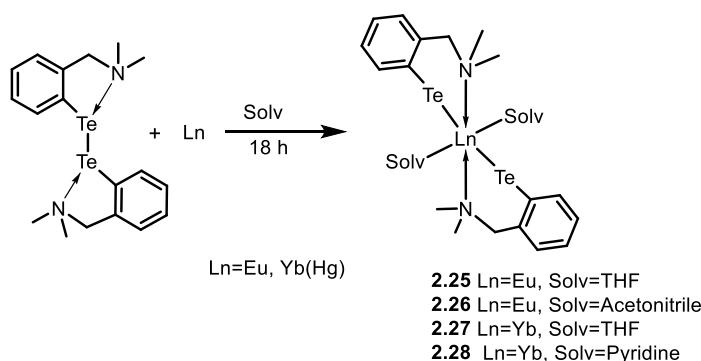
Scheme 2.3. Synthesis of lanthanoid complexes of 2-(dimethylamino)methyl)phenyl tellurolate ligand, **2.25-2.28.**

The same observation was also made in the reaction of 8,8'-diquinolyl dichalcogenide, **2.24** with lanthanoid metals, wherein Ln undergoes similar oxidative addition to give divalent, monomeric complexes of the form [Ln(ENC$_9$H$_{12}$)$_2$(Solv)$_n$] (Ln=Eu,Yb, E=Te, Solv=THF, DME), **2.29-2.30** (Scheme 2.4). However, unlike the earlier cases where 2-(dimethylamino)methyl)phenyl tellurolate ligand yielded hexacoordinated lanthanoid complexes (**2.25-2.28**), in case of the quinoline-8-tellurolate, a significant difference in coordination number of the resulting complexes was observed as evident from their molecular structures. For instance, in THF as solvent, it resulted in the isolation of heptacoordinated complex, [Eu(TeNC$_9$H$_6$)$_2$(THF)$_3$], **2.29**

where two quinoline moieties occupied four coordination sites and three coordination sites were occupied by THF molecules. On the other hand, in solvent DME, the coordination from two tellurolate ligand and two DME molecules resulted in octacoordinated complex, [Eu(TeNC$_9$H$_6$)$_2$(DME)$_2$], **2.30**. The formation of high coordination number complexes in case of the quinoline-8-tellurolate ligand is attributed to the fact that, herein, unlike 2-(dimethylamino)methyl)phenyl tellurolate ligands, the quinoline moieties with their rigid aromatic ring occupy one side of the Ln metal, which consequently leave enough spaces for three THF (or tow DME) molecule to sit around Ln.
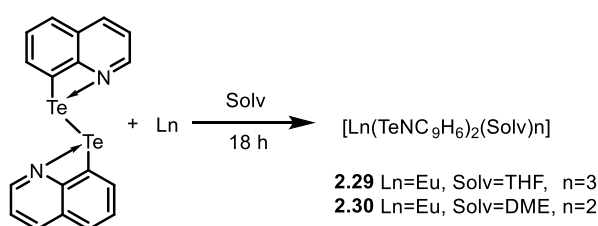
Scheme 2.4. Ln complexes of quinoline-8-tellurolate ligand, **2.29-2.30**

Interestingly, when the reaction of 8,8'-diquinolyl ditelluride, **2.24** was performed with Yb metal in DME at slightly harsh condition i.e. at 50 °C, the reaction took a different course and resulted in the formation of complex **2.31**(Scheme 2.5). In particular, one of the methoxy C−O bonds of the DME molecule underwent cleavage resulting in the formation of a 2-methoxethanonolate ligand, which eventually acts as bridging ligand to give rise to a Yb(III) complexes of the form [Yb(TeNC$_9$H$_{12}$)$_2$(μ-OCH$_2$CH$_2$OMe)]$_2$. Here, each Yb is heptacoordinated where two quinoline moieties occupy four coordination sites on each Yb molecule and rest of the three coordinations were satisfied by bridging methoxythanonolate ligand. Although, there is no dearth of literature reports regarding metal complexes bridged by methoxythanonolate ligand as the latter can be easily obtained by simple deprotonation of 2-methoxyethanol,[34] however only a few reports are available for transition/lanthanoid metal facilitated formation of methoxyethanolate ligand by the activation of DME molecule.[35] Nevertheless, the cleavage of solvent molecule such as THF during coordination to a lanthanoid metal is well documented in the literature and considered to be an interesting phenomenon.[36]
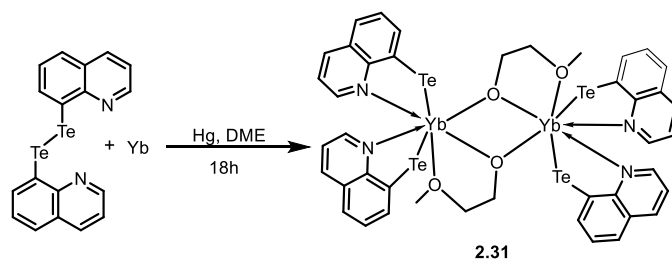
Scheme 2.5. DME bridged Yb complexes of quinoline-8-tellurolate ligand, **2.31.**

Due to the paramagnetic nature of the Eu complexes, hydrolysis NMR has been carried out by using triflic acid in D_2O and C_6D_6. It is worth noting that when lanthanoid tellurolate was hydrolysed in acidic medium, first it gave tellurol (RTe-H). The tellurol, being very unstable in acidic medium can undergo several competing reactions, such as oxidation to give ditelluride, telluroester, telluroxide etc. Liberation of elemental tellurium from the reaction is also expected in acidic medium. Consequently, hydrolysis NMR cannot be unambiguously used for the characterizations of the complexes. Nevertheless, the peaks corresponding to the ligands can be observed in the hydrolysed spectra along with the other peaks. Again, the Yb complexes were found to be extremely sensitive in nature, the crystals immediately turn black indicating its decomposition once it was removed from the mother liquor. This might be due to the de-solvation of the complex. Addition of dry THF from outside or any deuterated solvent does not re-dissolve the complexes, which in turn precluded the precise characterization of the complexes, **2.27-2.28, 2.31** by NMR studies. The percentage of metal has been determined by metal analyses which are carried out by titration of HCl-digested samples against Na_2H_2EDTA in hexamine-buffered solution with xylenol orange indicator. The metal percentages were found to be in agreement with the calculated values.

2.4 Structural studies

All samples were coated in viscous oil and mounted in a cryostream using the MX1 and MX2 macromolecular beamlines at the Australian Synchrotron, where the data and integration were completed by Blu-ice[37] and XDS[38] software programs, respectively. Structural solutions were obtained by Direct methods[39] and refined using full matrix least-squares methods against F2 using SHELX97[39] within the OLEX 2[40] interface

The molecular structure of **2.24** is shown in the Figure 2.6. Single crystals of 8,8'-diquinolyl ditelluride, **2.24** were obtained by slow evaporation from diethyl ether solution. It crystallises in triclinic fashion with space group *P-1*. The Te1–Te1A distance is found to be 2.710(12) Å. This distance is close to that of the Te–Te distance of reported for bis(2-naphthyl) ditelluride [2.7179(6) Å].[41] The Te–C bond lengths [Te1–C1 2.145(11) Å, Te1A-C1A 2.099(9) Å] correspond to typical Te–C single bond as suggested by Pauling (2.14 Å).[42a] The tellurium–nitrogen interatomic distances [N(1)···Te(1) 2.985(8) Å, N1A–Te1A 2.980(8) Å,] are larger than the sum of their covalent radii (2.70 Å)[42a-b] but are much shorter than the sum of the van der Waals radii for tellurium and nitrogen (3.65 Å).[42c] Consequently, the quinoline nitrogen is involved in strong secondary bonding interactions with the Te atom. However, the N···Te distances in compound **2.24** is significantly shorter as compared to compound **2.23** [2.903 Å and 2.848 Å].[41b] This observation correlates with the respective [125]Te NMR spectra of the compounds **2.23** and **2.24**, as a stronger secondary bonding interaction is expected to cause downfield shift of the [125]Te NMR resonance.
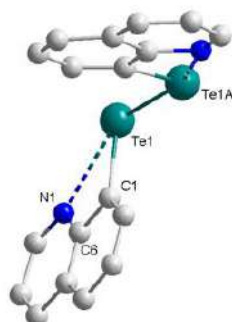
Figure 2.6. Molecular structure of 8,8'-diquinolyl ditelluride, **2.24**. Ellipsoids shown at 50% probability, hydrogen atoms removed for clarity

The molecular structures of Eu complexes of 2-(dimethylamino)methyl)phenyl tellurolate ligand, **2.25-2.26** are shown in the Figure 2.7. A comparative study of the selected bond lengths and bond angles of the complexes are listed in Table 2.1. In both these complexes, the six-coordinated lanthanoid metal atom sits on a crystallographically imposed center of inversion, containing two 2-(dimethylamino)methyl)phenyltellurolate ligands in *trans* arrangement. Each 2-(dimethylamino)methyl)phenyltellurolate ligand fills two coordination sites, one from the tellurium and the other from the nitrogen atom; both these atoms are involved in the formation of a six membered chelating ring to the metal. The rest of the two coordination sites around the

divalent metal centre are occupied by two solvent molecules. Both the complexes are isostructural where the geometry around the Ln metal centre is octahedral, both the tellurolate ligands occupying the *trans* position with the angle Te-Eu-Te1=180°, N–Eu–N1=180° and D–Eu–D1=180° (where D = donor atom of the solvent molecule). The nitrogen donor atom of tellurolate ligand furnishes an N1−Ln −Te1 bite angle of close to 90° in both cases (Table 1.1). In the molecular structure of the complexes **2.25** and **2.26**, of particular interest is the Eu−Te distance 3.2576(13) Å and 3.2258(8) Å respectively. This distance is significantly shorter as compared to the reported Eu−Te distance observed in the 1D polymer of [(THF)$_2$Eu(TeC$_6$H$_5$)2]$_\infty$ [3.335(2)-3.359(2)],[15] which is expected as in the latter Eu metals are bridged through Te atoms resulting in lengthening of the Eu−Te bond distance. However, the absolute Eu−Te bond distance in complexes **2.25** and **2.26** cannot accurately be explained by Shannon's radii, as the predicted value (3.37Å) is significantly longer than the value observed experimentally.[43]

2.25   **2.26**
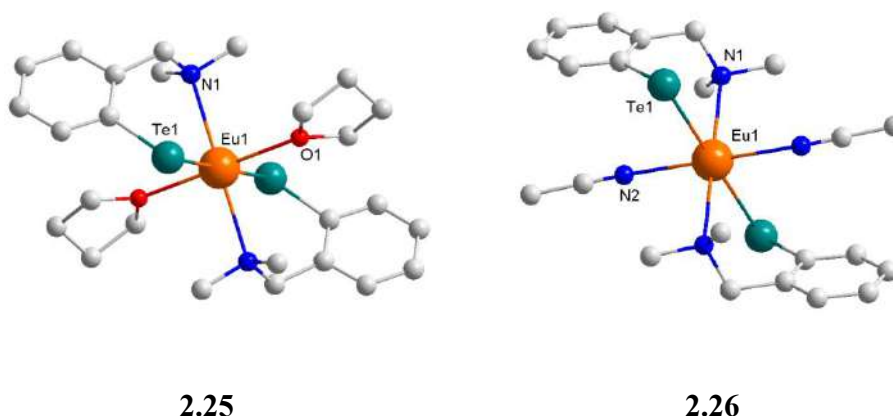
Figure: **2.7.** Molecular structure of [Eu(TeNC$_9$H$_{12}$)$_2$(THF)$_2$], **2.25**. and [Eu(TeNC$_9$H$_{12}$)$_2$(THF)$_2$] **2.26**. Ellipsoids shown at 50% probability, hydrogen atoms removed for clarity

In cases of the molecular structures of ytterbium tellurolate complex [Yb(TeNC$_9$H$_{12}$)$_2$(THF)$_2$] **2.27** and [Yb(TeNC$_9$H$_{12}$)$_2$(pyridine)$_2$] **2.28** (Figure 2.8), the Yb−Te distances are found to be 3.1611(12) and 3.1535(6)Å respectively. Both these distances are in same the range of Yb−Te distances (3.13-3.21Å) observed in the 1D coordination polymer [(THF)$_2$Yb(μ-TeC$_6$H$_5$)$_2$·^{1}/$_2$THF]$_\infty$.[15] As expected from Shannon's radii, the Yb−Te distances in **2.27** and **2.28** are significantly shorter than reported for heptacoordinated ytterbium tellurolate, (pyridine)$_5$Yb(TePh)$_2$ [3.248(1) and 3.315(1)Å],[31] and Cp*$_2$Yb(TePh)(NH$_3$) [3.039(1)Å].[44]

According to Shannon's ionic radii, there is 0.15 Å difference between the ionic redii of Eu(II) and Yb(II) for coordination number 6.[43] Consequently, one would expect the Eu−Te bond length to be 0.15 Å longer than that of Yb−Te bond distance. In our observation, the actual change in Ln-Te distances while moving from Eu to Yb is found to be in the range 0.06-0.1 Å.
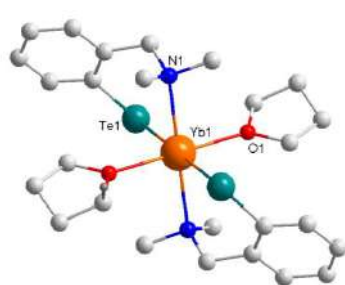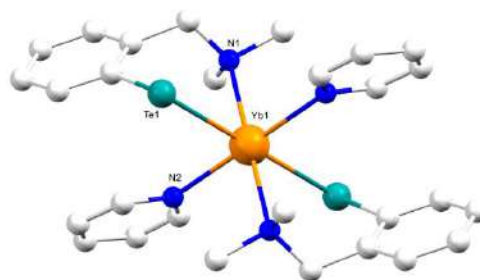
2.27   **2.28**

Figure 2.8. Molecular structures of [Yb(TeNC$_9$H$_{12}$)$_2$(THF)$_2$], **2.27** and [Yb(TeNC$_9$H$_{12}$)$_2$(pyridine)$_2$], **2.28**. Ellipsoids shown at 50% probability, hydrogen atoms removed for clarity.

Table 2.1. Selected bond lengths (Å) and angles (°) in the crystal structures of complex **2.25-2.31**

(Here D= Donor atom of the solvent molecule)

	2.25	2.26	2.27	2.28	2.29	2.30	2.31
Ln1-Te1	3.2576(13)	3.2258(8)	3.1611(12)	3.1535(6)	3.3011(10)	3.2702(14)	3.0101(19)
Ln1-Te2	3.2576(13)	3.2258(8)	3.1611(12)	3.1535(6)	3.2715(10)	3.2702(14)	3.022(2)
Ln1-N1	2.660(3)	2.677(3)	2.566(3)	2.593(4)	2.640(8)	2.729(8)	2.48(2)
Ln1-N2	2.660(3)	2.677(3)	2.566(3)	2.593(4)	2.682(8)	2.729(8)	2.47(2)
Ln1-D1	2.581(3)	2.653(3)	2.475(2)	2.571(4)	2.608(8)	2.730(8)	2.433(16)
Ln1-D2	2.581(3)	2.653(3)	2.475(3)	2.571(4)	2.560(7)	2.662(8)	2.184(14)
Ln1-D3					2.568(7)	2.662(8)	2.221(13)
Ln1-D4						2.730(8)	
Te1-Ln1-Te2	180.0	180.0	180.0	180.0	176.78(2)	107.93(4)	172.70(6)
N1-Ln1-N2	180.0	180.0	180.0	180.0	77.8(2)	124.2(4)	72.9(7)
N1-Ln1-Te1	82.62(6)	80.81(6)	84.79(7)	84.01(10)	67.39(18)	67.14(18)	73.6(5)
N1-Ln1-Te2	97.38(6)	99.19(6)	95.21(6)	95.99(10)	113.71(18)	80.68(19)	99.9(5)
N2-Ln1-Te1	97.38(6)	99.19(6)	95.21(6)	95.99(10)	116.01(18)	80.7(2)	101.2(7)
N2-Ln1-Te2	82.62(6)	80.81(6)	84.79(6)	84.01(10)	67.19(18)	67.14(18)	73.3(7)

The molecular structures of complexes **2.29** and **2.30** are shown in Figure 2.9. As mentioned earlier, when the tellurolate ligand has been changed from 2-(dimethylamino)methyl)phenyltellurolate to quinoline-8-tellurolate, there are significant changes in the coordination environment around the complexes. In particular, in THF quinoline-8-tellurolate resulted in seven coordinated europium complex [Eu(TeNC$_9$H$_6$)$_2$(THF)$_3$] **2.29**, whereas in DME, it afforded eight coordinated complex Eu(TeNC$_9$H$_6$)$_2$(DME)$_2$] **2.30**. In both the complexes, quinoline nitrogen atoms made five membered chelating rings with the metal centres. In complex **2.29**, the two quinoline-8-tellurolate ligands occupy axial position where both the tellurium atoms are *trans* to each other, as evident from Te1−Eu−Te2 angle of 176.78 (2) Å. Three THF molecules reside in a T-shape arrangement with Eu atom. The two nitrogen donor atoms from both the tellurolate ligands furnish an N1−Eu1−N2 angle of 77.8 (2) Å indicating their *cis* arrangement around Eu metal centre. However, a completely different spatial arrangement of the quinoline-8-tellurolate ligands is observed in complex **2.30**, as evident from the remarkable difference in Te1-Eu1-Te2 angle [107.93(4) Å] and N1−Eu1−N2 angle [124.2(4) Å] in comparison to that of the **2.29**. In complex **2.30**, the eight-coordinate Eu atom sits on a crystallographically imposed centre of inversion. The Eu−Te bond distances in **2.29** [3.2715(10) and 3.3011(10) Å] and **2.30** [3.2702(14) Å] are slightly longer than that observed for **2.25** and **2.26**. The N−Eu−Te bite angles in complex **2.29** are found to be 67.19 (18) Å and 67.39 (18) Å. A similar bite angle [67.14(18) Å] is observed in **2.30**. Expectedly, these bite angles are significantly smaller as compared to that of hexacoordinated complex **2.25** and **2.26**.

1.29   **1.30**
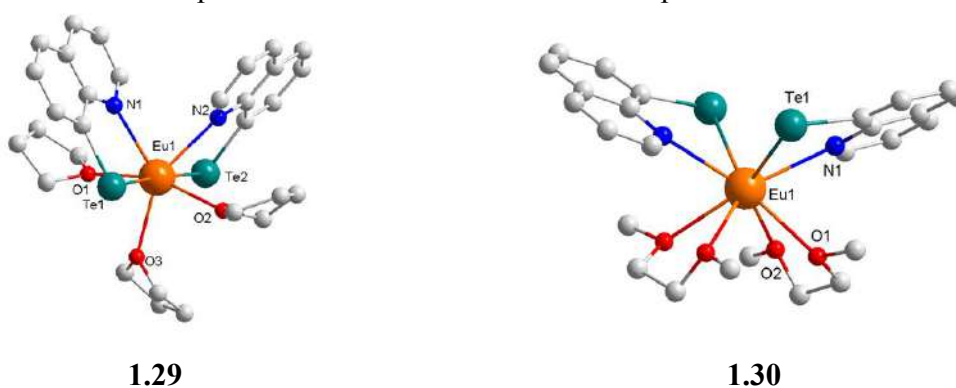
Figure 2.9. Molecular structure of **2.29** and **2.30**. Ellipsoids shown at 50% probability, hydrogen atoms removed for clarity.

The molecular structure of **2.31** is shown in Figure 2.10 which infers a dimeric structure with crystallographically imposed inversion center. Here each trivalent Yb metal centers is coordinated to two quinoline-8-tellurolate ligands. The two metal centres are bridged by alkoxy oxygen atom of two methoxyethanolate ligands thereby forming a Yb_2O_2 core with μ_2-bridging oxygen atom. The distance of the bridging oxygen atoms from the metal centres are 2.184(14) Å (Yb1−O2) and 2.221 (13) Å (Yb1−O2′). These Yb−O distances are close to the bridging bonds observed [2.198 (3) and 2.191 (3) Å] in the dimeric complex [Cp′YbCl(μ-OC$_2$H$_4$OMe)]$_2$ [where, Cp′ = 1,2,4-(Me$_3$C)$_3$C$_5$H$_2$].[35c] The coordinative bond distance of 2.433(16) Å between the Yb metal centre and the oxygen atom is significantly longer than the Yb−O bridging bonds. The non-bonding distance between the two metal centres is 3.589 (2) Å, which is in agreement with the distance observed in [Cp′YbCl(μ-OC$_2$H$_4$OMe)]$_2$ [3.5874(8) Å]. While comparing with **2.27** and **2.28,** the Yb−Te distances [3.011(19) and 3.022 (2) Å] in **2.31** are observed to be significantly shorter. The Te1−Yb−Te2 angle of 172.70(6)° indicates a *trans* arrangement of the quinoline-8-tellurolate ligand around Yb metal with respect to Te atom, whereas the *cis* arranged N1−Yb−N2 furnishes an angle of 72.9(7) Å. Again the O1−Yb1−O2 distance is found to be 70.6(5)°, which is in agreement with that of 70.36(12)° observed in [Cp′YbCl(μ-OC$_2$H$_4$OMe)]$_2$.
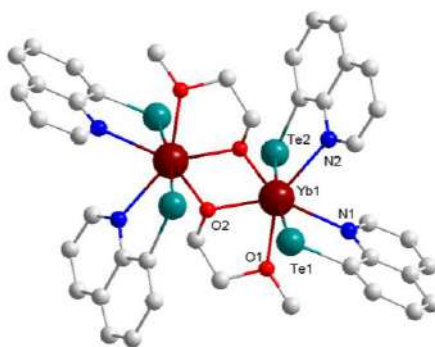
Figure 2.10. Molecular structure of [Yb(TeNC$_9$H$_{12}$)$_2$ (μ-OCH$_2$CH$_2$OMe)]$_2$, **2.31**. Ellipsoids shown at 50% probability, hydrogen atoms removed for clarity.

The Crystal Data and Structural Refinement for Complexes **2.24-2.31** are shown in Table 2.2.

Compound	2.24	2.25	2.26	2.27	2.28	2.29	2.30	2.31
Empirical formula	$C_{18}H_{12}N_2Te_2$	$C_{26}H_{40}EuN_2O_2Te_2$	$C_{22}H_{30}EuN_4Te_2$	$C_{26}H_{40}YbN_2O_2Te_2$	$C_{28}H_{34}YbN_4Te_2$	$C_{30}H_{36}EuN_2O_3Te_2$	$C_{26}H_{32}EuN_2O_4Te_2$	$C_{30}H_{36}EuN_2O_3Te_2$
Formula weight	511.50	819.76	757.66	840.84	854.83	879.77	848.97	343.67
Crystal system	Triclinic	Triclinic	Monoclinic	Triclinic	Monoclinic	Monoclinic	Monoclinic	Monoclinic
Space group	*P*-1	*P*-1	*P*2₁/*n*	*P*-1	*P*2₁/*n*	*Cc*	*C2/c*	*P2₁/c*
a (Å)	7.630(15)	8.8280(18)	11.816(2)	8.7450(17)	9.6700(19)	15.388(3)	24.233(5)	12.849(3)
b (Å)	8.560(17)	9.2710(19)	8.9240(18)	9.3620(19)	9.6300(19)	13.511(3)	7.9050(16)	12.442(3)
c (Å)	24.973(5)	9.906(2)	12.943(3)	9.856(2)	15.880(3)	16.413(3)	18.925(4)	16.120(3)
α (°)	89.93(3)	62.16(3)	90	61.78(3)	90	90	90	90
β (°)	86.24(3)	88.57(3)	101.86(3)	89.63(3)	101.33(3)	116.10(3)	125.74(3)	110.44(3)
γ (°)	89.95(3)	89.07(3)	90	88.73(3)	90	90	90	90
V (Å³)	1627.56(6)	716.7(3)	1335.7(5)	710.8(3)	1449.9(5)	3064.61(13)	2942.4(14)	2414.8(9)
Z	4	1	2	1	2	4	4	4
D_{calcd} (g/cm³)	2.088	1.899	1.884	1.964	1.958	1.907	4.369	4.727
Range of θ	6.84 to 58.28	4.65 to 52.72	6.24 to 52.778	4.66 to 52.738	4.57 to 52.742	4.216 to 52.042	6.656 to 52.812	4.708-52.756
Absorption coefficient (mm⁻¹)	3.582	4.207	4.503	5.324	5.220	3.945	18.454	25.116
Final $R(F)$	R1 =	R1 = 0.0233,	R1 = 0.0257,	R1 = 0.0316, wR2	R1 = 0.0333, wR2	R1 = 0.0295,	R1 = 0.1099,	R1 = 0.1190,

[I>2σ(I)][a]	R1 = 0.0652, wR2 = 0.1630	wR2 = 0.0514	wR2 = 0.0609	= 0.0888	wR2 = 0.0696		wR2 = 0.2900	wR2 = 0.3120
wR(F²) indices [I>2σ(I)]	R1 = 0.1099, wR2 = 0.2155	R1 = 0.0239, wR2 = 0.0517	R1 = 0.0276, wR2 = 0.0619	R1 = 0.0318, wR2 = 0.0890	R1 = 0.0425, wR2 = 0.0809	R1 = 0.0318, wR2 = 0.0704	R1 = 0.1139, wR2 = 0.2956	R1 = 0.1398, wR2 = 0.3328
Data / restraints / parameters	4369/0/199	2879/0/153	2691/0/136	2868/0/153	2947/0/162	5757/2/344	2882/0/159	4920/0/248
Goodness-of-fit on F²	0.768	1.143	1.079	1.131	1.056	1.048	1.313	1.089

Definitions: $R(F_o) = \Sigma||F_o - F_c||/\Sigma|F_o|$ and $wR(F_o^2) = \{\Sigma[w(F_o^2 - F_c^2)^2]/\Sigma[w(F_c^2)^2]\}^{1/2}$

2.5 Computational studies

2.5.1 Computational Details

Although no experiment has been carried out to calculate the magnetic properties of the synthesized complexes, however, it was envisaged to theoretically explore the magnetic behaviour of the complexes. All the first principle calculations have been performed using MOLCAS 8.0 and ORCA 4.0.1 programme package.[45, 46] In MOLCAS for estimating magnetic anisotropic properties we have employed CASSCF-RASSI-SO method. For this basis sets were chosen from ANO-RCC (atomic natural orbital-relativistic core contracted) basis set library-ANO-RCC-VTZP for Lanthanides (Ln = Yb, Eu) and Te center, ANO-RCC-VTZ for N, O centres and ANO-RCC-VDZ for C and H centres. Douglas-Kroll-Hess Hamiltonian was used to incorporate the scalar relativistic effect into the calculation. During the CASSCF (complete active space self-consistent field) step n electrons in metal 4f orbitals i.e., CAS(n,7) was chosen. In case of Yb seven doublet roots and for Eu one octet and 48 sextet roots were allowed to interact in the RASSI-SO (Restricted Active Space State Interaction-Spin Orbit) step. The g-tensors and other Spin-Hamiltonian parameters were computed using SINGLE_ANISO module.

We have also performed CASSCF-LFT (ligand field theory) calculations in ORCA 4.0.1 software. Here for Eu we have employed relativistic SARC-DKH-TZVP basis, DKH-def2-TZVP(-f) basis for O, N, Sapporo-DKH3-DZP basis for Te and DKH-def2-SVP basis set for C and H. In the CASSCF step, 7 electrons in 7 4f orbitals were correlated with 1 octet and 48 sextets. The LFT operator has been introduced on the top of CASSCF wavefunction.

Also DFT (density functional theory) calculations have been carried out in Gaussian 09 programme (version D.01).[47] Here unrestricted-B3LYP functional was used along LANL2DZ for Te, CSDZ basis set for Ln and TZVP for rest of the atoms. Further NBO (Natural Bond Orbital) analysis was performed using Gaussian NBO version 3.1.

2.5.2 Theoretical Study on [Eu(TeNC₉H₆)₂(THF)₃], 2.29

A representative theoretical calculations on Eu^{2+} complex have been performed on **2.29**. Since, it is $4f^7$ system, therefore possesses no orbital contribution to the magnetic moment. Being a spin only system the ground state is stated as totally symmetric ^8S term. The CASSCF computed shows that the first excited sextet state is ~36000 cm^{-1} apart from the ground state [Figure

2.11(a)]. Very small second order spin-orbit coupling splits the M_S levels into four Kramers doublets. The computed g tensors show an isotropic 2.00 value. Thus very weak spin-orbit coupling splits the M_S levels from a ground state to 1st excited state with computed energy gap of 0.17 cm^{-1} (see Figure 2.11(a) inset). Ligand field *f*-orbital splitting diagram shows a very small splitting which is close 600 cm^{-1}. The correlated CASSCF-LFT orbitals are shown in Figure 2.11(b). This figure also indicates a pure *f*-orbital character of the complex.
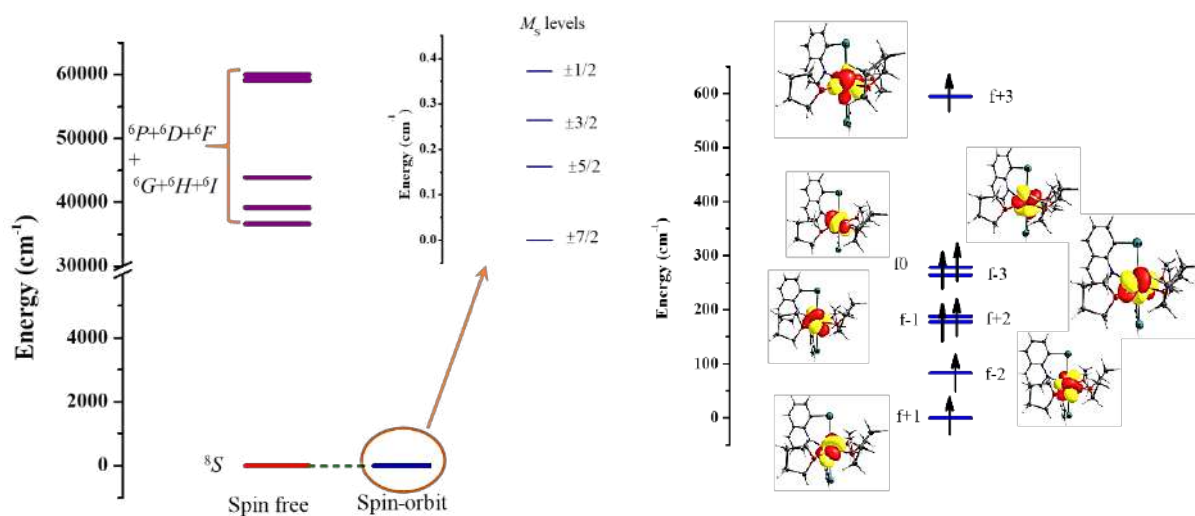
Figure 2.11. (a) (Left) Spin-free and spin-orbit energy states computed from CASSCF+RASSI-SO method of Eu complex. (b) (Right) Ligand field splitting diagram of 4*f*-orbitals of the Eu complex computed from CASSCF-LFT method.

Therefore, the DFT computed shows a spherically symmetric spin density of 7.034 value (Figure 2.12). From the spin density plot it is observed that there is a significant alpha spin polarization on the Eu^{2+} centre exist from surrounding coordinating atoms. Hence the coordinating atoms show a beta spin density -0.0016 on Te, −0.007 on N and −0.001 on O atoms (Figure 2.12). NBO analysis confirms that the seven 4*f* orbitals on Eu centre are purely metal centered (99.99%) *f*-character orbitals.
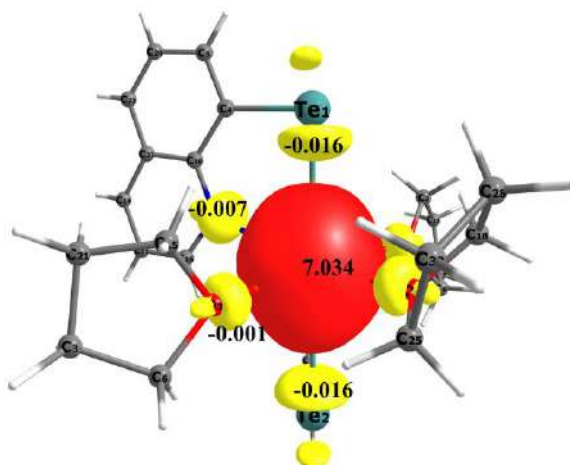
Figure 2.12. Spin density plot of the **2.29** with isosurface value of 0.0002 e/bohr^3.

2.5.3 Theoretical Study on [Yb(TeNC$_9$H$_{12}$)$_2$ (μ-OCH$_2$CH$_2$OMe)]$_2$, 2.31

This Yb(III) dimer showed some interesting magnetic anisotropy which was studied with *ab initio* methods. Since Yb(III) is a f^{13} system, so it has only one unpaired electron in 4f orbital. Due to strong spin-orbit coupling, it's ground state spin-free composed of ^{2}F term with a ground state J (L+S coupling constant) consist of 7/2. Therefore, the spin-orbit ground state has four Kramers doublets (KDs) from which molecular magnet property arises. The CASSCF+RASSI+SO+SINGLE_ANISO calculations reveals an effective energy barrier of 274 cm^{-1}, which is theoretically one of the highest reported spin reversal barrier (U$_{eff}$) for a single Yb(III) centre [Figure 2.13(a)]. During single_aniso we have substituted one Yb(III) centre with diamagnetic Lu(III) species. Although this reported barrier is very high but small magnetic exchange interaction may reduce or increase this barrier.

The computed ground state major magnetic anisotropy axes for the two Yb centres, i.e., g$_{ZZ}$ axes have been shown together in Figure 2.13(b). The centres have nearly equivalent symmetry and hence the g$_{ZZ}$ axes are almost parallel to each other. Since, the symmetry around the Yb centre is not exactly pentagonal bipyramidal (D$_{5h}$) so the g$_{ZZ}$ axis is not exactly along the Yb−Te bond axis but somewhat tilted. Since Yb(III) is a prolate ion and the stronger donating ligands such as O, N atoms are in equatorial position while weaker donating telluride is in axial position,

the ground state wave function depicts a pure (94%) J = ±7/2 ground state (see Table **2.3**). The g values also support an axial type anisotropy with a small rhombic part gz = 7.55, gy= 0.37 and gx= 0.22. From Figure 2.13(a), the ground state quantum tunnelling shows a small 0.09 value (red dotted line). The first excited state is 274 cm^{-1} apart and the gz angle indicates a relaxation of magnetization via this 1st excited state. The relaxation pathway reveals a Raman+Orbach type of relaxation (black dotted arrow + red dotted arrow) with an effective barrier of 274 cm^{-1} [see Figure 2.13(a)]. Since it is a dimer, so magnetic interaction could play an important role in reducing or increasing the effective energy barrier. This much of high barrier height for a single Yb(III) is reported to be one of the highest U$_{eff}$ and therefore may show single molecule magnet (SMM) properties which further require experimental magnetic DC/AC.[48-50]

Table 2.3. *Ab initio* computes spin-orbit energy levels along with g-tensor values and wavefunction decomposition.

Ab initio Energy of the Kramers' pairs	g_x	g_y	g_z	Angle between g_z axes	Wavefunction analysis
0.0	0.22	0.37	7.55	-	94%|±7/2⟩
273.6	1.38	1.57	6.20	58°	45%|±5/2⟩, 30%|±1/2⟩
322.5	1.61	1.96	5.10	81°	21%|±5/2⟩, 14%|±3/2⟩
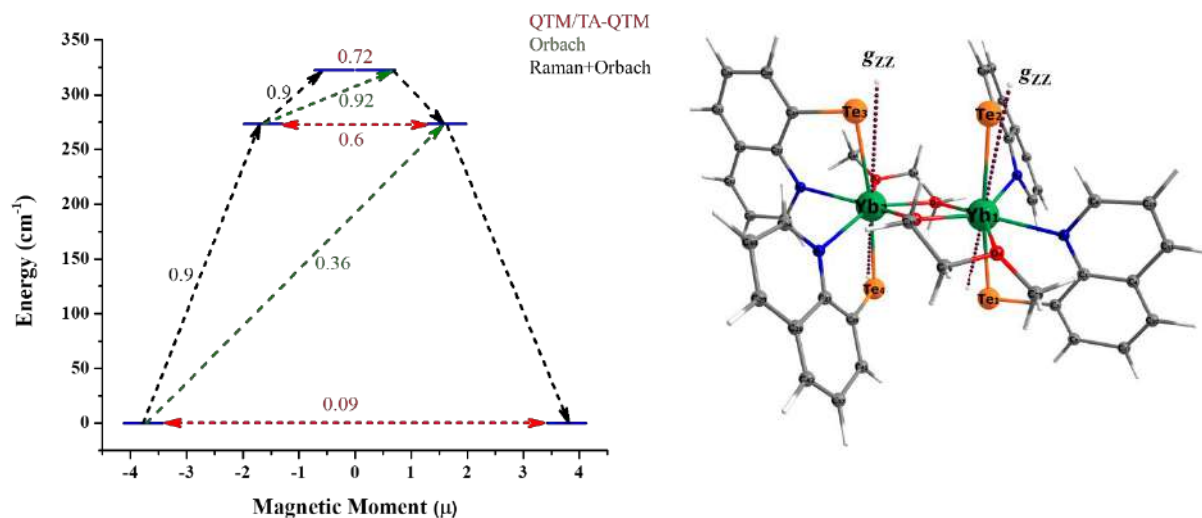
Figure 2.13. (a) (Left) SingleAniso computed magnetization reversal barrier with the relaxation mechanisms. (b) (Right) g_{ZZ} axes direction on the two Yb(III) centre.

2.6 Conclusion

A series of monomeric Eu(II) and Yb(II) tellurolate complexes are synthesized by using hybrid, Intramolecular Chalcogen Bonding stabilized organotellurolate ligands, namely 2-(dimethylamino)methyl)phenyltellurolate and quinoline-8-tellurolate ligand. In all the complexes the donor atoms from side arms, which were involved in secondary bonding interaction with tellurium (N···Te), form six membered [in case of 2-(dimethylamino)methyl)phenyltellurolate ligand] or five membered [in case of quinoline-8-tellurolate ligand] chelating rings with the metal centre. It is, in fact, the Ln···N interactions, together with the steric bulk of the ligands, which prevented the formation of higher order aggregates and confined the molecules to monomers. Although the synthesis of monomeric lanthanoid chalcogenolate complexes has still remained a challenging task in inorganic chemistry, herein we have provided the detailed insight into the age-old academic curiosity on the Ln-chlacogen bonds. All the complexes are characterized by single crystal X-ray diffraction studies. From the structural characterizations of the complexes, it can be inferred that the Ln-chalcogen bond lengths in all the complexes can be predicted from ionic radius summation rules. However, some degree of covalent bonding also contribute to the stability of the complexes. While only a handful reports are available on monomeric ytterbium tellurolate complexes, there is no report available on the isolation and

structural characterization of monomeric europium tellurolate complexes to best of our knowledge. As such the europium complexes reported here are first of their kinds for any tellurolate ligand.

2.7 Experimental section

All the manipulations were carried out under nitrogen atmosphere using standard Schlenk techniques unless otherwise noted. Solvents were purified and dried by standard procedures and were distilled prior to use. ^{1}H (400 MHz and 500 MHz), ^{13}C (100.56 MHz and 125 MHz), ^{77}Se (76.3 MHz) and ^{125}Te (157.97 MHz) nuclear magnetic resonance spectra were recorded on Bruker AV 400 and Bruker AV 500 spectrometers at 25 °C. Chemical shifts are cited with respect to Me$_3$Si as internal standard (^{1}H and ^{13}C) and Me$_2$Se (^{77}Se) and Me$_2$Te (^{125}Te) as external standards. IR spectra were collected using an Agilent Cary 630 attenuated total reflectance (ATR-IR) spectrometer between 4000 and 600 cm^{-1}. Microanalyses were performed by the Elemental Analysis Service of London Metropolitan University (UK). Metal analyses were performed by titration of HCl-digested samples against Na$_2$H$_2$EDTA in hexamine-buffered solution with Xylenol orange indicator

Synthesis of bis[2-(dimethylaminomethyl)phenyl] ditelluride, 2.23[33a]

To a stirred solution of N,N-dimethylbenzylamine (1.53 cm^3, 1.37 g, 10.2 mmol) in dry diethyl ether (50 cm^3) 1.6 mol dm^{-3} solution of *n*-butyllithium in hexane (6.4 cm^3, 10.2 mmol) was added dropwise by a syringe. A white slurry of the lithiated product was obtained on stirring for 32h at ambient temperature. Tellurium powder (0.80 g, 10.2 mmol) was added and stirring was continued for 4h for complete consumption of tellurium. The reaction mixture was then poured into a beaker containing aqueous NaHCO$_3$ and oxygen was passed at a moderate rate for half an hour. The product was extracted with diethyl ether. The organic layer was separated, dried over anhydrous Na$_2$SO$_4$ and was evaporated to dryness to give a yellow oil. To this methanol was added (5 cm^3) and the solution was allowed to diffuse slowly. The yellow coloured solid obtained was recrystallized in chloroform to give the pure titled compound.

^{1}H NMR (400 MHz, CDCl$_3$): δ (ppm) 8.01-7.98 (d, 2H), 7.15- 6.98(m, 6H, Ar-H), 3.55 (s, 4H, CH$_2$), 2.30 (s, 12H, NMe$_2$).

^{13}C NMR (100 MHz, CDCl$_3$): δ (ppm) 140.8, 138.9, 129.1, 128.0, 127.7, 113.0, 66.3, 43.8.

^{125}Te NMR (500 MHz, CDCl$_3$): δ (ppm) 353.2 ppm

Synthesis of 8,8'-diquinolyl ditelluridee, 2.24

To a vigorously stirred mixture of powdered NaOH (1.5 g, 38.0 mmol), tellurium powder (2.0 g, 25.0 mmol) and DMF (20 ml), 100% hydrazine hydrate (1 ml, 25.0 mmol) was added dropwise at room temperature. The mixture was stirred for 7h. 8-bromoquinoline (4.2 g, 25.0 mmol) was added drop-wise to the reaction mixture and refluxed for 3 days. After all the starting material was consumed, as evident by TLC, the reaction was stopped and diluted with water. The mixture was extracted with diethyl ether (4×100 ml) and the organic layer was dried over anhydrous sodium sulphate. Removal of solvent *in vacuo* afforded the titled compound as a yellow crystalline solid.

Yield: 78 %, m.p.: 200°C.

^{1}H NMR (400 MHz, CDCl$_3$)**:** 9.0 (d, 2H), 8.2 (dd, 2H), 8.0 (dd,2H), 7.7 (dd,2H), 7.5(dd,2H),7.3(dd,2H).

^{13}C NMR (100 MHz, CDCl$_3$)**:** 149.5, 146.8, 136.3, 131.5, 128.8, 128.2, 127.4, 125.8, 121.7

^{125}Te NMR (500 MHz, CDCl$_3$)**:** 220.2 ppm

Synthesis of [Eu(TeNC$_9$H$_6$)$_2$(THF)$_2$], 2.25

In a Schlenk flask, Eu fillings (0.23g, 1.52 mmol) and bis[2-(dimethylamino)methyl]phenyl]ditelluride (0.2 g, 0.38 mmol) were taken in THF and reaction mixture was stirred for 18h. The reaction mixture was filtered through filtering cannula to remove the excess metal. The volume of filtrate was reduced under vacuum to *ca.* 10 mL and the flask was stored at −30 °C. Dark yellow coloured crystals were obtained after 15 days and examined by X-ray crystallography.

Yield: 74%, m.p. 158°C

Elemental analysis Calcd (%) for C$_{26}$H$_{40}$EuN$_2$O$_2$Te$_2$ (819.772): C 38.09, H 4.92, N 3.42; found C 37.91, H 4.86, N 3.41

ν_{max} (nujol)/cm^{-1}: 3038.7 w, 2957.5 s, 2925.1 s, 2856.7 s, 2782.5 w, 2414.2 w, 2272.5 w, 1884.2 w, 1577.2 m, 1457.0 s, 1374.484 m, 1313.0 w, 1246.2 m, 1174.9 m, 1023.2 s, 950.0 w, 918.6 m, 868.1 m, 835.0 m, 800.8 s, 751.6 s.

^{1}H NMR (Hydrolysed) (400 MHz, CDCl$_3$): 7.93 (4H, br), 7.36 (8H, br), 7.15 (4H, br), 3.95 (8 H, br), 3.58 (2H, br), 2.57 (12H, br), 1.72(2 H, br)

Synthesis of [Eu(TeNC$_9$H$_6$)$_2$(Acetonitrile)$_2$], 2.26

Same procedure has been followed for synthesis of **2.26**. In a Schlenk flask, freshly prepared Eu filings (0.23 g, 1.52mmol) and bis[2-(dimethylamino)methyl]phenyl]ditelluride (0.20 g, 0.38 mmol) were taken in THF and reaction mixture was stirred for 18h. The reaction mixture was filtered through filtering cannula to remove the excess metal. The volume of filtrate was reduced under vacuum to *ca*. 10 mL and the flask was stored at −30°C. Dark orange coloured crystals were obtained after 1 month.

Yield: 79%, m.p. 158°C

Elemental analysis Calcd (%) for C$_{22}$H$_{30}$EuN$_4$Te$_2$ (757.674): C 34.88, H 3.99, N 7.39; found C 35.23, H 3.78, N 7.43

Eu: 19.93 (Calcd. 20.06%)

ν_{max} (nujol)/cm^{-1}: 2920 m, 2833 w, 1619 w, 1499 s, 1456 m, 1359 w, 1275 s, 1232 w, 1128 s, 1091 m, 1039 m, 941 m

Synthesis of [Yb(TeNC$_9$H$_6$)$_2$(THF)$_2$], 2.27

Small amounts of Hg^0 (2 drops) were added to Yb (0.26 g, 1.50 mmol) filings in 10 mL THF and the reaction mixture was allowed to stir for 1.5h. Bis[2-(dimethylamino)methyl]phenyl]ditelluride (0.20 g, 0.38 mmol) was dissolved in 10 mL THF and was transferred to the reaction mixture. The reaction mixture was stirred for 18h at room temperature. Excess metals were removed through filtration. The filtrate was concentrated to ca. 5-7 mL and kept in −30°C. After 1 month dark red coloured crystal of **2.27** was obtained.

Yield: 85%, m.p. turn black at 178°C.

Elemental analysis Calcd (%) for C$_{26}$H$_{40}$YbN$_2$O$_2$Te$_2$ (840.872): C 37.14, H 4.80, N 3.33; found C 37.29, H 4.93, N 3.19

Yb: 20.39 (Calcd. 20.58%)

ν_{max} (nujol)/cm^{-1}: 2924.5 s, 2854.9 s, 2781.1 w, 2723.5 w, 2283.1 w, 1578.6 m, 1457.1 m, 1374.3 w, 1260.7 m, 1094.0 m, 1021.2 m, 841.3 w, 799.1 m, 746.2 w

Synthesis of [Yb(TeNC$_9$H$_6$)$_2$(pyridine)$_2$], 2.28

Same protocol has been followed for the synthesis of **2.28** where small amounts of Hg^0 (2 drops) were added to Yb filings (0.26 g, 1.50 mmol) in 10 mL pyridine and the reaction mixture was allowed to stir for 1.5h. Bis[2-(dimethylamino)methyl)phenyl]ditelluride (0.20 g, 0.38 mmol) was dissolved in 5 mL pyridine and was transferred to the reaction mixture. The reaction mixture was stirred for 18h at room temperature. Excess metals were removed through filtration. The filtrate was concentrated to half and kept in −30°C. After 1 month dark red coloured crystal of **2.28** was obtained.

Yield: 85%, m.p. turn black at 178°C.

Elemental analysis Calcd (%) for $C_{28}H_{34}YbN_4Te_2$ (854.862): C 39.34, H 4.01, N 6.55; found C 39.11, H 4.17, N 6.89

Yb: 19.99 (Calcd 20.24%)

ν_{max} (nujol)/cm^{-1}: 2924.8 s, 2855.1 s, 2728.7 w, 2313.9 w, 1595.7 w, 1460.0 m, 1377.0 w,1261.1 w, 1147.6 w, 1029.2 w, 743.6 w, 702.0 w

Synthesis of [Eu(TeNC$_9$H$_6$)$_2$(THF)$_3$], 2.29

In a Schlenk flask, freshly prepared Eu (0.17 g, 1.11mmol) filings and 8,8′-diquoline ditelluride (0.15 g, 0.29 mmol) were taken in 15 mL THF and reaction mixture was stirred for 18h. The reaction mixture was filtered through filtering cannula to remove the excess metal. The volume of filtrate was reduced under vacuum to *ca*. 5 mL and the flask was stored at −30 °C. Yellow coloured crystals were obtained after 3 weeks and examined by X-ray crystallography.

Yield: 72 %, m.p. 187°C.

Elemental analysis Calcd (%) for $C_{30}H_{36}EuN_2O_3Te_2$ (879.782): C 40.96, H 4.12, N 3.18; found C 40.82, H 4.20, N 3.25

ν_{max} (nujol)/cm^{-1}: 2924.4 s, 2856.9 s, 2684.4 w, 2414.1 w, 2317.9 w, 1795.1 w, 1663.7 w, 1586.0 m, 1486.9 m, 1457.0 s, 1413.4 m, 1376.7 m, 1288.2 m, 1205.0 m, 1126.2 m, 1064.5 m, 1034.6 s, 959.4 m, 892.2 m, 825.2m, 792.5 m

^{1}H NMR (Hydrolysed) (400 MHz, CDCl$_3$): 6.1(2H, dd), 4.9(1H, br), 4.88 (4H, br), 4.49(2H, br), 4.37 (1H, t), 4.2 (2H, m)

Synthesis of [Eu(TeNC$_9$H$_6$)$_2$(DME)$_2$], 2.30

Same protocol has been followed for the synthesis of 1.3h where in a Schlenk flask, Eu metal (0.17 g, 1.11mmol) and 8,8´-diquoline ditelluride (0.15 g, 0.29 mmol) were taken in 15 mL DME and reaction mixture was stirred for 18h. The reaction mixture was filtered through filtering cannula to remove the excess metal. The volume of filtrate was reduced under vacuum to *ca.* 5-7 mL and the flask was stored at −30°C. Orange coloured crystals were obtained after 3 weeks and examined by X-ray crystallography.

Yield: 76 %, m.p. 191°C.

Elemental analysis Calcd (%) for $C_{26}H_{32}EuN_2O_4Te_2$ (843.702): C 37.01, H 3.82, N 3.32; found C 37.09, H 4.01, N 2.57

v_{max} (nujol)/cm^{-1}: 2924.8 s, 2855.3 m, 1595.9 w, 1453.1 m, 1372.4 w, 1297.1 w, 1261.9 w, 1200.6 w, 1114.5 w, 1066.0 m, 1024.2 w, 954.9 w, 858.6 w, 819.3 m, 785.6 m.

^{1}H NMR (Hydrolysed) (400 MHz, CDCl$_3$): 8.50(1H, br), 8.12 (1H, dd), 7.36(1H, br), 7.07 (1H, br), 6.86 (1H, br), 6.7 (1H, br), 3.05(2H, s), 2.93 (3H, s)

Synthesis of [Yb(TeNC$_9$H$_6$)$_4$($\mu_2{}^{\wedge}$O C$_3$H$_7$O$_2$)$_2$], 2.31

In a Schlenk flask, small amounts of Hg^0 (2 drops) were added to Yb filings (0.26 g, 1.50 mmol) in 10 mL DME and the reaction mixture was allowed to stir for 1.5h. 8,8´-diquoline ditelluride (0.20 g, 0.38 mmol) was dissolved in 5 mL DME and was transferred to the reaction mixture. The reaction mixture was stirred for 18 h at 50 °C. Excess metals were removed through filtration. The filtrate was concentrated to half and kept in −30 °C. After 15-20 days dark red coloured crystals of **2.31** were obtained.

Yield: 61%, turns black at 185°C

Elemental analysis Calcd (%) for $C_{42}H_{38}Yb_2N_4O_4Te_4$ (1519.2980): C 33.20, H 2.52, N 3.69; found C 33.04, H 2.58, N 3.81

v_{max} (nujol)/cm^{-1}: 2924.6s, 2285.5w, 1941.5w, 1588.9m, 1456.3s, 1375.8s, 1290.7m, 1208.0s, 1097.0s, 1042.3s, 966.9m, 862.8w, 619.2s

2.8 References:

1. Regulacio, M. D.; Bussmann, K.; Lewis, B.; Stoll, S. L. *J. Am. Chem. Soc.* **2006**, *128*, 11173.

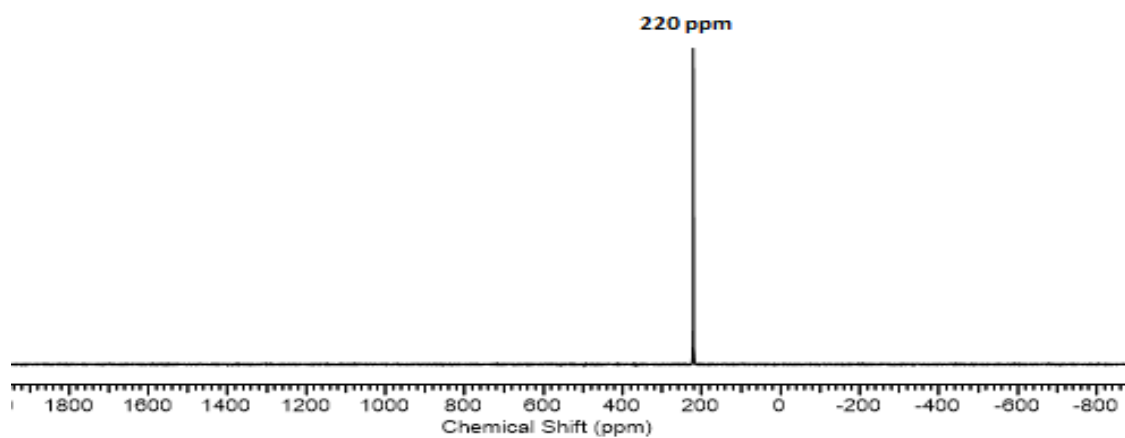2. Kim, J.Y.; Livinghouse, T. *Org. Lett.* **2005**, *7*, 1737.

3. Arndt, S.; Trifonov, A.; Spaniol, T.P.; Okuda, J.; Kitamura, M.; Takahashi, T. *J. Organomet. Chem.* **2002**, *647*, 158.

4. Kuriki, K.; Koiki, Y.; Okamoto, Y. *Chem. Rev.* **2002**, *102*, 2347.

5. Kumar, G. A.; Riman, R. E.; Chen, S.;Smith, D.; Ballato, J.; Banerjee, S.; Kornienko, A.; Brennan, J. G. *Appl. Phys. Lett*. **2006**, *88*, 91902.

6. Berg, D.J.; Andersen, R.A.; Zalkin, A. *Organometallics* **1988**, *7*, 1858.

7. Mashima, K.; Nakayama, Y.; Shibahara, T.; Fukumoto, H.; Nakamura, A. *Inorg. Chem.* **1996**, *35*, 93.

8. Mashima, K.; Nakayama, Y.; Fukumoto, H.; Kanehisa, N.; Kai, Y.; Nakamura, A. *J. Chem. Soc. Chem. Commun.* **1994** , 2523.

9. Freedman, D.; Melman, J. H.; Emge, T. J.; Brennan, J. G. *Inorg. Chem.* **1998**, *37* 4162.

10. Fitzgerald, M.; Emge, T. J.; Brennan, J. G. *Inorg. Chem.* **2002**, *41*, 3528.

11. Evans, W. J.; K. Miller, A.; Lee, D. S.; Ziller, J. W. *Inorg. Chem*. **2005**, *44*, 4326.

12. Freedman, D.; Melman, J. H.; Emge, T. J.; Brennan, J. G. *Inorg. Chem.* **1998**, *37*, 4162.

13. Freedman, D.; Emge, T. J.; Brennan, J. G. *Inorg. Chem*. **1999**, *38*, 4400.

14. Freedman, D.; Emge, T. J.; Brennan, J. G. *J. Am. Chem. Soc*. **1997**, *119*, 11112.

15. Khasnis, D. V.; Brewer, M.; Lee, J.; Emge, T. J.; Brennan, J. G. *J. Am. Chem. Soc.* **1994**, *116*, 7129.

16. (a) Lissner, F.; T. Schleid, *Z. Anorg. Allg. Chem.* **2004**, *630*, 1741. (b) Lissner, F.; Schleid, T. *Z. Anorg. Allg. Chem*. **2005**, *631*, 1119. (c) Schurz, C. M.; Talmon-Gros, P.; Lissner, F.; Schleid, T. *Solid State Sci.* **2013**, *17*, 140. (d) Foltin, M. L.; Schleid, T. *Z. Anorg. Allg. Chem***. 2015,** *641***,** 292; (e)Lissner, F.; Foltin, M. L.; Schleid T. *Eur. J. Inorg. Chem.* **2018**, 3014.

17. Lissner, F.; Schleid, T. *Z. Anorg. Allg. Chem.* **1994**, *620*, 2003.

18. (a)Lissner, F.; Schleid, T. *Z. Anorg. Allg. Chem.* **2006**, *632*, 1167. (b) Lissner, F.; Schleid, T. *Inorganics* **2017**, *5*, 2.

19. (a) Lissner, F.; Schleid, T. *Z. Anorg. Allg. Chem.* **2005**, *631*, 427. (b) Lissner, F.; Schleid, T. *Z. Anorg. Allg. Chem.* **2016**, *642*, 1038.

20. Zitzer, S.; Schleid, Th. *Z. Anorg. Allg. Chem.* **2010**, *636*, 1050.
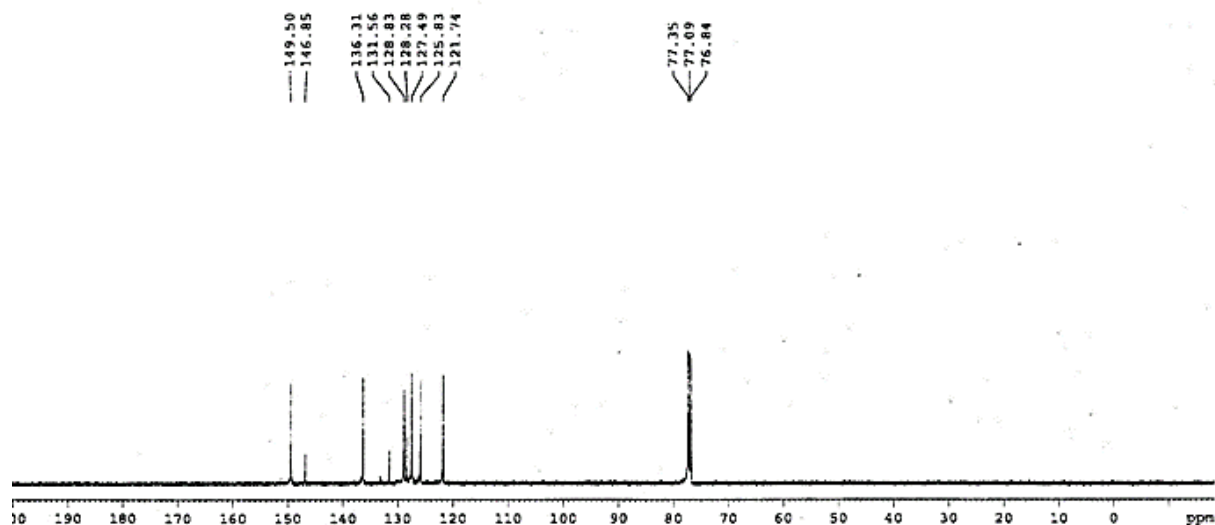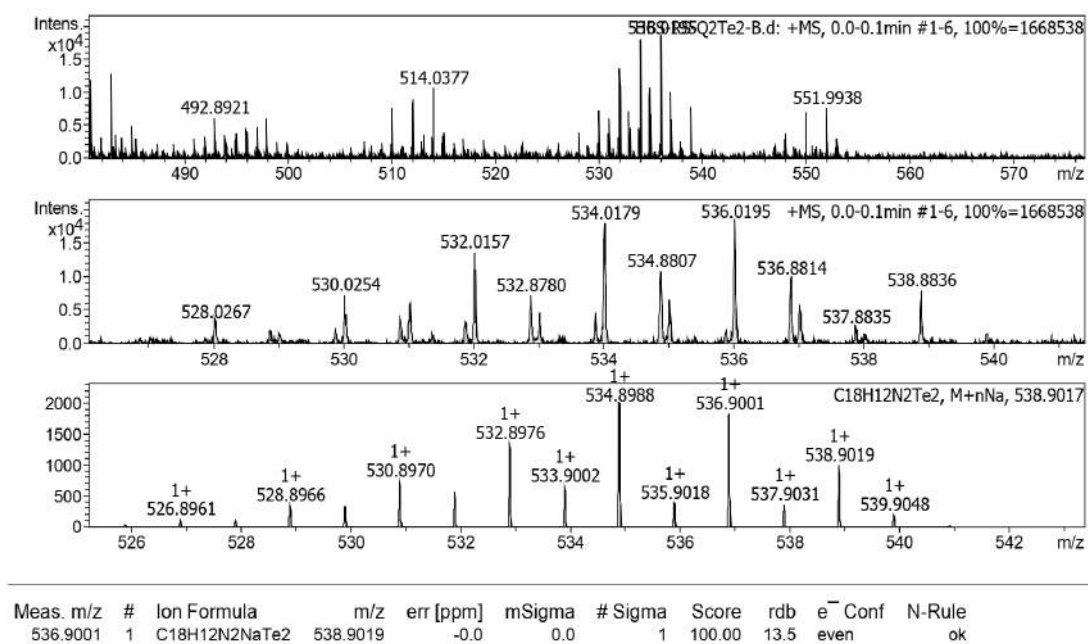
21. Charkin, D. O.; Black, C.; Downie, L.; Sklovsky, D.; Berdonosov, P. S.; Olenev, A.; Zhou, W.; Lightfoot, P.; Dolgikh, V. A. *J. Solid State Chem.* **2015**, *232*, 56.

22. Charkin, D. O.; Zitzer, S. Greiner, S.; Dorofeev, S. G.; Olenev,A. V.; Berdonosov, P. S.; Schleid, T.; Dolgikh,V. A. *Z. Anorg. Allg. Chem.* **2017**, *643*, 1654.

23. Poremba, P.; Noltemeyer, M.; Schmidt, H.-G.; Edelmann; F. T., *J. Organomet. Chem.* **1995**, *501*, 315.

24. Mashima, K.; Shibahara,T.; Nakayama, Y.; Nakamura, A. *J. Organomet. Chem.* **1998**, *559*, 197.

25. Niemeyer, M. *Eur. J. Inorg. Chem.* **2001**, 1969.

26. Hauber, S. O.; Niemeyer, M. *Chem. Commun.* **2007**, *3*,275.

27. Pernin, C. G.; Ibers J. A. *Inorg. Chem.* **2000,** *39,* 1216.

28. Wedler, M.; Noltemeyer, M.; Pieper, U.; Schmidt, H-G.; Stalke D.; Edelmann, F. T., *Angew. Chem. Int. Ed. Engl.* **1990**, *29*, 894

29. Hillier, A. C.; Liu, S.-Y.; Sella, A., Elsegood, M. R. J. *Inorg. Chem.* **2000**, *39*, 2635.

30. Lee, J.; Freedman, D.; Melman, J.H.; Brewer, M.; Sun, L.; Emge, T.J.; Long, F.H., Brennan, J.G. *Inorg. Chem.* **1998,** *37*, 2512

31. Brewer, M.; Khasnis, D.; Buretea, M.; Berardini, M., Emge, T. J., Brennan, J.C. *Inorg. Chem.* **1994**, *33*, 2743.

32. (a) Nishibayashi, Y.; Segawa, K.; Singh, J. D.; Fukuzawa, S.; Ohe, K.; Uemura, S. *Organometallics* **1996**, *15*, 370. (b) Nishibayashi, Y.; Singh, J. D.; Segawa, K.; Fukuzawa, S.; Uemura, S. *J. Chem. Soc., Chem. Commun.* **1994**, 1375. (c) Jones, P. G.; Laube, J.; Thone, C. *Inorg. Chem.* **1997**, *36*, 2097. (d) Kienitz, C. O.; Thone, C.; Jones, P. G. *Inorg. Chem.* **1996**, *35*, 3990. (e) Bonasia, P. J.; Arnold, J. *J. Organomet. Chem.* **1993**, *449*, 147. (f) Khasnis, D. V.; Buretea, M.; Emge, T. J.; Brennan, J. G. *J. Chem. Soc., Dalton Trans.* **1995**, 45. (g) Mugesh, G.; Singh, H. B.; Butcher, J. R. *J. Organomet. Chem.* **1999**, *577*, 243. (h) Mugesh, G.; Singh, H. B.; Butcher, J. R. *Eur. J. Inorg. Chem.* **1999**, 1229. (i) Mugesh, G.; Singh, H. B.; Patel, P. R.; Butcher, J. R. *Inorg. Chem.* **1998**, *37*, 2663.

33. (a) Kaur, R.; Singh, H. B.; Butcher, R. J. *Organometallics* **1995**, *14*, 4755. (b) Dreis, A. M.; Douglas, C. J. *J. Am. Chem. Soc.* **2009**, *131*, 412.

34. (a) Evans, W. J.; Greci, M. A.; Ziller, J. W. *Inorg. Chem.* **1998**, *37*, 5221. (b)Yu, Y.; Yuan, D.; Wang, Y.; Yao, Y. *J. Organomet. Chem.* **2016**, *819*, 37.

35. (a) Gun'ko, Y. K.; Hitchcock, P. B.; Lappert, M. F. *J. Organomet. Chem.* **1995**, *499*, 213. (b) Trifonov, A. A.; Spaniol T. P.; Okuda, J. *Dalton Trans.* **2004**, 2245. (c) Walter, M. D.; Bentz, D.; Weber, F.; Schmitt, O.; Wolmershäuser, G.; Sitzmann, H. *New J. Chem.* **2007**, *31*, 305.

36. (a) Evans, W. J.; Dominguez, R.; Hanusa, T. P. *Organometallics* **1986**, *5*, 1291. (b) Aspinall H. C.; Tillotson, M. R.; *Inorg. Chem.*, **1996**, *35*, 2163. (c) Evans, W. J.; Ulibarri, T. A.; Chamberlain, L. R.; Ziller, J. W.; Alvarez, D. *Organometallics* **1990**, *9*, 2124. (d) Schumann, H.; Glanz, M.; Hemling, H.; Görlitz, F. H. *J. Organomet. Chem.* 1993, **462**, 155.

37. McPhillips, T. M.; McPhillips, S. E.; Chiu, H.-J.; Cohen, A. E.; Deacon, A. M.; Ellis, P. J.; Garman, E.; Gonzalez, A.; Sauter, N. K.; Phizackerley, R. P.; Soltis, S. M.; Kuhn, P. *J. Synchrotron Radiat.* **2002**, *9*, 401.

38. Kabsch, W. *J. Appl. Crystallogr.* **1993**, *26*, 795.

39. Sheldrick, G. *Acta Cryst.* **2008**, *A64*, 112.

40. Dolomanov, O. V.; Bourhis, L. J.; Gildea, R. J.; Howard, J. A. K., Puschmann, H. *J. Appl. Crystallogr.* **2009**, *42*.

41. (a) Sandman, D. J.; Li, L.; Tripathy, S. *Organometallics* **1994**, *13*, 348. (b) Mugesh, G.; Panda, A.; Kumar, S.; Apte, S. D.; Singh, H. B.; Butcher, R. J. *Organometallics* **2002**, *21*, 884.

42. (a) Pauling L. In The Nature of the Chemical Bond, 3rd ed.; Cornell University Press: Ithaca, NY, 1960. (b) P. Pyykkö, M. Atsumi, *Chem. Eur. J.* **2009**, *15*, 186. (b) A. Bondi, *J. Phys. Chem*. **1964**, *68*, 441.

43. Shannon, R. D. *Acta Crystallogr*. **1976**, *A32*, 751.

44. Berg, D. J.; Andersen, R. A.; Zalkin, A. *Organometallics* **1988**, *7*, 1858.

45. Aquilante, F.; Autschbach, J.; Carlson, R. K.; Chibotaru, L. F.; Delcey, M. G.; De Vico, L.; Fdez. Galván, I.; Ferré, N.; Frutos, L. M.; Gagliardi, L.; Garavelli, M.; Giussani, A.; Hoyer, C. E.; Li Manni, G.; Lischka, H.; Ma, D.; Malmqvist, P. Å.; Müller, T.; Nenov, A.; Olivucci, M.; Pedersen, T. B.; Peng, D.; Plasser, F.; Pritchard, B.; Reiher, M.; Rivalta, I.; Schapiro, I.; Segarra-Martí, J.; Stenrup, M.; Truhlar, D. G.; Ungur, L.; Valentini, A.; Vancoillie, S.; Veryazov, V.; Vysotskiy, V. P.; Weingart, O.; Zapata, F.; Lindh, R. *J. Comp. Chem*. **2016**, *37*, 506.

46. Neese, F. *Wiley Interdiscip. Rev.: Comput. Mol. Sci.* **2018**, *8*, e1327.

47. Frisch, M. J.; Trucks, G. W.; Schlegel, H. B.; Scuseria, G. E.; Robb, M. A.; Cheeseman, J. R.; Scalmani, G.; Barone, V.; Mennucci, B.; Petersson, G. A.; Nakatsuji, H.; Caricato, M.; Li, X.; Hratchian, H. P.; Izmaylov, A. F.; Bloino, J.; Zheng, G.; Sonnenberg, J. L.; Hada, M.; Ehara, M.; Toyota, K.; Fukuda, R.; Hasegawa, J.; Ishida, M.; Nakajima, T.; Honda, Y.; Kitao, O.; Nakai, H.; Vreven, T.; Montgomery, J. A.; Peralta, J. E.; Ogliaro, F.; Bearpark, M.; Heyd, J. J.; Brothers, E.; Kudin, K. N.; Staroverov, V. N.; Kobayashi, R.; Normand, J.; Raghavachari, K.; Rendell, A.; Burant, J. C.; Iyengar, S. S.; Tomasi, J.; Cossi, M.; Rega, N.; Millam, J. M.; Klene, M.; Knox, J. E.; Cross, J. B.; Bakken, V.; Adamo, C.; Jaramillo, J.; Gomperts, R.; Stratmann, R. E.; Yazyev, O.; Austin, A.; Cammi, J. R.; Pomelli, C.; Ochterski, J. W.; Martin, R. L.; Morokuma, K.; Zakrzewski, V. G.; Voth, G. A.; Salvador, P.; Dannenberg, J. J.; Dapprich, S.; Daniels, A. D.; Farkas, Ö.; Foresman, J. B.; Ortiz, J. V.; Cioslowski, J.; Fox, D. J. *Gaussian 09 (Revisions D.01), Gaussian, Inc.*, Wallingford CT, U.S.A., **2013.**

48. Wu, D-Q.; Shao, D.; Wei, X-Q.; Shen, F-X.; Shi, L.; Zhang, Y-Q. Wang, X-Y. *Dalton Trans*. **2017**, *46*, 12884.

49. Gavrikov, A. V.; Efimov, N. N.; Dobrokhotova, Z.V.; Ilyukhin, A. B.; Vasilyev, P. N.; Novotortsev, V.M. *Dalton Trans.* **2017**, *46*, 11806.

50. Gavrikov, A. V.; Efimov, N. N.; Ilyukhin, A. B.; Dobrokhotova, Z. V.; Novotortsev, V. M. *Dalton Trans.* **2018**, *47*, 6199.

2.9 Representative Spectra of Some Compounds
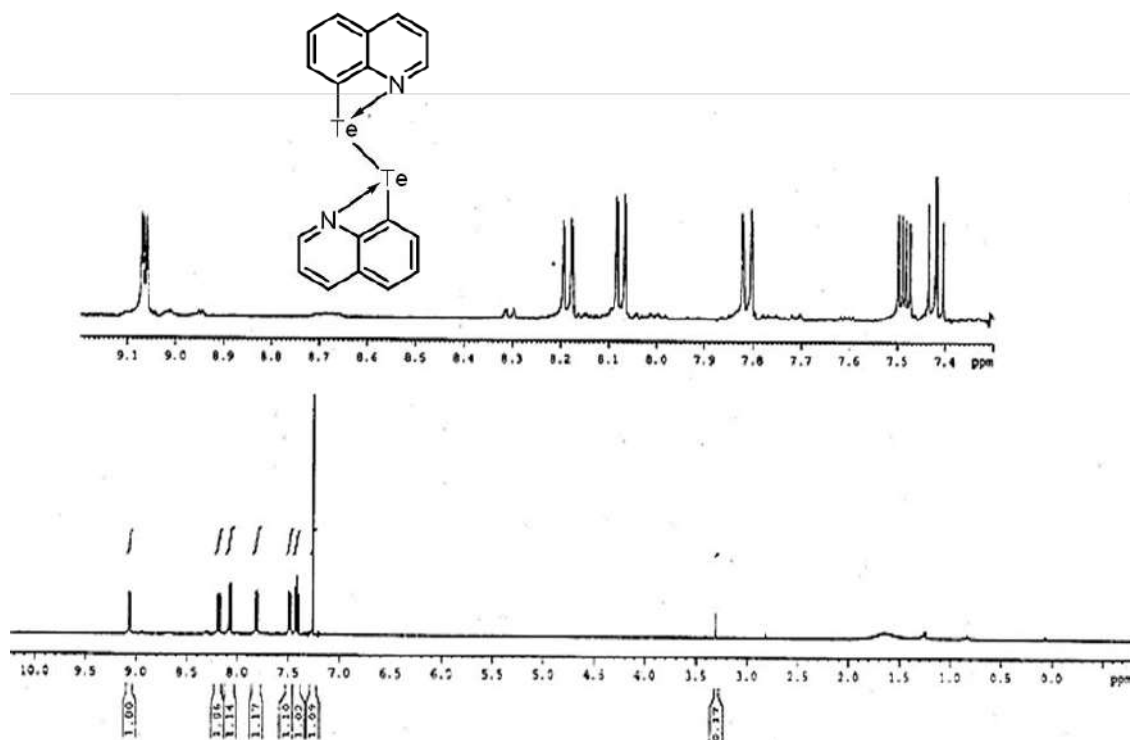
Figure 2.14. ^{1}H NMR spectrum of **2.24**

Figure 2.15. ^{125}Te NMR spectrum of **2.24**

Figure 2.15. ^{13}C NMR spectrum of **2.24**

Meas. m/z	#	Ion Formula	m/z	err [ppm]	mSigma	# Sigma	Score	rdb	e⁻ Conf	N-Rule
536.9001	1	C18H12N2NaTe2	538.9019	-0.0	0.0	1	100.00	13.5	even	ok

Figure 2.15. HRMS of **2.24**

3

Synthesis and Characterization of *cis*-Dichloridobis(8-quinolinethiolato)tin(IV)

and Bis(8-sulfanylquinolinium) hexachloridostannate(IV) Derivatives

3.1 Introduction

The inorganic complexes of 8-quinolinol (oxine) as well as its sulfur analogue 8-quinolinethiol (thiooxine) have garnered profound interest with respect to their synthesis, fascinating structural features and promising applications in different fields of chemistry and biology.[1] However compared to organotin oxinates,[2] the studies of organotin thiooxinates are much less prevalent. Tanaka *et al.*, in 1964, have reported the synthesis of diorganotin bis(8-quinolinolates) by reacting ethanolic solution of dialkyl- or diphenyltin dichloride with 8-hydroxyquinoline.[3] The first molecular structure of diorganotin bis(8-quinolinolates) namely, dimethyltin bis(8-hydroxyquinolinate) was reported by Schlemper.[2b] Later on, Archer *et al.* reported the synthesis and structural aspects of dichloridobis(8-quinolinolato)tin(IV) by reaction of anhydrous tin dichloride with 8-hydroxyquinoline.[4] The work has been expanded considerably wherein different substituted organotin 8-quinolinolates have been synthesised and their *in vitro* cytotoxicity has been examined.[5] For instance, by comparison with cisplatin, organotin quinolinolates like $[Sn(ClQ)_2Cl_2]$, $[Sn(BrQ)_2Cl_2]$ and $[Sn(ClIQ)_2Cl_2]$ (HClQ = 5,7-dichloro-8-hydroxyquinoline, H-BrQ = 5,7-dibromo-8-hydroxyquinoline, H-ClIQ = 5-chloro-7-iodo-8-hydroxyquinoline) show significant anti-proliferative activity toward tumour cell lines.[5c]

Bis(8-sulfanylquinolinium) hexachloridostannate(IV) has been identified as a reactive intermediate in various reactions. For example, in 1908, Edinger reported the presence of bis(8-sulfanylquinolinium) hexachloridostannate(IV) as an intermediate in the conversion of 8-quinolinesulfonic acid in to 8-quinolinethiol.[6] Similar reaction sequences have been extensively used afterwards to study the miscellaneous chemistry associated with 8-quinolinethiol.[7] Lubenets *et al.* utilized bis(8-sulfanylquinolinium) hexachloridostannate(IV) to react with sodium hydroxide in presence of sodium tartrate to synthesise sodium 8-quinolinethiolate,[8] and its use is prevalent in the literature.[9] However, although bis(8-sulfanylquinolinium) hexachloridostannate(IV) has played a significant role as an intermediate in the progression of organotin thiooxinates chemistry, there is no structural characterisation reported to the best of our knowledge. Herein, we report the isolation and structural characterisation of bis(8-sulfanylquinolinium) hexachloridostannate(IV). Additionally, we have explored some interesting reaction behaviour of this compound in different solvents.

3.2 Results and discussion

The synthesis of bis(8-sulfanylquinolinium) hexachloridostannate(IV) salt **3.2** was accomplished by following the reported procedure wherein 8-quinolinesulfonyl chloride, **3.1** (synthesised by reacting quinoline-8-sulfonic acid with phosphorus pentachloride) was treated with tin(II) dichloride dihydrate in the presence of hydrochloric acid to afford as yellow crystalline solid.[6] During the course of the work, to our surprise, we observed that **3.2** shows interesting behaviour in different organic solvents. In particular, compound **3.2** when recrystallized from chloroform or dichloromethane, yielded *cis*-dichloridobis(8-quinolinethiolato) tin(IV), **3.3**. However, when recrystallized from methanol, it afforded crystals of 8,8'-dithiodiquinolinium hexachloridostannate (IV), **3.4** (Scheme 1).

The behaviour of **3.2** in DMSO has also been investigated and it provides a convenient approach for the synthesis of diquinolinyl-8,8'-disulfide, **3.5**. In particular, **3.2** in an excess of DMSO and exposed to air oxidised affording diquinolinyl-8,8'-disulfide, **3.5**. The formation of the disulfide is enhanced when **3.2** was heated at 120 °C in the presence of air. During the reaction, dimethyl sulfide gas was evolved and its cessation indicated the complete transformation to the disulfide. The reaction medium when treated with mercuric chloride gave a white precipitate of mercurous chloride signifying the presence of Sn^{II}. Synthetically, this reaction is advantageous as it is quite simple to carry out and more importantly, does not require an added oxidant like potassium ferricyanide or a phase transfer catalytic system like CBr_4/18-crown-6/benzene which compounds have been previously used.[10]

Since compound **3.2** shows variable behaviour in different solvents with different compounds being subsequently isolated, it complicates its characterisation by NMR spectroscopy. In the ^1H NMR spectra of **3-5**, six discrete resonances are observed in the range 7-9 ppm, which correspond to the quinoline protons. The $^{119}Sn\{^1H\}$ NMR spectrum of **3.3** shows a single resonance at δ -392 ppm. This value is in agreement with the value expected for a six coordinate Sn(IV) complex.[11] In the ESI-MS (positive mode) spectrum of **3.2**, the molecular ion peak at *m*/z 160.0228 corresponds to the {[**Cat**-H]}$^+$ ion. In the ESI-MS spectrum of complex **3.3**, the molecular ion peak at *m*/z = 474.9143 (98.36%) is attributed to the positively charged species [**3.3**-Cl]$^+$, indicating the lability of the metal-chloride bond. Such a dissociation of one or two chloride ligands from the metal centre is common.[5c] The other prominent peak at m/z = 599.9664 (65.80%) could be assigned to tri(8-thioquinolinyl)stannonium ion. The observed isotopic patterns for both the peaks fit well with

theoretical isotopic distributions. Similarly, the ESI MS spectrum of **3.4** exhibits two prominent mass peaks, which are assigned to {[**Cat**-H]}$^+$ (m/z 321.0507, 100%) and {[**Cat**-2H+Na]}$^+$ (m/z 343.0351, 97.20%) respectively. The molecular ion peak for **3.5** at m/z 321.0635 corresponds to the [**3.5**+H]$^+$ ion.
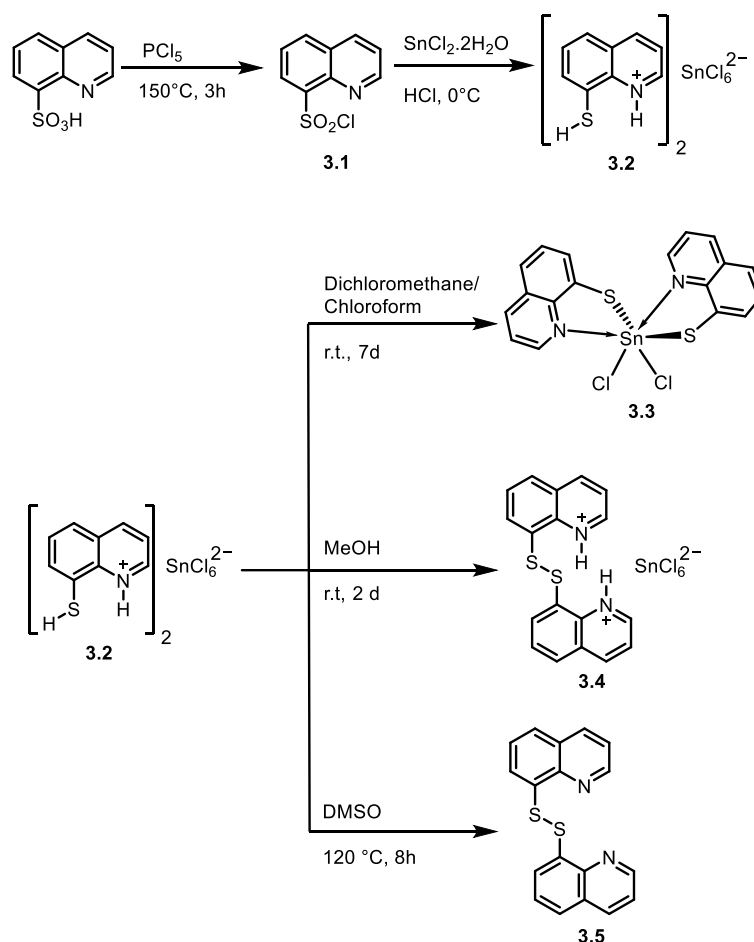
Scheme 3.1. Synthetic route to dichloridobis(8-quinolinethiolato)tin(IV), **3.3** and quinolinium hexachloridostannate(IV) derivatives **3.2**, **3.4** and diquinolyl-8,8'-disulfide, **3.5**.

3.3 Structural studies

During the crystallization of dichloridobis(quinoline-8-thiolato)tin(IV) **3.3**, we succeeded in isolating two polymorphs **3.3m** and **3.3t**. Complex **3.3m** obtained by evaporation of a saturated dichloromethane solution, crystallizes in the monoclinic space group *C2/c*, whereas **3.3t**, obtained by evaporation of a chloroform solution, crystallizes in the triclinic space group *P-1*. The molecular structure of **3.3m** is presented in Figure. 3.1 and selected bond lengths and bond angles are presented in Table 3.1. The single-crystal X-ray diffraction determinations reveals that the hexacoordinated metal centre of the Sn^{4+} ion in

both **3.3m** and **3.3t**, is chelated by two 8-quinolinethiolate anions and coordinated by two _cis_-chloride ions. The co-ordination environment of Sn^{IV} is distorted octahedral and the N-donor atoms as well as the chloride ligands are in a _cis_ arrangement. On the other hand, the sulfur atoms of the 8-quinolinethiolate anions are _trans_ to each other. The Sn^{IV} atom lies on a two-fold axis so that the two 8-hydroxyquinoline ligands are related by symmetry.
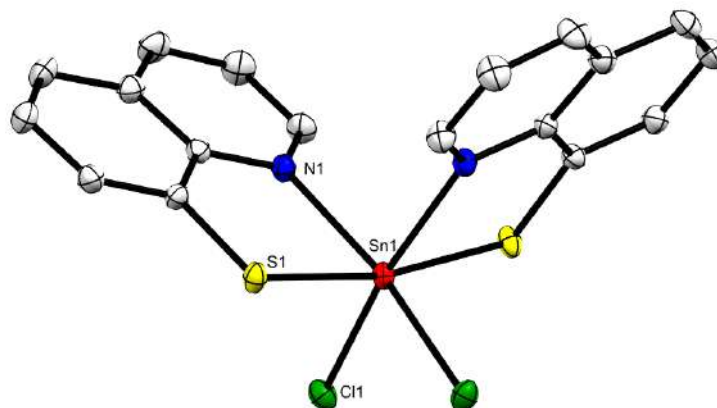

Figure 3.1. ORTEP diagram of dichloridobis(8-quinolinethiolato)tin(IV), **3m** plotted with 50% probability displacement ellipsoids**.**

Comparing the molecular structure of dichloridobis(8-quinolinethiolato)tin(IV), **3.3** with its O- analogue, dichloridobis(8-quinolinolato)tin(IV)[4], both have similar spatial arrangements of the ligands around the metal centre. In both the polymorphs, **3.3m** and **3.3t**, the bond lengths around the metal atom (Sn–N, Sn–Cl) are in the same range. However, in complex **3.3t**, $\angle$ S-Sn-S is closer to linear, $\angle$ Cl-Sn-Cl wider and $\angle$ N-Sn-N smaller than the corresponding angles of **3.3m** (Table 3.1). The Sn–S bond length in **3.3m** is observed to be 2.4168(4) Å. This distance is expectedly longer than the Sn-O distance of dichloridobis(8-quinolinolato)tin(IV) [2.030(3)Å][4] but shorter in dichloridobis(2-pyridinethiolato)tin(IV) [2.4739(3)°Å, 2.4770(4) Å],[12] as in the latter the pyridinethiolate ligands are involved in the formation of four membered chelating rings to the metal centre. Again the Sn-S distances in **3.3m** is somewhat longer than that of dibenzylchlorido(8-quinolinethiolato)tin(IV) [2.386(2) Å].[9d] As this difference is much less than the 0.07 Å expected for the change in coordination number from the Shannon radii,[13] Sn-S bond length of dibenzyltin(IV) compound may be lengthened by the two Sn-C bonds. The Sn-N and Sn-Cl bond lengths in **3.3m** (Table 3.1) are significantly longer than those in dichloridobis(8-quinolinolato)tin(IV) [2.209(4) and 2.379(2)Å respectively] and dichloridobis(2-pyridinethiolato)tin(IV) [ave. 2.264(1) and ave. 2.40245(4) Å respectively], but shorter than in dibenzylchlorido(8-quinolinethiolato)tin(IV)

[2.367(4) and 2.475(5) Å respectively]. The S-Sn-S angle in **3.3m** exhibits a significant deviation from linearity with an angle of 169.35(2) Å, but in dichloridobis(2-pyridinethiolato)tin(IV), this S-Sn-S angle deviates more from the planarity [154.55(1) Å].[12]

Although, bond lengths of **3.3m** and **3.3t** are similar, **3.3m** and **3.3t** show non-identical and interesting packing behaviour associated with bond angle differences. In the monoclinic structure, only half of the complex is crystallographically unique; hence π-stacking interactions in two perpendicular directions are identical with a centroid-centroid separation of 4.001 Å (Figure 3.2). On the other hand, in the triclinic structure, the whole complex is crystallographically unique, and therefore π-stacking interactions in the two perpendicular directions are different, with an infinite chain in one direction and a pair of complexes in the other (Figure 3.3). The corresponding centroid-centroid distances associated with these two non-identical face-to-face π-π interactions are 4.008 and 3.856 Å.
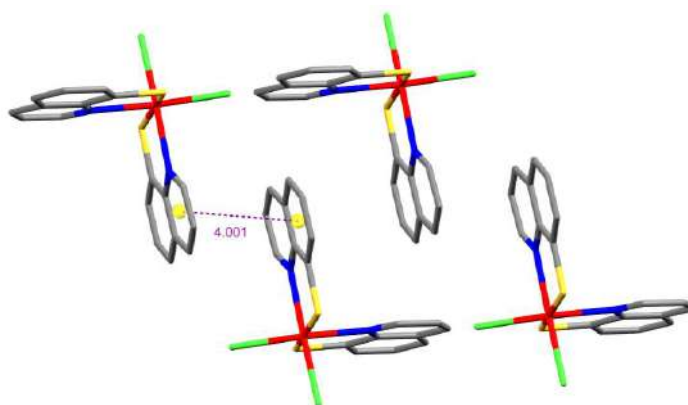

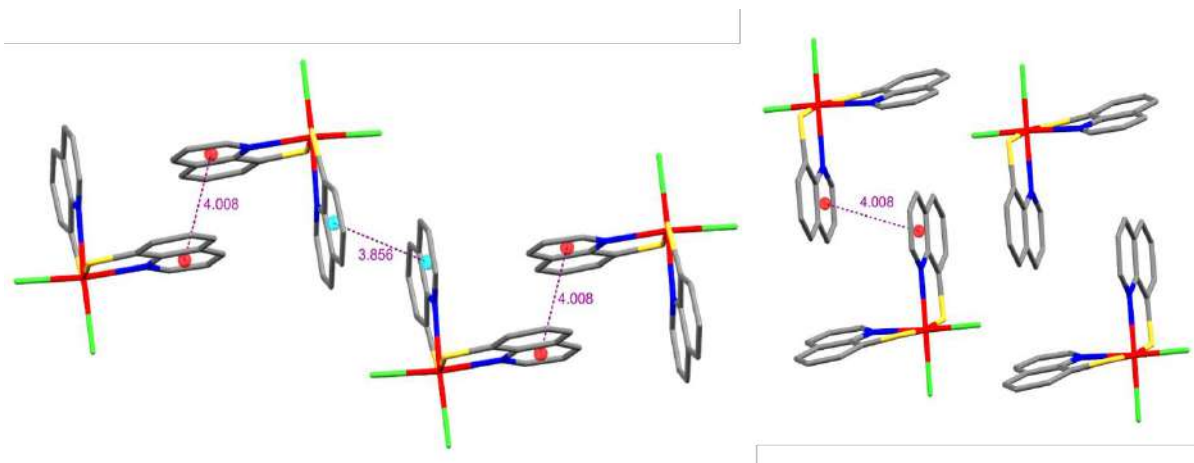**Figure 3.2.** π-stacking in the monoclinic structure **3.3m**.

Figure 3.3. π-stacking in the triclinic structure **3.3t** (two perpendicular views).

The molecular structure of compound **3.2** and **3.4** are shown in Figures **3.4** and **3.5** respectively. In the triclinic structure of compound **3.2**, one asymmetric unit contains one 8-sulfanylquinolinium ion and half of a $[SnCl_6]^{2-}$ anion with Sn^{IV} on the edge of the unit cell. In the anionic entity of **3.2**, the Sn^{IV} atom is six-fold coordinated by chloride ions, forming an octahedral arrangement. The Sn^{IV} atom sits on a crystallographically imposed center of inversion with three different Sn−Cl bond distances, Sn1−Cl1 2.4121(18) Å, Sn1−Cl2 2.4371(18) Å and the one participating in intermolecular H-bonding with the quinolinium ion, Sn1−Cl3 is 2.4332(18) Å. All the equatorial Cl-Sn-Cl angles are close to right angle, ranging from 90.09(6)° to 90.57(6)°, while the axial angles are 180°. These bond distances and bond angles agree well with that of the reported compounds containing octahedral $[SnCl_6]^{2-}$ anion.[14a,b] The quinolinium N-atom participates in the formation of intermolecular (N−H···Cl) hydrogen bond with the chloride ions of a hexachloridostannate anion with a H-bonding distance of 2.391 Å. In the cationic entity, the C−S bond length is observed to be 1.772(8) Å indicating its single bond nature.[14c]
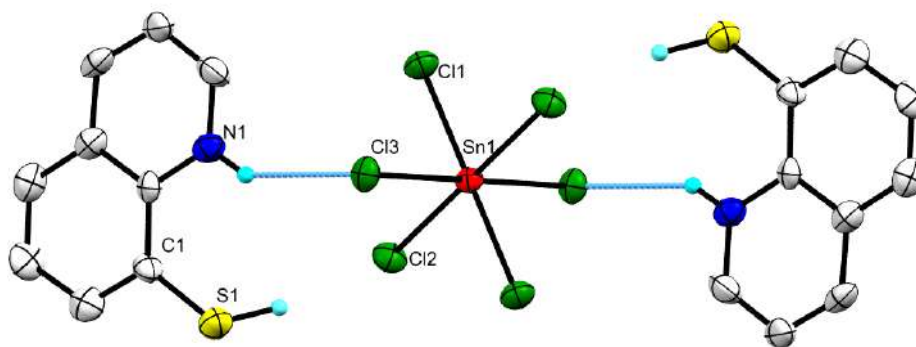
Figure 3.4. ORTEP diagram of bis(8-sulfanylquinolinium) hexachloridostannate(IV), **3.2** plotted with 50% probability displacement ellipsoids.

The monoclinic structure of compound **3.4** consists of one 8,8′-dithioquinolinium cation and one hexachloridostannate anion. In the anionic entity, the Sn(IV) adopts a distorted octahedral geometry. In comparison to compound **3.2**, the Sn–Cl bond lengths vary in a wider range between 2.4118(7) Å and 2.4640(7) Å. The equatorial Cl-Sn-Cl angle deviates somewhat from right angles, ranging from 86.74(2)° to 92.78(2)°, while the axial Cl-Sn-Cl angles lie in the range from 174.52(2)° to 178.13(2)°. In the cationic entity of compound **3.4**, the S1–S2 distance is 2.0554(9) Å which is slightly longer than that observed in diquinolyl-8,8'-disulfide [2.039 (2) Å].[15] Again, in comparison to the Pauling single bond covalent radii [Σr_{cov}(S, S) = 2.04 Å], the S1–S2 distance in **3.4** is slightly longer.[13] Both the C-S bond distances of 1.776(2) Å and 1.778(2) Å, which are similar to the C–S bond in compound **3.2** [1.772(8) Å] and somewhat shorter than that observed in diquinolyl-8,8'-disulfide [1.780(3) and 1.784(3) Å]. In the molecular structure of diquinolyl-8,8'-disulfide, both the sulfur atoms and one quinoline ring reside in one plane, the dihedral angle between the two ring planes is 78.1(1) Å. However, in compound **3.4**, the second sulfur atom deviates from the ring plane and sits at a distance of 0.968 Å above the plane.
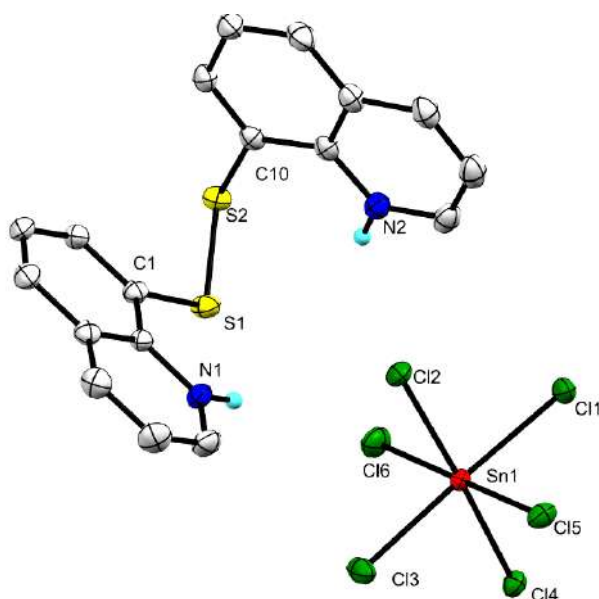
Figure 3.5. ORTEP diagram of 8,8'-dithiodiquinolinium hexachloridostannate(IV), **3.4** plotted with 50% probability thermal ellipsoids.

Table 3.1. Selected bond lengths [Å] and bond angles (°) for compounds **3.2**, **3.3m**, **3.3t** and **3.4**.

3.2

Sn1–Cl1 2.4121(18)   Sn1–Cl2 2.4371(18)   Sn1–Cl3 2.4332(18)   S1–C1 1.772(8)

Cl1-Sn1-Cl2 90.18(7)   Cl1-Sn1-Cl3 90.09(6)   Cl2-Sn1-Cl3 90.57(6)

3.3m

S1– Sn1 2.4168(4)   N1– Sn1 2.2876(15)   N1´– Sn1 2.2875(15) Cl1–Sn1 2.4358(5)

S1–C1 1.7504(18)

N1-Sn1-S1 80.38(3)   N1-Sn1-Cl1 88.31(4)   C1-S1-Sn1   100.25(5)

Cl1-Sn1-Cl1´ 91.64(2)   N1-Sn1-N1´ 93.78(8)   S1-Sn1-S1´   169.35(2)

N1-Sn1-Cl1´ 169.12(3)

3.3t

S1– Sn1 2.4401(16)   S2–Sn1 2.4435(16)   N1– Sn1 2.293(4)   N2– Sn1 2.283(4)

Cl1–Sn1 2.4388(14) Cl2–Sn1 2.4287(13) S1–C1 1.755(5)   S2–C18 1.765(6)

N1-Sn1-S1 80.42(12)   N1-Sn1-Cl1 90.70(12)   N1-Sn1-Cl2 169.39(12)

N1-Sn1-N2 86.86(16)   Cl1-Sn1-Cl2 94.48(5)   S1-Sn1-S2 172.11(5)

C1-S1-Sn1 99.81(17)   C18-S2-Sn1 98.92(17)   N2-Sn1-S2   80.47(11)

N2-Sn1-Cl2 89.96(11)   N2-Sn1-Cl1 167.74(11)

3.4

Sn1−Cl1 2.4319(7)   Sn1−Cl2 2.4405(7)   Sn1−Cl3 2.4640(7)   Sn1−Cl4 2.4118(7)

Sn1−Cl5 2.4271(8)   Sn1−Cl6 2.4208(8)   S1−S2   2.0554(9)   S1−C1 1.778 (2)

S2−C10 1.776(2)

C1-S1-S2 104.85(7)	C10-S2-S1 103.20(7)	Cl1-Sn1-Cl2 89.842(18)
Cl1-Sn1-Cl3 174.52(2)	Cl1-Sn1-Cl4 91.285(17)	Cl1-Sn1-Cl5 87.976(19)
Cl1-Sn1-Cl6 92.78(2)	Cl2-Sn1-Cl3 88.842(18)	Cl2-Sn1-Cl4 176.518(19)
Cl2-Sn1-Cl5 91.41(4)	Cl2-Sn1-Cl6 86.88(4)	Cl3-Sn1-Cl4 90.338(17)
Cl3-Sn1-Cl5 86.74(2)	Cl3-Sn1-Cl6 92.46 (2)	Cl4-Sn1-Cl5 91.92(4)
Cl4-Sn1-Cl6 89.77(4)	Cl5-Sn1-Cl6 178.13(2)	

3.4 DFT Optimised Geometry

In order to have more insight into the bonding in the synthesised compounds a detailed computational study has been carried out. All the geometry optimization and subsequent single point calculations were carried out using Density Functional Theory (DFT) method in the Gaussian 09 program.[16] Geometry optimization has been performed using hybrid B3LYP-D3 functional with SDD basis set and SDD pseudopotential on Sn and Ahlrichs split valence polarization (SVP) basis set on rest of the atoms. The computed structural parameters in the optimized geometries show good agreement with the respective X-ray diffraction crystallographic data, which attests to the accuracy of the optimized structures. A special mention goes to the structure of compound **3.4** where the Sn1−Cl6 bond undergoes elongation after optimization [Sn1−Cl6$_{crystal}$ = 2.4208(8) Å; Sn1−Cl6$_{calc}$ = 2.781 Å]. This can be attributed to the appearance of a new weak hydrogen bonding interaction between Sn1−Cl6 with the proximal −N−H atoms of the quinolinium ion after optimisation.

The natural charges (in a.u.) obtained from Natural Population Analysis (NPA) reveal that both the polymorphs **3.3m** and **3.3t** show identical natural charges (Figure 3.6a). In particular, in both the structures, a positive charge of 1.599 a.u. is centred on the Sn centres. The natural charges on respective first coordination sphere atoms are S (-0.207), Cl (-0.482)

and N (-0.571), with delocalization of charges decreasing in the order S⁻ > Cl⁻ > N. While comparing the natural charges in **3.2** and **3.4**, it was observed that due to the unsymmetrical nature of compound **3.4**, NPA charges on Cl atoms are less symmetrically distributed as compared to compound **3.2** [Figure 3.6(b-c)]. In particular, the two Cl atoms in **3.4** which are closer to the N-H protons, *i.e.*, Cl2 and Cl6 experience more negative charge *i.e.*, -0.526 and -0.571 a.u. respectively compared to distal Cl atoms, *i.e.*, Cl4 (-0.463 a.u.) and Cl5 (-0.476 a.u.). Furthermore, in case of compound **3.4**, the natural charges on the two quinolinium nitrogen atoms [N1 (0.519 a.u.) and N2 (0.510 a.u.)] are slightly more negative than that of quinolinium nitrogen atoms of compound **3.2** [N (0.495 a.u.)].
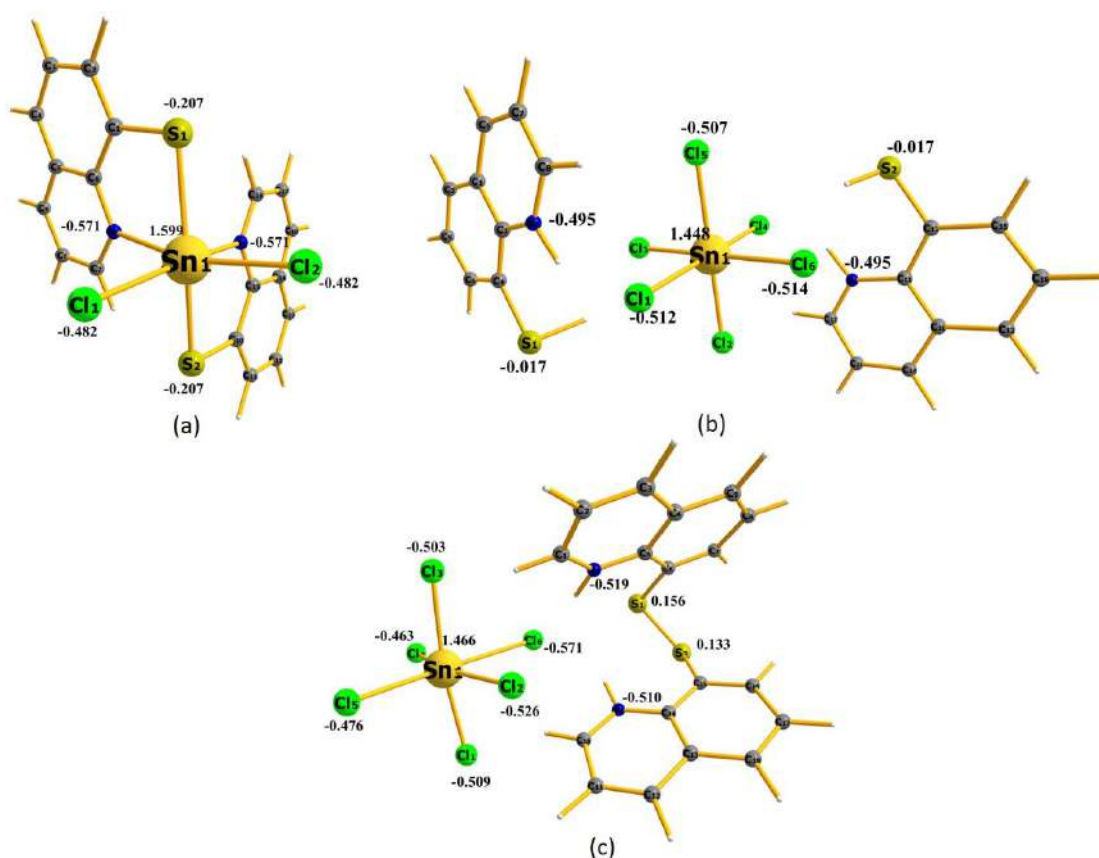
Figure 3.6. NPA atomic charges of the atoms on the optimised structure of compound (a) **3.3m/3.3t**, (b) **3.2** and (c) **3.4**. Colour code: Sn-golden yellow, S- yellowish green, Cl-bright green, N-deep blue, C- dark grey and H-light grey.

3.5 Vibrational study: Raman spectroscopy

Since the Raman vibrations are associated with the spatial relationship and interactions of the ligand(s) with the metal centre, the experimentally observed Raman vibrations of a compound in combination with DFT calculated values can give useful insight into the

molecular structure of the compound. The calculations of Raman vibrations for compound **3.2-3.4** have been performed on the optimized geometry with the same level of theory and basis functions that was used for the optimisation of the compounds (*vide supra*). For an O_h symmetry, out of the six normal modes of vibration, three *viz.* $v_1(A_{1g})$, $v_2(E_g)$ and $v_5(F_{2g})$ are Raman active.[17] Along the series of synthesized compounds **3.2-3.4**, a moderate to very good agreement between the experimental and theoretically obtained values is observed (Table 3.2). In compound **3.2**, the intense band at 308 cm^{-1} could be attributed to the frequency of the purely symmetric Sn−Cl stretching vibration (v_1), which has been aptly reproduced by the theoretically computed value (287 cm^{-1}). Successive weak bands at 238 cm^{-1} and 242 cm^{-1} in the experimental and calculated Raman spectra respectively could be assigned to distinctive antisymmetric stretching (v_2) of Sn−Cl bond. The weak band observed at 173 cm^{-1} in the theoretically calculated Raman spectrum could be assigned to the mixed contributions from counter ions and Sn-Cl (v_5) vibration. The corresponding experimental band was not observed as it is below the low frequency limit (250 cm^{-1}) of the instrument used. In case of compound **3.4**, all the Sn−Cl bond vibrations in the experimental as well as theoretical spectrum have been shifted to higher energy band compared to compound **3.2**. In particular, in the experimentally obtained spectrum of **3.4**, the v_1 mode of vibration was observed at 313 cm^{-1}. The corresponding theoretically calculated value was shifted to 329 cm^{-1}. Similarly, while the the experimental v_2 vibration was observed at 261 cm^{-1}, the corresponding calculated value shifted to 266 cm^{-1}. Again, the theoretically calculated value for the v_5 vibration was observed at 176 cm^{-1}. The slight disparity observed in the Raman vibrations of compound **3.2** and **3.4** might be attributed to the variable interactions of the $[SnCl_6]^{2-}$ moieties with the corresponding cationic entity. The experimentally observed vibrations at 475 cm^{-1} and 427 cm^{-1} for compound **3.4** could be assigned to the –S-S- vibrations. These values are in good agreement with the theoretically observed values of 471 cm^{-1} and 416 cm^{-1}, respectively. The polymorphs **3.3m** and **3.3t** exhibit identical Raman vibrations. In particular, the Raman band originating from Sn−Cl vibration appeared at 310 cm^{-1}, while its theoretical value was observed at 323 cm^{-1}. The experimental Raman band at 387 cm^{-1} could be assigned to the combination of Sn-S stretching vibrations and ligand vibrations. The band at 338 cm^{-1} in the theoretically computed spectrum corresponds to Sn−Cl and mixed Sn−S stretching vibrations.

Table 3.2. Comparison between experimental and computed Raman vibrations (in cm^{-1}) of compounds **3.2**-**3.4**.

3.2		3.3m		3.3t		3.4		Assignment of Raman vibrations
Exp	Calc	Exp	Calc	Exp	Calc	Exp	Calc	
308	287					313	329	ν(Sn-Cl) (ν_1)
238	242					261	266	ν(Sn-Cl) (ν_2)
–	173					–	176	ν(Sn-Cl) (ν_5) + counter ionic vibrations
						475, 427	471, 416	ν(S-S)
		310	323	310	323			ν(Sn-Cl)
		387	338	387	338			ν(Sn-S) + ν(Sn-Cl)

3.6 Natural Bond Orbital (NBO) Analysis

To investigate the nature of bonding and orbital participation in **3.3** (**3.3m** and **3.3t**), a detailed NBO analysis has been performed on the optimized geometry using Gaussian NBO 3.1 package. Since both the complexes (**3.3m** and **3.3t**) resulted in identical optimised structures, NBO analysis also afforded identical results. The contributions of the orbitals, electron occupancies and stabilization energies (ΔE) of the Sn-S/N/Cl interactions of donor and acceptor NBOs for **3.3m** and **3.3t** are given in Table 3.3. The NBO analysis indicates that in both the complexes strong coordinate covalent donor-acceptor (Lewis-non-Lewis) interactions take place between the Sn^{4+} and S$^-$ ions. The Sn-S interactions in each complex are attributed to two prominent interactions. In one case, the S atom donates its lone pair of orbital to the antibonding *s*-orbital of the Sn atom with second order perturbation energy of 419.0 kcal/mol [Figure 3.7(a)]. In the second type of interaction, S atom donates its lone pair of orbital to the antibonding *p*-orbital of the Sn atom with stabilisation 139.5 kcal/mol [Figure 3.7(b)]. Taken together, the second order perturbation energies of Sn-S interactions suggest that they are substantial contributors to stability of the complexes.
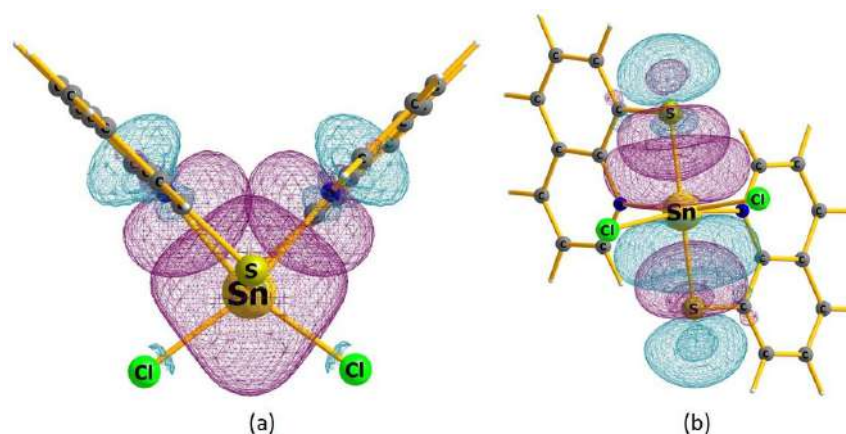
Figure 3.7. Natural Bond Orbital (NBO) plots of **3.3m/3.3t** showing (a) lp(S)$_{sp}{}^{5.23}$→lp*(Sn)$_s$ and (b) lp(S)$_{sp}{}^{5.23}$→lp*(Sn)$_p$ interactions.

Table 3.3. Donor-Acceptor (Lewis-non-Lewis) type interaction along with their stabilization energy, occupation number (in parenthesis red coloured) and hybridization of complex **3.3m/3.3t**

Donor(Lewis) NBO and wave function decomposition	Acceptor (Non-Lewis) NBO and wave function decomposition	Stabilization Energy (kcal/mol)
S1 (LP) – (1.534) – s-16.03% + p-83.79%	Sn1 (LP*) – (1.056)- s-99.71%	419.0
S1 (LP) – (1.534) – s-16.03% + p-83.79%	Sn1 (LP*) – (0.496)- p-100.00%	139.5
S2 (LP) – (1.534) – s-16.03% + p-83.79%	Sn1 (LP*) – (1.056)- s-99.71%	419.0
S2 (LP) – (1.534) – s-16.03% + p-83.79%	Sn1 (LP*) – (0.496)- p-100.00%	139.5
N1 (LP) – (1.790) – s-21.61% + p-78.38%	Sn1 (LP*) – (1.056)- s-99.71%	58.8
N1 (LP) – (1.790) – s-21.61% + p-78.38%	Sn1 (LP*) – (0.415)- p-100.00%	19.3
N1 (LP) – (1.790) – s-21.61% + p-78.38%	Sn1 (LP*) – (0.405)- p-99.85%	33.7
N2 (LP) – (1.790) – s-21.61% + p-78.38%	Sn1 (LP*) – (1.056)- s-99.71%	58.8
N2 (LP) – (1.790) – s-21.61% + p-78.38%	Sn1 (LP*) – (0.415)- p-100.00%	19.3
N2 (LP) – (1.790) – s-21.61% + p-78.38%	Sn1 (LP*) – (0.405)- p-99.85%	33.7
Cl1 (LP) – (1.603) – s-19.32%+ p-80.49%	Sn1 (LP*) – (1.056)- s-99.71%	136.0
Cl1 (LP) – (1.603) – s-19.32%+ p-80.49%	Sn1 (LP*) – (0.415)- p-100.00%	88.6

Cl1 (LP) – (1.603) – s-19.32%+ p-80.49%	Sn1 (LP*) – (0.405)- p-99.85%	43.6
Cl2 (LP) – (1.603) – s-19.32%+ p-80.49%	Sn1 (LP*) – (1.056)- s-99.71%	136.0
Cl2 (LP) – (1.603) – s-19.32%+ p-80.49%	Sn1 (LP*) – (0.415)- p-100.00%	88.6
Cl2 (LP) – (1.603) – s-19.32%+ p-80.49%	Sn1 (LP*) – (0.405)- p-99.85%	43.6

The NBO analysis for Sn-S bond in **3.3m/3.3t** was further corroborated by Atoms in Molecules (AIM) analysis, which indicates almost identical values for the Sn-S bonds in complexes **3.3m** and **3.3t**. The corresponding topological parameters for the Sn-S bond critical points (bcps) in **3.3m** and **3.3t** are given in Table 3.4 and their corresponding Laplacian of electron density [$\nabla^2\rho(r)$] plots are shown in Fig.3.8.

Table 3.4. S-Sn Bond critical points for the **3m** and **3t**.

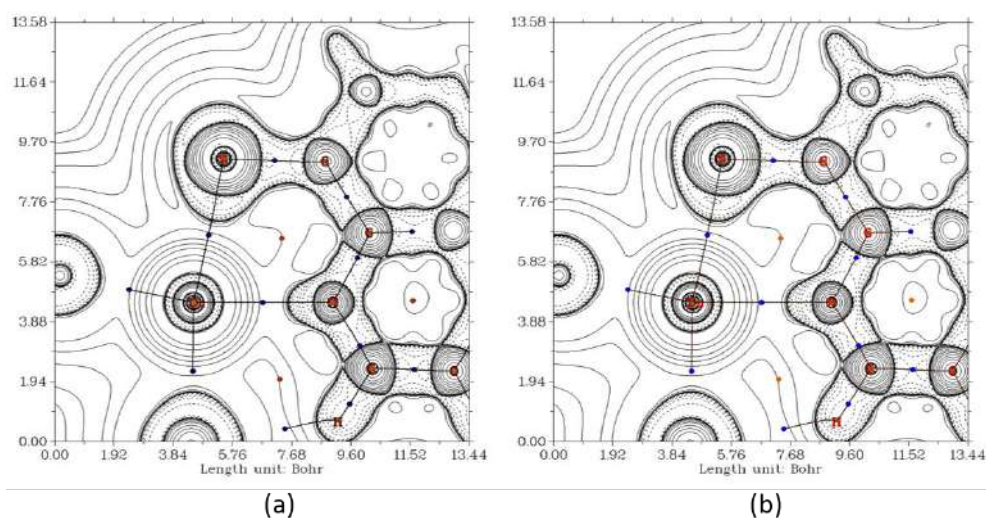| Compounds	$\rho(r)$	$\nabla^2\rho(r)$	V(r)	G(r)	H(r)
3.3m	0.06740	0.10041	-0.03068	-0.01371	-0.01697
	0.06740	0.10041	-0.03068	-0.01371	-0.01697
3.3t	0.06742	0.10045	-0.03690	-0.01371	-0.01698
	0.06742	0.10045	-0.03690	-0.01371	-0.01698

Figure 3.8. Laplacian of electron density [$\nabla^2\rho(r)$] plots for (a) **3.3m** and (b) **3.3t**.

Apart from the strong Sn−S interactions in both complexes **3.3m** or **3.3t**, the quinolinium N-atoms and the Cl⁻ anions make donor-acceptor (Lewis-non Lewis) interactions with the Sn^{4+}

ion (Figure 3.8). In both the cases, Sn acceptor orbitals (anti-bonding) are either pure *s*-character or pure *p*-character in nature. Stronger interactions are observed when the acceptor orbital of Sn has *s*-character and the relatively weaker interactions are observed with the *p*-orbital of Sn (Table 3.3). While both the N-atoms use their $sp^{3.63}$ hybridized lone pair as a donor orbital [Figure 3.8(a-c)], the Cl-atoms in each complex use their more polarizable $sp^{4.17}$ hybridized orbitals for bonding [Figure 3.8(d-f)]. Among the N and Cl donor atoms, Cl⁻ shows stronger stabilization energy with Sn, as it carries a negative charge and have more polarizable *p*-orbitals.
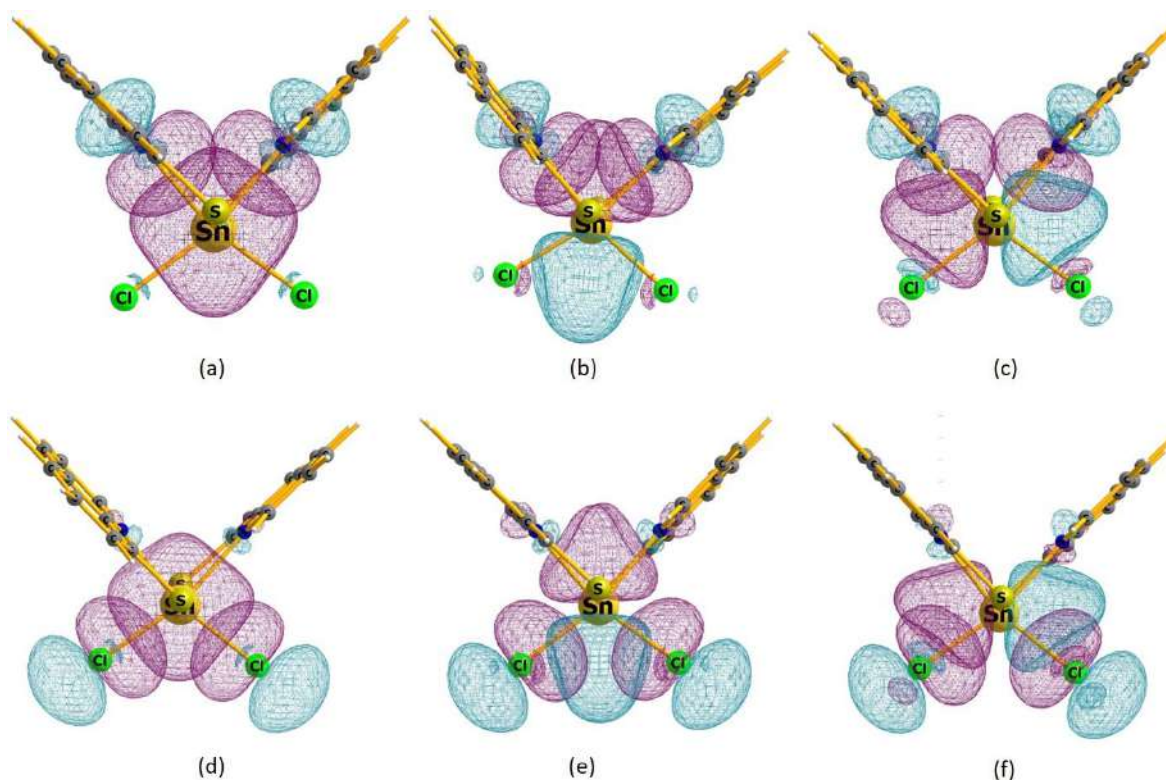

Figure 3.8. Natural bond orbital (NBO) plots showing (a-c) Sn-N and (d-f) Sn-Cl interactions.

The plots of frontier molecular orbitals reveal that the non-bonding chloride π-orbitals of $[SnCl_6]^{2-}$ moieties make the major contribution to the HOMO in compounds **3.2** and **3.4**, whereas in complex **3.3** it comes from the sulfur non-bonding π-orbitals (Figure 3.9). In all three compounds, the LUMO is localized mostly on the quinolinium ring. For compounds **3.2** and **3.3**, the HOMO-LUMO energy gap practically remains unchanged (ΔE = 78.37 kcal/mol and 78.50 kcal/mol respectively), whereas at compound **3.4,** it decreases sharply to 55.47

kcal/mol. A sharp decrease in the HOMO-LUMO gap in compound **3.4** in comparison to **3.2** can be attributed to the strong π-accepting nature of the two quinolinium N-H system.
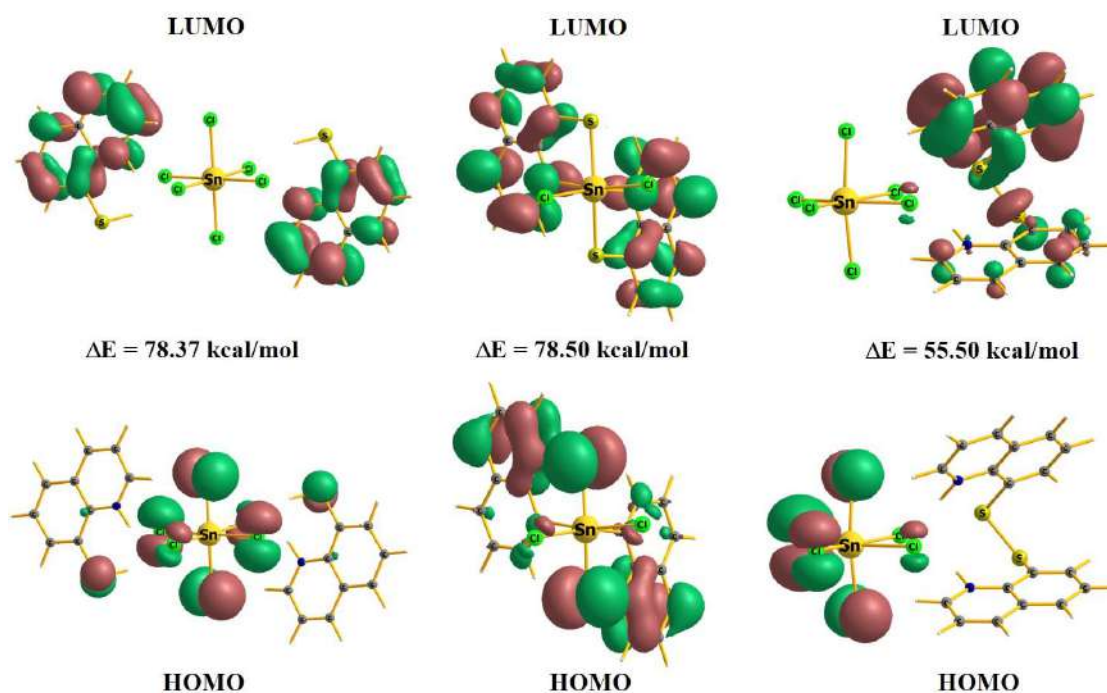

Figure 3.9. Frontier molecular orbitals of complexes **3.2**-**3.4** and their HOMO-LUMO energy gaps.

3.7 Conclusions

Bis(8-sulfanylquinolinium) hexachloridostannate(IV), **2** has been isolated and its characterisation has been accomplished by ESI-MS, Raman and IR spectroscopy and single crystal X-ray diffraction studies. The variable reaction behaviour of **2** in different solvent was explored. The nature of bonding between the sulfur and the tin in complexes **3m** and **3t** was examined by DFT calculations. It is observed that in both complexes **3m** and **3t**, a strong coordinate covalent donor-acceptor (Lewis-non Lewis) interaction takes place between Sn^{4+} ion and S^- of 8-quinolinethiolate ligand. The overall electron contributions of tin atom and the 8-quinolinethiolate ligands towards HOMO and LUMO in all the complexes **2-4** were derived by DFT calculations.

3.8 Experimental section

X-ray Crystallography Data

All samples were coated in viscous oil and mounted in a cryostream on the respective diffractometers: a Bruker APEX II CCD diffractometer (for **3.3m**), with integration and absorption corrections completed using Apex II program suite,[18] a Rigaku Saturn724+ (for **3.2**) with refinement and data reduction done using CrysAlis(Pro) 1.171.38.43 (Rigaku OD, 2015) and the MX1 (for **3.3t** and **3.4**) macromolecular beam-lines at the Australian Synchrotron, where the data collection and integration were completed using the Blu-ice[19] and XDS[20] software programs, respectively. The structures were solved using direct methods, refined with the least-squares methods against F^2 using SHELXL[21] and expanded using Fourier techniques, all within the OLEX 2[22] software suite. Part of crystallographic work was conducted using the MX1 beamline at the Australian Synchrotron, which is part of ANSTO.[23]

General

IR spectra were collected as solid samples using an Agilent Cary 630 attenuated total reflectance (ATR-IR) spectrometer between 4000 and 600 cm^{-1}. ^1H and ^{13}C spectra were recorded on either a Bruker DPX300 or a Bruker AV 500 MHz spectrometers at 25 °C spectrometer, and chemical shifts were referenced to the residual ^1H and ^{13}C resonances of the deuterated solvents. Melting points were determined in glass capillaries and are reported uncalibrated. Microanalyses were performed by the Elemental Analysis Service of London Metropolitan University (UK). Raman spectra were collected using a Renishaw Raman Microscope RM2000, using 782nm excitation.

Synthesis

8-quinolinesulfonyl chloride, 3.1

Quinoline-8- sulfonic acid (2.00 g, 9.57 mmol) was thoroughly mixed with phosphorus pentachloride (2.50 g, 12.00 mmol) in a glove bag and heated under a N_2 environment at 150° in a round bottom flask for 3 h. The liquid reaction mixture was poured on to crushed ice and neutralised with $NaHCO_3$. The pale yellow precipitate was filtered off and dried to give **8-quinolinesulfonyl chloride, 3.1** (1.87 g, 86%), m.p. 121-124°C. (lit. 118-122°C[24])

ν_{max}(neat)/cm^{-1} 3086 (vw), 3045 (vw), 2108 (vw), 1609 (vw), 1593 (m), 1558 (m), 1492 (m), 1460 (w), 1368, 1311 (vw), 1291 (vw), 1246 (vw), 1208(m), 1169 , 1148 , 1069 (vw), 1054

(vw), 1032(m), 898 (vw), 838 , 789 , 767 , 682(m), 666(s); **^{1}H NMR** (400 MHz, CDCl$_3$) δ 9.25 (dd, J = 4.2, 1.5 Hz, 1H), 8.55 (dd, J = 7.5, 1.0 Hz, 1H), 8.33 (dd, J = 8.3, 1.4 Hz, 1H), 8.24 (d, J = 8.2 Hz, 1H), 7.71 (t, J = 7.9 Hz, 1H), 7.65 (dd, J = 8.3, 4.3 Hz, 1H); **^{13}C NMR** (400 MHz, CDCl$_3$) δ 152.48, 142.98, 139.48, 136.76, 136.42, 131.89, 129.44, 125.09, 122.95; **MS (ESI$^+$)**, *m*/z [M+Na]$^+$ Calcd for C$_9$H$_6$ClNNaO$_2$S, 249.9700; found 249.9691.

Bis(8-sulfanylquinolinium) hexachloridostannate(IV), 3.2

8-Quinolinesulfonyl chloride (1.00 g, 4.40 mmol) was dissolved in 32% hydrochloric acid (12.00 ml) and slowly added to excess tin(II) dichloride dihydrate (5.00 g, 22.19 mmol) in 32% hydrochloric acid (6 ml). On cooling in an ice bath, yellow crystals separated out, which were filtered off and washed with 50% v/v hydrochloric acid to give yellow coloured Bis(8-sulfanylquinolinium) hexachloridostannate(IV), **3.2** (2.40 g, 83%), m.p. 176 °C.

ν$_{max}$(neat)/cm^{-1} 3652(vw), 3171(vw), 3091(m), 3015(m), 2645(vw), 2461(m), 2374(vw), 2323(vw), 2107(vw), 2048 (vw), 1701 (vw), 1621 (m), 1595 (m), 1542, 1499 (vw), 1406 (w), 1374 (m), 1280(m), 1232 (w), 1201 (m), 1156 (w), 1116 (vw), 1063 (vw), 979 (w), 960 (vw), 926 (vw), 874 (vw), 815 , 763 , 662 (w); **Raman**(780nm excitation), v̄(cm^{-1}) 1569(m), 1499(vw)1420(w), 1366(s), 1224(w), 1081(w), 997(w), 857(w), 806(w), 683(vw), 553(s), 533(m), 457(m), 403(m), 346(s), 308(m), 238(vw); **MS (ESI$^+$)** *m*/z {[**Cat**-H]}$^+$ Calcd for C$_9$H$_6$NS, 160.0215; found. 160.0228.

***Cis*-Dichloridobis(8-quinolinethiolato)tin(IV), 3.3**

Compound **3.2** (1.00 g, 1.52 mmol) was dissolved in dichloromethane or chloroform (5.00 ml) by slight heating. The yellow coloured solution was filtered, and the filtrate was kept at room temperature for slow evaporation. After 1 week, bright yellow coloured crystals of dichloridobis(quinoline-8-thiolato)tin(IV) was obtained. (**3.3m**, 0.56 g, 72% from dichloromethane; **3.3t**, 0.46 g, 59% from chloroform), compound decomposed at 240 °C. Both the polymorphs show inconsiderable differences in characterisations, hence characterisations of **3.3t** is included here.

ν$_{max}$(neat)/cm^{-1} 3278(vw), 3249(vw), 3172(vw), 3082(vw), 3044(vw), 2993(m), 2362(vw), 2343(vw), 2115(vw), 1933 (vw), 1624 (w), 1598 (m), 1544(m), 1437(vw), 1402 (m), 1368 (m), 1286(m), 1263 (vw), 1212 (m), 1140 (w), 1012 (w), 976(m), 848 (vw), 798 (m), 788 (m), 751 , 738 , 719 , 668 (m), 655 (m); **^{1}H NMR** (500 MHz, DMSO-*d$_6$*) δ 9.02 (dd, *J* = 4.3, 1.6 Hz, 2H), 8.44 (dd, *J* = 8.3, 1.3 Hz, 2H), 8.00 (dd, *J* = 7.2, 1.0 Hz, 2H), 7.94 (d, *J* = 8.0 Hz,

2H), 7.69 (dd, J = 8.2, 4.3 Hz, 2H), 7.43 (t, J = 7.6 Hz, 2H); ^{13}**C NMR** (500 MHz, DMSO-d_6) δ 150.86, 148.42, 137.30, 136.67, 128.75, 128.04, 127.84, 122.91, 114.89; ^{119}**Sn{^{1}H} NMR** (500 MHz, DMSO-d_6) δ -392; **Raman** (780nm excitation), $\bar{\upsilon}$(cm^{-1}) 1374(s), 1216(vw), 838(w), 800(w), 722(w), 702(w), 662(m), 545(s), 508(w), 473(w), 387(m), 310(s), 250(w); **HRMS (ESI$^+$)**, m/z (98.36%) [M-Cl]$^+$ Calcd for $C_{18}H_{12}ClN_2S_2Sn$, 474.9140; found, 474.9143; m/z (65.80%) [(RS)$_3$Sn, R = 8-quinolinyl]$^+$ Calcd for $C_{27}H_{18}N_3S_3Sn$, 599.9680; found, 599.9664; **Elemental analysis**, Found C 42.26, H 2.44, N 5.32; Calcd. for $C_{18}H_{12}Cl_2N_2S_2Sn$ C 42.39, H 2.37, N 5.49.

8,8'-Dithiodiquinolinium hexachloridostannate, 3.4

Compound **3.2** (1.00 g, 1.52 mmol) was dissolved in methanol (5.00 ml) by slight heating. The yellow coloured solution was filtered, and the filtrate was kept at r.t. for slow evaporation. After 1 week bright yellow coloured crystals of 8,8'-dithiodiquinolinium hexachloridostannate, **3.4** were obtained (0.56 g, 57%). m.p. 173 °C.

ν_{max}(neat)/cm^{-1} 3367(vw), 3271(vw), 3138(vw), 3065(vw), 2951(m), 2373 (vw), 2301(vw), 2108(vw), 1989 (vw), 1918(vw), 1626 (w), 1597 (m), 1544(m), 1404(vw), 1366 (m), 1287(m), 1212 (m), 1005 (vw), 978 (vw), 794 (m), 758 (m), 738(m) , 727(m) , 699 (m), 656 (m), 597(m); ^{1}**H NMR** (500 MHz, DMSO-d_6) δ 9.03 (t, J = 7.0 Hz, 2H), 8.43 (d, J = 8.2 Hz, 2H), 8.00 (d, J = 7.1 Hz, 2H), 7.93 (t, J = 7.7 Hz, 2H), 7.71 – 7.64 (m, 2H), 7.44 (dt, J = 15.3, 7.6 Hz, 2H), 5.77 (s, 2H); ^{13}**C NMR** (500 MHz, DMSO-d_6) δ 150.84, 148.42, 137.29, 136.68, 128.73, 128.03, 127.83, 122.89, 114.92, 55.39; **MS (ESI$^+$)**, m/z (100%) [**Cat**-H]$^+$ Calcd. for $C_{18}H_{13}N_2S_2$, 321.0515; found 321.0507, m/z (97.20%) [**Cat**-2H+Na]$^+$ Calcd. for $C_{18}H_{12}N_2NaS_2$, 343.0334; found 343.0351; **Raman**(780nm excitation), $\bar{\upsilon}$(cm^{-1}) 1595(vw), 1543(vw), 1440(w), 1367(m), 1228(w), 1140(vw), 1068(w), 980(vw), 928(vw), 832(w), 804(w), 720(w), 661(m), 547(m), 525(w), 475(m), 427(w), 393(vw), 313(s), 261(vw), 230(w).

Diquinolyl-8,8'-disulfide, 3.5

Compound **3.2** (1.00 g, 1.52 mmol) was dissolved in excess DMSO (8.00 ml) and heated for 8h at 120 °C in presence of air. The reaction mixture was allowed to cool down to room temperature. Compound **3.5** was obtained as white crystalline solid (0.45 g, 92%). m.p. 204 °C (lit. 206°C)[10].

¹H NMR (500 MHz, CDCl₃) δ 8.98 (dd, J = 4.3, 1.6 Hz, 2H), 8.20 – 8.16 (m, 4H), 7.73 (t, J = 6.2 Hz, 2H), 7.50 (dd, J = 8.2, 4.3 Hz, 2H), 7.32 (t, J = 7.6 Hz, 2H); **¹³C NMR** (500 MHz, CDCl₃) δ 149.69, 148.92, 137.16, 136.33, 128.15, 127.73, 126.85, 121.68, 115.21; **MS (ESI⁺)**, (m/z) [M+H]⁺ Calcd. for $C_{18}H_{13}N_2S_2$, 321.0515; found 321.0635.

3.9 References

1. (a) Prachayasittikul, V.; Prachayasittikul, S.; Ruchirawat, S.; Prachayasittikul, V. *Drug Des Devel. Ther*. **2013**, *7*, 1157. (b) Dholariya, H. R.; Patel, K. S.; Patel, J. C.; Patel, A. K.; Patel, K. D. *Med. Chem. Res*. **2013**, *22*, 5848. (c) Choi, B. Y.; Jang, B. G.; Kim, J. H.; Seo, J. N.; Wu, G.; Sohn, M.; Chung, T. N.; Suh, S. W. *Neurobiol. Dis*. **2013**, *54*, 382. (d) Scattolin, T.; Visentin, F.; Santo, C.; Bertolasi, V.; Canovese, L. *Dalton Trans*. **2016**, *45*, 11560. (e) Rao, H.; Yu, W. -Q.; Zheng, H. -Q.; Bonin, J.; Fan, Y. -T.; Hou, H. -W. *J. Power Sources*. **2016**, *324*, 253.(f) Canovese, L.; Visentin, F.; Scattolin, T.; Santo, C.; Bertolasi, V. *Polyhedron*. **2017**, *129*, 229. (g) Sánchez, A. C.; Santos, C. M.; Padrón, J. M.; Ballesté, R. M.; Ranninger, C. N.; Alemán, J.; Cabrera, S. *J. Inorg. Biochem*. **2017**, *174*, 111.

2. (a) McGrady, M. M.; Tobias, R. S. *J. Am. Chem. Soc*. **1965**, *87*, 1909. (b) Schlemper, E. O. *Inorg. Chem*. **1967**, *6*, 2012. (c) Jain, V. K.; Mason, J.; Saraswat, B. S.; Mehrotra, R. C. *Polyhedron*. **1985**, *4*, 2089. (d) Kawasaki, Y. *Org. Magn. Reson*. **1970**, *2*, 165.

3. Tanaka, T.; Komura, M.; Kawasaki, Y.; Okawara, R. *J. Org. Chem.* **1964**, *1*, 484.

4. Archer, S. J.; Koch, K. R.; Schmidt, S. *Inorg. Chim. Acta*. **1987**, *126*, 209.

5. (a) Fazaeli, Y.; Najafi, E.; Amini, M. M.; Ng, S. W. *Acta Cryst*. **2009**, *E65*, m270. (b) Lo, K. M.; Ng, S. W. *Acta Cryst*. **2009**, *E65*, m719. (c) Chen, Z. F.; Peng, Y.; Gu, Y. -Q.; Liu, Y. -C.; Liu, M.; Huang, K. -B.; Hu, K.; Liang, H. *Eur. J. Med. Chem*. **2013**, *62*, 51.

6. Edinger, A. *Ber. Dtsch. Chem. Ges*. **1908**, *41*, 937.

7. (a) Banfield, J. *J. Org. Chem.* **1960**, *25*, 300. (b) Corsini, A.; Fernando, Q.; Freiser, H. *Anal. Chem*. **1963**, *35*, 1424. (c) Dalziel, J. A. W.; Kealey, D. *Analyst*. **1964**, *89*, 411. (d) Henkel, G.; Krebs, B.; Schmidt, W. *Angew. Chem. Int. Ed.* **1992**, *31*, 1366.

8. Lubenets, V. I.; Stadnitskaya, N. E.; Novikov, V. P. *Russ. J. Electrochem*. **2000**, *36*, 851.

9. (a) Mido, Y.; Sekido, E. *B. Chem. Soc. JPN*. **1971**, *44*, 2127. (b) Lindoy, L. F.; Livingstone, S. E.; Lockyer, T. N. *Aust. J. Chem*. **1966**, *19*, 1391. (c) Pecha, L.; Bankovskis, J.; Kemme, A.; Bel'sky, V.; Silin, E.; Asaks, J. *Chem. Heterocycl. Compd*. **2002**, *38*, 695. (d) Kellö, E.; Vrábel, V.; Lyčka, A.; Sivý, J. *Acta Cryst*. **1993**, *C49*, 1943.

10. Abele, E.; Abele, R.; Lukevics, E. *J. Chem. Research (S)*. **1999**, 624.

11. (a) Otera, J. *J. Organomet. Chem.* **1981**, *221*, 57. (b) Holeček, J.; Nádvorník, M.; Handlíř, K.; Lyčka, A. *J. Organomet. Chem.* **1986**, 315, 299. (c) Schmiedgen, R.; Huber, F.; Preut, H.; Ruisi, G.; Barbierit, R. *Appl. Organomet. Chem.* **199**4, *8*, 397. (d) Tyagi, A.; Kedarnath, G.; Wadawale, A.; Jain, V. K.; Kumar, M.; Vishwanadh, B. *RSC Adv.*, **2015**, *5*, 62882.

12. Wächtler, E.; Gericke, R.; Kutter, S.; Brendler, E.; Wagler, J. *Main Group Met. Chem.* **2013**, *36*, 181.

13. Shannon, R. D. *Acta Crystallogr*. **1976**, *A32*, 751.

14. (a) Rademeyer, M. *Acta Cryst.* 2004, *C60*, m55. (b) Kessentini, A.; Dammak, T.; Belhouchet, M. *J. Mol. Struct.* **2017**, *1149*, 818. (c) Pauling L. *In The Nature of the Chemical Bond*, 3rd ed.; Cornell University Press: Ithaca, NY, **1960**.

15. Yuchi, A.; Shiro, M.; Yasui, T. *Anal. Sci.* **1990**, *6*, 923.

16. Frisch, M. J.; Trucks, G. W.; Schlegel, H. B.; Scuseria, G. E.; Robb, M. A.; Cheeseman, J. R.; Scalmani, G.; Barone, V.; Mennucci, B.; Petersson, G. A.; Nakatsuji, H.; Caricato, M.; Li, X.; Hratchian, H. P.; Izmaylov, A. F.; Bloino, J.; Zheng, G.; Sonnenberg, J. L.; Hada, M.; Ehara, M.; Toyoto, K.; Fukuda, R.; Hasegawa, J.; Ishida, M.; Nakajima, T.; Honda, Y.; Kitao, O.; Nakai, H.; Vreven, T.; Montgomery, J. A., Jr.; Peralta, J. E.; Ogliaro, F.; Bearpark, M.; Heyd, J. J.; Brothers, E.; Kudin, K. N.; Staroverov, V. N.; Kobayashi, R.; Normand, J.; Raghavachari, K.; Rendell, A.; Burant, J. C.; Iyengar, S. S.; Tomasi, J.; Cossi, M.; Rega, N.; Millam, J. M.; Klene, M.; Knox, J. E.; Cross, J. B.; Bakken, V.; Adamo, C.; Jaramillo, J.; Gomperts, R.; Stratmann, R. E.; Yazyev, O.; Austin, A. J.; Cammi, R.; Pomelli, C.; Ochterski, J. W.; Martin, R. L.; Morokuma, K.; Zakrzewski, V. G.; Voth, G. A.; Salvador, P.; Dannenberg, J. J.; Dapprich, S.; Daniels, A. D.; Farkas, O.; Foresman, J. B.; Ortiz, J. V.; Cioslowski, J.; Fox, D. J. Gaussian 09, revision D.01; Gaussian, Inc.: Wallingford, CT, 2013.

17. Nakamoto, K. Editor. *Infrared and Raman Spectra of Inorganic and Coordination Compounds, Part A: Theory and Applications in Inorganic Chemistry, Sixth Edition* **2009** (John Wiley & Sons, Inc.).

18. Allen, F. H. *Acta Crystallogr, Sect B: Struct Sci.* **2002**, *B58*, 380.

19. McPhillips, T. M.; McPhillips, S. E.; Chiu, A. H. -J.; Cohen, E.; Deacon, A. M.; Ellis, P. J.; Garman, E.; Gonzalez, A.; Sauter, N. K.; Phizackerley, R. P.; Soltis, S. M.; Kuhn, P. *J. Synchrotron Radiat.* **2004**, *9*, 401.

20. Kabsch, W. *J. Appl. Crystallogr*. **1993**, *26*, 795.

21. (a) Sheldrick, G. M. *Acta Crystallogr, Sect A: Found. Crystallogr.* **2008**, *64*, 112. (b) Sheldrick, G. Acta Crystallogr., Sect. A: Cryst. Struct. Commun., **2015**, *71*, 3-8. (c) Sheldrick, G. Acta Crystallogr., Sect. C: Fundam. Crystallogr., **2015**, *71*, 3-8.

22. Dolomanov, O. V.; Bourhis, L. J.; Gildea, R. J.; Howard, J. A. K. *J. Appl. Crystallogr.* **2009**, *42*, 339.

23. Cowieson, N. P.; Aragao, D.; Clift, M.; Ericsson, D. J.; Gee, C.; Harrop, S. J.; Mudie, N.; Panjikar, S.; Price, J. R.; Riboldi-Tunnicliffe, A.; Williamson, R.; Caradoc-Davies, T. *J. Synchrotron Radiat.* **2015**, *22*, 187-190.

24. H. S. Lee, *Can. J. Chem.* **1963***, 41,* 1646.

3.10 Supplementary table

Table 3.5. Refinement details for the X-ray structures of **3.2**, **3.3m**, **3.3t**, **3.4**

Compound	3.2	3.3m	3.3t	3.4
Crystal system	Monoclinic	Monoclinic	Triclinic	Monoclinic
Space group	*P2₁/n*	*C2/c*	*P-1*	*P2₁/n*
Empirical formula	$C_{18}H_{16}Cl_6N_2S_2Sn$	$C_{18}H_{12}Cl_2N_2S_2Sn$	$C_{18}H_{12}Cl_2N_2S_2Sn$	$C_{19}H_{16}Cl_8N_2S_2Sn$
Formula weight	655.84	510.01	510.01	738.75
T/K	150(2)	123(2)	123(2)	123(2)
a [Å]	10.2402(11)	15.4999(8)	8.0780(16)	13.870(3)
b [Å]	9.9690(9)	8.4072(4)	9.3260(19)	11.326(2)
c [Å]	12.3557(12)	14.5149(7)	13.252(3)	17.080(3)
α [°]	90	90	96.93(3)	90
β [°]	109.198(12)	107.818(3)	91.63(3)	104.45(3)
γ [°]	90	90	112.90(3)	90
V [A³]	1191.2(2)	1800.72(16)	909.9(4)	2598.2(10)
Z	2	4	2	4
$\rho_{cal}g/cm^3$	1.829	1.881	1.862	1.889
μ/mm⁻¹	1.931	1.951	1.931	1.981
GOF	1.056	1.049	1.039	1.034
2θ range (deg)	5.374 - 49.992	5.896 - 60.518	3.106 - 52.744	4.358 - 63.632
Refs collected	8626	9216	13104	33136
Unique/observed	2091	2683	3693	7332
Parameters	134	114	226	297
R_{int}	0.1026	0.0286	0.0891	0.0368
R_{1,} wR2[I>2σ(I)]	0.0552, 0.1068	0.0215, 0.0484	0.0613, 0.1503	0.0312, 0.0789
R_{1,} wR2[I>2σ(I)]	0.0888, 0.1250	0.0254, 0.0503	0.0675, 0.1569	0.0342, 0.0807

Table 3.6. Comparison of bond lengths (in Å) and bond angles (in °) between X-ray structures and optimized structures of **3.2-3.4**

Compound 3.2

Selected Structural Parameters	X-ray geometry	Optimized geometry
Sn1−Cl3	2.4332	2.529
Sn1−Cl1	2.4121	2.471
Sn1−Cl2	2.4371	2.492
S1−C1	1.772	1.782
Cl1-Sn1-Cl2	90.18	89.63
Cl1-Sn1-Cl3	90.09	89.12
Cl2-Sn1-Cl3	90.57	90.98

Complex 3.3m/3.3t

Selected Structural Parameters	X-ray geometry		Optimized geometry
	3.3m	3.3t	
S1− Sn1	2.4168	2.4401	2.513
S2−Sn1	2.4168	2.4435	2.513
N2− Sn1	2.2876	2.293	2.388
N1− Sn1	2.2875	2.283	2.388
Cl1−Sn1	2.4358	2.4388	2.409
Cl2−Sn1	2.4358	2.4287	2.409
S1−C1	1.7504	1.755	1.761
S2−C18	1.7504	1.765	1.761
N1-Sn1-S1	80.38	80.42	78.13
N2-Sn1-S2	80.38	80.47	78.13
N1-Sn1-Cl1	88.31	90.70	87.66
N2-Sn1-Cl2	88.31	89.96	87.70
N1-Sn1-Cl2	169.12	169.39	162.97
N2-Sn1-Cl1	169.12	167.74	162.94
C1-S1-Sn1	100.25	99.81	100.44
C18-S2-Sn1	100.25	98.92	100.44
Cl1-Sn1-Cl2	91.64	94.48	106.55
N1-Sn1-N2	93.78	86.86	80.07
S1-Sn1-S2	169.35	172.11	165.85

Compound 3.4

Selected Structural Parameters	X-ray geometry	Optimized geometry
Cl1−Sn1	2.4319	2.487
Cl2−Sn1	2.4405	2.602
Cl3−Sn1	2.4640	2.481
Cl4−Sn1	2.4118	2.399
Cl5−Sn1	2.4271	2.397
Cl6−Sn1	2.4208	2.781
S1−S2	2.0554	2.130
S1−C1	1.776	1.785
S2−C10	1.778	1.786
C1-S1-S2	104.85	102.25
C10-S2-S1	103.20	105.15
Cl1-Sn1-Cl2	89.842	86.38
Cl1-Sn1-Cl3	174.52	171.82
Cl1-Sn1-Cl4	91.285	91.45
Cl1-Sn1-Cl5	87.976	93.32
Cl1-Sn1-Cl6	92.78	87.94
Cl2-Sn1-Cl3	88.842	88.58
Cl2-Sn1-Cl4	176.518	164.87
Cl2-Sn1-Cl5	91.41	91.74
Cl2-Sn1-Cl6	86.88	78.56

Cl3-Sn1-Cl4	90.338	91.74
Cl3-Sn1-Cl5	86.74	93.26
Cl3-Sn1-Cl6	92.46	84.75
Cl4-Sn1-Cl5	91.92	103.34
Cl4-Sn1-Cl6	89.77	86.40
Cl5-Sn1-Cl6	178.13	170.12

3.11 Representative Spectra of 3.3t
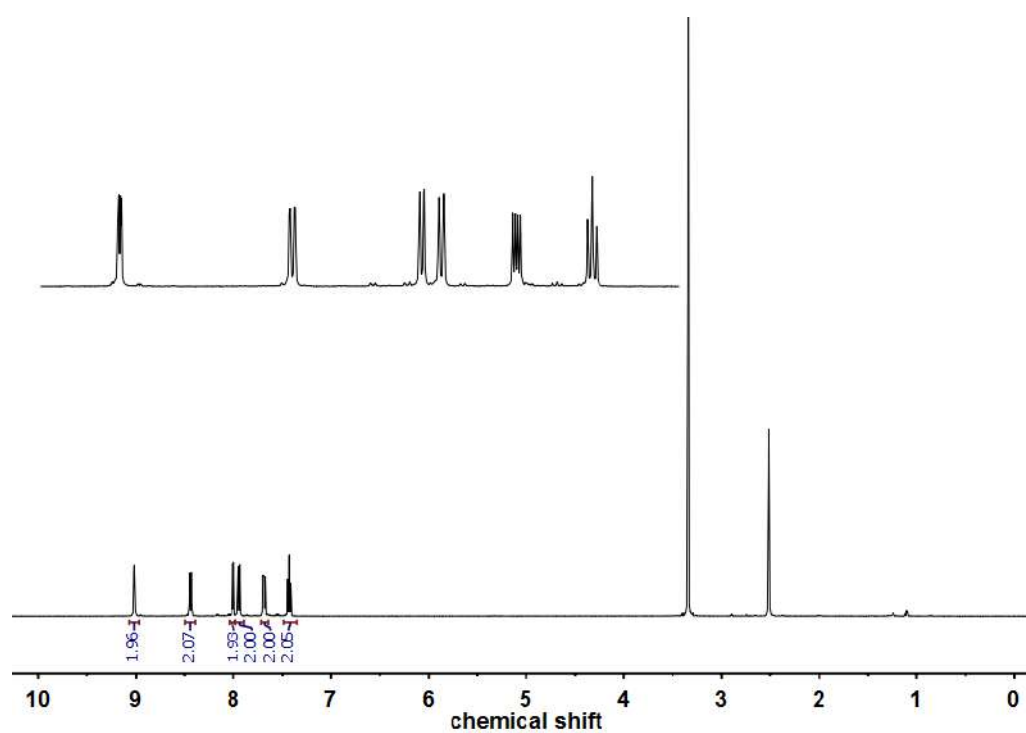
Figure 3.10. ^{1}H NMR Spectrum of **3.3t**.
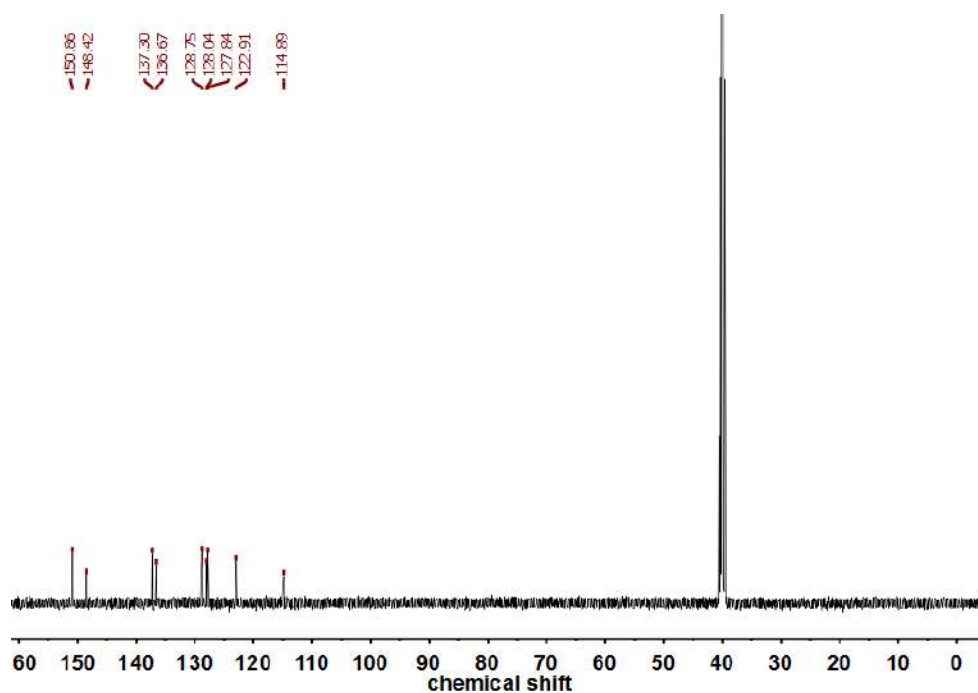
Figure 3.11. ¹³C NMR Spectrum of **3**.**3t.**
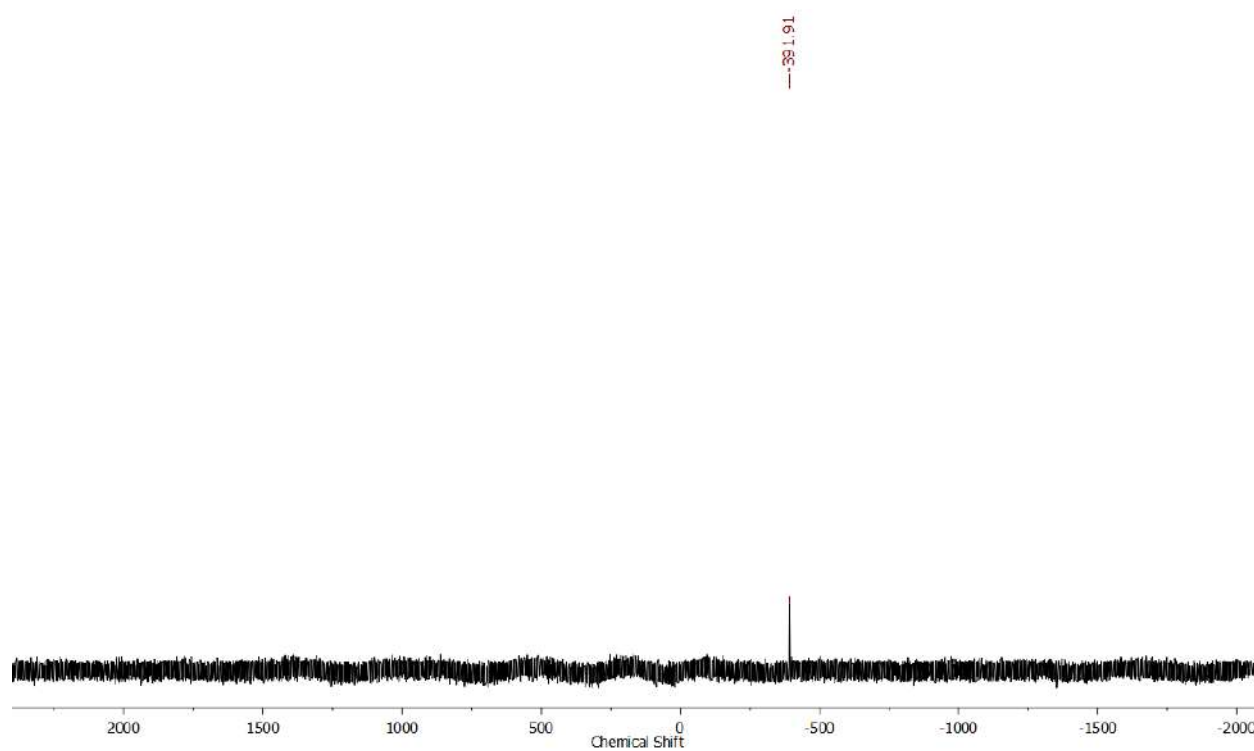
Figure 3.12. ^{119}Sn$\{^1$H$\}$ NMR Spectrum of **3.3t**.
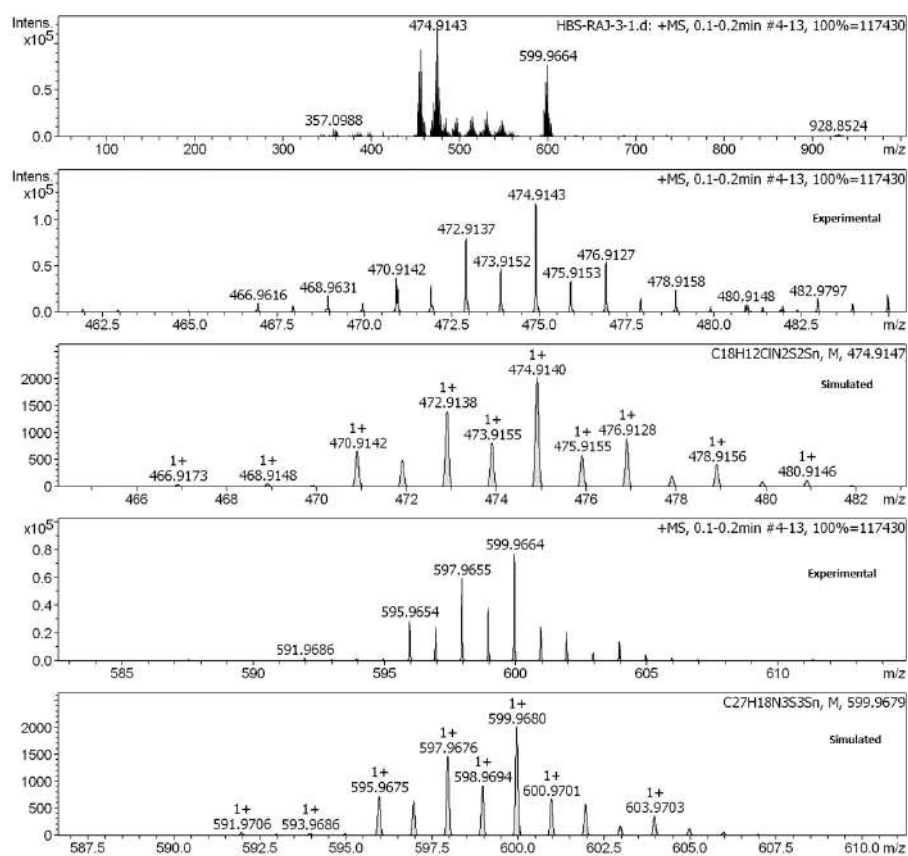
Figure 3.13. ESI-Mass Spectrum of **3.3t**.

4

An Insight into the Redox Activity of Ru and Os Complexes of N,N´-Bis(2-pyridyl)benzene-1,2-diamine Ligand: Structural, Electrochemical and DFT Analyses

4.1 Introduction

Over the last few decades, N, N′-disubstituted 1,2-diaminobenzenes have gained profound interest owing to their expedient applications in various aspects of chemistry, for example, as a building block for supramolecular arrays,[1,2] in synthesizing N-heterocyclic carbenes[3,4] and their analogues such as N-heterocyclic phospheniums,[5] germylenes, stannylenes,[6,7] boroles[8,9] and plumbylenes[10,11] species to name a few. Apart from these notable applications, N, N′-disubstituted 1,2-diaminobenzene derivatives have been considered as one of the preferred choices of ligand frameworks for transition metal complexes.[12] The most intriguing feature of N, N′-disubstituted 1,2-diaminobenzenes as a ligand is their 'redox non-innocent' behavior, a term given by Jørgensen[13] to ligands that have variable, energetically accessible levels that can actively participate in redox processes, giving rise to an apparent ambiguity in oxidation states. Starting from mere academic curiosities, the redox non-innocence of a ligand is now considered to be a fascinating electronic phenomenon and has become a well-appreciated avenue in coordination chemistry.[14] Another interesting development of redox non-innocent ligands is their ability to function as an 'electron reservoir' for assisting multi-electron transformations in metals that have otherwise limited redox activity.[14b,h-j,15] As such, N, N′-disubstituted 1,2-diaminobenzenes can undergo two successive one-electron oxidations, thereby offering variable oxidation states to the bonded metal atom. The dianionic ligand, L^{2-} can undergo one electron oxidation to form the *o*-diiminosemiquinone radical ($L^{\cdot-}$) and the latter can further endure one electron oxidation, thereby resulting into a fully oxidized *o*-diiminoquinone (L^{0}) (Fig. 4.1).
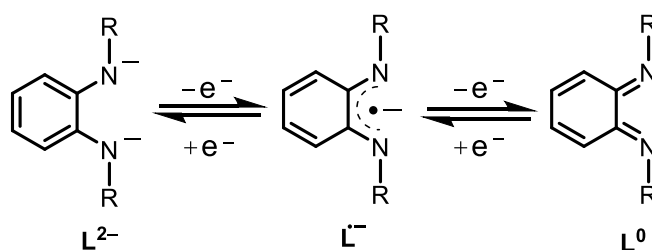

Fig. 4.1. Redox transformations of N, N′-disubstituted 1,2-diaminobenzenes.

It is apparent that modification of the donor atoms or the substituent 'R' in N, N′-disubstituted 1,2-diaminobenzenes can significantly alter the electronic structures of the resulting

metal complexes. For example, when 2-aminothiophenol, where one of the donor atom was replaced with sulfur, was reacted with CpRu^{II}Cl(PPh$_3$)$_2$, the sulfur atom was found to take part in the redox activity of the resulting complex [(PPh$_3$)CpRu^{II}(L)]Cl (where, L = 6-iminocyclohexa-2,4-dienethione) (Chart 4.1, compound **4.1**).[16] Contrastingly, in case of complexes **4.2** and **4.3**, where the flanking arms in *o*-phenylenediamine contain neutral sulfur donor atoms, the redox reactivity was solely localized on the *o*-phenylenediamine backbone and the sulfur being a neutral donor did not take part in the electron transfer processes.[16-17] Interesting redox behavior was also manifested when *o*-phenylenediamine was flanked with phenolate groups. For example, when tetra-dentate ligand, N, N´-bis(3,5-di-tert-butyl-2-hydroxy-phenyl)-1,2-phenylenediamine, was reacted with [Cu(NCCH$_3$)](ClO$_4$) or Zn(BF$_4$)$_2$·2H$_2$O, it was observed that the resulting complexes, **4.4** (M = Cu) and **4.5** (M = Zn) showed redox activity localized on both at the *o*-phenylenediamine backbone as well as on the flanking phenolate groups.[18] Similar results were also observed when the redox behavior of the Mo or Zr complexes of the same ligand were examined.[19,20] However, in case of complex **4.6**, where the the flanking arms in *o*-phenylenediamine was changed to aniline groups the redox activity was only restricted to the flanking aniline groups rather than on the *o*-phenylenediamine backbone.[21] In a recent development, Lahiri and co-workers have reported Ru complexes of N, N´-diphenyl-*o*-benzoquinonediimine embedded with a series of different ancillary ligands. They found that π-acceptor co-ligands such as 2,2'-bipyridine (bpy) in **4.7** and 2-(phenylazo)pyridine (pap) in **4.8** can extend their role to redox activity of the complexes in addition to their typical spectator role.[12i]
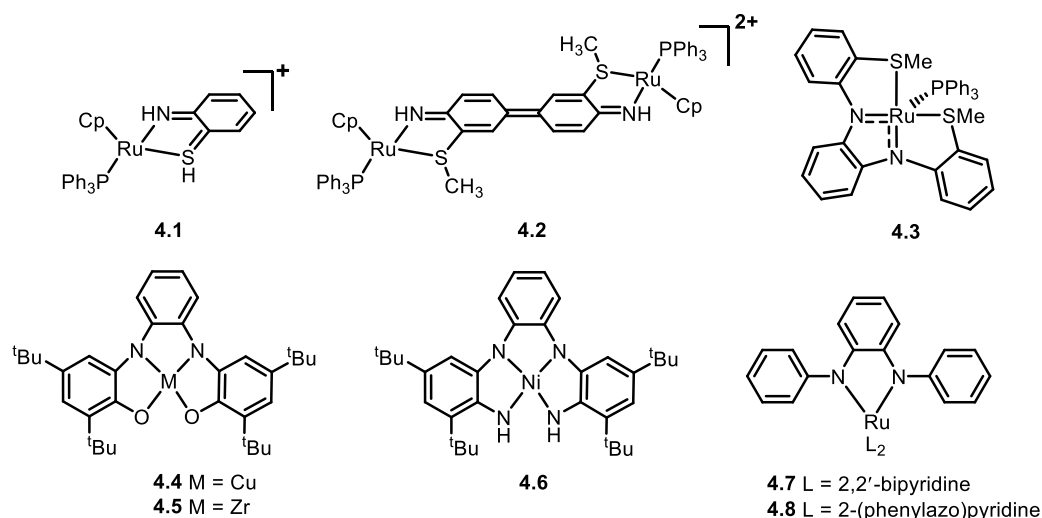
Chart 4.1. Representative examples of metal complexes of N, N′-disubstituted 1,2-diaminobenzene derivatives showing diverse redox behavior.

In the present work, we have incorporated two pyridine rings as flanking arms to *o*-phenylenediamine and have explored the redox innocent properties of the new ligand, namely N, N′-bis(2-pyridyl)benzene-1,2-diamine, **H₂L** with Ru and Os precursors. We anticipated that incorporation of a π-acceptor group to the flanking arms would significantly modulate the redox properties of the resulting complexes. It was further envisaged to compare the electronic structural properties of the synthesized complexes with similar reported complexes wherein different substituents were present in the flanking arms of *o*-phenylenediamine. It is worth mentioning that, although the synthesis of **H₂L** was reported earlier,[22] however, its ligation properties, to our knowledge, have not been explored yet. Thus, the synthesized complexes, **4.9**-[**4.11**]ClO₄ are of considerable interest with respect to their general coordination chemistry as well as the non-innocent behavior of the ligand.

4.2 Results and discussion

Ligand **H₂L** was prepared by following the reported procedure wherein *o*-phenylenediamine was reacted with 2-bromopyridine at 195 °C for 1h.[22] The metal precursors *cis*-[Ru^{II}(acac)₂(CH₃CN)₂],[23] [Ru^{III}(Ph-trpy)(Cl₃)][24] and *cis*-[Os^{II}(bpy)₂Cl₂][25] (*cis* configuration with respect to chlorine, pyridine and nitrogen atoms) [acac = 2,4-pentanedionate, Ph-trpy = 4′-phenyl-2,2′:6′,2″-terpyridine, bpy = 2,2′-bipyridine] were prepared as reported. The mononuclear

complexes [Ru^{III}(acac)$_2$(Py-bqdi)], (**4.9**), [Ru^{II}(Ph-trpy)(Py-bqdi)Cl], (**4.10**) and [Os^{II}(bpy)$_2$(Py-bqdi)](ClO$_4$), ([**4.11**]ClO$_4$), where Py-bqdi = N, N´-dipyridyl-*o*-benzoquinonediimine were synthesized in a single step reaction between the ligand (**H₂L**) and the respective metal precursors; *cis*-[Ru^{II}(acac)$_2$(CH$_3$CN)$_2$], [Ru^{III}(Ph-trpy)(Cl$_3$)] and *cis*-[Os(bpy)$_2$Cl$_2$] respectively in the presence of Et$_3$N in polar protic solvent medium (*e.g.* ethanol or methanol) at elevated temperature (Scheme 4.1). All the synthesized complexes were purified by alumina column chromatography by a gradient elusion with a dichloromethane/acetonitrile mixture.
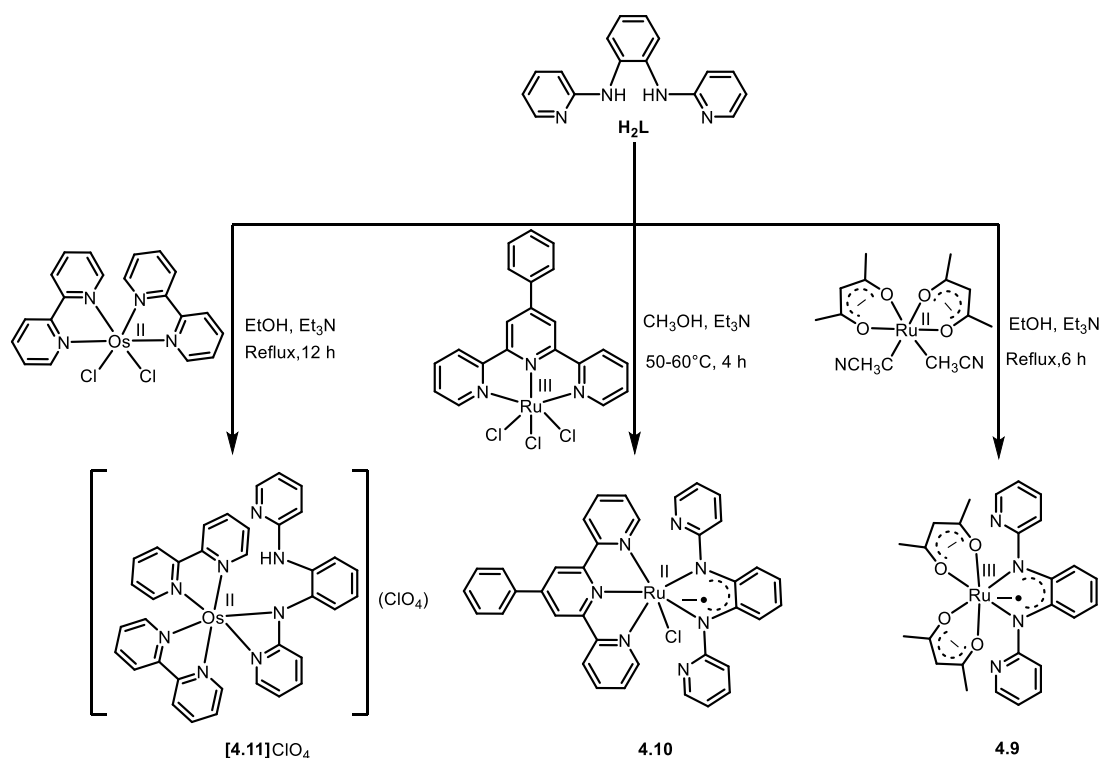
Scheme 4.1. Synthetic route for complexes **4.9**-[**4.11**]ClO$_4$.

The identity of the complexes was validated using various analytical techniques like mass spectrometry (ESI-MS), conductivity, NMR and UV-Vis-NIR spectroscopy, which substantiate the structure of the complexes in their respective electronic states. The molar conductivities show **4.9** and **4.10** are non-electrolytes and [**4.11**]ClO$_4$ is a 1:1 electrolyte. In the ^{1}H NMR spectrum complex **4.9** exhibits aromatic proton resonances corresponding to the ligand (**H₂L**) in the region of 6-8 ppm. A single resonance at 5.08 ppm can be ascribed to the methine proton at the acetylacetonate backbone, while the methyl groups of the acetylacetonate display singlet resonances at 1.86 ppm and 1.85 ppm respectively. On the other hand, complex [**4.11**]ClO$_4$

exhibits overlapping proton resonances corresponding to bipyridine and the ligand respectively in the range 6.5-8.3 ppm. The N-H resonance was not observed in the ^{1}H NMR spectrum, however, ν(N-H) is evident in the IR spectrum.

4.3 Structural elucidation

The identity of complex **4.9** was further validated by single crystal X-ray diffraction study. The single crystals of **4.9** were obtained from the slow evaporation of a solution of **4.9** in a *n*-hexane/chloroform mixture. An ORTEP view of complex **4.9** is shown in Fig. 4.2 and crystallographic data and structure refinement parameters are given in Table 4.4. The spatial arrangement of the Ru(III) ion is distorted octahedral and is defined by a N_2O_4 donor set. Of particular interest are the C1−N1 and C2−N2 distances, which are of 1.335(6) Å and 1.342(5) Å respectively. These bond distances are in good agreement with those observed [1.336(3) Å and 1.346(3) Å] in [Ru^{III}(acac)$_2$(Ph-bqdi)] where Ph-bqdi = N, N´-diphenyl-*o*-benzoquinonediimine.[12i] While comparing the C−N and C−C intra-ring bond distances in **4.9** with the literature values,[12i-j, 26-27] it can be inferred that in complex **4.9**, the ligand is in the semiquinone state (L$^{\bullet-}$). The Ru1−N1 [1.981(4) Å] and Ru1−N2 [1.991(4) Å] bond distances and N1−Ru1−N2 bite angle [79.19(18)°] in **4.9** are comparable to those observed in [Ru^{III}(acac)$_2$(Ph-bqdi)] [Ru1−N1=1.963(2) Å, Ru1−N2=1.982(19) Å and ∠ N1−Ru1−N2=80.10(9)°][12i]. The Ru−O(acac) bond lengths and associated angles are in good agreement with the data observed in related complexes.[28]
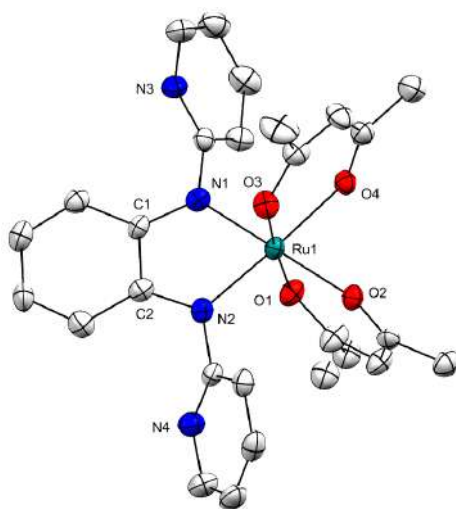

Fig. 4.2. Molecular structure of **4.9**; thermal ellipsoids are set at the 50% probability level.

An ORTEP view of complex **4.10** is shown in Fig. 4.3. Single crystals of complex **4.10** were obtained by slow evaporation of a *n*-hexane/dichloromethane solution. The geometry around Ru(II) ion is distorted octahedral wherein its coordination environment is completed by a N_5Cl donor set. The chloride ligand is *trans* to the N2 atom with a *trans* angle of 172.9(3)°. The C1−N1 bond distance is 1.37(1) Å, which is on the longer side of the C−N double bond values and resembles more that of a C−N distance observed in the fully reduced dianionic catecholate form.[27] On the other hand, the C2−N2 distance of 1.368(1) Å corresponds to a typical C−N double bond. Again, the C1−N1 distance in **4.10** is considerably longer than the C=N distances [1.317(9) Å and 1.316(9) Å] observed in [Ru(trpy)(Cl)(bqdi)]ClO₄ [bqdi = *o*-benzoquinonediimine; trpy = 2, 2′:6′,2′′-terpyridine].[29a] Again, the C1−C6 bond length of 1.42 (1) Å is shorter than normal C−C single bonds. Hence, from these observations, it can be inferred that like in complex **4.9**, the ligand in **4.10** is also in semiquinone state (L$^{\bullet-}$). The Ru1−N1 and Ru1−N2 bond distances are 2.007(8) Å and 1.991 (7) Å respectively, which are in agreement with that of complex **4.9** [1.980(4) Å and 1.991(4) Å] and [Ru(trpy)(Cl)(bqdi)]ClO₄ [1.985(6) Å and 1.991(7) Å].[29a] The N1−Ru1−N2 bite angle of 78.1(3)° is smaller than that observed in **4.9** [79.19(18)°]. The Ru1−Cl1 distance [2.404 (2) Å] and Ru-N (Ph-trpy) distances [Ru1−N5 {2.058 (6) Å}, Ru1−N6 {1.978 (7) Å}, Ru1−N7 {2.080 (6) Å}] of **4.10** are in good agreement with the data reported for related molecules.[29]
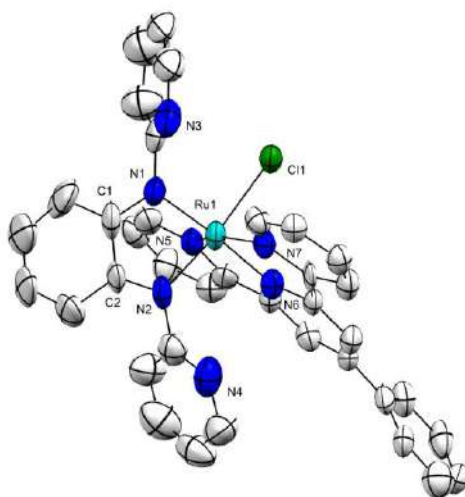

Fig. 4.3. Molecular structure of **4.10**; thermal ellipsoids are set at the 50% probability level.

The molecular structure of complex [**4.11**]ClO$_4$ is shown in Fig. 4.4. Single crystals of complex [**4.11**]ClO$_4$ were obtained by slow evaporation of its *n*-hexane/dichloromethane solution. The geometry of the Os(II) ion is distorted octahedral and is coordinated to one nitrogen atom (N1) of the *o*-phenylenediamine core, one nitrogen atom (N3) from the flanking pyridine group and two bipyridyl ancillary ligands. The remaining positive charge on the Os ion is balanced by a perchlorate counter anion. Interestingly, the second N-<u>H</u> hydrogen of the *o*-phenylenediamine did not undergo deprotonation during the reaction and eventually did not take part in coordination to the metal center. The N1 atom and the pyridyl nitrogen (N3) make a four-membered chelating ring with the Os center with a N1−Os1−N3 bite angle of 62.0(1)°. It is worth noting that complex [**4.11**]ClO$_4$ is the first example of an osmium complex of any benzoquinonediimine ligand, which contains a four-membered chelating ring. Being part of the four-membered chelating ring, this bite angle is significantly smaller than the N1−Os1−N3 angle observed in Os(H$_2$)(HNC$_6$H$_4$NMe)(P^{i}Pr$_3$)$_2$ [76.2(2)°][26] and Os(H$_2$)(HNC$_6$H$_4$NH)(P^{i}Pr$_3$)$_2$ [76.35(15)°][30a], where the nitrogen atoms are part of five-membered chelating rings. The Os1−N1 and Os1−N3 bond distances are 2.146(3) and 2.090(3) Å respectively. The C1−N1 bond distance is 1.411(5) Å. While comparing with the related literature values,[26-28] it can be inferred that this value clearly approaches that of a single bond, and hence the best description of [**4.11**]ClO$_4$ is [Os^{II}(bpy)$_2$(LH$^-$)Cl](ClO$_4$), where the negative charge is localized on the N1 atom. The Os−N (bpy) bond lengths and associated angles are in good agreement with the data observed in related Os(II) complexes.[30]
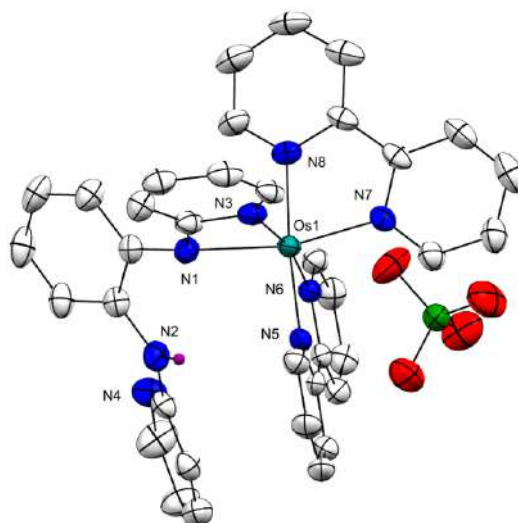
Fig. 4.4. Molecular structure of [**4.11**]ClO$_4$; thermal ellipsoids are set at the 50% probability level.

4.4 Electrochemistry

Electrochemical techniques like cyclic voltammetry and differential pulse voltammetry provide a better perception about accessible redox states within the molecule. Compounds **4.9**, **4.10** and [**4.11**]$^+$ demonstrate one oxidation (O1) and one (R1) or two successive reductions (R2 and R3) waves in the potential range 0.12–1.21 V and −0.43 to −1.71 V versus SCE in CH$_3$CN. The respective electrochemical parameters are represented in Fig. 4.5 and Table 4.1. Appreciable differences in the potentials between the first oxidation (O1) and reduction process (R2), [ΔE = 1.29 V, 1.64 V and 1.56 V, respectively for **4.9**, **4.10** and [**4.11**]$^+$] translate to a high value of the comproportionation constant (K_c) [10^{21}, 10^{27} and 10^{26}], thereby indicating high stability of the native states. Depending on the nature of the donor/acceptor co-ligands, a considerable shift in potentials could be observed for the accessible charged states. In particular, the strong electron donating nature of the acac$^−$ co-ligands in **4.9** makes the first oxidation easier and the first reduction more difficult to access as compared to **4.10** owing to the π-accepting nature of the terpyridine co-ligand. Moreover, the oxidation potential in the pyridine containing benzoquinonediimine complex (**4.9**) shifts to a positive value as compared to the analogous phenyl containing benzoquinonediimine (Ph-bqdi) complex, [Ru(acac)$_2$(Ph-bqdi)][12i], while the

reduction potentials shift to less negative values, an outcome which is attributed to the electron withdrawing nature of the pyridine ring.
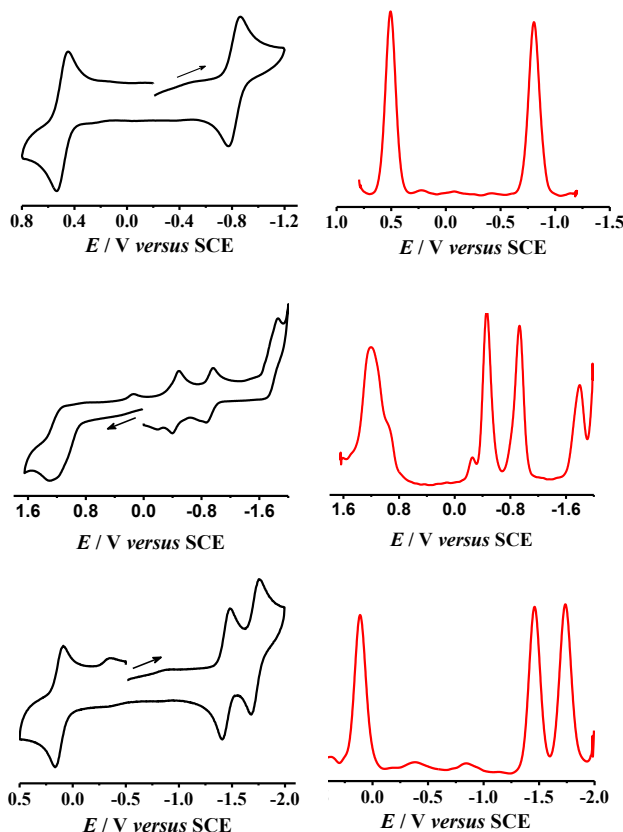

Fig. 4.5. Cyclic (black) and differential pulse (red) voltammograms of (a) **4.9** (b) **4.10** and (c) [**4.11**]ClO$_4$ in CH$_3$CN/0.1 M Et$_4$NClO$_4$.

In complex **4.10**, the irreversible wave corresponding to the Ru^{II}/Ru^{III} oxidation indicates that the oxidized species (**4.10/4.10$^+$**) is not stable on the cyclic voltammetric scale. This is quite similar to the oxidation profile of the previously reported complex [Ru(trpy)(bqdi)].[29a] The effect of the electron accepting nature of the pyridine ring of the pendant arm is evident from the change in electronic potentials as compared to corresponding tpm/trpy [tpm = tris(pyrazolyl)methane, trpy = 2,2′:6′,2″-terpyridine] containing derivatives of benzoquinonediimine.[29a,31a] The first reduction (R1; **4.10/4.10$^-$**) could be associated with the ligand backbone, while the successive reduction (R2; **4.10$^-$/4.10^{2-}**) takes place on trpy based orbitals. These assignments are validated by Mulliken spin density calculations (vide infra) and in agreement with that of the similar reported complexes.[29a,31] The difference in π-donation

capability of osmium and bipyridine could be held accountable for the change in electronic potentials in complex [**4.11**]$^+$. The presence of negative charge derived from the anionic nitrogen atom is primarily responsible for the very low oxidation potential of complex [**4.11**]$^+$ resulting in the formation of a ligand centered radical, while successive reduction processes could be attributed to the presence of low-lying π^*-acceptor orbitals of bipyridine. More precise assignment of oxidation states is discussed with the help of EPR spectroscopy in combination with theoretically computed Mulliken spin density values (*vide infra*).

Table 4.1. Electrochemical data^a for **4.9**-[**4.11**]ClO$_4$ and comparison with related complexes.

Complex	$E°_{298}[V](\Delta E_p[mV])^b$					$K_c{}^c$	
	O2	O1	R1	R2	R3	$K_{c1}{}^e$	$K_{c2}{}^f$
4.9	-	0.48(90)	-0.81(100)	-	-	7.3 x10^{21}	-
4.10	-	1.21(90)	-0.43(90)	-0.92(80)	-1.86^d	6.2 x10^{27}	2.0 x10^8
[**4.11**](ClO$_4$)	-	0.12(70)	-1.44 (80)	-1.71(70)	-	2.7 x10^{26}	3.7 x10^4
[Ru(acac)$_2$(Ph-bqdi)]^g		0.36(60)	-1.05(70)	-	-	7.9 x10^{23}	-
[Ru(acac)$_2$(bqdi)]^h	-	0.53	-0.96	-	-	1.7 x10^{25}	-
[Ru(trpy)(bqdi)]^i	1.32(90)	0.94(70)	-0.54(70)	-0.70(60)	-1.27 (140)		
[Ru(tpm)(bqdi)]^j	-	0.82(80)	-0.79(80)	-1.39^d	-		-

^{a}From cyclic voltammetry in CH$_3$CN/0.1 M Et$_4$NClO$_4$ at 100 mV s^{-1}. ^{b}Potential in V versus SCE; peak potential differences $\Delta E_p[mV]$(in parentheses).^{c}Comproportionation constant from $RT\ln K_c = nF(\Delta E)$. ^{d}Irreversible. $^e K_{c1}$ between O1 and R1. $^f K_{c2}$ between R1 and R2. ^{g} Ph-bqdi= N, N′-diphenyl-*o*-benzoquinonediimine. ^{h}bqdi= *o*-benzoquinonediimne. ^{i}trpy= 2,2′:6′,2″-terpyridine. ^{j}tpm= tris(pyrazolyl)methane

4.5 EPR spectroscopy, spin density analysis and redox series

EPR spectroscopy serves as an indispensable tool for assessing contributions of metal or ligand or mixed metal-ligand of the singly occupied molecular orbitals of paramagnetic states. Hence, precise assignments of oxidation state can be done unambiguously with the help of EPR

spectroscopy in combination with calculated spin densities. Quite expectedly, due to larger values of the spin-orbit coupling constant for the Ru/Os atom as compared to the C, H or N atoms, the *g*-values deviate significantly from the ideal value of 2.0023. The EPR spectra of electrochemically oxidized or reduced states have been recorded in a frozen solution of the samples in CH_3CN at 77K. Representative EPR spectra of paramagnetic states are illustrated in Fig. 4.6 and the values of the respective parameters have been summarized in Table 4.2. The theoretically calculated spin density diagram and respective values are given in Fig. 4.7 and Table 4.3 respectively.
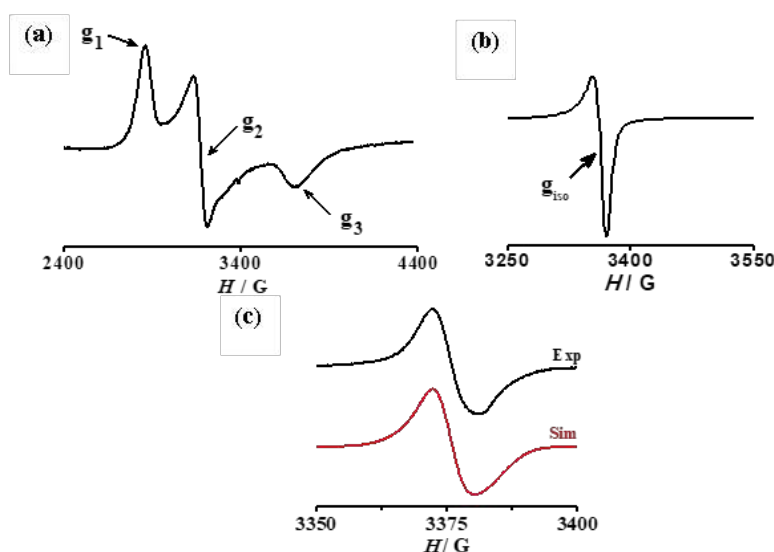
Fig. 4.6. EPR spectra after *in situ* oxidation of (a) [**4.9**], (b) [**4.11**]ClO_4 and native state of (c) [**4.10**] at 77 K in CH_3CN /0.1 M Et_4NClO_4.

Compound **4.9**, designated as $Ru^{III}/Pybq^{•-}$, failed to display any EPR spectrum which might be attributed to the antiferromagnetic coupling between the low-spin Ru(III) (S =½) and the ligand based radical (S = ½). This is clearly reflected in the DFT calculated [Fig. 4.12; Broken symmetry (BS) analysis] Mulliken spin density distributions of Ru: 0.216/0.939, Pybq(L): -0.203/1.012 in singlet/triplet energy states respectively. A preferential stabilization of the singlet state [BS(1,1) S =0] over the triplet state (S =1) could be attributed to significant energy difference between the two states. This is further evident by diamagnetic nature of the ^1H NMR spectrum of **4.9** (*vide supra*). Upon oxidation, it exhibits the characteristic metal-based rhombic EPR signal corresponding to the Ru^{III} (d^5) state as confirmed from the <*g*> value of 2.122 and a large anisotropic parameter of 0.542. Moreover, the 80% contribution (as indicated by Mulliken

spin density calculation) of metal spin in the oxidized state (4.9^+) adds further validation to the ligand-based transformation of $\{Pybq^{\bullet-} \rightarrow Pybq^0\}$ leaving metal center as the sole contributor towards the overall spin.

Table 4.2. EPR Data for the complexes[a]

Complex	g	g_1	g_2	g_3	$\langle g \rangle$[b]	Δg[c]
4.9^+	-	2.369	2.136	1.828	2.122	0.541
4.10	2.003	-	-	-	-	-
4.11^{2+}	2.005	-	-	-	-	-

[a]In CH_3CN/0.1 M Et_4NClO_4.at 125 K, [b]$\langle g \rangle = \{(1/3)(g_1^2 + g_2^2 + g_3^2)\}^{1/2}$, [c]$\Delta g = g_1 - g_3$.
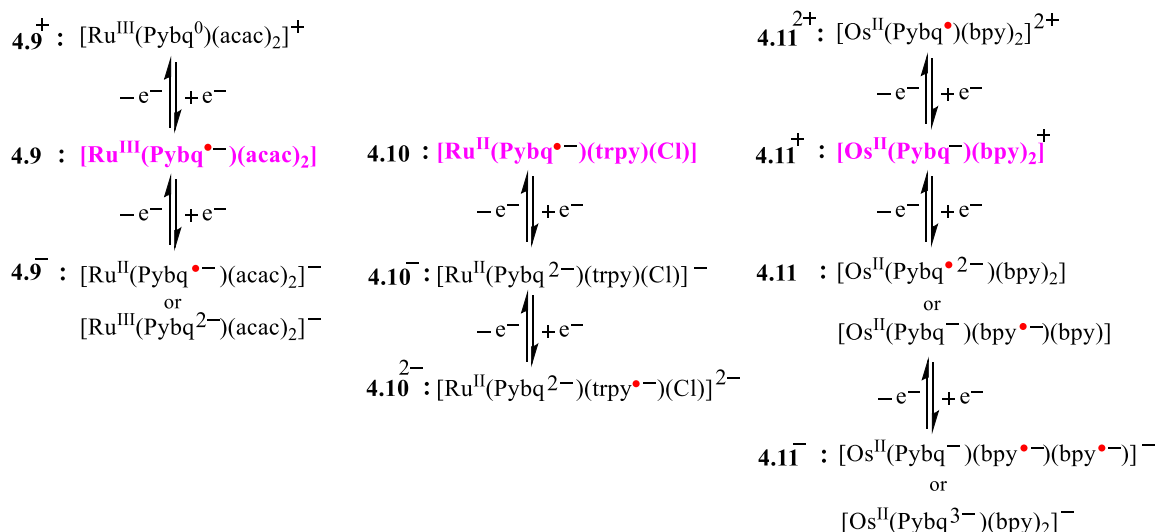
Complex **4.10** exhibits a broad isotropic signal with a g_{iso} value of 2.003, which points towards the formation of a radical anion in the native state $\{Ru^{II}(Pybq^{\bullet-})\}$. The irreversible nature of the oxidation process in the case of complex **4.10**, precludes observation of any EPR spectrum upon oxidation. Upon reduction (R1), no signal was observed quite expectedly due to the doubly reduced dianionic ligand indicating a ligand-based first reduction $\{Pybq^{\bullet-} \rightarrow Pybq^{2-}\}$. While, the successive reduction (R2; **4.10$^-$**/**4.10^{2-}**) takes place on trpy based orbitals, which is substantiated by Mulliken spin density calculations (Table 4.6) and are in agreement with that of the similar reported complexes.[29a, 31] The native state of compound **4.11$^+$** is EPR silent due to the diamagnetic nature of the ground state. The oxidized species, **4.11^{2+}** displays an isotropic EPR signal with a g value of 2.005 along with 71% ligand contribution to overall spin density indicating a ligand-based oxidation process. No EPR signals were observed upon reduction which is expected to be composed of bipyridine ($bpy^{\bullet-}$) based spin.

Table 4.3. DFT calculated Mulliken spin densities for paramagnetic forms of **4.9^n**, **4.10^n** and **4.11^n** (n= −1 to +2)

complexes	Ru/Os	Q(L)	bpy	trpy	acac
4.9$^+$(*S*=1/2)	0.807	0.120	-		0.073
4.9$^-$(*S*=1/2)	0.408	0.578	-		0.014
4.10(*S*=1/2)	0.126	0.715	-	0.159	-
4.11^{2+}(*S*=1/2)	0.244	0.715	0.041		-
4.11(*S*=1/2)	0.260	-0.150	0.890		
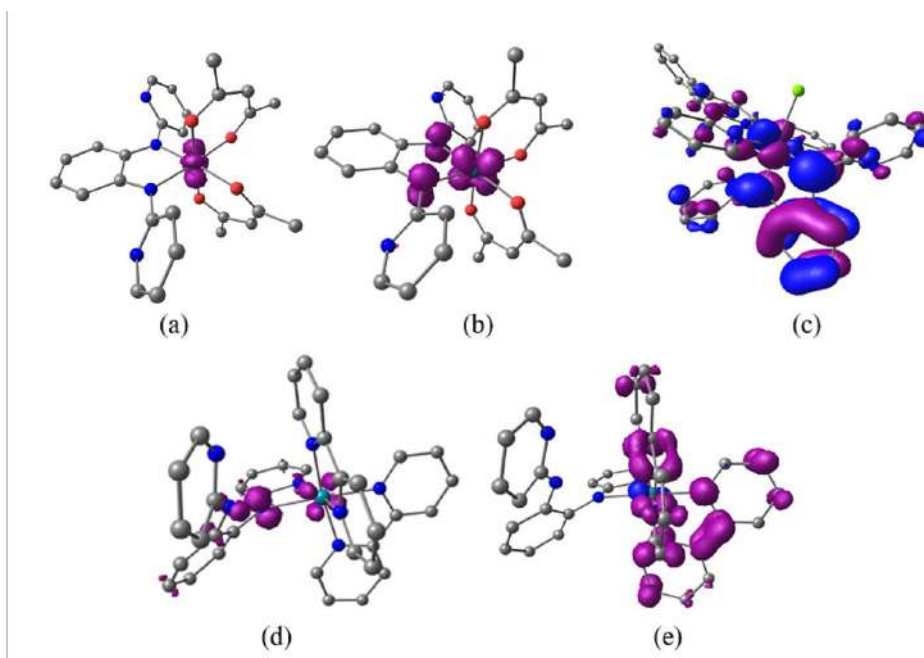
Fig. 4.7. DFT calculated Mulliken spin density plots of (a) **4.9$^+$** (*S*= 1/2) (b) **4.9$^-$** (*S*= 1/2) (c) **4.10** (*S* = 1/2), (d) **4.11^{2+}** (*S*= 1/2) and (e) **4.11** (*S*= 1/2).

Based on these observations obtained by the combined studies of electrochemistry, theoretically formulated Mulliken spin density and EPR spectroscopy, the best possible representations of the redox formulation across the series of complexes [**4.9**, **4.10** and **4.11$^+$**] are depicted in Scheme 2. The native forms are marked in pink.

4.9$^+$: [Ru^{III}(Pybq^0)(acac)$_2$]$^+$

$-e^-$ ⇅ $+e^-$

4.9 : **[Ru^{III}(Pybq$^{\bullet-}$)(acac)$_2$]**

$-e^-$ ⇅ $+e^-$

4.9$^-$: [Ru^{II}(Pybq$^{\bullet-}$)(acac)$_2$]$^-$
or
[Ru^{III}(Pybq^{2-})(acac)$_2$]$^-$

4.10 : **[Ru^{II}(Pybq$^{\bullet-}$)(trpy)(Cl)]**

$-e^-$ ⇅ $+e^-$

4.10$^-$: [Ru^{II}(Pybq^{2-})(trpy)(Cl)]$^-$

$-e^-$ ⇅ $+e^-$

4.10^{2-} : [Ru^{II}(Pybq^{2-})(trpy$^{\bullet-}$)(Cl)]$^{2-}$

4.11^{2+} : [Os^{II}(Pybq$^{\bullet}$)(bpy)$_2$]$^{2+}$

$-e^-$ ⇅ $+e^-$

4.11$^+$: **[Os^{II}(Pybq$^-$)(bpy)$_2$]$^+$**

$-e^-$ ⇅ $+e^-$

4.11 : [Os^{II}(Pybq$^{\bullet 2-}$)(bpy)$_2$]
or
[Os^{II}(Pybq$^-$)(bpy$^{\bullet-}$)(bpy)]

$-e^-$ ⇅ $+e^-$

4.11$^-$: [Os^{II}(Pybq$^-$)(bpy$^{\bullet-}$)(bpy$^{\bullet-}$)]$^-$
or
[Os^{II}(Pybq^{3-})(bpy)$_2$]$^-$

Scheme 4.2. Assignments of oxidation states across the redox series of **4.9^n**, **4.10^n** and **4.11^n** (native forms are marked in pink, the free radicals are depicted on red).

4.6 UV-Vis-NIR spectroscopy

The electronically accessible paramagnetic states of the complexes **4.9**, **4.10** and [**4.11**]$^+$ could be analyzed by controlled potential coulometry in association with UV-vis-NIR spectroscopy (Fig. 4.8). Multiple transitions observed in the region are summarized in Table 4.4, while the nature of the transitions could be assigned on the basis of the TD-DFT calculations (ESI). Compound **4.9**, displays a moderately intense transition at 529 nm which can be described as ligand-to-metal charge transfer (LMCT) involving π-orbitals (L$^{\bullet-}$) of the partially reduced ligand to dπ orbitals of metals. While one electron oxidized species **4.9$^+$** exhibits Ru(dπ)→L(π^*) MLCT band at 556 nm which further validates a ligand based oxidation process as stated before (*vide supra*). Quite obviously presence of the pyridine ring results in a hypsochromic shift of the band position by ~10 nm as compared to the phenyl substituted analogous compound [Ru(acac)$_2$(Ph-bqdi)].[12i]
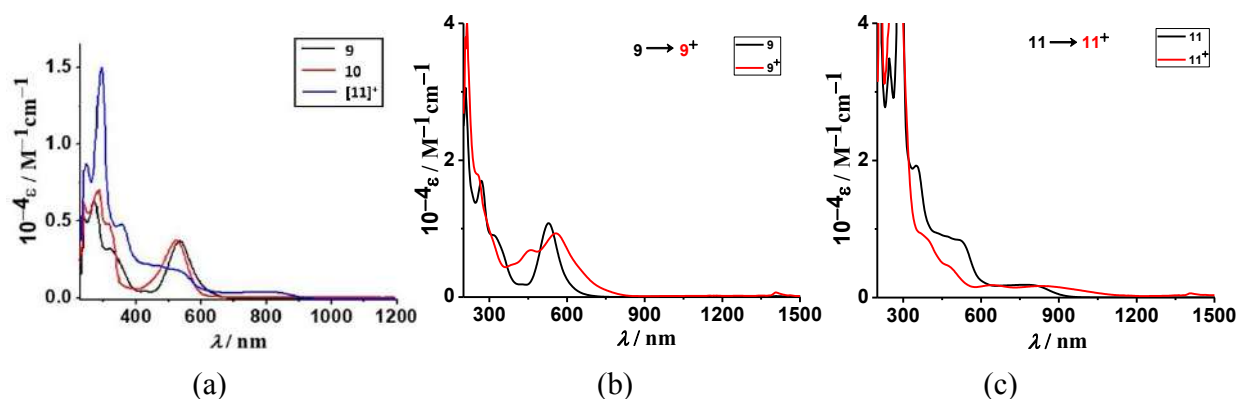
Fig. 4.8. UV-vis-NIR spectra of complexes (a) **4.9** (black), **4.10** (red), and [**4.11**]ClO₄ (blue) in acetonitrile. Spectroelectrochemical responses of (b) **4.9** and (c) **4.11** upon oxidation in CH₃CN / 0.1 M Bu₄NClO₄.

On the other hand compounds **4.10** and [**4.11**]⁺ exhibit absorption bands with high intensity at 521 nm and 528 nm respectively corresponding to the characteristic metal to ligand charge transfer transitions (MLCT), while the appearance of several higher energy peaks can be assigned to ligand-to-ligand charge transfer (LLCT) transitions.[12] Complex [**4.11**]²⁺ displays a broad band corresponding to the $Os(d\pi) \rightarrow L(\pi^*)$ MLCT transition arising out of the generation of a possible radical at the ligand center.

Table 4.4. UV-visible spectral data of **4.9, 4.10,** and [**4.11**]ClO₄ in acetonitrile solutions.

Complex	λ[nm] (ε [M⁻¹cm⁻¹])
4.9	270(17050), 319(9060), 529(10790)
4.9⁺	257(17740), 455(6860), 556(9350)
4.10	284(6920), 317(4770), 521(3760)
[**4.11**]⁺	295(34940), 350(19330), 528(8290), 778(1900)
[**4.11**]²⁺	394(8600), 481(4300),8 56(1730)

It is worth mentioning that a slight disparity in position of the spectral bands on moving from **4.9** to **4.10** to [**4.11**]ClO₄ is mainly due to the variation in σ-donating (acac) and π-acceptor (trpy and bpy) capabilities of ancillary ligands.

4.7 Conclusion

A series of Ru and Os complexes has been synthesized by using the bidentate ligand N, N′-bis(2-pyridyl)benzene-1,2-diamine. The experimental information in combination with theoretical investigations point out the intricate details about the electronic structure formulation of benzoquinonediimine in the presence of π-acceptor pyridyl groups attached to NH arms. Although the exact valence structure formulation of the aforesaid benzoquinonedimine ligand has remained a point of debate in the literature, herein we have highlighted the possible redox states of the metals as well as the ligands in all three complexes. It is observed that due to the incorporation of the π-acceptor pyridyl group, a minor variation in the electronic properties of [Ru(acac)$_2$(Py-bqdi)] has been observed in comparison to that of the similar reported complexes.[12i-j,29a,31] However, due to the combined effect of a π-acceptor 'ph-trpy' co-ligand as well as pyridyl side arms, the effects were more pronounced in [Ru(Ph-trpy)(Py-bqdi)]. The osmium complex, [Os(bpy)$_2$(Py-bqdi)](ClO$_4$) also shows interesting electronic behaviour, wherein it makes use of the negative charge of the mono deprotonated ligand in the native form. Here, the electrochemically induced oxidations are found to be ligand based (71%), while the reductions are purely bpy based (89%). Complex [Os(bpy)$_2$(Py-bqdi)](ClO$_4$) is found to be interesting from the structural point of view, as it involves the formation of a four-membered chelate ring of the ligand with Os metal. It is noteworthy that the formation of a four-membered chelation ring with Os metal centre is the first of its kind for any benzoquinonedimine ligand.

4.8 Experimental section

All the reactions were performed under nitrogen atmosphere by using standard Schlenk techniques and were occasionally monitored by using thin layer chromatography (TLC). The starting materials and solvents were purchased from commercial sources. Solvents were purified by standard techniques.^{1}H (400 MHz and 500 MHz) NMR spectra were recorded on Bruker AV 400 MHz and Bruker AV 500 MHz spectrometers at 25 °C. Chemical shifts are cited with respect to Me$_4$Si as an internal standard for ^{1}H NMR. Electron spray mass spectra (ESI-MS) were carried out using a Q-tof micro (YA-105) mass spectrometer. The electrical conductivities were measured by an autoranging conductivity meter (Toshcon Industries, India). The EPR spectra were recorded on a Bruker EMX Plus instrument. A PAR model 273A electrochemistry system was used to carry out the cyclic voltammetric and differential pulse voltammetric measurements of the complexes. Platinum wire working and auxiliary electrode and an aqueous

saturated calomel reference electrode (SCE) were used in a three-electrode configuration. Tetraethylammonium perchlorate (TEAP) was used as the supporting electrolyte (substrate concentration $\approx 10^{-3}$M; standard scan rate 100 mVs^{-1}). The half-wave potential, $E^0{}_{298}$, was set to equal $0.5(E_{pa}+E_{pc})$, in which E_{pa} and E_{pc} are anodic and cathodic cyclic voltammetry peak potentials, respectively. A platinum wire-gauze working electrode was used for the constant potential coulometry experiments.

Synthesis of [Ru(acac)$_2$(Ph-bqdi)], 4.9

A mixture comprising **H$_2$L**[22] (0.038 g, 0.144 mmol) and NEt$_3$ (0.031 g, 0.306 mmol) in 25 mL EtOH was stirred at room temperature for 15 min under a nitrogen atmosphere. The metal precursor, *cis*-[Ru(acac)$_2$(CH$_3$CN)$_2$][23] (0.055 g, 0.144 mmol) in 15 mL EtOH was added to the reaction mixture which was refluxed for 6 h. After completion of the reaction, solvents were removed under vacuum to get the crude product. The purification was done on a neutral alumina column and the pink colored compound corresponding to **4.9** was obtained by using a CH$_2$Cl$_2$:CH$_3$CN (20:1) solvent mixture as eluent.

Yield: 0.068 g (84%). m. p. 157-159 °C. MS (ESI+, CH$_3$CN): m/z{[**4.9**+H]}$^+$ Calc: 561.10; Found: 561.12. ^{1}H NMR in CDCl$_3$ [δ/ ppm(J/Hz)] $=\delta$ 8.46 (dd, $J = 4.9$, 1.2 Hz, 2H), 7.73 (td, $J = 7.8$, 1.9 Hz, 2H), 7.69 – 7.57 (m, 2H), 7.44 (d, $J = 8.0$ Hz, 2H), 7.30 – 7.22 (m, 2H), 6.78 – 6.75 (m, 2H), 5.08 (s, 2H), 1.87 (d, $J = 3.9$ Hz, 6H), 1.85 (s, 6H). Molar conductivity $\{\Lambda_M\ (\Omega^{-1}\ cm^2\ M^{-1})$, CH$_3$CN}: 8. Anal. Calc. for C$_{26}$H$_{26}$N$_4$O$_4$Ru: C, 55.81; H, 4.68; N, 10.01; Found C, 55.73; H, 4.89; N, 10.17.

Synthesis of [Ru(Ph-trpy)(Ph-bqdi)(Cl)], 4.10

A methanolic solution (15 ml) of **H$_2$L**[22] (0.056 g, 0.213 mmol) and Et$_3$N (0.045 g, 0.448 mmol) was stirred at room temperature for 15 min. The precursor complex, [Ru(Ph-trpy)Cl$_3$][24] (0.110 g, 0.213 mmol) in 10 mL CH$_3$OH was added followed by a heating at 55-60 °C for 4 h. The resulting purple colored solution was then evaporated under reduced pressure to obtain a dark colored solid which was then subjected to a neutral alumina column. The purple colored pure complex **4.10** was obtained by using a CH$_2$Cl$_2$:CH$_3$CN (5:1) solvent mixture as eluent.

Yield: 0.093 g (62%). m. p. 184 °C. MS (ESI+, CH$_3$CN): m/z{[**4.10**]}$^+$ Calc: 706.12; Found: 706.11. Molar conductivity $\{\Lambda_M\ (\Omega^{-1}\ cm^2\ M^{-1})$, CH$_3$CN}: 27. Anal. Calc. for C$_{37}$H$_{27}$ClN$_7$Ru: C, 62.93; H, 3.85; N, 13.88; Found C, 63.07; H, 3.98; N, 14.17.

Synthesis of [Os(bpy)₂(Ph-bqdi)](ClO₄), [4.11]ClO₄

A mixture containing **H₂L**[22] (0.050 g, 0.190 mmol) in 10 mL EtOH and Et₃N (0.040 g, 0.400 mmol) was stirred for 15 min followed by a subsequent addition of metal precursor, [Os(bpy)₂Cl₂][25] (0.109 mg, 0.190 mmol). The resulting mixture was then refluxed overnight. The color of the solution gradually changes from reddish-brown to deep brown. After completion of the reaction, the solution was evaporated and the crude reaction mixture was subjected to a neutral alumina column. The desired brown color band was eluted by a CH_2Cl_2:CH_3CN (4:1) solvent mixture and evaporated to obtain the pure complex [**4.11**]ClO₄.

Yield: 0.114 mg (69%). m. p. 197 °C. MS (ESI+, CH_2Cl_2): m/z{[**4.11**]⁺} Calc: 765.21; Found: 765.22. ¹H NMR in DMSO-d_6 [δ/ ppm (J/Hz)] = δ 8.24 (s, 4H), 8.07 (dd, J = 5.0, 1.2 Hz, 4H), 7.67 – 7.60 (m, 4H), 7.49 (ddd, J = 8.9, 7.2, 2.0 Hz, 4H), 7.07 – 6.99 (m, 4H), 6.76 – 6.63 (m, 8H). FTIR (KBr): ν(N-H) 3390 cm⁻¹, ν(ClO₄⁻) 1089, 622 cm⁻¹. Molar conductivity {Λ_M (Ω^{-1} cm² M⁻¹), CH_3CN}: 114. Anal. Calc. for $C_{36}H_{29}ClN_8O_4Os$: C, 50.08; H, 3.39; N, 12.98; Found C, 49.93; H, 3.18; N, 12.77.

Caution: Perchlorate salt of metal complexes with organic ligands are potentially explosive. Adequate precaution should be taken while handing of such compounds.

4.9 References

1. Bensemann, I.; Gdaniec, M.; Łakomecka, K.; Milewska, M. J.; Połoński, T. *Org. Biomol. Chem*. **2003**, 1, 1425.

2. Bensemann, I.; Gdaniec, M.; Połoński, T. *New J. Chem*. **2002**, *26*, 448.

3. Wang, H.; Xia, Y.; Lv, S.; Xu, J.; Sun, Z. *Tetrahedron Lett*. **2013**, *54*, 2124.

4. Grieco, G.; Blacque, O.; Berke, H. *ActaCryst*. **2011**, *E67*, o2066.

5. Ould, D. M. C.; Rigby, A. C.; Wilkins, L. C.; Adams, S. J.; Platts, J. A.; Pope, S. J. A.; Richards, E.; Melen, R. L. *Organometallics* **2018**, *37*, 712.

6. Krupski, S.; Pöttgen, R.; Schellenberg, I.; Hahn, F. E. *Dalton Trans*. **2014**, *43*, 173.

7. Druzhkov, N. O.; Kazakov, G. G.; Shavyrin, A. S.; Baranov, E. V.; Egorova, E. N.; Piskunov, A. V.; Abakumov, G. A. *Inorg. Chem. Commun*. **2018**, *90*, 92.

8. Weber, L.; Kahlert, J.; Böhling, L.; Brockhinke, A.; Stammler, H. -G.; Neumann, B.; Harder, R. A.; Low, P. J.; Fox, M. A. *Dalton Trans*. **2013**, *42*, 2266.

9. Weber, L.; Halama, J.; Werner, V.; Hanke, K.; Böhling, L.; Chrostowska, A.; Dargelos, A.; Maciejczyk, M.; Raza, A. -L.; Stammler, H. -G.; Neumann, B. *Eur. J. Inorg. Chem*. **2010**, 5416.

10. Hahn, F. E.; Heitmann, D.; Pape, T. Eur. J. *Inorg. Chem*. **2008**, 1039.

11. Heitmann, D.; Pape, T.; Hepp, A.; Mück-Lichtenfeld, C.; Grimme, S.; Hahn, F. E. *J. Am. Chem. Soc*. **2011**, *133*, 11118.

12. (a) Chłopek, K.; Bothe, E.; Neese, F.; Weyhermüller, T.; Wieghardt, K. *Inorg. Chem*. **2006**, *45*, 6298;

   (b) Khusniyarov, M. M.; Weyhermüller, T.; Bill, E.; Wieghardt, K. *Angew. Chem., Int. Ed*. **2008**, *47*, 1228;

   (c) Blackmore, K. J.; Joseph, N. L.; Ziller, W.; Heyduk, A. F.; *J. Am. Chem. Soc*. **2008**, *130*, 2728;

   (d) Samanta, S.; Goswami, S. *J. Am. Chem. Soc*. **2009**, *131*, 924;

   (e) Janes, T.; Rawson, J. M.; Song, D. *Dalton Trans*. **2013**, *42*, 10640;

   (f) Munhá, R. F.; Zarkesh, R. A.; Heyduk, A. F. *Inorg. Chem*. **2013**, *52*, 11244;

   (g) van der Meer, M.; Manck, S.; Sobottka, S.; Plebst, S.; Sarkar, B. *Organometallics* **2015**, *34*, 5393;

(h) Roy, S. K.; Sengupta, D.; Rath, S. P.; Saha, T.; Samanta, S.; Goswami, S. *Inorg. Chem*. **2017**, *56*, 4966;

(i) Das, A.; Ghosh, P.; Plebs, S.; Schwederski, B.; Mobin, S. M.; Kaim, W.; Lahiri, G. K. *Inorg. Chem*. **2015**, *54*, 3376;

(j) Kalinina, D.; Dares, C.; Kaluarachchi, H.; Potvin, P. G.; Lever, A. B. P. *Inorg. Chem*. **2008**, *47*, 10110; and references therein.

(k) Chatterjee, S.; Singh, P.; Fiedler, J.; Baková, R.; Záliš, S.; Kaim, W.; Goswami, S. *Dalton Trans.* **2009**, 7778.

13. Jørgensen, C. K. *Coord. Chem. Rev.* **1966**, *1*, 164.

14. (a) Kaim, W.; Schwederski, B. *Coord. Chem. Rev.* **2010**, 2*54*, 1580;

(b) Chirik, P. J. *Science* **2010**, *327*, 794;

(c) Dzik, W. I.; Zhang, X. P.; de Bruin, B. *Inorg. Chem*. **2011**, *50*, 9896;

(d) Chirik, P. J. *Inorg. Chem*. **2011**, *50*, 9737;

(e) Zhu, D.; Thapa, I.; Korobkov, I.; Gambarotta, S.; Budzelaar, P. H. M. *Inorg. Chem*. **2011**, *50*, 9879;

(f) Kaim, W. *Inorg. Chem*. **2011**, *50*, 9752;

(g) Kaim, W. *Eur. J. Inorg. Chem.* **2012**, 343;

(h) Lyaskovskyy, V.; de Bruin, B. *ACS Catal*. **2012**, *2*, 270;

(i) Praneeth, V. K. K.; Ringenberg, M. R.; Ward, T. R. *Angew. Chem., Int. Ed.* **2012**, *51*, 10228;

(j) Luca, O. R.; Crabtree, R. H. *Chem. Soc. Rev. 2013*, *42*, 1440;

(k) Mandal, A.; Grupp, A.; Schwederski, B.; Kaim, W.; Lahiri, G. K. *Inorg. Chem*. **2015**, *54*, 7396;

(l) Mondal, P.; Das, A.; Lahiri, G. K. *Inorg. Chem*. **2016**, *55*, 1208;

(m) Vijaykumar, G.; Pariyar, A.; Ahmed, J.; Shaw, B. K.; Adhikari, D.; Mandal, S. K. *Chem. Sci*. **2018**, *9*, 2817;

(n) Wada, K.; Sakaushi, K.; Sasaki, S.; Nishihara, H. *Angew. Chem., Int. Ed.* **2018**, *57*, 1.

(o) Storr, T.; Mukherjee, R. *Inorg. Chem*. **2018**, *57*, 9577.

15. (a) Bouwkamp, M. W.; Bowman, A. C.; Lobkovsky, E.; Chirik, P. J. *J. Am. Chem. Soc*. **2006**, *128*, 13340;

(b) Haneline, M. R.; Heyduk, A. F. *J. Am. Chem. Soc*. **2006**, *128*, 8410;

(c) Sylvester, K. T.; Chirik, P. J. *J. Am. Chem. Soc*. **2009**, *131*, 8772;

(d) Smith, A. L.; Hardcastle, K. I.; Soper, J. D. *J. Am. Chem. Soc*. **2010**, *132*, 14358;

(e) Dzik, W. I.; van der Vlugt, J. I.; Reek, J. N. H.; de Bruin, B. *Angew. Chem., Int. Ed*. **2011**, *50*, 3356;

(f) Mukherjee, A.; Sen, T. K.; Ghorai, P. K.; Mandal, S. K. *Sci. Rep*. **2013**, 3;

(g) Kärkäs, M. D.; Åkermark, T.; Chen, H.; Sun, J.; Åkermark, B. *Angew. Chem., Int. Ed***. 2013**, *52*, 4189;

(h) Broere, D. L. J.; Plessiusa, R.; van der Vlugt, J. I. *Chem. Soc. Rev*. **2015**, 44, 6886.

16. Ghosh, P.; Mandal, S.; Chatterjee, I.; Mondal, T. K.; Goswami, S. *Inorg. Chem*. **2015**, *54*, 6235.

17. Durgaprasad, G.; Luna, J. A.; Spielvogel, K. D.; Haas, C.; Shaw, S. K.; Daly, S. R. *Organometallics* **2017**, *36*, 4020.

18. Chaudhuri, P.; Hess, M.; Müller, J.; Hildenbrand, K.; Bill, E.; Weyhermüller, T.; Wieghardt, K. *J. Am. Chem. Soc.* **1999**, *121*, 9599.

19. Hänninen, M. M.; Paturi, P.; Tuononen, H. M.; Sillanpää, R.; Lehtonen, A. *Inorg. Chem*. **2013**, *52*, 5714.

20. Blackmore, K. J.; Lal, N.; Ziller, J. W.; Heyduk, A. F. *J. Am. Chem. Soc*. **2008**, *130*, 2728.

21. Ciccione, J.; Leconte, N.; Luneau, D.; Philouze, C.; Thomas, F. *Inorg. Chem*. **2016**, *55*, 649.

22. Gdaniec, M.; Bensemann, I.; Połoński, T. *ActaCryst*. **2004**, *C60*, o215.

23. (a) Kobayashi, T.; Nishina, Y.; Shimizu, K.; Satô, G. P. *Chem. Lett*. **1988**, 1137;
    (b) Kasahara, Y.; Hoshino, Y.; Shimizu, K.; Satô, G. P. *Chem. Lett*. **1990**, 381.

24. (a) Matias, T. A.; Mangoni, A. P.; Toma, S. H.; Rein, F. N.; Rocha, R. C.; Toma, H. E.; Araki, K. *Eur. J. Inorg. Chem*. **2016**, 5547;
    (b) Benavides, P. A.; Matias, T. A.; Araki, K. *Dalton Trans*. **2017**, *46*, 15567.

25. (a) Lay, P. A.; Sargeson, M.; Taube, H. *Inorg. Synth*. **1986**, *24*, 291;
    (b) Ghosh, B. K.; Goswami, S.; Chakravorty, A. *Inorg. Chem*. **1983**, *22*, 3358.

26. Ferrando-Miguel, G.; Wu, P.; Huffman, J. C.; Caulton, K. G. *New J. Chem*. **2005**, *29*, 193.

27. Bhattacharya, S.; Gupta, P.; Basuli, F.; Pierpont, C. G. *Inorg. Chem*. **2002**, *41*, 5810.

28. (a) Nair, R. B.; Yeung, L. K.; Murphy, C. J. *Inorg. Chem*. **1999**, *38*, 2536;

    (b) Bennett, M. A.; Heath, G. A.; Hockless, D. C. R.; Kovacik, I.; Willis, A. C. *Organometallics* **1998**, *17*, 5867;

    (c) Maji, S.; Sarkar, B.; Mobin, S. M.; Fiedler, J.; Urbanos, F. A.; Jimenez-Aparicio, R.; Kaim, W.; Lahiri, G. K. *Inorg. Chem*. **2008**, *47*, 5204.

29. (a) Maji, S.; Patra, S.; Chakraborty, S.; Janardanan, D.; Mobin, S. M.; Sunoj, R. B.; Lahiri, G. K. *Eur. J. Inorg. Chem*. **2007**, 314;

    (b) Patra, S.; Sarkar, B.; Ghumaan, S.; Patil, M. P.; Mobin, S. M.; Sunoj, R. B.; Kaim, W.; Lahiri, G. K. *Dalton Trans*. **2005**, 1188;

    (c) Chanda, N.; Mobin, S. M.; Puranik, V. G.; Dutta, A.; Niemeyer, M.; Lahiri, G. K. *Inorg. Chem*. **2004**, *43*, 1056;

    (d) Mondal, B.; Puranik, V. G.; Lahiri, G. K. *Inorg. Chem*. **2002**, *41*, 5831;

    (e) Sens, C.; Rodriguez, M.; Romero, I.; Llobet, A. *Inorg. Chem*. **2003**, *42*, 8385;

    (f) Hartshorn, C. M.; Maxwell, K. A.; White, P. S.; DeSimone, J. M.; Meyer, T. J. *Inorg. Chem*. **2001**, *40*, 601;

    (g) Claustro, I.; Abate, G.; Sanchez, E.; Acquaye, J. H. *Inorg. Chim. Acta* **2003**, *342*, 29.

30. (a) Baya, M.; Esteruelas, M. A.; Oñate, E. *Organometallics* **2011**, *30*, 4404;

    (b) Ghosh, P.; Ray, R.; Das, A.; Lahiri, G. K. *Inorg. Chem*. **2014**, *53*, 10695;

    (c) Bhattacharya, S.; Pierpont, C. G. *Inorg. Chem*. **1992**, *31*, 35;

    (d) Gobetto, R.; Nervi, C.; Romanin, B.; Salassa, L. *Organometallics* **2003**, *22*, 4012.

31. (a) Agarwala, H.; Ehret, F.; Dutta, A. C.; Maji, S.; Mobin, S. M.; Kaim, W.; Lahiri, G. K. *Dalton Trans*. **2013**, *42*, 3721;

    (b) Das, A.; Ghosh, T. K.; Chowdhury, A. D.; Mobin, S. M.; Lahiri, G. K. *Polyhedron* **2013**, *52*, 1130.

4.10 Supplementary table

Table 4.4. Refinement details for the X-ray structures of **4.9, 4.10** and [**4.11**]ClO$_4$

Compound	4.9	4.10	[4.11]ClO$_4$
Formula	C$_{26}$H$_{26}$N$_4$O$_4$Ru	C$_{37}$H$_{27}$ClN$_7$Ru	C$_{45}$H$_{38}$ClN$_8$O$_4$Os
Crystal System	Hexagonal	Monoclinic	Triclinic
Space group	*P6$_1$*	*C2/c*	*P-1*
T/K	293(2)	293(2)	293(2)
a [Å]	10.6783(2)	11.4893(9)	11.8605(2)
b [Å]	10.6783(2)	29.335(2)	13.5233(3)
c [Å]	37.8191(7)	24.2604(17)	14.3278(3)
α [°]	90	90	67.070(2)
β [°]	90	97.376(7)	76.321(2)
γ [°]	120	90	67.853(2)
V [A^3]	3734.62(16)	8109.1(11)	1949.49(8)
Z	6	8	2
ρ$_{cal}$g/cm^3	1.493	1.157	1.670
μ/mm^{-1}	0.669	0.483	3.396
GOF	1.071	1.052	1.040
2θ range (deg)	4.404 - 49.992	3.252 – 49.998	3.45- 50
Refs collected	70939	22929	15002
Unique/observed	4377	6979	6844
Parameters	414	416	532
R$_{int}$	0.0902	0.1119	0.0581
R$_1$, wR2[I>2σ(I)]	0.0296, 0.0721	0.0919, 0.2408	0.0326, 0.0717
R$_1$, wR2[I>2σ(I)]	0.0305, 0.0727	0.1463, 0.2968	0.0381, 0.0744

BS(1,1) $S = 0$ **BS(1,1) $S = 1$**

Energy: **-1620.3734138 Hartrees**   **-1620.3618940 Hartrees**

$$\Delta E: E(S=1) - E(S=0) = 2528.3038 \text{ cm}^{-1}$$
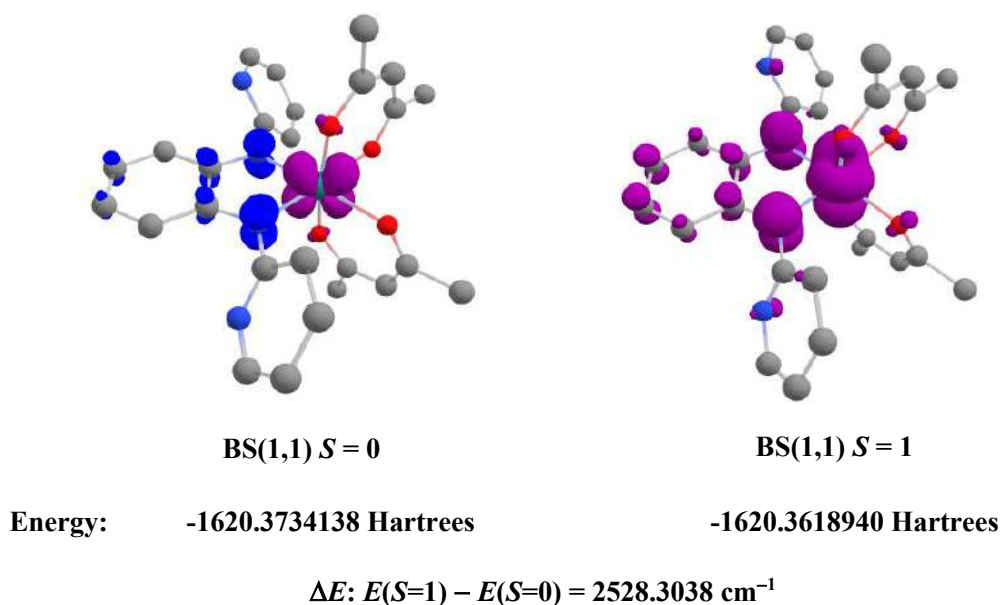
Fig. 4.9. Broken-symmetry calculations for **4.9**.

Table 4.5. Energies of DFT optimized structures of **4.9^n**, **4.10^n** and **4.11^n**.

Complex	E (Hartrees)		$\Delta E_{\text{(HE-LE)}}{}^a$
	$S = 0$	$S = 1$	
4.9	-1620.2877337	-1620.2792849	0.008448 Hartrees 1854.121674 cm^{-1} 22.18022569 kJ/mol
4.10$^+$	-2363.4703366	-2363.4524890	0.017847 Hartrees 3916.9637216 cm^{-1} 46.857302069 kJ/mol
4.10$^-$	-2363.7017708	-2363.6821612	0.019609 Hartrees 4303.67802 cm^{-1} 51.4834334 kJ/mol
4.11^{2-}	-1918.4441264	-1918.4457844	0.001658 Hartrees 363.8889365 cm^{-1} 4.353079332 kJ/mol

^{a}HE = Spin state in higher in energy; LE = Spin state in lower in energy.

Table 4.6. Selected DFT calculated MO compositions of **4.9^n**, **4.10^n** and **4.11^n**.

Complex	MO	fragments	%contribution
4.9 (S=0)	HOMO LUMO	Ph-bqdi/Ru/acac Ru/Ph-bqdi/acac	61/32/07 62/19/19
4.9$^+$ (S=1/2)	β-LUMO	Ph-bqdi/Ru/acac	69/19/12
4.9$^-$ (S=1/2)	SOMO	Ph-bqdi/Ru/acac	74/21/05
4.10 (S=1/2)	SOMO β-LUMO	Ph-bqdi/Ru/Ph-trpy/Cl Ph-trpy/Ru/Ph-bqdi/Cl	69/21/08/01 88/06/05/01
4.10$^+$ (S=0)	LUMO	Ph-bqdi/Ru/Ph-trpy/Cl	70/23/06/02
4.10$^-$ (S=0)	HOMO LUMO	Ph-bqdi/Ru/Ph-trpy/Cl Ph-trpy/Ru/Ph-bqdi/Cl	75/13/11/00 82/14/03/02
4.10^{2-} (S=1/2)	SOMO	Ph-trpy/Ru/Ph-bqdi/Cl	79/15/05/01
4.11$^+$ (S=0)	HOMO LUMO	Ph-bqdi/Os/bpy bpy/Os/ Ph-bqdi	80/12/08 92/06/02
4.11^{2+} (S=1/2)	β-LUMO	Ph-bqdi/Os/bpy	67/23/10
4.11 (S=1/2)	SOMO α-LUMO	bpy/Os/ Ph-bqdi bpy/Os/ Ph-bqdi	92/06/02 82/15/03
4.11$^-$ (S=1)	SOMO	bpy/Os/ Ph-bqdi	80/16/04
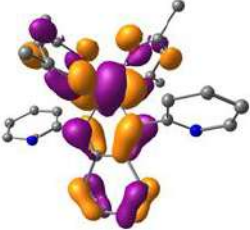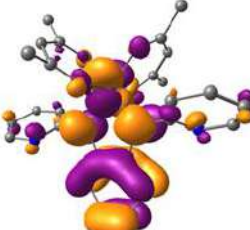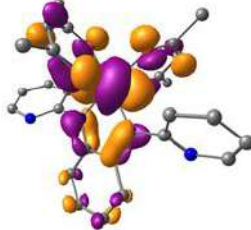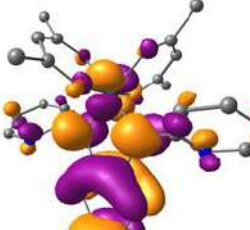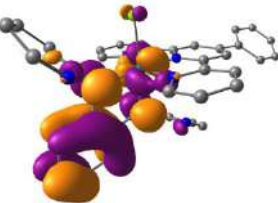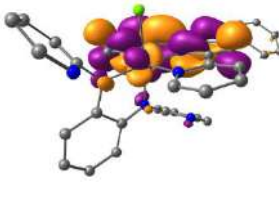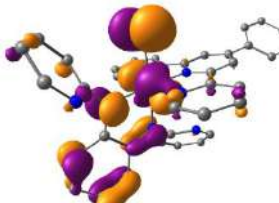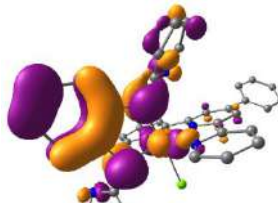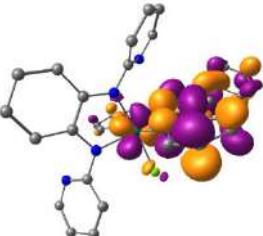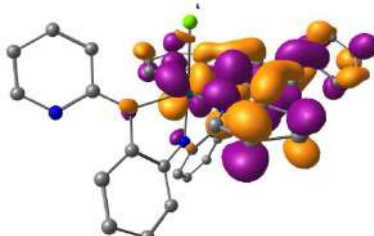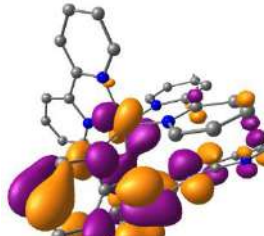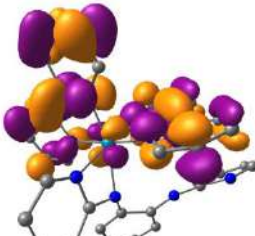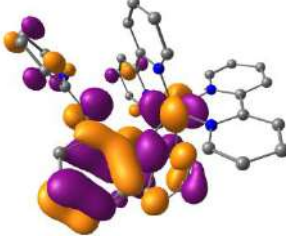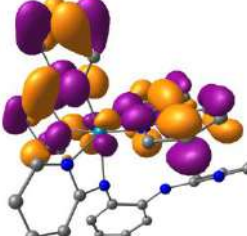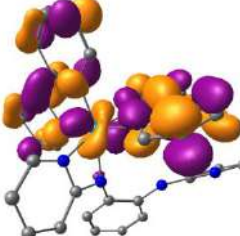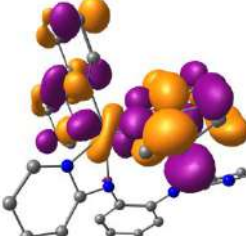
4.9 (HOMO)	**4.9** (LUMO)	**4.9**$^+$(β-LUMO)	**4.9**$^-$(SOMO)
4.10 (SOMO)	**4.10** (β-LUMO)	**4.10**$^+$(LUMO)	**4.10**$^-$(HOMO)
4.10$^-$(LUMO)	**4.10**$^{2-}$(SOMO)	**4.11**$^+$(HOMO)	**4.11**$^+$(LUMO)
4.11^{2+}(β-LUMO)	**4.11** (SOMO)	**4.11**(α-LUMO)	**4.11**$^-$(SOMO)

Table 4.7. Experimental and TD-DFT calculated electronic transitions for **4.9**[n], **4.10** and **4.11**[n].

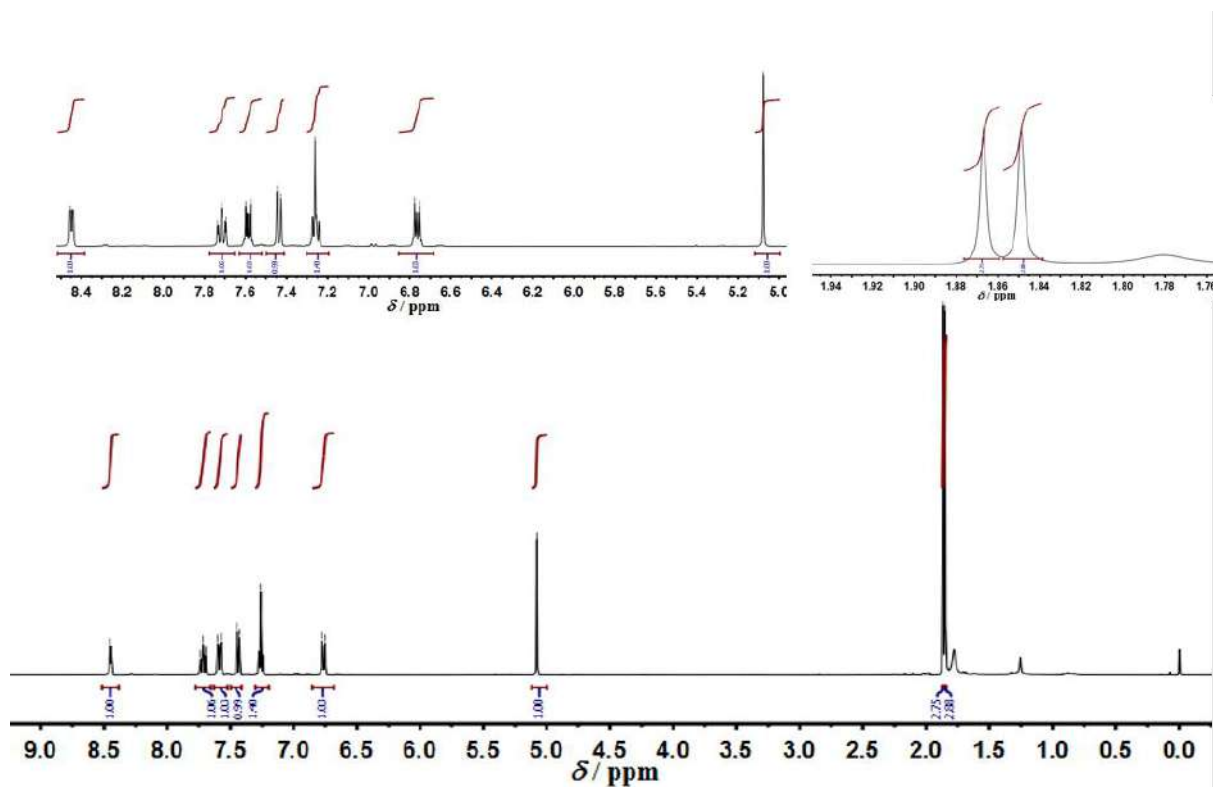| λ/nm expt. (DFT)	ε /$M^{-1}cm^{-1}$ (f)	Key transition	Character
4.9 (*S*=0)			
529(582)	10790(0.14)	HOMO-2→LUMO(0.64)	Ru(dπ)/Py-bqdi(π)/acac(π)→Py-bqdi(π*)/Ru(dπ)
319(327)	9060(0.05)	HOMO-1→LUMO+2(0.62)	Ru(dπ)/acac(π)→Py-bqdi(π*)
270(293)	17050(0.02)	HOMO-1→LUMO+4(0.61)	Ru(dπ)/acac(π)→acac(π*)
4.9[+] (*S*=1/2)			
556(539)	9350(0.02)	HOMO-2(α)→LUMO(α)(0.78)	Py-bqdi(π)/Ru(dπ)→Py-bqdi(π*)
455(475)	6860(0.06)	HOMO-3(α)→LUMO(α)(0.73)	Ru(dπ)/Py-bqdi(π)→Py-bqdi(π*)
257(303)	17740(0.02)	HOMO-1(β)→LUMO+3(β)(0.53)	acac(π)/ Py-bqdi(π)→acac(π*)
		HOMO(β)→LUMO+2(β)(0.53)	acac(π)/ Py-bqdi(π)→Py-bqdi(π*)
4.10 (*S*=0)			
521(522)	3760(0.02)	HOMO-1(β)→LUMO+2(β)(0.85)	Ru(dπ)/Cl(π)→Py-bqdi(π*)
317(342)	4770(0.01)	HOMO-2(β)→LUMO+4(β)(0.60)	Ru(dπ)/Py-bqdi(π)→Py-trpy(π*)
284(310)	6920(0.06)	HOMO-4(β)→LUMO+2(β)(0.53)	Py-bqdi(π)/Cl(π)→Py-bqdi(π*)
4.11[+] (*S*=0)			
778(711)	1900(0.01)	HOMO→LUMO(0.98)	Py-bqdi(π)→bpy(π*)
528(536)	8290(0.02)	HOMO-2→LUMO(0.56)	Os(dπ)→bpy(π*)
350(367)	19330(0.06)	HOMO-1→LUMO+4(0.53)	Py-bqdi(π)/ Os(dπ)→bpy(π*)
295(297)	34940(0.09)	HOMO-6→LUMO(0.60)	Py-bqdi(π)→bpy(π*)
4.11[2+] (*S*=1/2)			
856(781)	1730(0.08)	HOMO-3(β)→LUMO(β)(0.97)	Py-bqdi(π)/ Os(dπ)→Py-bqdi(π*)
481(473)	4300(0.01)	HOMO-1(α)→LUMO(α)(0.51)	Py-bqdi(π)/ Os(dπ)→Py-bqdi(π*)
394(383)	8600(0.02)	HOMO(α)→LUMO+2(α) (0.64)	Py-bqdi(π)/→bpy(π*)

4.11 Representative Spectra

Fig. 4.10. ^{1}H NMR spectrum of complex **4.9**. Inset showing expanded aromatic and aromatic region.

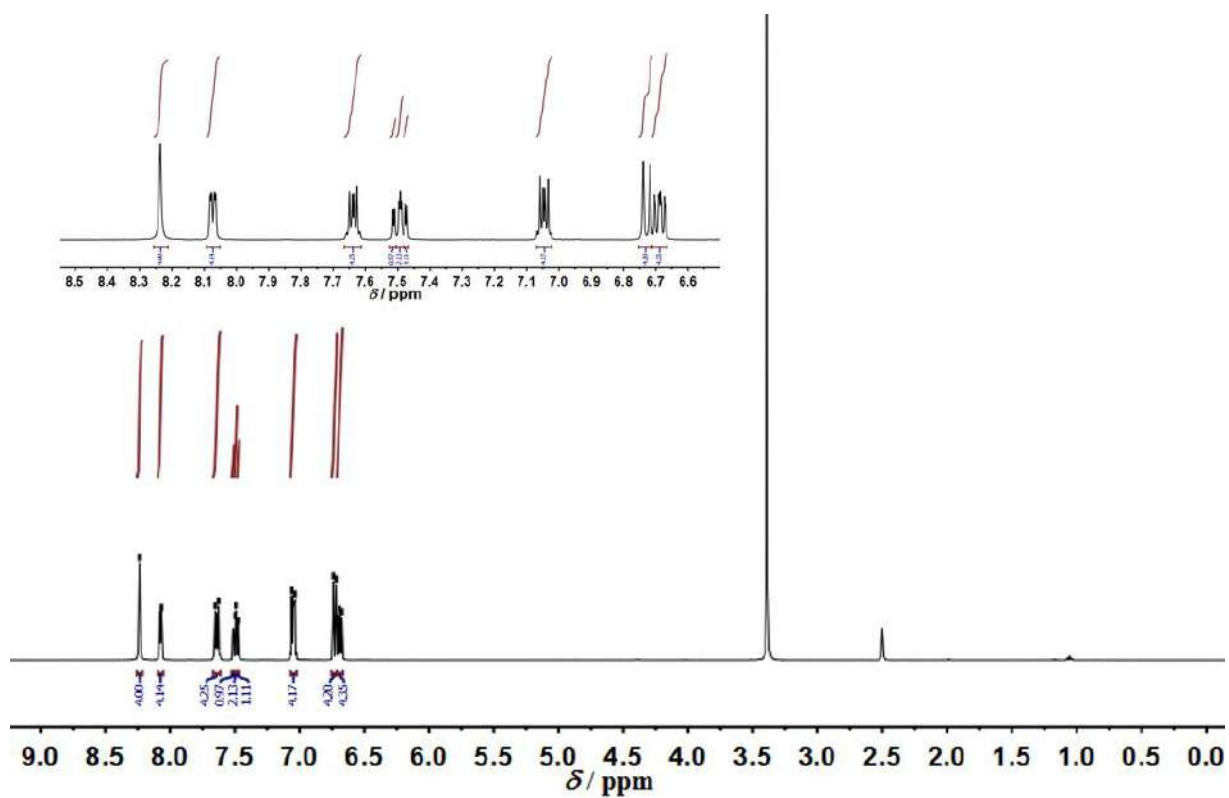**Fig. 4.11.** ^{1}H NMR spectrum of **[4.11]**(ClO₄). Inset showing expanded aromatic region.
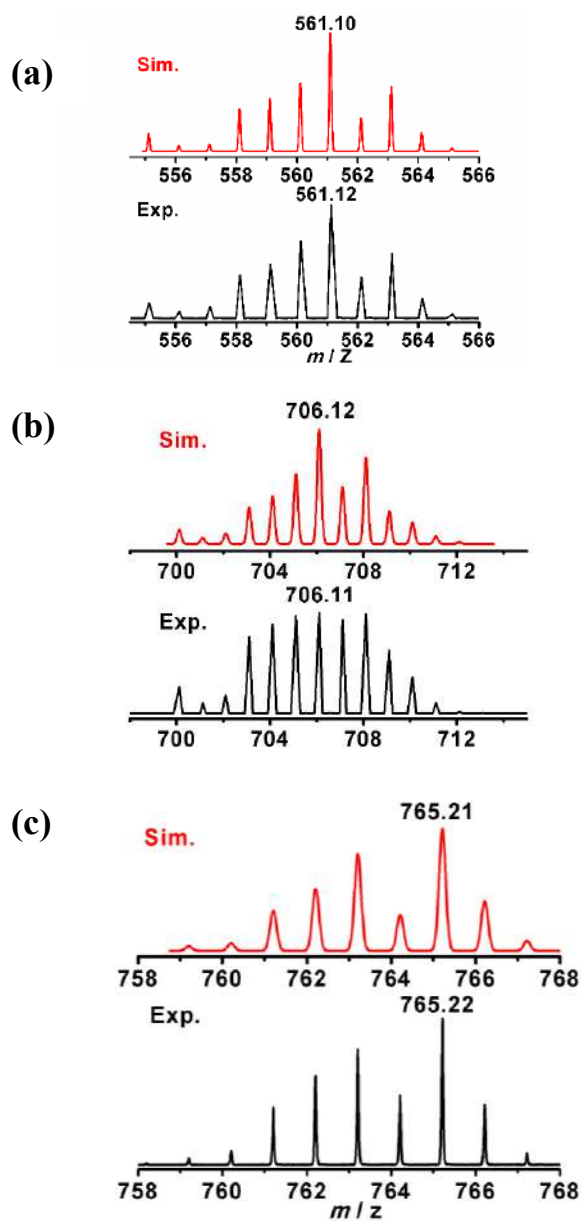
Fig. 4.12. ESI-mass spectra (positive mode) of (a) **4.9**, (b) **4.10** and (c) [**4.11**]$^+$ in CH$_3$CN. (experimental spectra are depicted in black, simulated patterns are depicted in red)

5

Synthesis and Characterization of Pyrrole Based NNN-Pincer Ligands and their Complexes

5.1 Introduction

'Pincer ligands' are a class of ligands consisting of donor atoms which are capable of coordinating in a tridentate manner to the central metal atom, thus, giving rise to the phenomenon of chelation. *Pincer* literally means the presence of blunt ends for gripping things, which is what the donor atoms in the ligand do, *i.e.,* hold the central metal atom in a particular coordination mode (preferably meridionally). Chelation makes the structure versatile enough to modify them and provide the dual combination of stability as well as reactivity with metal complexes; both of which are crucial in coordination chemistry. Throughout the past few decades, the chemistry of pincer ligands has been unambiguously developed to be one of the most exciting and esteemed field of organometallic chemistry.[1-5] In fact, during the last few years, several landmark discoveries have been achieved from the chemistry of pincer ligands with different metals.[6-18] The chemistry of pincer ligand was brought to light by Moulton *et al.*, in 1976 whereby they synthesized a series of transition metal (Ni, Pd, Pt, Rh, Ir) complexes stabilised by PCP-tridentate pincer ligand.[19] Succeeding report was by van Koten *et al.*, in 1978 wherein they introduced the family of NCN-pincer ligand.[20]

Of late, amidst various pincer ligands, NNN-pincer ligands based on pyrrole framework have drawn significant interest with respect to their interesting structural properties and applications. Some of the recent developments on pyrrole based NNN-pincer ligands and their complexes, especially with respect to their synthetic strategies and applications are outlined here. For example, in 2000, Huang *et al.*, first reported the synthesis of 2,5-bis[(dimethylamino)methyl]pyrrolate zirconium complex **5.1** by treating tetrakis(diethylamido)zirconium with 2,5-bis[(dimethylamino)methyl)]pyrrole (Scheme 5.1).[21]
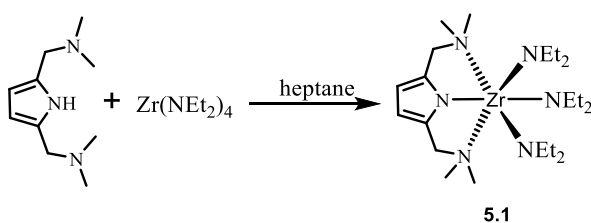

Scheme 5.1. Synthesis of Zr complex **5.1**.

In the succeeding year, they extended the work to synthesise aluminium complex **5.2** of the same pincer ligand.[22] They further isolated aluminium dimethyl complex **5.3** by alkylating **5.2** with methyl iodide. (Scheme 5.2).
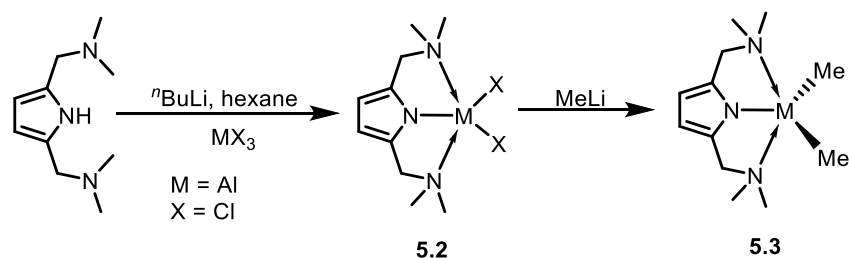
Scheme 5.2. Synthesis of Al complexes of NNN-pincer ligands 2,5-bis[(dimethylamino)methyl)]pyrrole.

The coordination chemistry of 2,5-bis[(dimethylamino)methyl)]pyrrole with other group 13 elements (Ga, In) was also reported by reacting the lithiated ligand with the respective metal halides (Scheme 5.3).[23] Reactions of complexes, **5.4a-b** with alkyl lithium afforded dialkylated complexes, **5.5a-b**. It was further observed that **5.4b** has the tendency to act as Lewis acid, as it can easily accept water molecules when exposed to open atmosphere, thereby affording water-bridged complex, **5.6**.
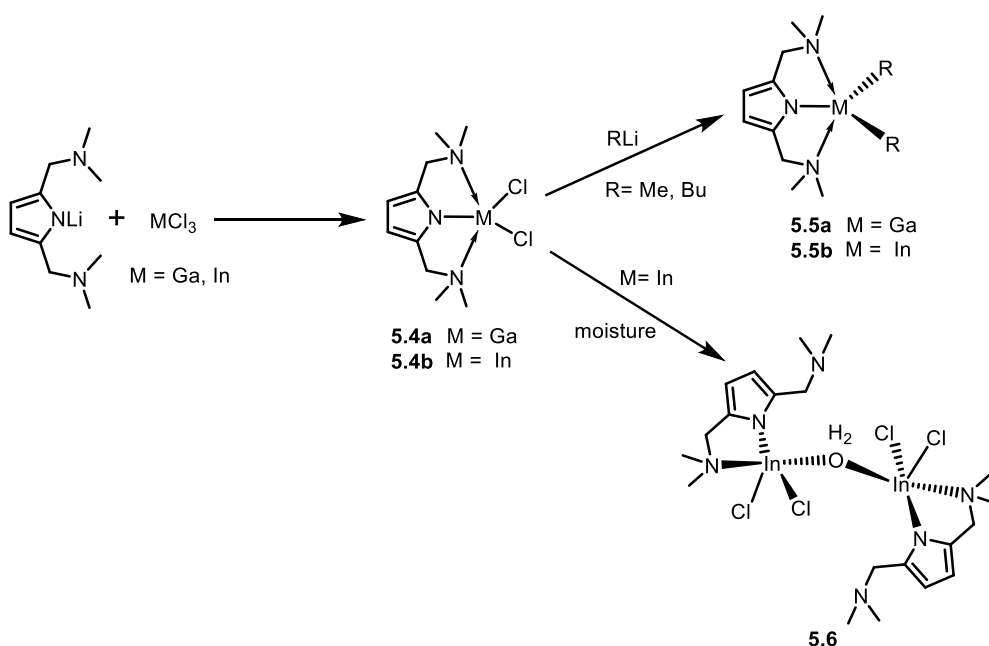
Scheme 5.3. Synthesis of five coordinated gallium and indium complexes **5.5a-b**, **5.6a-b** stabilized by NNN-pincer ligand.

In 2005, Banerjee *et al.*, have synthesized titanium pyrrolyl complex [$C_4H_2N(2,5-CH_2NMe_2)_2$]Ti(NEt$_2$)$_3$, **5.7** by treating 2,5-bis[(dimethylamino)methyl)]pyrrole with Ti(NMe$_2$)$_4$ (Scheme 5.4).[24] From the solid state structure of complex **5.7**, it was observed that only one side arm was coordinated to the metal centre, while the other arm remained free.
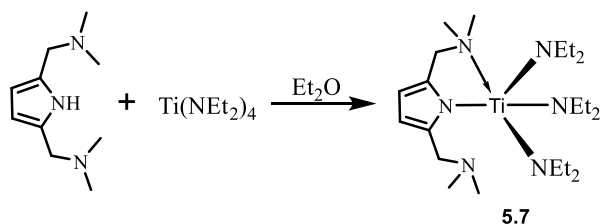
Scheme 5.4. Synthesis of titanium pyrrolyl complex $[C_4H_2N(2,5-CH_2NMe_2)_2]Ti(NEt_2)_3$, **5.7**.

The titanium complex, **5.7** has been used as an effective catalyst for a new class of multi-component coupling reaction involving alkyne, hydrazine and isonitrile named as *iminohydrazination of alkynes* (Scheme 5.5). The catalytic activity of $[C_4H_2N(2,5-CH_2NMe_2)_2]Ti(NEt_2)_3$ in *iminohydrazination* was examined with different substrates and it was observed that it holds wide scope for being used in internal and terminal alkynes, alkyl and aryl isonitriles and alkyl- and aryl-containing 1,1-disubstitutedhydrazines.
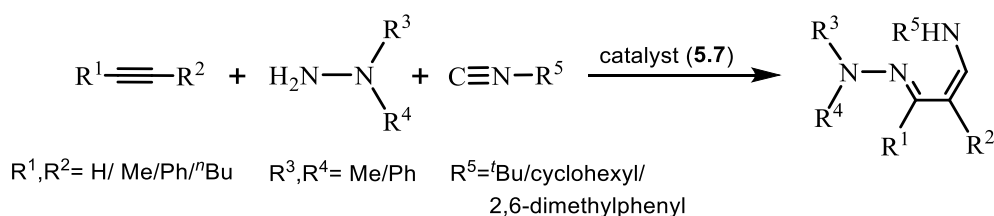

Scheme 5.5. The general outline of "iminohydrazination of alkynes" catalyzed by **5.7**.

Recently, Lee and co-workers have reported a series of zirconium and hafnium complexes of 2,5-bis[(dimethylamino)methyl)]pyrrole (Scheme 5.6). They have further reported the applicability of these complexes in ring opening polymerisation of ε-caprolectum.[25] Reactions of 2,5-bis[(dimethylamino)methyl)]pyrrole with $M(NEt_2)_4$ (M = Zr/Hf) afforded complexes **5.8a-b** which on further treatment with 2,6-di-tert-butylphenol, *tert*-butanol resulted in the formation of complexes **5.9a-b** and **5.10a-b** respectively. It is worth noting that due to the presence of multiple reactivity centres, complexes **5.9a-b** and **5.10a-b** can act as initiators for ring opening polymerization of ε-caprolectum.
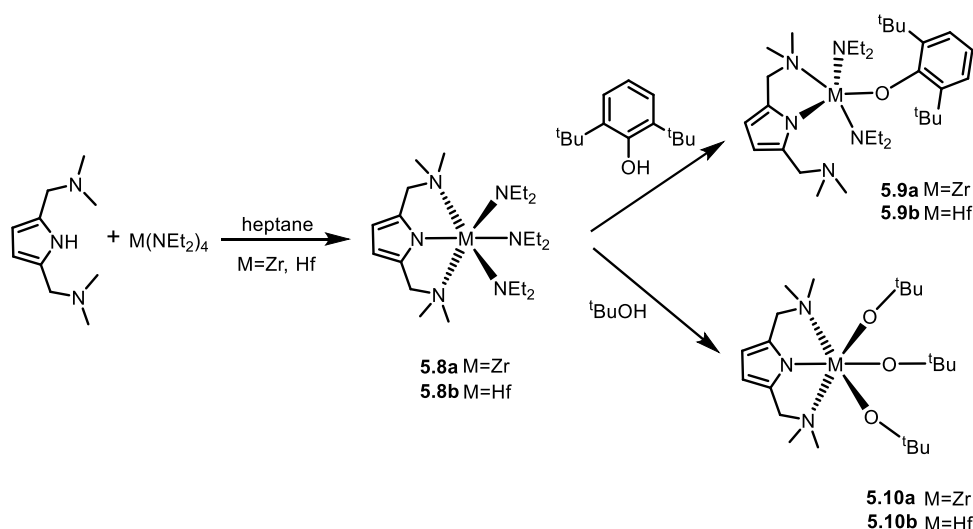
Scheme 5.6. Synthesis of zirconium and hafnium alkoxide and amide complexes of 2,5-bis[(dimethylamino)methyl)]pyrrole.

Stalke and co-workers have changed the side arms of the pyrrole ring from dimethyl amine to pyrrolidine and reported a new pyrrole based pincer ligand namely, 2,5-bis[(pyrrolidino)methyl]pyrrole. They have utilised this ligand for synthesising complex, **5.11a-c** with group 14 elements (Ge, Sn, Pb) (Scheme 5.7) and performed theoretical studies to explore the bonding between metal and pyrrole nitrogen atom.[26] The theoretical studies unveil that the pyrrole pincer ligand binds to the metal with covalent bond. In addition to that, there is substantial π-back donation from pyrrole to metal which causes decrease in the aromaticity of the pyrrole in the metal complexes as compared to the ligand. At the same time, there is coordination from the two donors of chelating arms, which further stabilizes the pyrrole metal bond. They further noticed that pyrrole-metal interaction decreases while descending the group 14. This indicates that the stability of the metal complex of pyrrole based pincer ligand depends upon the π-accepting nature of the metals.
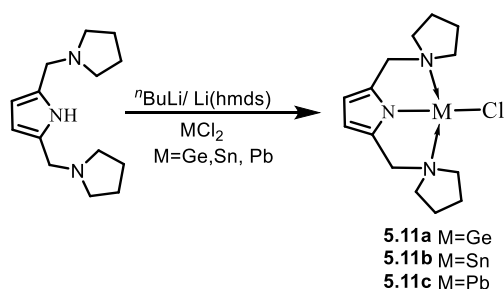
Scheme 5.7. Synthesis of complexes, **5.11a-c** of 2,5-bis[(pyrrolidino)methyl]pyrrole with group 14 elements.

Iva Vránová *et al.,* recently reported the synthesis of antimony and bismuth complexes **5.12a-b** stabilised by the same NNN-pincer ligand, 2,5-bis[(pyrrolidino)methyl]pyrrole (Scheme 5.8) and performed theoretical studies.[27]


5.12a M=Sb
5.12b M=Bi
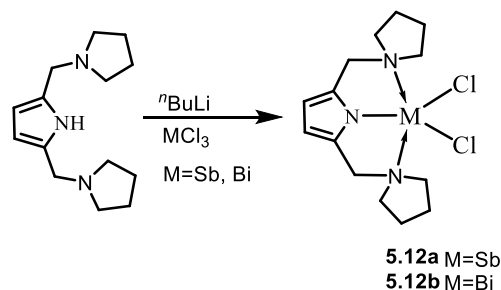
Scheme 5.8. Synthesis of antimony and bismuth complex, **5.12a-b** of 2,5-bis[(pyrrolidino)methyl]pyrrole.

From theoretical investigations they observed that like the previous cases, the Sb/Bi–N bond was a covalent 2e-2c bond. The strength of additional N→M (M = Sb or Bi) intramolecular interactions was comparable with the carbanionic NCN analogues,[9,12,28-30] thereby proving to be a promising ligand for stabilization of antimony and bismuth compounds similar to classical pincer-type ligands.

Based on the literature reports available for pyrrole based NNN-pincer ligands, it is apparent that this very class of pincer ligands is not well explored, especially with respect to their transition metal complexes and group 16 complexes. While still in its infancy, the chemistry of pyrrole based NNN-pincer ligands sincerely demands design and development of new ligand family in order to explore their bonding facets with metals and probable applications in contemporary coordination chemistry. In the present work, three pyrrole based NNN-pincer ligands with variable chelating arms, *viz.* 2,5-bis[(dimethylamino)methyl]pyrrole, 2,5-bis[(pyrrolidino)methyl]pyrrole and 2,5-bis[(piperidino)methyl]pyrrole are synthesised and it was envisaged to explore their chemistry with group 16 elements (Se and Te) especially with respect to the nature of N E (E=Se, Te) bond. It is further envisaged to synthesise transition metal complexes of the aforementioned ligands and to explicitly study the structural aspects of the complexes.

5.2 Results and discussion

Ligand 2,5-bis[(dimethylamino)methyl] pyrrole, **L¹** was prepared by Mannich reaction following the reported procedure wherein pyrrole was treated with formaldehyde and dimethylamine solution in presence of acetic acid (Scheme 5.9).[31] The Same protocol was applied for the synthesis of 2,5-bis[(pyrrolidino)methyl]pyrrole, **L²** and 2,5-bis[(piperidino)methyl] pyrrole, **L³** by using pyrrolidine and piperidine as starting material respectively.
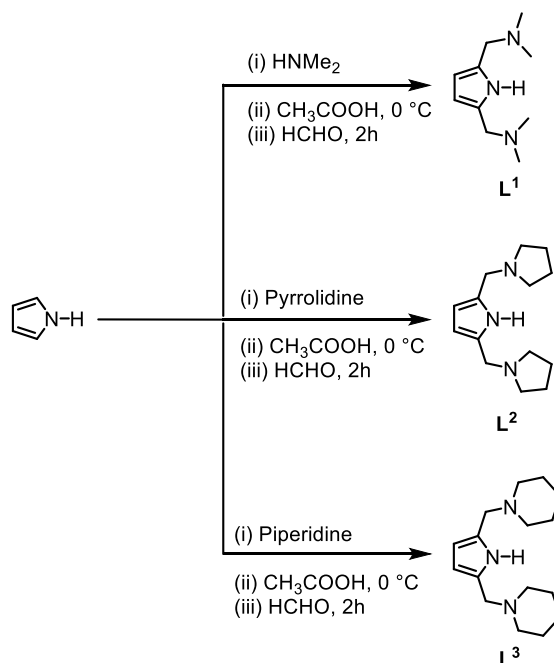

Scheme 5.9. Synthetic routes for the pyrrole based NNN-pincer ligands, 2,5-bis[(dimethylamino)methyl] pyrrole, **L¹**, 2,5-bis[(pyrrolidino)methyl] pyrrole, **L²** and 2,5-bis[(piperidino)methyl]pyrrole, **L³**.

Ligands **L¹** was viscous in nature, while **L²** and **L³** were white crystalline solids. All three compounds were characterised by m.p., NMR, IR and mass spectrometry. The proton NMR spectra of **L¹** and **L²** exactly matched with literature values.[26, 31] Like ligands **L¹** and **L²**, in the ¹H spectra of **L³**, the pyrrolyl protons resonated at 5.87 ppm, while the 'N–H' proton shows resonance around 8.6 ppm. IR spectra for all three ligands show a broad peak around 3300 cm⁻¹ signifying the presence of the N–H peak.

To unveil the characteristics of N−Te/Se bond, a series of reaction have been carried out. In particular, first the lithiated ligand *viz.,* Li[NC$_4$H$_2$(CH$_2$NMe$_2$)$_2$-2,5] was synthesised by treating the ligand **L¹** with 1.1 equivalent of *ⁿ*BuLi at −78 °C in diethyl ether (Scheme 5.10). The lithiated product was then treated with Te/Se powder followed by aerial oxidation to

afford the dichalcogenides, **5.13-5.14**. In another approach, the lithiated product was treated with Te/Se metal and then bromobenzene was added to synthesize unsymmetrical monotellurides, **5.15-5.16**.
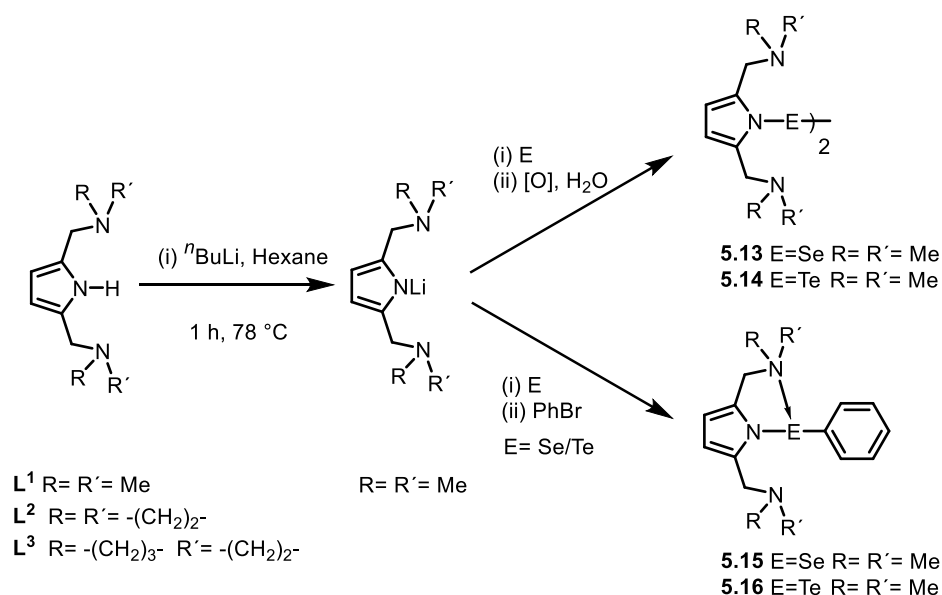
Scheme 5.10. Synthetic route for the chalcogen complexes of NNN-pincer pyrrolyl ligand.

Both dichalcogenides and monochalcogenides were purified by column chromatography using *n*-hexane as eluent. However, it was observed that the dichalcogenide compounds were not stable under ambient condition and in other organic solvents, as it immediately gave white colored intractable solid. These, in turn precluded their detailed characterisations through ^{1}H NMR. However, the ^{77}Se NMR could be obtained by recording the spectra directly from the reaction aliquots, which substantiated the formation of the compounds. In particular, the ^{77}Se NMR for diselenide **5.13** was observed at 465 ppm. For ditelluride **5.14**, [125]Te NMR resonance was observed at 225 ppm. The ^{1}H NMR spectrum of compounds **5.15** exhibited aromatic proton resonance corresponding to the phenyl protons in the range 7-8 ppm, while the resonance at ~6 ppm corresponded to the pyrrolyl protons. The "methane" and "methyl" protons showed resonances at ~3.4 and ~2.2 ppm respectively. Quite similar resonances were also observed for compound **5.16**. Compound **5.15** depicted signal at 229 ppm in the ^{77}Se NMR spectrum. The corresponding [125]Te NMR resonance for compound **5.16** was observed at 109 ppm. In the mass spectra (positive ion mode) of **5.15,** the molecular ion peak at *m/z* = 338.1133 was assigned to [M+H]$^+$ ion. Similarly, [M+H]$^+$ ion of compound **5.16** exhibited molecular ion peak at *m/z* = 388.1021.

To synthesize transition metal complex, in particular, Pd complex of $\mathbf{L^1}$, the lithiated ligand $Li[NC_4H_2(CH_2NMe_2)_2-2,5]$ was treated with $Pd(COD)Cl_2$ (Scheme 5.11). The reaction afforded compound **5.17** in 68% yield. In ^1H NMR spectrum of the complex, the characteristic signal for pyrrole N<u>H</u> proton at 8.66 ppm disappeared which indicated that metalation took place at the pyrrole nitrogen atom. In the mass spectra (positive ion mode) of **5.17,** the two intense peaks at *m*/z 286.0783 and 327.1143 were assigned to $[PdNC_4H_2(CH_2NMe_2)_2]^+$ and $\{[PdNC_4H_2(CH_2NMe_2)_2]+(CH_3CN)\}^+$ respectively. Interestingly, the solid state structure of the complex revealed an additional coordination of dimethyl amine to the Pd centre (*vide infra*).
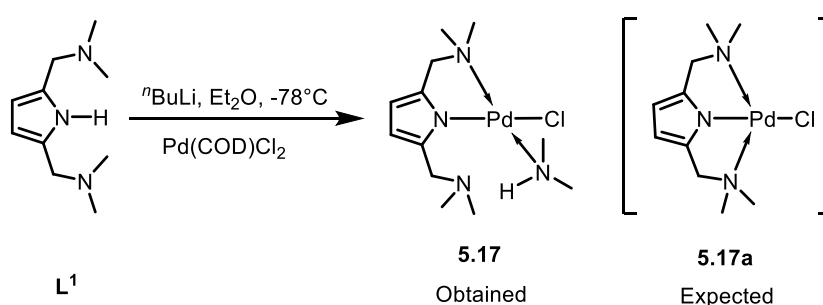
Scheme 5.11. Synthetic route for complex **5.17** via lithiation route.

In another approach, to obtain the metal complex, the –N<u>H</u> proton of the ligand $\mathbf{L^2}$ was first removed by addition of trimethylamine at room temperature. Successive addition of $Pd(COD)Cl_2$ led to the displacement of COD, and resulted in the formation of complex **5.18** (Scheme 5.12). However, in the case of $Pt(COD)Cl_2$, the chloride ions behaved as leaving groups, resulting in the formation of the complexes, **5.19-5.20**.
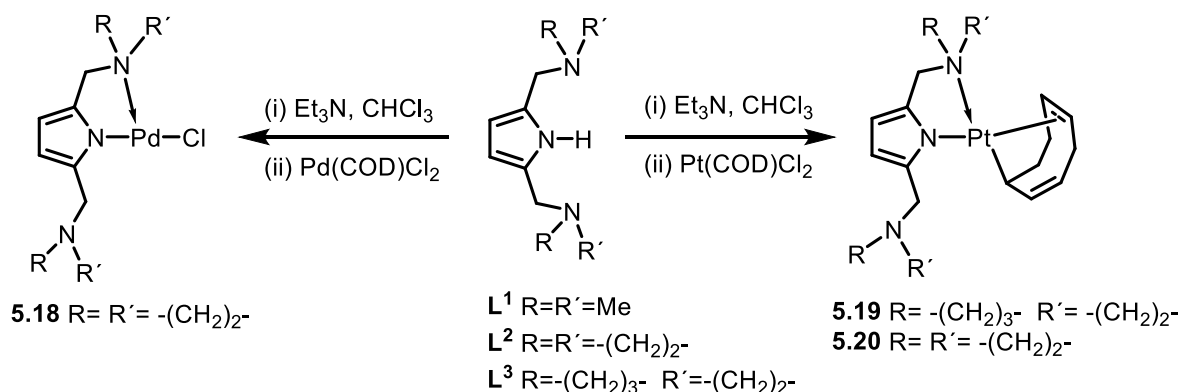
Scheme 5.12. Synthetic route for Pd and Pt complexes of NNN-pincer pyrrolyl ligands.

Interestingly, in both complexes **5.19-5.20**, the cyclooctadiene moiety experienced a Pt-induced deprotonation in the position α to one of the double bonds followed by formation of a new double bond via 1,2-shift. This afforded 2,5-cyclooctadienyl ligand. It is worth mentioning that during the isomerisation process, one of the former π-bonded carbon atoms changed its coordination mode to C–Pt σ-bond. The possible pathway for the formation of 2,5-cyclooctadienyl ligand from COD deprotonation via Pt induced C–H activation is depicted in Figure 5.1. A similar kind of C–H activation of the COD ligand has been reported by Neumüller *et al.* by reaction of hexaphenylcarbodiphosphorane[36] ($Ph_3P=C=PPh_3$) with $Pt(COD)Cl_2$.
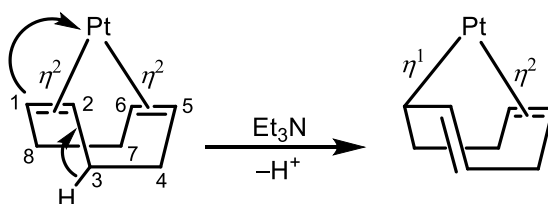

Figure 5.1. Possible pathway for the Pt induced C-H activation of COD to give 2,5-cyclooctadienyl ligand.

In the mass spectra (positive ion mode) of **5.19**, the molecular ion peak at *m*/z 585.2529 corresponded to {M+Na}$^+$ ion. Similarly, in the mass spectra of complex **5.20**, the molecular ion peak at *m*/z 534.2317 corresponded to {M+H }$^+$ ion. In the ^{1}H NMR spectrum of complex **5.19**, the disappearance of –N<u>H</u> resonance at 8.6 ppm indicated the coordination of the metal to the pyrrole nitrogen atom. A slight change in the chemical shift for the pyrrole proton and methine were observed as compared to the corresponding chemical shift in the ligand. The multiplet observed between 4.9-5.1 ppm corresponds to olefinic protons from 2,5-cyclooctadiene. However, due to the fluxional nature of the piperidine rings and possible overlap with aliphatic protons of the co-ligand, a cluster of peaks was observed in the aliphatic region 1.5-3.1 ppm, which precluded the adequate integration of the peaks in NMR spectra. Similar observation was also made in the ^{1}H NMR spectrum of complex **5.20**, where a cluster of peak was observed corresponding to the overlap of pyrrolidine proton with the aliphatic protons of the co-ligand. Similar complicacy in the NMR study has also been reported by Neumüller *et al*. for their complex [C_8H_{11})Pt($C_6H4PPh_2CPPh_3$)].[36]

5.3 Structural Studies

5.3.1 X-ray crystallographic studies

5.3.1.1 Molecular structure of 2,5-bis[(piperidino)methyl]pyrrole, L³

The single crystals of ligand **L³** were obtained by slow evaporation of the compound from CHCl₃/*n*-hexane mixture. It crystallises in triclinic crystal system with space group *P-1*. In the molecular structure (Figure 5.2), the pyrrolidine rings and the methylene linkers reside in same plane. The bond lengths and the associated bond angles in compound **L³** [C1−C2 137.2(18), C2−C3 141.96(17), C3−C4 137.91(12), C1−C11−N3 113.02(10), C4−C5− N2 114.94(17)] are in good agreement with the value observed in the molecular structure of free pyrrole and **L²**.[26,32]
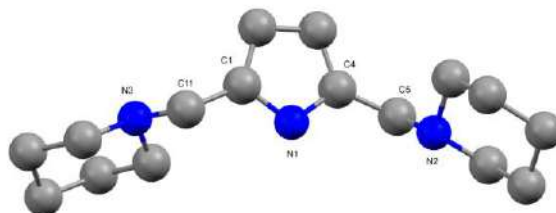

Figure 5.2. Molecular structure of **L³**. All the hydrogen atoms are omitted for clarity.

5.3.1.2 Molecular structure of compound 5.17

The molecular structure of complex **5.17** is shown in Figure 5.3. It crystalizes in monoclinic system with space group $P12_{1/c1}$. The geometry around Pd ion is distorted square planar and it is in +2 oxidation state. The tetra-coordinated Pd ion is coordinated to the nitrogen atom of the central pyrrole ring, one nitrogen atom (N2) from the flanking dimethylamine group and one chloride ligand. Interestingly the fourth coordination site is occupied by one HNMe₂ group, which might have come from the decomposed product. The central ring is positioned *trans* to the chloride ligand. The Pd1−N1(pyrrole) distance in complex **5.17** is found to be 2.019(3) Å. This bond distance is consistent with the Pd−N(pyridyl) distance of 1.996(8) Å observed in [Pd(N-N´-N´´)Cl]Cl, where N-N´-N´´ = 2,6-bis[(dimethylamino)methyl]pyridine.[33] However, the Pd1−N1(pyrrole) distance in **5.17** is considerably longer than the Pd−N(pyridyl) distance of 1.956(2) Å observed in Pd(pipNNN)Cl]Cl {pip = (2,6-bis(piperidylmethyl)pyridine)} and Pd−N(phenyl) distance of

[1.927(3) Å and 1.922(3) Å] observed in Pd(pipNCN)Br.[34] In complex **5.17,** the N2 atom from side arm makes a five membered chelating ring with the metal centre with a bite angle of 81.63(12)º. This bite angle is comparable with that observed in [Pd(pipNNN)Cl]Cl [82.31(8)°, 81.44(8)°], [Pd(N-N′-N′′)Cl]Cl [80.9(3)°, 80.8(3)°] and Pd(pipNCN)Br [81.56(11)°, 81.63(11)°]. The corresponding Pd1-N2 distance is found to be 2.091(3) Å. This distance is again in good agreement with that observed in [Pd(pipNNN)Cl]Cl [2.109(2) Å, 2.133(2) Å], [Pd(N-N′-N′′)Cl]Cl [2.094(7) Å, 2.099(7) Å] and Pd(pipNCN)Br [2.128(2), 2.126(3)Å]. The Pd1−N4 distance is 2.046(3) Å. The −N<u>H</u> hydrogen of HNMe₂ group is found to be engaged in intramolecular hydrogen bonding with N3 atom with a distance of 1.804 Å. The Pd1−Cl1 distance for **5.17** [2.3285(9) Å] is in good agreement with literature values.[33,34]
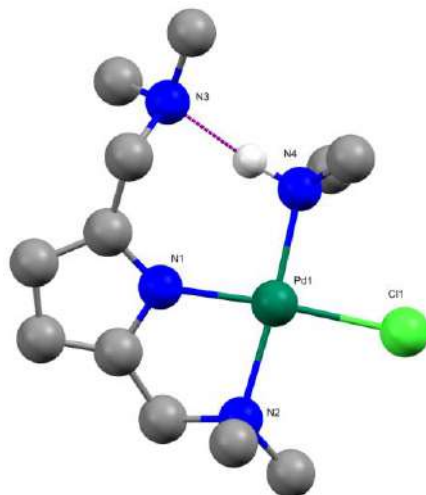

Figure 5.3. Molecular structure of compound **5.17**. All the hydrogen atoms are omitted for clarity.

5.3.1.3 Molecular structure of complex 5.18

The molecular structure of complex **5.18** is depicted in Figure 5.4. Single crystals of complex **5.18** were obtained by slow evaporation from a chloroform/tetrahydrofuran mixture. It crystallises in a monoclinic crystal system with space group *C2/c*. Like complex **5.17**, the geometry around Pd(II) centre in **5.18** is distorted square planar and the four coordination sites around the metal centre are occupied by central pyrrole nitrogen atom, one pyrrolidine nitrogen atom from one of the side arms, one chloride ligand and one THF molecule. Like the previous structure, the pyrrole nitrogen is *trans* to the chloride ligand. Of particular interest is the Pd1−N1(pyrrole) distance of 1.974(12) Å which is slightly shorter than the value observed in **5.15** [2.019(3) Å]. Again, this value is comparable with Pd−N(pyridyl) distance

of 1.956(2) Å and 1.996(8) Å observed in [Pd(pipNNN)Cl]Cl {pip = (2,6-bis(piperidylmethyl)pyridine)} and [Pd(N-N′-N″)Cl]Cl {N-N′-N″ = 2,6-bis[(dimethylamino)methyl]pyridine} respectively.[33-34] In complex **5.18**, ∠N2-Pd1-N1 bite angle is 84.3(5)°, which is slightly larger than the corresponding bite angle of 81.63 (12)° observed in **5.17**. The corresponding Pd1−N2 distance is found to be 2.103(11) Å which is consistent with value observed in **5.17** [2.091(3) Å]. The Pd1−N3 distance of 3.395 Å is too long to be coordinated to the metal centre. The Pd1−O(thf) distance is found to be 2.048(9) Å. The Pd1−Cl1 distance for **5.18** [2.328(3) Å] is almost identical to that of **5.17** [2.3285(9) Å].
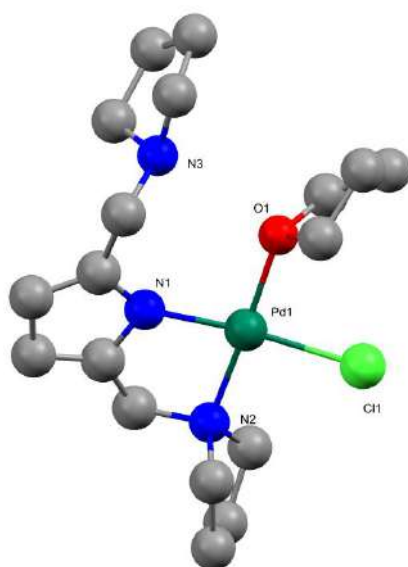

Figure 5.4. Molecular structure of Complex **5.18.** All the hydrogen atoms are omitted for clarity.

5.3.1.4 Molecular structure of complex 5.19

The molecular structure of complex **5.19** is depicted in Figure 5.5. Single crystals of complex **5.19** were obtained by slow evaporation from a chloroform/*n*-hexane mixture. It crystallises in a trigonal crystal system with space group *R-3*. The formal oxidation state of the Pt atom is +2. The arrangement of ligand around the metal centre is composed of three carbon atoms from the cyclooctadienyl moiety, the central nitrogen atom and one piperidino nitrogen atom from the side arm. The Pt1−N1 distance is 2.006(16) Å, which is in good agreement with the Pt−N(pyridyl) distance observed in [Py(tpy)Cl]Cl [2.019(5) Å] where tpy = 2,2′:6′,2″-terpyridine.[35] The Pt1−N3 coordination bond distance of 2.256(17) Å is significantly longer

than that of Pt1-N1 distance. The N3 atom of piperidino side arm makes a five membered chelating ring with ∠ N1-Pt1-N3 bite angle of 81.075(7)°. During the reaction, a deprotonation took place at C20 carbon of 1,4-cyclyoctadiene, followed by 1,2-shift which resulted in a new double bond between C20–C21 with a bond distance of 1.318(3) Å. The new 2,5-cyclooctadienyl ligand is coordinated to the Pt atom via a π-bond and a σ-bond. The C17 and C18 atoms coordinate to the metal centre in a η^2- fashion with C17–Pt1 and C18–Pt1 bond distances of 2.185(3) Å and 2.177(3) Å respectively. On the other hand C22 atom coordinates to the Pt centre in a η^1- fashion with bond distance of 2.042(2) Å. All these bond distances from the co-ligand to the Pt centre were in good agreement with value observed in [C_8H_{11})Pt($C_6H4PPh_2CPPh_3$)] where similar C–H activated cyclooctadienyl moiety was coordinated to the Pt centre.[36]
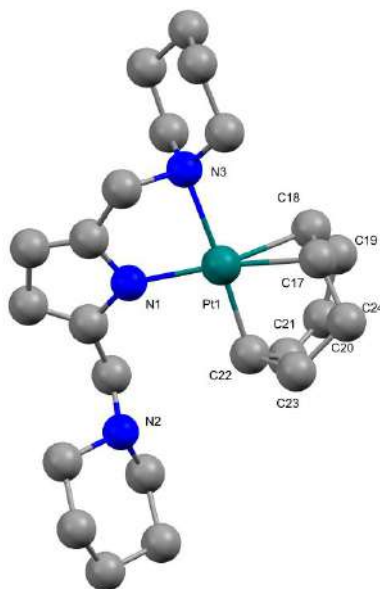

Figure 5.5. Molecular structure of Complex **5.19.** All the hydrogen atoms are omitted for clarity.

5.3.1.5 Molecular structure of complex 5.20

The molecular structure of complex **5.20** is depicted in Figure 5.6. Single crystals of complex **5.20** were obtained by slow evaporation from a chloroform/*n*-hexane mixture. It crystallises in a monoclinic crystal system with space group *P2/c*. Complex **5.20** is observed to be isostructural with complex **5.19,** where Pt(II) centre is coordinated to one 2,5-cyclooctadienyl ligand, pyrrole nitrogen atom and one nitrogen atom of side arm. The Pt1–N1 distance is found to be 2.029(2) Å, which is slightly longer than that observed in

complex **5.19** [2.006(16) Å]. On the other hand, the Pt1-N3 distance of 2.215(2) Å is slightly shorter than corresponding bond distance of **5.19** 2.256(17) Å. Like the previous case, The N<u>3</u> atom from the pyrrolidine side arm makes a five membered chelating ring with the metal centre with a ∠N1-Pt1-N3 bite angle of 80.20(10) Å. The other side arm did not take part in coordination to the metal centre. In complex **5.20**, The Pt1−C19 σ-bond distance is 2.061(3) Å, which is slightly longer than that observed in previous complex. Again, the π-bond distances between C15−Pt1 and C22−Pt1 are found to be 2.113(3) Å and 2.146(3) Å respectively.
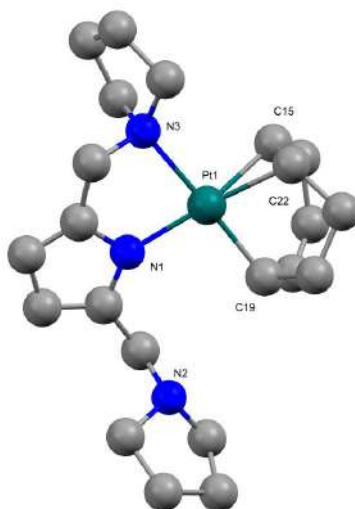

Figure 5.6. Molecular structure of Complex **5.20.** All the hydrogen atoms are omitted for clarity.

5.4 Computational studies

Since solid state structures were not obtained for compounds **5.13**-**5.16,** to get a better understanding about the nature of the bond between pyrrole nitrogen atom and chalcogen elements, electronic structure calculations have been carried out using Gaussian09[37] package by employing DFT method. Geometry optimizations were carried out using MPW1PW91 method; 6-311g(d) basis set for C, H, N, Cl and Se, 3-21g basis set for Te and Lanl2dz basis set for Pd have been undertaken. The optimized structures of compounds **5.13**, **5.14**, **5.15**, **5.16**, **5.17** and **5.17a** are given in Figure 5.7. The value obtained for minimum energy of compounds **5.13**, **5.14**, **5.15**, **5.16**, **5.17** and **5.17a** are given in Table 5.1.

Table 5.1. Optimized ground state energies of **5.13**, **5.14**, **5.15**, **5.16**, **5.17** and **5.17a.**

Compound	Energy (a.u.)
5.13	−5915.60036135
5.14	−14278.6760044
5.15	−3189.36921041
5.16	−7373.30201003
5.17	−833.086998019
5.17a	−697.895216424

From the optimized structures, it can be observed that in compound **5.13** and **5.14** none of the amine groups coordinate with Se/Te, though, in compound **5.14** each tellurium has weak interactions with one of the amine groups. In compounds **5.15** and **5.16**, one of the amine groups coordinates with Se/Te and the other amine group remains free. In compound **5.17** and **5.17a,** one of the amine groups from the pyrrole ligand coordinates with Pt and the other amine group remains free. It is worth noting that the ground state energy of Compound **5.17** is significantly lower than that of **5.17a**. This indicates that the Pd centre takes up its four coordination from a HNMe$_2$ to attain lower energy of the overall molecule, which might have come from the decomposition of the ligand.
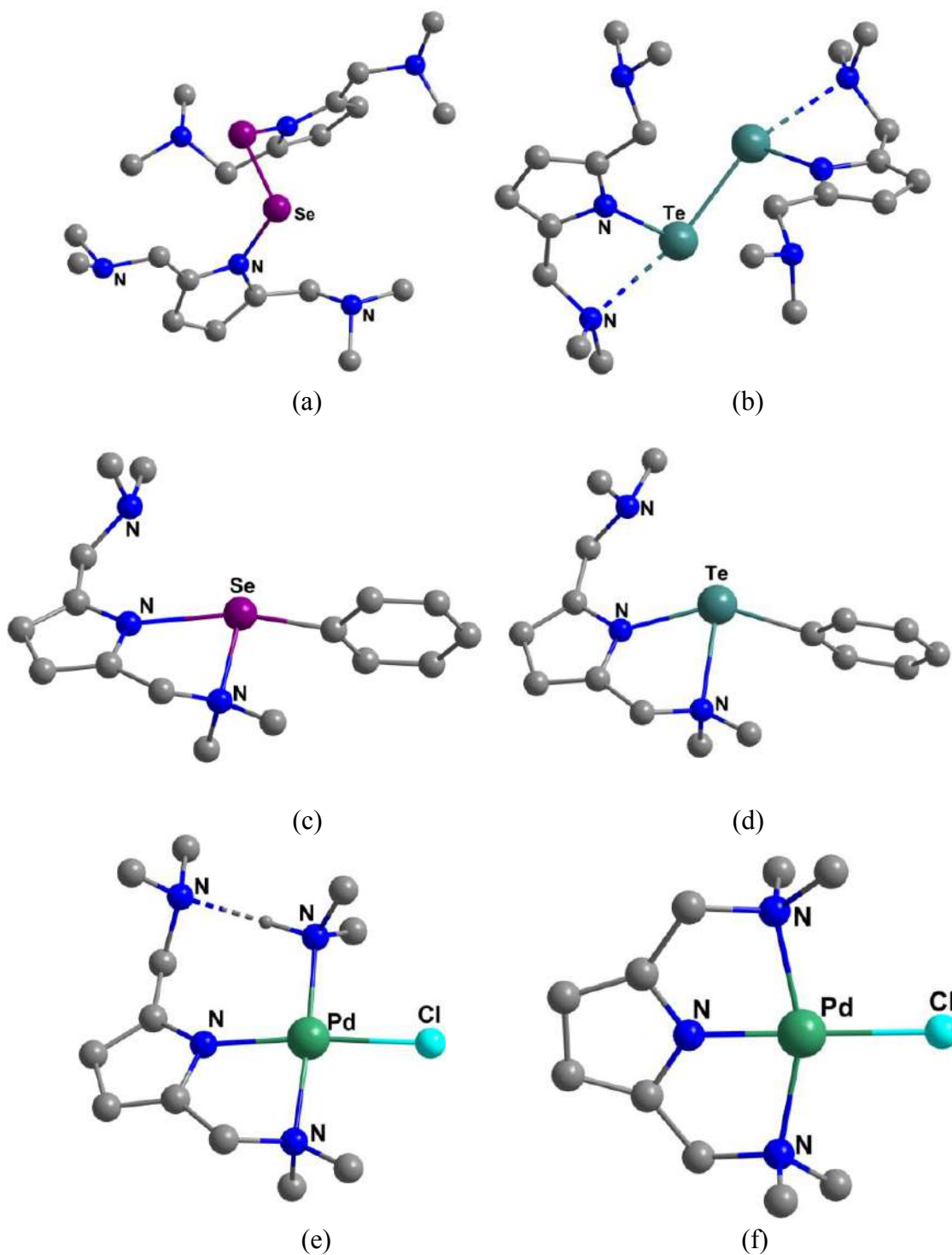
Figure 5.7. Optimized structures of compound (a) **5.13**, (b) **5.14**, (c) **5.15**, (d) **5.16**, (e) **5.17**, and (f) **5.17a**.

5.5 NBO analysis

From NBO analysis,[38] it can be concluded that in compound **5.15,** selenium has three bonds around it, one bond with phenyl group (Se32−C33), second bond with amine group from the side chain (N30−Se32) and the last bond is with pyrrole (N1−Se32) where N1 gives its lone pair to σ* of Se32−C33 bond (Figure 5.8). Same is the case for compound **5.16** where Te has three bonds around it *i.e.* first bond with phenyl group (Te32−C33), second bond with amine group of side chain (N30−Te32) where N30 donates its lone pair to LP* of Te and the third bond with pyrrole (N1−Te32) in which again N1 donates its lone pair to LP* of Te. In compound **5.17** palladium is bound with two nitrogen (N2 and N42) by proper coordination bond and N40 donates it lone pair to the σ* of Pd−N42. The NBO involved in these bindings and the energies of these interactions are given in Table 5.2.
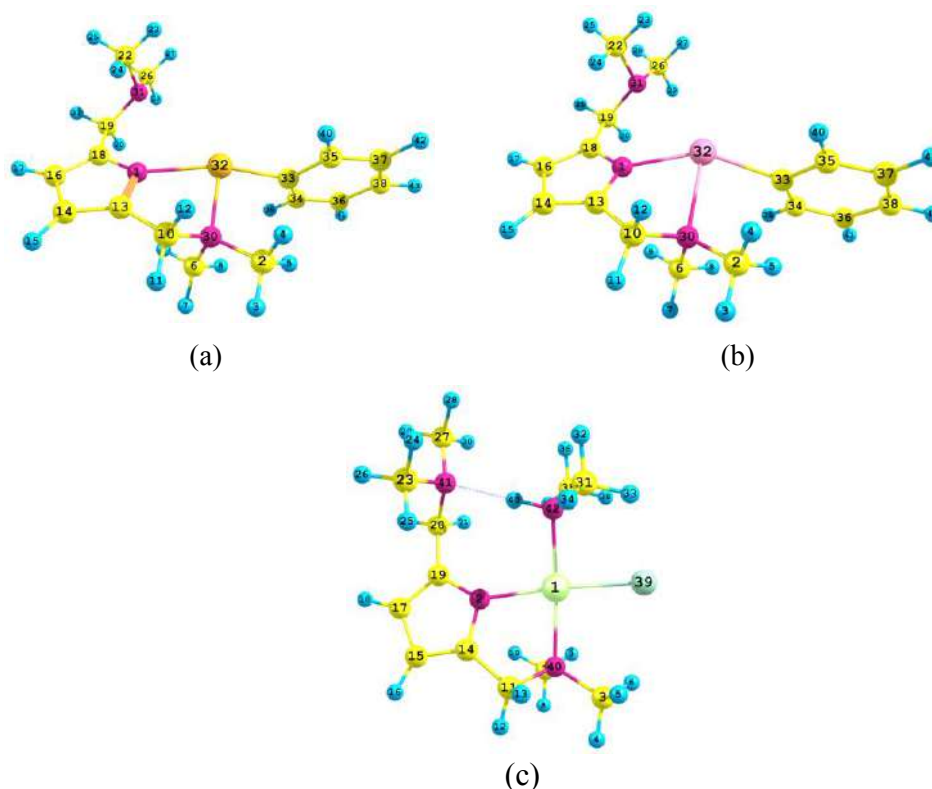

(a) (b)

(c)

Figure 5.8. Optimized structure of compound (a) **5.15**, (b) **5.16** and (c) **5.17** on which NBO analysis has been performed.

Table 5.2. Bond properties of (a) **5.15**, (b) **5.16** and (c) **5.17.**

Compound	Bond	Occupancy	Energy (Kcal/mol)
5.15	BD (1) N 30 -Se 32	0.97404	-0.54214
5.15	BD (1)Se 32 - C 33	0.97665	-0.53380
5.16	BD (1)Te 32 - C 33	0.97750	-0.44401
5.16	BD (1)Pd 1 - N 2	0.96113	-0.47932
5.16	BD (1)Pd 1 - N 42	0.95762	-0.46896
	Donor NBO	**Accepter NBO**	
5.15	83. LP (1) N 1	/441. BD*(1)Se 32 - C 33	13.67
5.16	93. LP (1) N 1	/ 97. LP*(3)Te 32	66.90
5.16	93. LP (1) N 30	/ 97. LP*(3)Te 32	31.46
5.17	77. LP (1) N 40	/369. BD*(1)Pd 1 - N 42	21.51
5.17	70. LP (1) N 39	/411. BD*(1) N 41 -Pt 43	34.10

5.6 Conclusion

In this report a series of pyrrole based NNN pincer ligands with variable side arms have been synthesised, viz. 2,5-bis[(dimethylamino)methyl] pyrrole, **L¹**, 2,5-bis[(pyrrolidino)methyl] pyrrole, **L²** and 2,5-bis[(piperidino)methyl] pyrrole, **L³** and their reactions with group 16 elements (Se and Te) and d^8 transition metals (Pd, Pt) are explored. Due to the instability of the dichalcogenide compounds, their detailed characterisations could not be achieved. However, the ^{77}Se/^{125}Te NMR data substantiate the formation of the compounds. While attempting to synthesise d^8 metal complexes, when the lithiated ligand Li[NC₄H₂(CH₂NMe₂)₂-2,5] was treatment with Pd(COD)Cl₂ it afforded complex of the form [C₄H₂N(2,5-CH₂NMe₂)₂]PdCl(HNMe₂)₃, where an additional coordination of dimethylamine to Pd centre was observed. This might have resulted from decomposition of the starting material. In another approach, when ligand **L²** was treated with Pd(COD)Cl₂ in the presence

of trimethylamine, the displacement of COD resulted in the formation of L^2Pd(II)Cl complex. On the other hand, when Pt(COD)Cl$_2$ was used the metal precursor, the chloride ions behaved as leaving groups. Interestingly, a Pt induced C–H activation took place on the cyclooctadiene moiety, thereby resulting two different modes of coordination (η^2 and η^1) to the metal centre. It is worth noting that, in both experimentally and theoretically optimised structures of the complexes, while one side arms of the ligand coordinates to the metal and the other arm does not participate in the coordination. This bidentate behaviour of the pyrrole based NNN-pincer ligands is also observed in literature.

5.7 Experimental Section

All the manipulations were carried out under nitrogen or argon atmosphere using standard Schlenk techniques unless otherwise noted. Solvents were purified and dried by standard procedures and were distilled prior to use. ^{1}H (400 MHz and 500 MHz), ^{13}C (100.56 MHz and 125 MHz), ^{77}Se (76.3 MHz) and ^{125}Te (157.97 MHz) nuclear magnetic resonance spectra were recorded on Bruker AV 400 and Bruker AV 500 spectrometers at 25 °C. Chemical shifts are cited with respect to Me$_3$Si as internal standard (^{1}H and ^{13}C) and Me$_2$Se (^{77}Se) and Me$_2$Te (^{125}Te) as external standards. The ESI mass spectra are recorded on a Q-Tof micro (YA-105) mass spectrometer.

Synthesis of 2,5-bis[(dimethylamino)methyl]pyrrole, L^1

A round bottomed flask was charged with 30% dimethylamine solution (85 mL). To it glacial acetic acid (45 g) was added dropwise at 0°C. After addition of aqueous formaldehyde solution (65 mL) drop-wise to the reaction mixture, freshly distilled pyrrole (25 g) was added to it at 0°C. The reaction mixture was stirred at same temperature for 2h. The reaction was quenched by addition of 30% conc. KOH solution maintaining the temperature at 0°C this resulted in a dense layer of the required compound which was subsequently separated out and was stored at lower temperature away from light over KOH pallet.

Yield: 69.00 g (30%).

^{1}H NMR (400 MHz, CDCl$_3$): δ (ppm) 9.32 (s, 1H), 5.89 (s, 2H), 3.35 (s, 4H), 2.17 (s, 12H).

^{13}C NMR (100 MHz, CDCl$_3$): δ (ppm) 128.92, 107.43, 56.69, 44.95.

Synthesis of 2,5-bis[(pyrrolidino)methyl]pyrrole, L^2

In a round bottomed flask, glacial acetic acid (45 g) was added drop-wise to pyrrolidine solution (74 mL) at 0°C. After the addition of aqueous formaldehyde solution (65 mL) drop-wise to the reaction mixture, a freshly distilled pyrrole (25 g) was added to it at 0°C. The reaction mixture was stirred at 0°C for 2h. The reaction was quenched by addition of 30%

conc. KOH solution maintaining the temperature at 0°C, this resulted in a dense layer of the required compound which was subsequently separated out and finally it was extracted from acetone which gives the title compound as a white solid. The compound was preferably stored at lower temperature keeping away from light.

Yield: 85 %, **m.p.** 53°C

^{1}H NMR (400 MHz, CDCl₃): δ (ppm) 8.66 (s, 1H), 5.87 (s, 2H), 3.39 (s, 4H), 2.33 (broad, 8H), 1.55 (quin, J = 5.60 Hz, 8H), 1.42 (s, 4H).

^{13}C NMR (100 MHz, CDCl₃): δ (ppm) 128.57, 107.06, 56.34, 54.40, 26.05, 24.50.

Synthesis of 2,5-bis[(piperidino)methyl]pyrrole, L^3

In a round bottomed flask, glacial acetic acid (45 g) was added drop-wise to piperidine solution (63.63 mL) at 0°C. After the addition of aqueous formaldehyde solution (65 mL) drop-wise to the reaction mixture, a freshly distilled pyrrole (25 g) was added to it at 0°C. The reaction mixture was stirred at 0°C for 2h. The reaction was quenched by addition of 30% conc. KOH solution maintaining the temperature at 0°C which resulted in a dense layer of the desired compound this was subsequently separated out and finally it was extracted from acetone which gives the title compound as a white solid. The compound was stored at lower temperature keeping away from light.

Yield: 88 %

M.P. 56 °C

^{1}H NMR (400 MHz, CDCl₃): δ (ppm) 8.66 (s, 1H), 5.87 (s, 2H), 3.39 (s, 4H), 2.33 (broad,8H), 1.55 (quin,8H), 1.42 (s, 4H).

^{13}C NMR (100 MHz, CDCl₃): δ (ppm) 128.57, 107.06, 56.34, 54.40, 26.05, 24.50.

Synthesis of compounds 5.13, 5.14

In a round bottomed flask, ligand **L^1** (0.5 g, 2.7 mmol) was charged with 20 mL of diethyl ether. To it 1.6 mol dm^{-3} solution of ^{n}butyllithium in n-hexane (1.9 cm^3, 3.1 mmol) was added dropwise by a syringe at −78 °C. The reaction mixture was stirred at the same temperature for one hour to give a light yellow coloured lithiated compound Li[C₄H₂N(CH₂NMe₂)-2,5]. Elemental chalcogen (selenium and tellurium) (0.22 g Se/0.35 g Te, 2.7 mmol) was added and the stirring was continued for an additional 1 h at 0 °C and 2 h at room temperature. The oxygen was bubbled through the solution for 10 min and the resulting mixture was poured into a beaker containing cold aqueous NaHCO₃ solution. Then oxygen was bubbled for an additional 15 min. The yellow oily product was extracted with

ether and then washed with water. The organic phase was separated, dried over Na_2SO_4, and filtered. The filtrate was concentrated to give a yellow coloured dense liquid.

5.13: ^{77}**Se NMR** (76 MHz, CDCl$_3$): δ (ppm) 465

5.14: ^{125}**Te NMR**(126 MHz, CDCl$_3$): δ (ppm) 225

^{1}**H NMR**: the ^{1}H spectra for both the compounds were found to be complex and could not be integrated

Synthesis of compound 5.15

In a round bottomed flask, ligand **L^1** (0.5 g, 2.7 mmol) was dissolved in 20 mL of diethyl ether. To it 1.6 mol dm^{-3} solution of *n*-BuLi in hexane (1.9 cm^3, 3.1 mmol) was added dropwise by a syringe at −78 °C. The reaction mixture was stirred at the same temperature for one hour to give a light yellow coloured lithiated compound Li[C$_4$H$_2$N(CH$_2$NMe$_2$)-2,5]. Selenium powder was (0.22 g , 2.7 mmol) was added and the stirring was continued for an additional 1 h at 0 °C and 2 h at room temperature. PhBr (0.43 g, 2.7 mmol) was added to the reaction mixture and was further stirred for 12 hours at room temperature. The reaction mixture was quenched with water and the compound was extracted in dichloromethane solution. The organic layer was extracted, dried over Na_2SO_4 and the solvent was removed to give the compound **5.15**.

Yield: 0.42 g (96%).

^{1}**H NMR** (400 MHz, CDCl$_3$): δ (ppm) 7.58 (m, 2H), 7.22 (m, 3H), 5.88 (s, 2H), 3.39 (s, 4H), 2.20 (s, 4H).

^{13}**C NMR** (100 MHz, CDCl$_3$): δ (ppm) 128.51, 127.40, 124.00, 120.17, 131.52, 109.63, 56.86, 40.78, 25.57

^{77}**Se NMR** (76 MHz, CDCl$_3$): (ppm) 229

ESI-MS (positive mode): [C$_{16}$H$_{24}$N$_3$Se]$^+$ *m*/z = 338.1133 (observed), 338.1130 (calculated).

Synthesis of compound 5.16

A similar procedure as described above was followed for the synthesis of **5.16**. To the lithiated ligand Li[C$_4$H$_2$N(CH$_2$NMe$_2$)-2,5], tellurium powder was (0.35 g , 2.7 mmol) was added and the stirring was continued for an additional 1 h at 0 °C and 5 h at room temperature. PhBr (0.43 g, 2.7 mmol) was added to the reaction mixture and was further stirred for 12 hours at room temperature. A similar workup afforded compound **5.16**.

Yield: 0.42 g (96%).

^{1}**H NMR** (400 MHz, CDCl$_3$): δ (ppm) 7.83-7.82 (m, 2H), 7.25-7.17 (m, 3H), 5.99 (s, 2H), 3.39 (s, 4H), 2.24 (s, 4H).

^{13}C NMR (100 MHz, CDCl$_3$): δ (ppm) 128.51, 127.40, 124.00, 120.17, 131.52, 109.63, 56.86, 40.78, 25.57.

^{125}Te NMR (126 MHz, CDCl$_3$): δ (ppm) 109

ESI-MS (positive mode): [C$_{16}$H$_{24}$N$_3$Te]$^+$ *m*/z = 388.1021 (observed), 388.1028 (calculated).

Synthesis of [{C$_4$H$_2$N(CH$_2$NMe$_2$)$_2$-2,5}PdCl], 5.17

In a round bottomed flask, ligand **L^1** (0.5g. 2.7 mmol) was charged with 20 mL of diethyl ether. To it 1.6 mol dm^{-3} solution of *n*-butyllithium in hexane (1.9 cm^3, 3.1 mmol) was added dropwise by a syringe at −78 °C. The reaction mixture was stirred at the same temperature for one hour to give a light yellow coloured lithiated compound Li[C$_4$H$_2$N(CH$_2$NMe$_2$)-2,5]. The metal precursor, Pd (COD)Cl$_2$ (0.79 g, 27 mmol) was added to the reaction mixture at −78 °C and was stirred overnight at room temperature. After completion of the reaction, the solvent was removed *in vacuo*. The resulting solid was dissolved in dichloromethane solution and filtered through celite. The filtrate was concentrated to dryness and the resultant solid was recrystallized from diethyl ether to afford light reddish coloured crystalline title compound.

^{1}H NMR (400 MHz, CDCl$_3$): δ (ppm) 9.32 (s, 1H), 5.89 (s, 2H), 3.35 (s, 4H), 2.17 (s, 12H).

ESI-MS (positive mode): [M+CH3CN]$^+$ *m*/z = 327.1143 (observed), 327.0801 (calculated).

Synthesis of complex 5.18

In a round bottomed flask, ligand **L^2** (0.5 g, 2.1 mmol) was disolved 20 mL of freshly dried chloroform. To it Et$_3$N (0.44mL, 3.21 mmol) solution was added and the reaction mixture was stirred for half an hour. The metal precursor, Pd(COD)Cl$_2$ (0.61 g, 2.1mmol) was added to the reaction mixture and stirred for 24h. The dark yellow colored solution was filtered through celite and dried under vacuum. The resulting solid was washed thoroughly with hexane to remove any unreacted ligand present. The desired compound was obtained as a yellow powder.

Yield: 69%

M.P. 178 °C

I.R. 2920 m, 2833 w, 1619 w, 1499 s, 1456 m, 1359 w, 1275 s, 1232 w, 1128 s, 1091 m, 1039 m, 941 m

ESI-MS (positive mode): [(M+Na -Cl)]$^+$ *m*/z = 361.0713 (observed), 361.0746 (calculated)

Synthesis of complex 5.19

In a round bottomed flask, ligand **L^3** (0.2g, 0.76 mmol) was charged with 20 mL of freshly dried chloroform. To it Et$_3$N (0.16mL, 1.14 mmol) solution was added and the reaction mixture was stirred for half an hour. Precursor Pt(COD)Cl$_2$ (0.28 g, 0.76 mmol) was added

to the reaction mixture and stirred for 24h. The dark yellow colored solution was filtered through celite and dried under vacuum. The resulting solid was washed thoroughly with hexane to remove any unreacted ligand present. The desired compound was obtained as a light yellow powder.

Yield: 47 %

M.P. 184°C

ESI-MS (positive mode): $[(M+Na)]^+$. $m/z = 585.2529$ (observed), 585.2533 (calculated).

I.R. 2924.5 s, 2854.9 s, 2781.1 w, 2723.5 w, 2283.1 w, 1578.6 m, 1457.1 m, 1374.3 w, 1260.7 m, 1094.0 m, 1021.2 m, 841.3 w, 799.1 m, 746.2 w

Synthesis of complex 5.20

A similar procedure as described before was followed for the synthesis of **5.20**. In a round bottomed flask, ligand L^2 (0.2 g, 0.85 mmol) was charged with 20 mL of freshly dried chloroform. To it Et$_3$N (0.18 mL, 1.28 mmol) solution was added and the reaction mixture was stirred for half an hour. Pt(COD)Cl$_2$ (0.32 g, 0.85 mmol) was added to the reaction mixture and stirred for 24h. The dark yellow colored solution was filtered through celite and dried under vacuum. The resulting solid was washed thoroughly with hexane to remove any unreacted ligand present. The desired compound was obtained as light yellow powder.

Yield: 34%

M.P. 179 °C

ESI-MS (positive mode): $m/z = 534.2317$(observed), 534.2395[calculated for $(M+H)^+$].

I.R. 2924.6s, 2285.5w, 1941.5w, 1588.9m, 1456.3s, 1375.8s, 1290.7m, 1208.0s, 1097.0s, 1042.3s, 966.9m, 862.8w, 619.2s

5.8 References

1. van der Boom, M. E.; Milstein, D. *Chem. Rev.* **2003**, *103*, 1759.
2. Moreno, I.; SanMartin, R.; Ines, B.; Herrero, M. T.; Domínguez, E. *Curr. Org. Chem.* **2009**, *13*, 878.
3. Milstein, D. *Top. Catal.* **2010**, *53*, 915.
4. Peris, E. Crabtree, R. H. *Chem. Soc. Rev.* **2018**, *47*, 1959.
5. Lawrence, M. A. W.; Green, K-A.; Nelson, P. N.; Lorraine, S. C. *Polyhedron* **2018**, *143*, 11.
6. Albrecht, M.; van Koten, G. *Angew. Chem., Int. Ed.* **2001**, *40*, 3750.

7. Jambor, R.; Kašná, B.; Kirschner, K. N.; Schürmann , M.; Jurkschat, K. *Angew. Chem., Int. Ed.* **2008**, *47*, 1650.

8. L.; Dostál, Jambor, R.; Růžička, A.; Lyčka, A.; Brus, J.; de Proft, F. *Organometallics* **2008**, *27*, 6059.

9. Dostál, L.; Jambor, R.; Růžička, A.; Jirásko, R.; Lochař, V.; Beneš, L.; de Proft, F. *Inorg. Chem.* **2009**, *48*, 10495.

10. Simon, P.; Proft, F. De; Jambor, R.; Růžička, A.; Dostál, L. *Angew.Chem. Int. Ed.* **2010**, *49*, 5468.

11. Khan, S.; Michel, R.; Dieterich, J. M.; Mata, R. A.; Roesky, H. W.; Demers, J.-P., Lange, A.; Stalke, D. *J. Am. Chem. Soc.* **2011**, *133*, 17889.

12. Casely, I. J.; Ziller, J. W.; Fang, M.; Furche F.; Evans, J. W. *J. Am. Chem. Soc.* **2011**, *133*, 5244.

13. Magdzinski, E.; Gobbo, P.; Martin, C. D.; Workentin, M. S.; Ragogna, P. J. *Inorg. Chem.* **2012**, *51*, 8425.

14. Singh, A. P.; Roesky, H. W.; Carl, E.; Stalke, D.; Demers, J. -P.; Lange, A. *J. Am. Chem. Soc.* **2012**, *134*, 4998.

15. Bouška, M.; Dostal, L.; Padělková, Z.; Herres-Pawlis, S.; Jurkschat, S. K.; Lyčka, A.; Jambor, R. *Angew. Chem., Int. Ed.* **2012**, *51*, 3478.

16. Khan, S.; Samuel, P. P.; Michel, R.; Dieterich J. M.; Mata, R. A.; Demers, J.-P.; Lange, A.; Roesky H. W.; Stalke, D. *Chem. Commun.* **2012**, *48*, 4890.

17. Flock, J.; Slujanovic, A.; Torvisco, A.; Schoefberger, W.; Gerke, B.; Pöttgen, R.; Fischer, R. C.; Flock, M. *Chem. Eur. J.* **2013**, *19*, 15504.

18. Chu, T.; Belding, L.; van der Art, A.; Dudding, T.; Korobkov, I.; Nikonov, G. I. *Angew. Chem., Int. Ed.* **2014**, *53*, 2711.

19. Moulton, C. J.; Shaw, B. L. *J. Chem. Soc., Dalton Trans*. **1976**, 1020.

20. Koten, G. V; Jastrzebski, J. T. B. H.; Noltes, J. G.; Spek, A. L.; Schoone, J. C. *J.Organomet. Chem*. **1978**, *148*, 233.

21. Huang, J.-H.; Kuo, P. -C.; Lee, G. -H.; Peng, S. –M. *J. Chin. Chem. Soc.* **2000,** *47,* 1191.

22. Huang, J.-H.; Chen, H.-J.; Chang, J.-C.; Zhou, C.-C.; Lee, G.-H.; Peng, S.-M. *Organometallics* **2001**, *20*, 2647.

23. Kuo, P. -C.; Huang, J.-H.; Hung, C. –H.; Lee, G. -H.; Peng, S. –M. *Eur. J. Inorg. Chem.* **2003**, 1440.

24. Banerjee, S.; Shi, Y.; Cao, C.; Odom, A. L. *J. Organomet. Chem*. **2005**, *690*, 5066.

25. Lee, W.-Y.; Hsieh, C. -C.; Hsu, J.-W.; Datta, A.; Linb, Y. –C.; Huang, J. –H.;Lee, T.-Y. *J. Organomet. Chem.* **2011**, *696*, 3816.

26. Maaß, C.; Andrada, D. M.; Mata, R. A.; Herbst-Irmer, R. and Stalke, D. *Inorg. Chem.* **2013**, *52*, 9539.

27. Vránová, I.; Jambor, R.; Růžička, A.; Hoffmann, A.; Herres-Pawlis, S.; Dostál, L. *Dalton Trans.* **2015**, *44*, 395.

28. Balazs, L.; H. Breunig, J.; Lork, E.; Soran, A.; Silvestru, C. *Inorg. Chem.* **2006**, *45*, 2341.

29. Casely, I. J.; Ziller, J. W.; Mincher, B. J.; Evans J. W. *Inorg. Chem.* **2011**, *50*, 1513.

30. Kindra, D. R.; Casely, I. J.; Fieser, M. E.; Ziller, J. W.; Furche, F.; Evans, J. W. *J. Am. Chem. Soc.* **2013**, *135*, 7777.

31. Kim, I. T.; Elsenbaumer, R. L. *Tetrahedron Lett.* **1998**, *39*, 1087.

32. Goddard, R.; Heinemann, O.; Krüger, C. *Acta Crystallogr., Sect. C: Cryst. Struct. Commun.* **1997**, *53*, 1846.

33. Markies, B.A.; Wijkens, P.; Boersma, J.; Kooijman, H.; Veldman, N.; Spek, A. L.; van Koten, G. *Organometallics* **1994**, *13*, 3244.

34. Tastan, S.; Krause, J. A.; Connick, W. B. *Inorg. Chim. Acta* **2006**, *359*, 1889.

35. Zhang, R.; Liang, Z.; Han, A.; Wu, H.; Du, P.; Lai, W.; Cao, R. *CrystEngComm.* **2014**, *16*, 5531.

36. Petz, W.; Kutschera, C.; Neumüller, B. *Organometallics* **2005**, *24,* 5038.

37. Frisch, M. J.; Trucks, G. W.; Schlegel, H. B.; Scuseria, G. E.; Robb, M. A.; Cheeseman, J. R.; Scalmani, G.; Barone, V.; Mennucci, B.; Petersson, G. A.; Nakatsuji, H.; Caricato, M.; Li, X.; Hratchian, H. P.; Izmaylov, A. F.; Bloino, J.; Zheng, G.; Sonnenberg, J. L.; Hada, M.; Ehara, M.; Toyoto, K.; Fukuda, R.; Hasegawa, J.; Ishida, M.; Nakajima, T.; Honda, Y.; Kitao, O.; Nakai, H.; Vreven, T.; Montgomery, J. A. Jr.; Peralta, J. E.; Ogliaro, F.; Bearpark, M.; Heyd, J. J.; Brothers, E.; Kudin, K. N.; Staroverov, V. N.; Kobayashi, R.; Normand, J.; Raghavachari, K.; Rendell, A.; Burant, J. C.; Iyengar, S. S.; Tomasi, J.; Cossi, M.; Rega, N.; Millam, J. M.; Klene, M.; Knox, J. E.; Cross, J. B.; Bakken, V.; Adamo, C.; Jaramillo, J.; Gomperts, R.; Stratmann, R. E.; Yazyev, O.; Austin, A. J.; Cammi, R.; Pomelli, C.; Ochterski, J. W.; Martin, R. L.; Morokuma, K.; Zakrzewski, V. G.; Voth, G. A.; Salvador, P.; Dannenberg, J. J.; Dapprich, S.; Daniels, A. D.; Farkas, O.; Foresman, J.

B.; Ortiz, J. V.; Cioslowski, J.; Fox, D. J. *Gaussian 09*, Revision A.02; Gaussian, Inc., Wallingford CT, 2009.

38. Reed, A. E.; Curtiss, L. A.; Weinhold, F. *Chem. Rev.* **1988**, *88*, 899.

5.9 Representative Spectra of Some Compounds
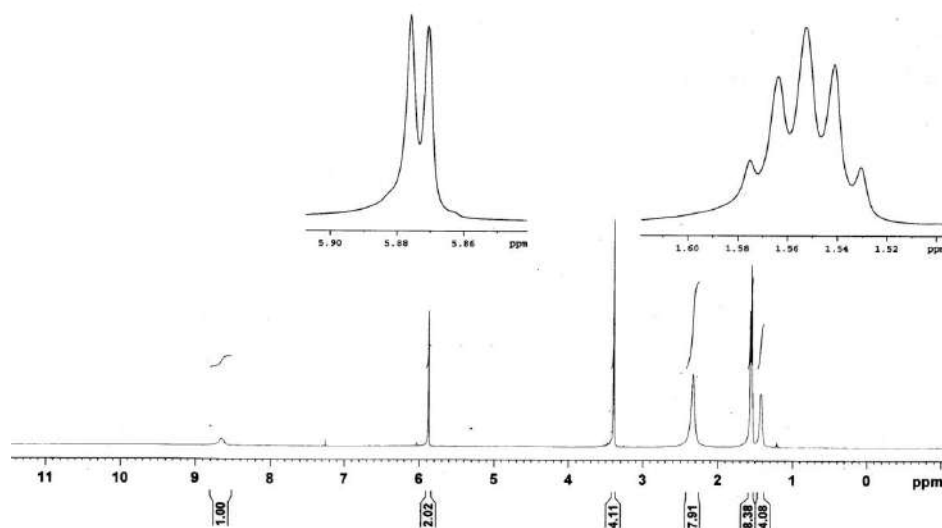
Figure 5.9. ^{1}H NMR spectrum of L^3
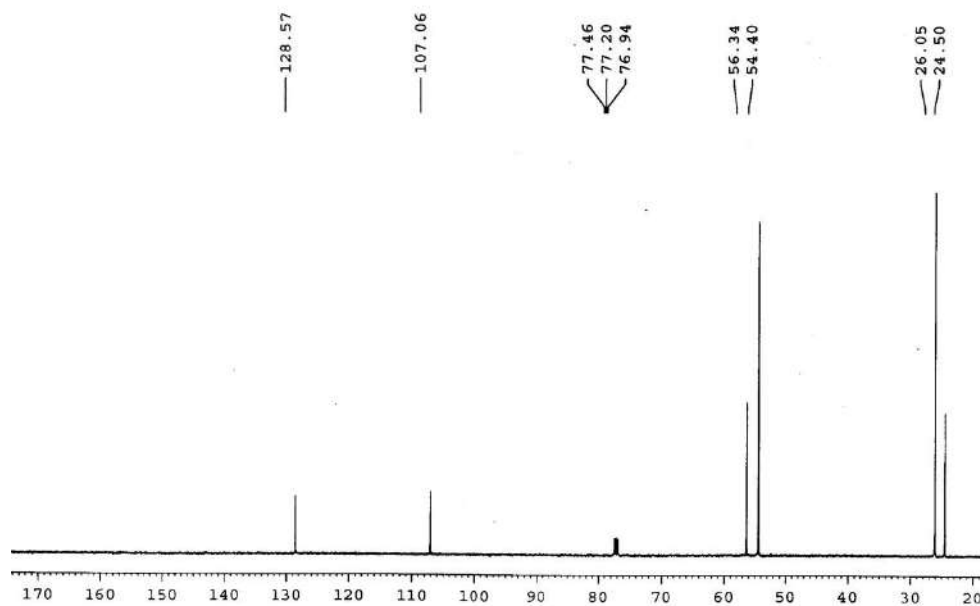
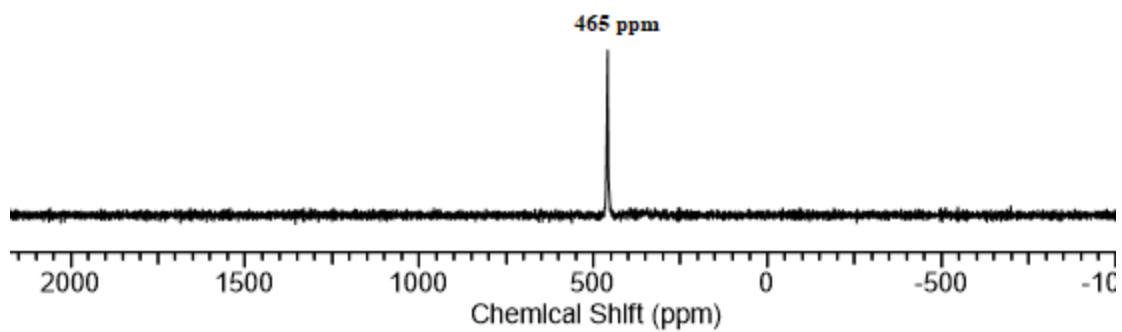**Figure 5.10. ^{13}C NMR spectrum of L^3**
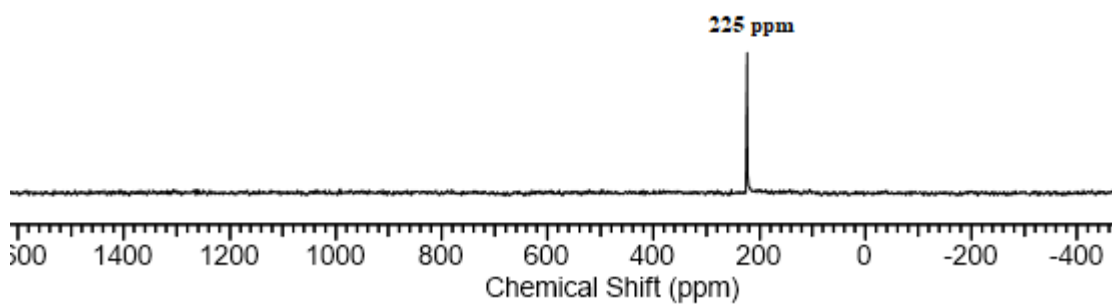
Figure 5.10. ⁷⁷Se NMR spectrum of 5.13

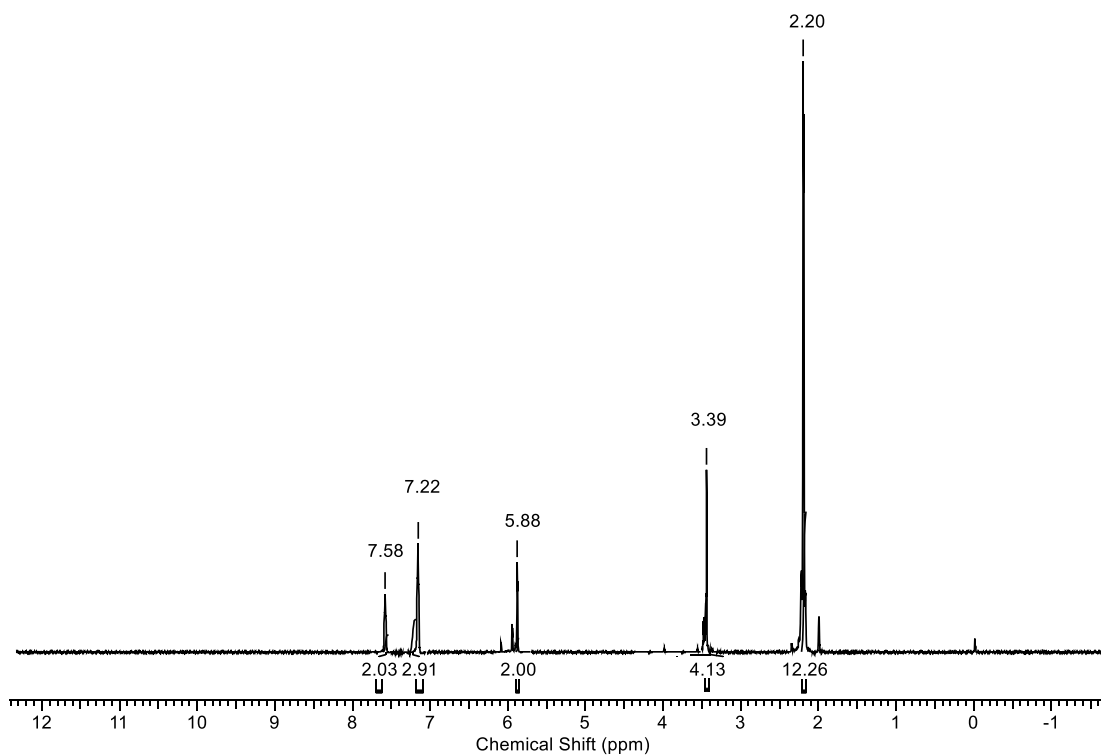

Figure 5.11. ¹²⁵Te NMR spectrum of 5.14

Figure 5.12. ^{1}H NMR spectrum of 5.15
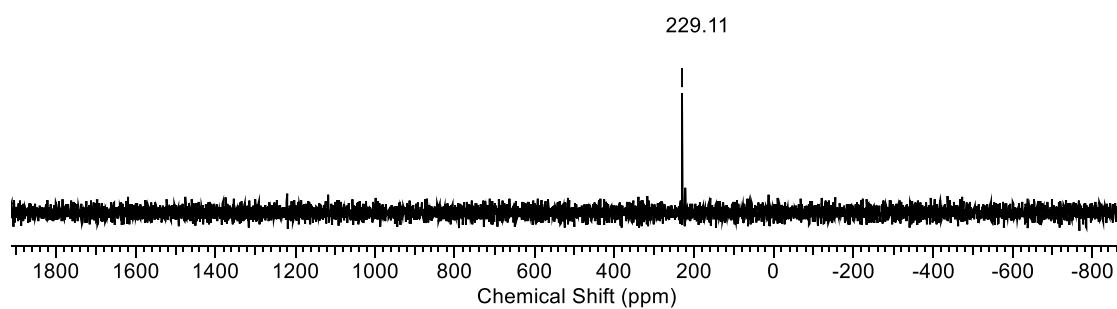
Figure 5.13. ^{77}Se NMR spectrum of 5.15
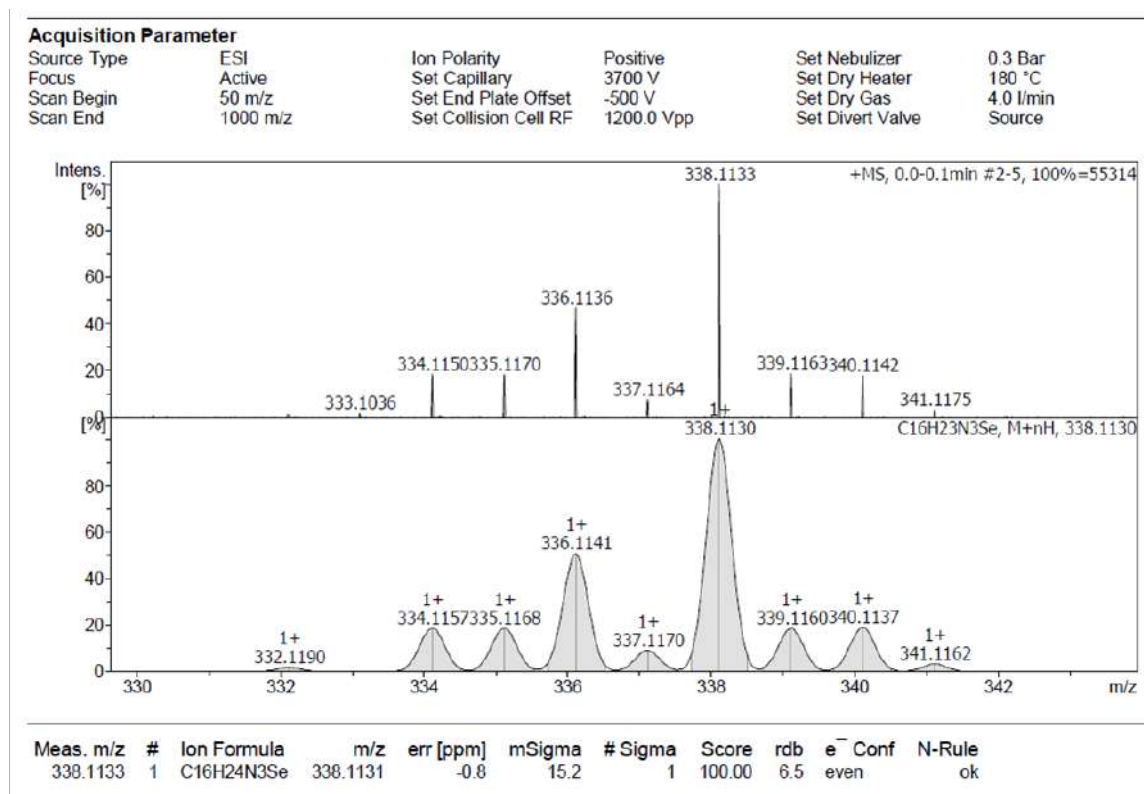
Figure 5.14. HRMS of 5.15

Appendix 1

Isolation of the Novel Example of a Monomeric Organotellurinic Acid

6.1 Introduction

The hydrolysis reactions of heavy main group metal and metalloid halides of period 5, REX_n (E = In, Sn, Sb, Te; X = Cl; n = 2-4) have been extensively studied. Based on the nature of organic groups or the reaction conditions used, the hydrolysis affords a large number of structurally diverse, multinuclear organo-oxo compounds ranging from dimers, cubes, drums, cages to clusters, which have found numerous expedient applications in contemporary chemistry.[1] In recent years, considerable efforts have been directed to isolate the basic monomeric units of the hydrolyzed products, *i.e.*, $RE(OH)_n/RE(O)(OH)_n$ (E = In, Sn, Sb, Te; n = 2-4). It is worth noting that, due to the highly Lewis acidic nature of the E (E = In, Sn, Sb, Te) center in a polar E=O bond, these compounds have an inherent tendency to undergo a high degree of aggregation. In fact, despite the use of sterically encumbered aryl substituents, the reactions afforded self-condensed/aggregated products and consequently the isolation/characterization of the basic building blocks of these hydrolyzed products is still a challenge.[2]

In group 16, the chemistry of organosulfinic(IV)[3] and organoseleninic(IV)[4] acids are well-established in the literature with respect to their well-defined structures, interesting reactivity profiles and promising applications in modern chemistry and biology. Although the first report on an organotellurium(IV) acid, known as an organotellurinic acid dates back to 1915,[5a] the studies on organotellurinic acids have not achieved significant success due to their ill-defined amorphous nature, high melting point and poor solubility in common organic solvents, in comparison to their lighter analogues (S, Se) and other telluroxane derivatives (telluroxides, tellurones, telluronic acids).[5,6] Among various tellurium compounds, tellurite glasses, a class of telluroxane derivatives containing a 'TeO_2' unit as a building block have gained significant attention for their promising optoelectronic properties.[7] However, the lack of precise structural information on these compounds has impeded their development as well as applications in modern technologies. The general protocol for the synthesis of tellurinic acids involves the alkaline hydrolysis of the corresponding aryltellurium trichlorides. Alternatively, tellurinic acid can be prepared by the oxidation of diorganoditellurides.[5f] Both these protocols often result in aggregated products in solution as well as in the solid state.[5a-c,8] Beckmann *et al.*, have used sterically demanding substituents for the synthesis of the first (and the only) example of a well-defined organotellurinic acid **6.1**, [2,6-$Mes_2C_6H_3Te(O)(OH)]_2$, Mes = $2,4,6-Me_3C_6H_2$ (Chart 6.1).[9] In the solid state, tellurinic acid **6.1** exists as a μ_2-oxo-bridged dimer featuring a four-membered Te_2O_2 ring.

6,1, Mes = 2,4, 6-Me₃C₆H₂

6.2, R = C₆H₅NNC₆H₄
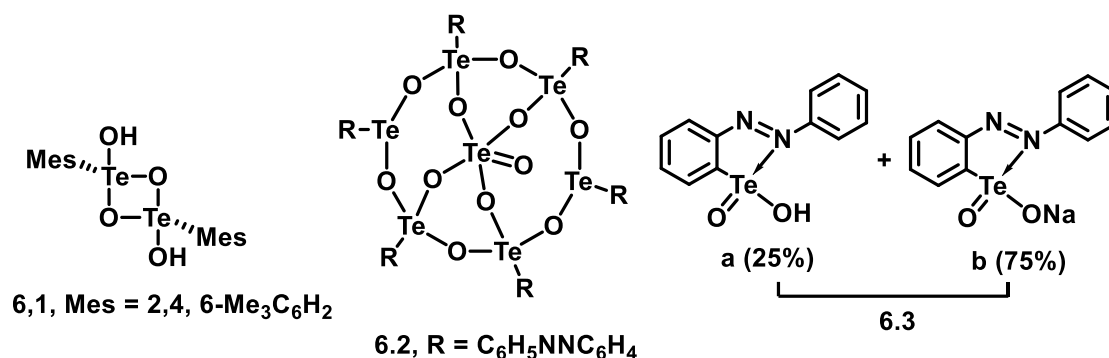
a (25%)   **b (75%)**

6.3

Chart 6.1 Dimeric organotellurinic acid **6.1**, heptanuclear telluroxane cluster **6.2** and co-crystal of monomeric tellurinic acid **6.3a** and its Na-salt **6.3b**.

In another approach, Srivastava *et al.* have attempted to utilize an Intramolecular Chalcogen Bonding (IChB) interaction for the isolation of discrete telluroxane moieties. In particular, the room temperature hydrolysis of the IChB stabilized aryltellurium trichloride, namely [2-(phenylazo)phenyl-*C, N'*]tellurium(IV) trichloride, followed by acidic work-up afforded a heptanuclear, covalent telluroxane cluster **6.2**.[10a] Interestingly, when the reaction was carried out under reflux condition in the absence of acid, co-crystals of monomeric tellurinic acid, **6.3a** and its sodium salt **6.3b** were obtained in a 1:3 ratio.[10b] Both the moieties **6.3** and **6.3a** are held together by multiple hydrogen bonding interactions through a ladder-type Na⁺ and water structure. It is worth mentioning that IChB has recently gained significant attention for stabilizing various otherwise unstable organo-main group compounds and can be best explained invoking the concept of σ-hole participation.[11] In group 14-16 compounds, along the extension of a covalent bond, a highly directional and localized region of depleted electron density (positive electrostatic potential) is observed, due to the anisotropic distribution of electron density and is known as a σ-hole. We envisaged that by using stronger IChB interactions in comparison to that in [2-(phenylazo)phenyl-*C, N'*]tellurium(IV) trichloride, the σ-hole could be fine-tuned to reduce the electrophilicity around the Te atom to isolate discrete, monomeric organotellurinic acid. In reported structures, there are a few aryltellurium trichlorides such as; [2-(4-ethyl-2-oxazolinyl)phenyl]tellurium(IV) trichloride, {2-[1-(3,5-dimethylphenyl)-2-naphthyl]-4,5-dihydro-4,4-dimethyloxazole}tellurium(IV) trichloride, which were stabilized by a much stronger IChB with N···Te bond distances lying in the range 2.2414 (18)-2.251 (3) Å, in comparison to that of [2-(phenylazo)phenyl-*C, N'*]tellurium(IV) trichloride [2.416 (5) Å].[12-14a] For our current study, we preferred [2-(2-pyridyl)phenyl-*C,N'*]tellurium(IV) trichloride, **6.4**, (ppy)TeCl₃ [ppy = 2-(2'-pyridyl)phenyl] as the starting material, as it is a robust system which could withstand highly alkaline reaction

conditions and where the N···Te distance was significantly short [2.277(3) Å] (*vide infra*). Herein, we report the quantitative, room temperature synthesis and comprehensive characterization of the first example of a stable, monomeric organotellurinic acid by alkaline hydrolysis of **4**.

6.2 Results and discussion

Precursor **6.4** was synthesized by the reaction of (ppy)HgCl and TeCl$_4$ as reported by McWhinnie and co-workers.[15] The hydrolysis of **6.4** with one equivalent of NaOH in methanol/water mixture at room temperature resulted in the formation of a stable, white crystalline solid of the partially hydrolyzed μ-oxo-bridged dinuclear telluroxane **6.5**, [(ppyTeCl$_2$)$_2$(μ-O)] in 89% yield (Scheme 6.1). When compound **6.4** was treated with three equivalents of NaOH under identical reaction condition, complete hydrolysis of **6.4** took place and afforded a highly crystalline white solid of the monomeric organotellurinic acid **6.6**, (ppy)Te(O)OH in 93% yield. The ^{1}H and ^{13}C NMR spectra of **6.5** and **6.6** identified pure products with characteristic signals and consistent integration values for the 2-(2´-pyridyl)phenyl moiety. Compound **6.6** is thermally stable, and no aggregation or condensation was observed even at elevated temperature. In the ESI-MS spectrum of **5**, the molecular ion peak at m/z 317.9832 could be assigned to [ppyTeCl]$^+$ (Calc. 317.2406) moiety. Noteworthingly, the observation of a molecular ion peak at m/z 317.9772 (Calc. 317.9769 [M+H]$^+$) for **6.6** by using High Resolution Electrospray Ionization Mass Spectrometry (HRMS) further validates the significant stability of tellurinic acid **6.6**. The ^{125}Te NMR spectrum of **6.5** exhibits single resonance at δ = 1406 ppm. This value is in good agreement with the similar partially hydrolyzed telluroxane, namely, [(8-Me$_2$NC$_{10}$H$_6$TeCl$_2$)$_2$(μ-O)] (δ = 1468 ppm)[8] and is considerably downfield shifted as compared with starting material **6.4** (δ = 1207 ppm). Similarly, the ^{125}Te NMR spectrum of **6.6** showed a single resonance signal at δ = 1468 ppm, which is comparable to that of the dimeric organotellurinic acid **6.1** (δ = 1403 ppm).[9] The FT-IR spectrum (KBr Pellet) of **6.6** exhibits sharp, intense bands at 3458 cm^{-1} and 659 cm^{-1}, which are assigned to OH and Te = O stretching vibrations respectively.
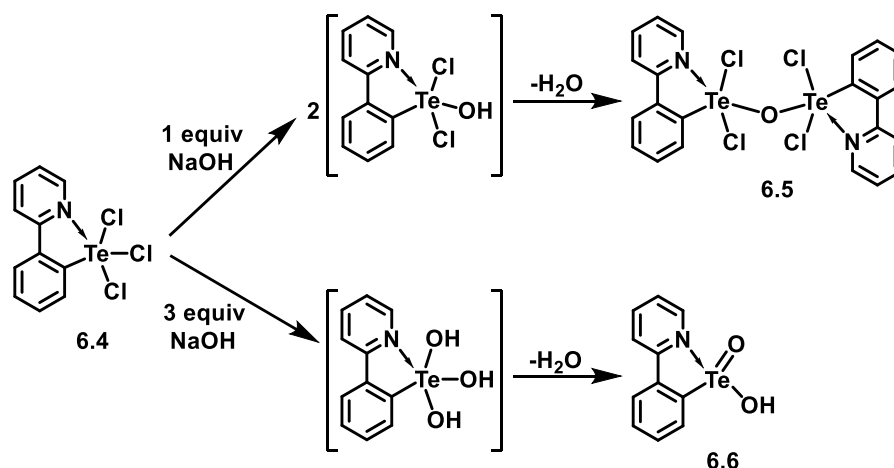
Scheme 6.1 Synthesis of **6.5** and **6.6** by controlled hydrolysis of **6.4**.

Though compound **6.4** has been known since 1992,[15] its structure has not been reported. It was crystallized either from hot methanol or methanol/ethanol (1:1) mixture to give two polymorph **6.4a** and **6.4b**. Crystallization from hot methanol afforded monomeric (ppy)TeCl₃ (**6.4a**, monoclinic) and crystallization from hot methanol/ethanol (1:1) mixture afforded dimeric (ppy)TeCl₃ (**6.4b**, orthorhombic). The metric parameters for the both systems are quite similar and the major difference being, (i) **6.4b** is linked by intermolecular Te···Cl contacts [3.457 (2) Å] resulting in a centrosymmetric dimer, (ii) polymorph **6.4b** crystallizes in chiral space group (P2₁2₁2₁) with Flack parameter -0.02(3) indicating optical purity of the crystal. The molecular structure of **6.4a** is described here (Fig. 6.1a; for the molecular structure of **6.4b** see Fig. 6.5). The geometry around the tellurium is distorted trigonal bipyramidal with two chlorine atoms in axial positions and nitrogen, tellurium, and a chlorine atom in equatorial positions. The N···Te distance is 2.277 (3) Å, which is considerably shorter than that observed in [2-(phenylazo)phenyl-*C, N′*]tellurium(IV) trichloride [2.416 (5) Å] and in good agreement with similar reported aryltellurium(IV) trichlorides containing *sp²* hybridized nitrogen atoms, namely [2-(4-ethyl-2-oxazolinyl)phenyl]tellurium(IV) trichloride [2.2414 (18) Å], [2-[1-(3,5-dimethylphenyl)-2-naphthyl]-4,5-dihydro-4,4-dimethyloxazole]tellurium(IV) trichloride [2.251 (3) Å], ([*N,N′*-dicyclohexyl-1-butane-2,3-diimine]tellurium(IV) trichloride [2.309(4) Å].[12-14] Again, the Te−Cl bond lengths and associated angles are in good agreement with the data observed in the aforementioned compounds.[12-14]

(a)   (b)
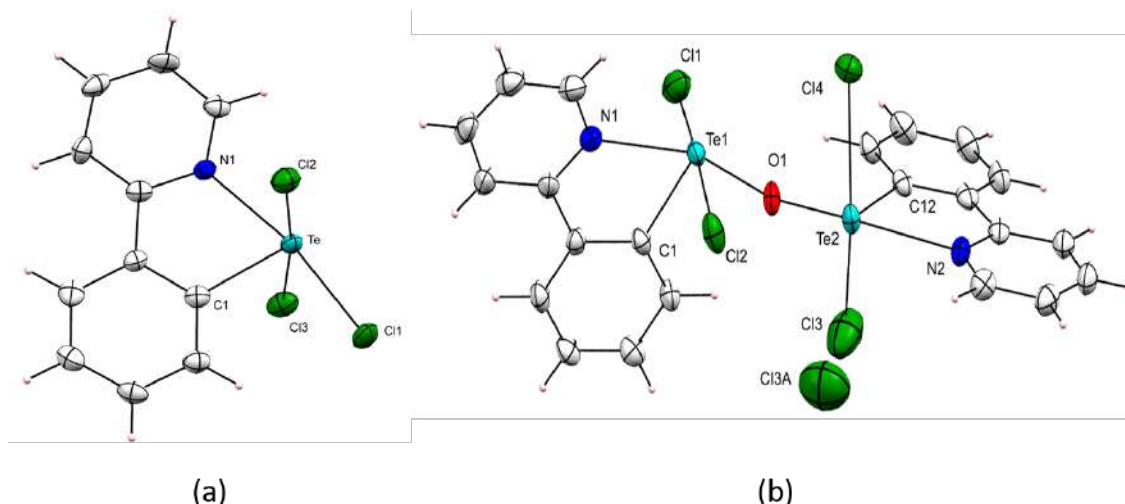
Fig. 6.1 Molecular structures of (a) **6.4a** and (b) **6.5**; thermal ellipsoids are set at the 50% probability level. Selected bond distances and bond angles [Å, °]: For **6.4a**, C1-Te 2.133 (5), N1-Te 2.277 (3), Cl1-Te 2.465 (1), Cl2-Te 2.482 (1), Cl3-Te 2.506 (1), N1-Te-C1 75.7 (2), N1-Te-Cl1 167.64 (9), N1-Te-Cl2 85.47 (9), N1-Te-Cl3 88.58 (9). For **6.5**, N1-Te1 2.413 (4), N2-Te2 2.425 (4), Te1-Cl1 2.542 (1), Te1-Cl2 2.515 (1), Te2-Cl3 2.164 (3), Te2-Cl4 2.741 (1), Te2-Cl3A 3.00 (1), Te1-O1 1.969 (3), Te2-O1 1.963 (3) (1), Te1-O1-Te2 124.90 (2), Cl1-Te1-Cl2 173.38 (5), Cl3-Te2-Cl4 171.88 (8).

In the molecular structure of **6.5** [Fig. 6.1b], the spatial arrangement of each Te atom is distorted trigonal bipyramidal and is defined by a $NCOCl_2$ donor set. The N···Te IChB distances of 2.413 (4) Å and 2.425 (4) Å are significantly longer than that of precursor **6.4** {2.277 (3) [**6.4a**] /2.286 (6) [**6.4b**], Fig. 6.5}, but shorter than that of [(8-$Me_2NC_{10}H_6TeCl_2)_2(\mu$-O)] [2.55 (1) Å].[8] The Te1-O1-Te2 angle of 124.90 (2)° resembles to that of [(8-$Me_2NC_{10}H_6TeCl_2)_2(\mu$-O)] [126.0 (5) Å]. The Te1-Cl1 and Te1-Cl2 bond lengths of 2.542 (1) Å and 2.515 (1) Å are in good agreement with that of [(8-$Me_2NC_{10}H_6TeCl_2)_2(\mu$-O)] [2.470 (5)-2.551 (5) Å]. Interestingly, one of the chlorine atom bonded to Te2 center undergoes ionization resulting in a shorter Te2-Cl3 bond [1.164 (3) Å], a longer Te2-Cl4 bond [2.741 (1) Å] and a weak Te···Cl3A interaction [3.00 (1) Å].

The molecular structure of **6.6** (crystallized as **6.6**.$2H_2O$), reveals that the geometry around the Te(IV) center is distorted trigonal bipyramidal, taking the N···Te IChB into account (Fig. 6.2a). The donor set CNO_2 makes spirocyclic arrangement around the Te center. The 2-phenylpyridine ring together with the Te atom and the OH group reside in a single plane, and the double bonded oxygen atom (O1) occupies the axial position. The donor

C and N atoms make C1-Te-O1 and N1-Te-O1 angles of 103.0(1)° and 87.00(9)° respectively with the double bonded oxygen. While the O1-Te-O2 angle is close to a right angle [96.0(1)°], the N1-Te-O2 angle is *transoid* with a value of 166.12(9)°. The C-N1-Te bond angle is 114.0 (2)°. The Te=O bond distance of 1.834(2) Å is significantly shorter in comparison to that of the dimeric tellurinic acid **6.1** [1.897 (5) Å], as in the latter the O atom is involved in bridging with two Te atoms.[9] The Te-OH bond distance in **6.6** is 1.966(2) Å, which compares well with the ideal Te-O single bond distance (2.04 Å)[16] and is significantly shorter than that observed in **6.1** [2.232(4) Å].[9] Particularly noteworthy in the molecular structure of **6.6**, is the N···Te IChB, which makes a planar five-membered ring with the Te atom. The N···Te bond distance of 2.411(2) Å in **6.6** is longer than typical Te-N single bonds [$\Sigma\ r_{cov}$ (Te, N) = 2.09 Å], and much shorter than the sum of the van der Waals radii for these atoms [$\Sigma\ r_{vdw}$ (Te, N) = 3.58 Å].[16-17] This N···Te distance in **6.6** is significantly shorter than that observed in **6.3** [2.694(3)/2.708(3) Å].[10b] Both the O-atoms of **6.6** are involved in hydrogen bonding with two water molecules with O1···H and O2···H distances of 1.94 (5) Å and 2.08 (4) Å respectively. In the packing diagram of **6.6**, unlike in tellurinic acid **6.1**, two adjacent molecules are oriented in a head-to-tail manner, and the Te and O atoms of the adjacent molecules are considerably separated [7.653(3) Å], thereby minimizing the probability for dimerization or intramolecular Te···O interactions. In addition, a π-arene interaction of two neighboring ppy moieties is observed as indicated by the centroid-centroid distance of 3.706 Å between them (Fig. 6.6).

To probe the role of the N-atom of the 2-phenylpyridine ring in assisting the mono-nuclearity of the synthesized aryltellurinic acid **6.6** and to understand the hitherto unknown bonding properties in monomeric aryltellurinic acid, DFT calculations were carried out using Gaussian 0.9 (Rev A.02) program[18] (functional: B3PW91;[19] mixed basis set: Te: SDB-cc-pVTZ;[20] C/H/N/O: 6-311+G**[21]). After a geometry optimization starting from the crystal coordinates, natural bond orbital (NBO) calculations were performed for compound **6.6**.[22] The NBO analysis inferred that the lone pair (*lp*) on the N-atom donates its electron density to the antibonding *p*-orbital (*p**) of the Te center, thereby resulting in the N→Te donor-acceptor interaction (Fig. 6.2b). The stabilization energy of 37.43 kcal/mol of the N→Te interaction indicates that it plays a significant role in the overall stability of the compound. Rani *et al.*, have recently observed a similar *lp*(N)→*p*(Te) interaction in a series of IChB stabilized aryltellurenium(II) cations where N···Te bond distances lie in the range of 2.210 (7) Å-2.287(2) Å.[23] Similar IChB interactions, where the lone pair of the donor atom interacts

with the vacant *p*-orbital are observed in other organo-main group compounds,[24] however, it is not prevalent in the case of organotellurium compounds and the electrons mostly populate the σ* orbital of the covalent bond *trans* to the donor atom. In a comparative study, when NBO analysis of the N→Te bond in compound **6.3** was performed where the N atom is more loosely bonded to the Te atom than in compound **6.6**, it was observed that the acceptor NBO is a σ* orbital of the Te-O single bond.
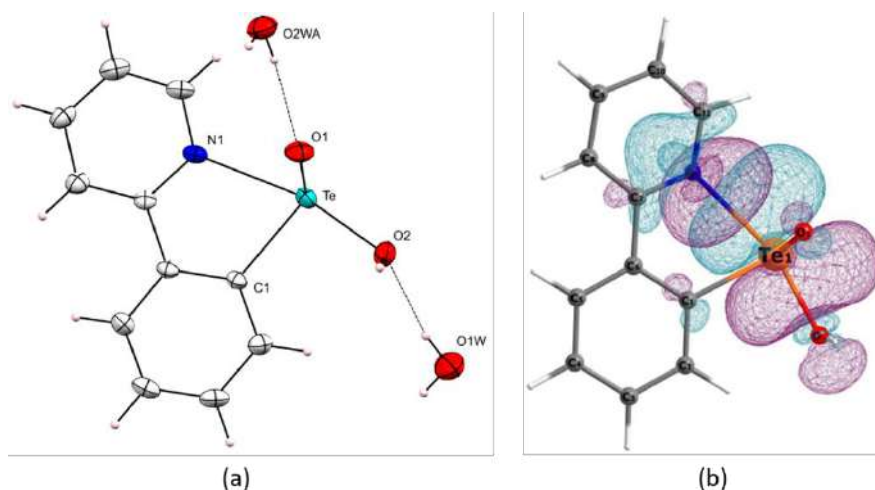

Fig. 6.2 (a) Molecular structure of **6.6**; thermal ellipsoids are set at the 50% probability level. Selected bond distances and angles [Å, °]: C1-Te 2.128 (3), N1···Te 2.411 (2), O1-Te 1.834 (2), O2-Te 1.966 (2), C1-Te···N 73.28 (9), N···Te-O1 87.00 (9), N···Te-O2 166.12(9), O1-Te-O2 96.00 (1), C-Te-O2 92.80 (1). (b) Natural bond orbital (NBO) plot showing the *lp*(N)→*p**(Te) interaction, stabilization energy, ΔE = 37.43 kcal/mol.

The electrostatic surface potential (ESP) map provides an important insight into the correlation of the σ-hole and IChB in **6.6**. To locate the position of the σ-hole, the structure of **6.6** was re-optimized by imposing a symmetry constraint around the pyridyl ring (*i.e.*, rotating the pyridyl ring with respect to the phenyl ring) so that there is no N···Te interaction present. The ESP of the modified structure showed a broad σ-hole region antipodal to the Te-O double bond (Fig. 6.3a). The disappearance of the original σ-hole in compound **6.6** (Fig. 6.3b) clearly indicates the direct involvement of the σ-hole in chalcogen bonding with the lone pair of the nitrogen atom, thereby resulting in considerable exhaustion of electrophilicity at the Te center to afford a stable monomeric unit. To quantitatively analyze the nature of bonding in **6.6,** the quantum theory of atoms in molecule (QTAIM) analysis was performed. The topological parameters of the N···Te bond critical point (bcp) suggest a predominantly

ionic character of the N···Te interaction with a significant mixing of covalent character. The AIM bond topology of **6.6** and the relevant topological parameters are included in Fig 6.7, Table 6.2).[25-26]
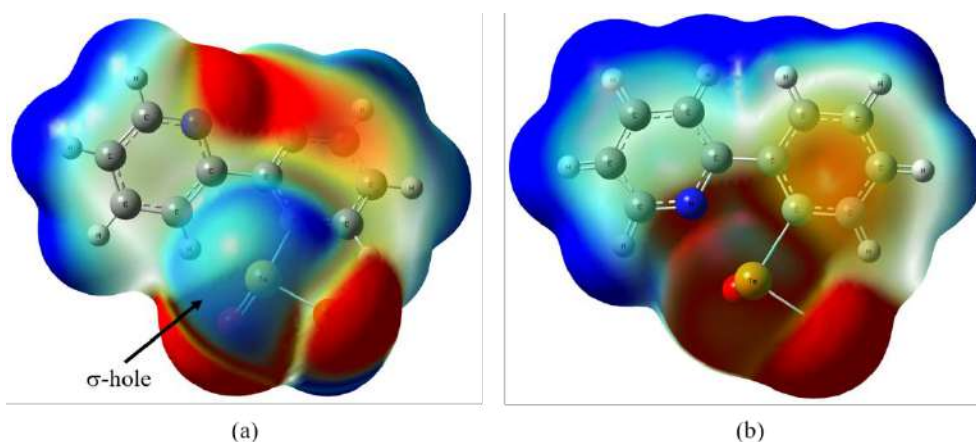

(a)   (b)

Fig. 6.3 (a) Electrostatic surface potential (ESP) map, $\rho(r) = 0.001$ a.u., showing the location of σ-hole antipodal to the Te=O bond in the absence of an N···Te IChB interaction. (b) ESP of **6.6** showing the disappearance of the σ-hole due to the presence of the N···Te IChB interaction. ESP s have been drawn on the Hirshfeld surfaces with potential in the range -0.02 a.u. (red)-0.02 a.u. (blue).

The attempted synthesis of an organotelluronic(VI) acid by the reaction of compound **6.6** with strong oxidizing agents such as H_2O_2 and $NaIO_4$ resulted in immediate precipitation of a white solid, which was insoluble in common organic solvents. In an alternative approach, when **6.7**, (ppyTe)$_2$[27] was treated with H_2O_2 in methanol at room temperature, the reaction resulted in the formation of μ-oxo bridged dimethyl ester [(ppy)Te(O)(OH)(OMe)]$_2$(O), **6.8** (Scheme 6.2). This is similar to the observation by Beckmann *et al.*, wherein the reaction of bis[8-(dimethylamino)-1-naphthyl] ditelluride, (8-Me$_2$NC$_{10}$H$_6$Te)$_2$ with H_2O_2 followed by crystallization from methanol afforded the dimethyl ester derivative of the diorganoditelluronic acid, [8-Me$_2$NC$_{10}$H$_6$Te(O)(OH)(OMe)]$_2$(O).[6e]
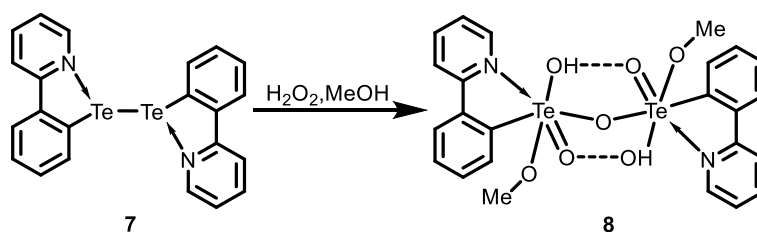
Scheme 6.2 Synthesis of **6.8** by H_2O_2 hydrolysis of **6.7**.

The ^{125}Te NMR chemical shift (δ 833 ppm) is in good agreement with [8-Me$_2$NC$_{10}$H$_6$Te(O)(OH)(OMe)]$_2$(O) (^{125}Te NMR: δ 885 ppm).[6e] The molecular structure of **6.8** is isostructural (Fig. 6.4a) with [8-Me$_2$NC$_{10}$H$_6$Te(O)(OH)(OMe)]$_2$(O), except the fact that in the place of 8-(dimethylamino) napthyl ring, 2-phenypyridine ring unit is bonded to each tellurium atom. The Te-O double bond distances [1.818 (4) Å, 1.820 (3) Å] and Te-O single bond distances [1.894 (3) Å – 2.000 (3) Å] are well comparable to that of [8-Me$_2$NC$_{10}$H$_6$Te(O)(OH)(OMe)]$_2$(O). Of particular interest is the N$\cdots$Te IChB distances of 2.269 (5) Å and 2.277 (4) Å, which are significantly shorter than that observed in [8-Me$_2$NC$_{10}$H$_6$Te(O)(OH)(OMe)]$_2$(O) [2.406 (8) Å and 2.384 (7) Å]. The structure of **6.8** was further examined by NBO analysis, which describes the N$\cdots$Te interaction as a *lp*(N)$\rightarrow$ σ*(Te-OH) donor-acceptor interaction with stabilization energy of 29.26 kcal/mol (Fig. 6.4b). There are two other contributions for N$\rightarrow$Te interactions; namely *lp*(N)$\rightarrow$$\sigma$*(Te-C) (21.59 kcal/mol) and *lp*(N)$\rightarrow$$\sigma$*(Te=O) (20.39 kcal/mol) which also play considerable role in the overall stability of the compound [Fig. 6.8].
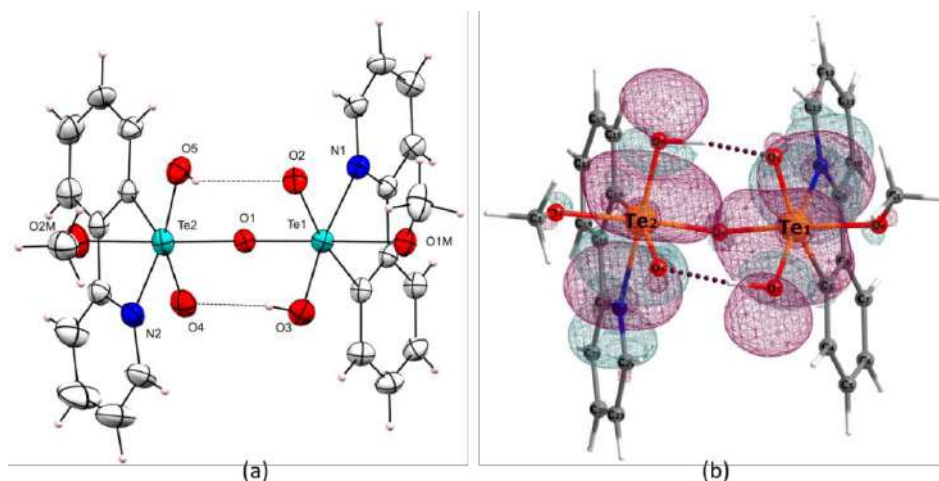
Fig. 6.4 (a) Molecular structure of **6.8**; thermal ellipsoids are set at the 50% probability level. Selected bond distances and angles [Å, °]: Te1-O1 2.000 (3), Te1-O2 1.820 (3), Te1-O3 1.894 (3), Te1-O1M 1.945 (3), N1···Te1 2.269 (5), Te2-O4 1.818 (4), Te2-O5 1.897 (3), Te2-O1 1.971 (3), Te2-O2M 1.949 (4), N2···Te2 2.277 (4), Te1-O1-Te2 122.8 (2). (b) Natural bond orbital (NBO) plot showing $lp(N) \rightarrow \sigma^*(Te\text{-}OH)$ interaction (isosurface value = 0.03), stabilization energy, $\Delta E = 29.26$ kcal/mol.

6.3 Conclusions

We report the σ-hole assisted synthesis of the novel example of a monomeric organotellurinic acid. Compound **6.6** is the first of its kind for any monomeric organo-acid of period 5 main group metals and metalloids (In, Sn, Sb and Te). The formation of the monomeric organotellurinic acid **6.6** is made possible by utilizing a rigid and planar pyridylphenyl ring where the N-atom makes a strong IChB by donating its lone pair of electrons to the antibonding *p*-orbital of the Te atom, and attenuates the electrophilicity around the Te center. We believe that like its lighter congeners, the availability of a monomeric organotellurinic acid species will stimulate interesting activity in the area of organometallics, materials and biochemistry. Efforts are underway to exploit the strong IChB capability of the 2-(2'-pyridyl)phenyl group to stabilize hitherto unknown diorganotelluronium dications and to explore the coordination behavior of the resultant cationic species towards transition metals.

6.4 Experimental Section

All manipulations were performed under a N_2 atmosphere using standard Schlenk techniques. Solvents were dried by following standard methods. The starting materials and solvents were purchased from commercial sources. (ppy)TeCl$_3$ was synthesized following reported procedure using (ppy)HgCl and TeCl$_4$.[15] (**Caution**: organomercury compounds are highly toxic. Adequate precaution should be taken while handing of such compounds). (ppyTe)$_2$ was synthesized by the treatment of ppyTeBr with an excess of hydrazine hydrate.[27] ^{1}H (400 and 500 MHz), ^{13}C (100 and 125 MHz) and ^{125}Te (126 MHz, 158 MHz) NMR spectra were recorded on Bruker AV 400 MHz and Bruker AV 500 MHz spectrometers at 25 °C. Chemical shifts cited were referenced to TMS (^{1}H, ^{13}C) as internal and Me$_2$Te (^{125}Te) as external standard. Electron spray mass spectra (ESI-MS) were performed on a Q-Tof micro (YA-105) mass spectrometer. Melting points were recorded in capillary tubes on a Veego VMP-1 instrument and are uncorrected. Elemental analyses were performed on a Carlo Erba Model 1106 elemental analyzer. Infrared spectra were recorded on a Perkin Elmer Spectrum One FT-IR spectrometer using KBr pellets.

Synthesis of compounds 6.5 and 6.6

To a solution of **6.4**[15] (0.200 g, 0.514 mmol) in methanol (15 mL), was added NaOH (0.200 g, 0.514 mmol for **6.5**, 0.061 g, 1.542 mmol for **6.6**) in water (2 mL). The reaction mixture was stirred at room temperature for 20 h, which resulted in a white precipitate. The precipitate was collected by filtration and dried under vacuum to get the pure product. Colorless crystals of **6.5** and **6.6** suitable for single-crystal diffraction analysis were obtained by slow evaporation from a methanol solution of **6.5** and **6.6** at room temperature respectively.

6.5: Yield 0.332 g (89%); m.p. 211-214 °C; ^{1}H NMR (500 MHz, DMSO-d_6) δ 8.58 (ddd, J = 4.8, 1.7, 0.9 Hz, 2H), 8.19 – 8.11 (m, 4H), 7.98 (td, J = 7.8, 1.8 Hz, 2H), 7.66 (dd, J = 7.1, 1.4 Hz, 2H), 7.51 (ddd, J = 7.4, 4.8, 0.9 Hz, 2H), 7.44 (dtd, J = 17.9, 7.3, 1.5 Hz, 4H); ^{13}C NMR (125 MHz, DMSO-d_6) δ 156.5, 150.3, 148.5, 141.9, 139.0, 138.4, 129.8, 128.7, 127.7, 124.0, 121.6; ^{125}Te (126 MHz, DMSO-d_6) δ 1406; MS (ESI+, CH$_3$OH): *m/z* 317.9832 (Observed) (Calc. 317.2406, [C$_{11}$H$_8$ClNTe]$^+$); Anal. Calc. for C$_{22}$H$_{16}$Cl$_4$N$_2$OTe$_2$: C, 36.63; H, 2.24; N, 3.88; Found C, 36.58; H, 2.10; N, 3.27.

6.6: Yield 0.152 g (93%); m. p. 188 °C; ^{1}H NMR (500 MHz, D$_2$O) δ 8.61 (d, J = 4.5 Hz, 1H), 8.22 – 8.14 (m, 3H), 8.08 (t, J = 7.4 Hz, 1H), 7.70 (p, J = 7.6 Hz, 2H), 7.53 (t, J = 6.3 Hz, 1H); ^{13}C NMR (125 MHz, D$_2$O) δ 151.8, 144.4, 141.4, 136.8, 132.6, 131.8, 130.4, 126.6, 125.1, 120.5; ^{125}Te (126 MHz, D$_2$O) δ 1468; MS (ESI+, CH$_3$OH): *m/z* 317.9772 (Observed) (Calc. 317.9769 {[**6**+H]$^+$}); FT-IR (KBr): ν(O-H) 3458 cm^{-1}, ν(Te=O) 659 cm^{-1}; Anal. Calc. for C$_{11}$H$_9$NO$_2$Te: C, 41.97; H, 2.88; N, 4.45; Found C, 41.78; H, 2.42; N, 4.65.

Synthesis of compound 6.8

To a solution of **6.7**, (ppyTe)$_2$^{27} (0.250 g, 0.440 mmol) in methanol (10 mL) was added H$_2$O$_2$ (35%, 3 mL), and the reaction mixture was refluxed for 18 h. The mixture was cooled down to room temperature. A white solid precipitated that was collected by filtration, dried under vacuum to get the pure compound **6.8**. Colorless crystals of **6.8** suitable for single-crystal diffraction analysis were obtained by slow evaporation from a chloroform solution of **6.8** at room temperature.

Yield 0.261 g (83%); m.p. 221-223 °C; ^{1}H NMR (400 MHz, CDCl$_3$) δ 8.79 – 8.75 (m, 2H), 8.29 (dd, J = 7.9, 1.1 Hz, 2H), 7.91 – 7.76 (m, 6H), 7.37 – 7.27 (m, 4H), 7.11 (td, J = 8.0, 1.4 Hz, 2H), 3.48 (s, 6H); ^{13}C NMR (125 MHz, CDCl$_3$) δ 156.5, 146.1, 140.2, 139.1, 137.1, 129.7, 127.0, 122.4, 120.6, 111.5, 50.8; ^{125}Te NMR (400 MHz, CD$_3$OD) δ 833; MS (ESI+, CH$_3$OH): *m/z* 333.9787 (Observed) (Calc. 333.9718, [C$_{11}$H$_{10}$NO$_3$Te]$^+$); FT-IR (KBr): ν(O-H) 3441 cm^{-1}, ν(Te=O) 734 cm^{-1}. Anal. Calc. for C$_{24}$H$_{24}$N$_2$O$_7$Te$_2$: C, 40.73; H, 3.42; N, 3.96; Found C, 40.43; H, 3.35; N, 3.85.

6.5 References

1. (a) R. R. Homes, *Acc. Chem. Res*., 1989, **22**, 190-197; (b) H. Puff, H. Reuter, *J. Organomet. Chem*., 1989, **373**, 173-184; (c) W. Uhl, M. Pohlmann, *Chem. Commun.*, 1998, 451-452; (d) V. Chandrasekhar, S. Nagendran, V. Baskar, *Coord. Chem. Rev*., 2002, **235**, 1-52, and references therein; (e) A. K. Jami, M. S. R. Prabhu, V. Baskar, *Organometallics*, 2010, **29**, 1137-1143; (f) J. Goura, V. Chandrasekhar, *Chem. Rev.*, 2015, **115**, 6854-6965, and references therein; (g) S. Yadav, H. B. Singh, M. Zeller, R. J. Butcher, *Organometallics*, 2017, **36**, 2067-2071.

2. (a) J. Beckmann, T. Heek, M. Takahash, *Organometallics*, 2007**, 26***, 3633-3635; (b) S. U. Ahmed, J. Beckmann, *Organometallics*, 2009, **28**, 6893-6901; (c) U. U. Ahmed, J. Beckmann, A. Duthie, *Chem. Asian J*., 2010, **5**, 160-168; (d) J. Brünig, E. Hupf, E. Lork, S. Mebs, J. Beckmann, *Dalton Trans*., 2015, **44**, 7105-7108.

3. a) W. E. Truce, A. M. Murphy, *Chem. Rev.*, 1951, **48**, 69-124; (b) J. L. Kice, K. W. Bowers, *J. Am. Chem. Soc*., 1962, **84,** 605-610; (c) K. Seff, E. G. Heidner, M. Meyers, K. N. Trueblood, *Acta Cryst*., 1969, **B25**, 350-354; (d) H. A. Woo, H. Z. Chae, S. C. Hwang, K.-S. Yang, S. W. Kang, K. kim, S. G. Rhee, *Science*, 2003, **300**, 653-656; (e) Z. A. Wood, L. B. Poole, P. A. Karplus, *Science*, 2003, **300**, 650-653; (f) S. Akter, L. Fu, Y. Jung, M. L. Conte, J. R. Lawson, W. T. Lowther, R. Sun, K. Liu, J. Yang, K. S. Carroll, *Nat. Chem. Biol*., 2018, **14**, 995-1004; (g) M. Griesser, J.-P. R. Chauvin, D. A. Pratt, *Chem. Sci.*, 2018, **9**, 7218-7229.

4. (a) J. H. Bryden, J. D. Mccullough, *Acta Cryst*., 1954, **7**, 833-838; (b) J. H. Bryden, J. D. Mccullough, *Acta Cryst*., 1956, **9**, 528-533; (c) T. Shimizu, I. Watanabe, N. Kamigata, *Angew. Chem. Int. Ed.*, 2001, **40**, 2460-2462; *Angew. Chem.*, 2001, **113**, 2526-2528; (d) H. Ungati, V. Govindaraj, M. Narayanan, G. Mugesh, *Angew. Chem. Int. Ed.*, 2019, **58**, 8156-8160; *Angew. Chem.*, 2019, **131**, 8240-8244; (e) K. H. Tan, W. Xu, S. Stefka, D. E. Demco, T. Kharandiuk, V. Ivasiv, R. Nebesnyi, V. S. Petrovskii, I. I. Potemkin, A. Pich, *Angew. Chem. Int. Ed.*, 2019, **58**, 9791-9796; *Angew. Chem.*, 2019, **131**, 9895-9901.

5. (a) K. Lederer, *Ber. Dtsch. Chem. Ges*., 1915, **48**, 1345-1350; (b) P. Thavornyutikarn, W. R. McWhinnie, *J. Organomet. Chem*., 1973, **50**, 135-143; (c) D. H. R. Barton, J. Finet, M. Thomas, *Tetrahedron*, 1986, **42**, 2319-2324; (d) Y. Nakashima, T. Shimizu, K. Hirabayashi, N. Kamigata, *Org. Lett*., 2004, **6**, 2575-2577; (e) Y. Nakashima, T. Shimizu, K. Hirabayashi, M. Yasui, M. Nakazato, F. Iwasaki, N. Kamigata, *Tetrahedron:*

Asymmetry, 2004, 3791-3797; (f) E. E. Alberto, L. M. Muller, M. R. Detty, *Organometallics*, 2014, **33**, 5571-5581.

6. (a) N. J. Beckmann, P. Finke, *Organotelluroxanes*, in: J. D. Woollins, R. Laitinen (Eds.), *Selenium and Tellurium Chemistry: from Small Molecules to Biomolecules and Materials*, Springer Berlin Heidelberg, 2011, **Ch. 7**, 151-177; (b) K. Srivastava, A. Panda, S. Sharma, H. B. Singh, *J. Organomet. Chem.*, 2018, **861**, 174-206, and references therein; (c) A. Gupta, R. Deka, H. B. Singh, R. J. Butcher, *J. Organomet. Chem.*, 2019, **894**, 10-17; (d) A. Gupta, R. Deka, A. Sarkar, H. B. Singh, R. J. Butcher, *Dalton Trans.*, 2019, **48**, 10979-10985; (e) J. Beckmann, J. Bolsinger, A. Duthie and P. Finke, *Organometallics,* 2012, **31**, 289-293.

7. (a) R. El-Mallawany, *Mater. Chem. Phys.*, 1999, *60*, 103-131; (b) R. El-Mallawany, *Mater. Chem. Phys.*, 2000, **63**, 109-115; (c) J. C. McLaughlin, S. L. Tagg, J. W. Zwanziger, *J. Phys. Chem. B*, 2001, **105**, 67-75; (d) M. I. Sayyed, H. Elhouichet, *Radiat. Phys. Chem.*, 2017*, **130***, 335-342; (e) N. S. Tagiara, D. Palles, E. D. Simandiras, V. Psycharis, A. Kyritsis, E. I. Kamitsos, *J. Non-Cryst. Solids*, 2017, **457**, 116-125.

8. J. Beckmann, J. Bolsinger, A. Duthie, *Chem. Eur. J.*, 2010, **17**, 930-940.

9. J. Beckmann, P. Finke, M. Hesse, B. Wettig, *Angew. Chem. Int. Ed.*, 2008, **47**, 9982-9984; *Angew. Chem.*, 2008, **120**, 10130-10133.

10. (a) K. Srivastava, S. Sharma, H. B. Singh, U. P. Singh, R. J. Butcher, *Chem. Commun.*, 2010, **46**, 1130-1132; (b) K. Srivastava, P. Shah, H. B. Singh, R. J. Butcher, *Organometallics*, 2011, **30**, 534-546.

11. (a) A. F. Cozzolino, P. J. W. Elder, I. Vargas-Baca, *Coord. Chem. Rev.*, 2011, **255**, 1426-1438, and references therein; (b) P. Politzer, J. S. Murray, T. Clark, *Phys. Chem. Chem. Phys.*, 2013, **15**, 11178-11189; (c) D. J. Pascoe, K. B. Ling, S. L. Cockrof, *J. Am. Chem. Soc.*, 2017, **139**, 15160-15167; (d) L. Brammer, *Faraday Discuss.*, 2017, *203*, 485-507; (e) K. Selvakumar, H. B. Singh, *Chem. Sci.*, 2018, **9**, 7027-7042, and references therein; (f) S. Benz, A. I. Poblador-Bahamonde, N. Low-Ders, S. Matile, *Angew. Chem. Int. Ed.*, 2018, **57**, 5408-5412; *Angew. Chem.*, 2018, **130**, 5506-5510; (g) M. Yang, D. Tofan, C.-H. Chen, K. M. Jack, F. P. Gabbaï, *Angew. Chem. Int. Ed.*, 2018, **57**, 13868-513872; *Angew. Chem.*, 2018, **130**, 14064-14068.

12. P. Rakesh, H. B. Singh, R. J. Butcher, *Dalton Trans.*, 2012, **41**, 10707-10714.

13. K. Kandasamy, S. Kumar, H. B. Singh, G. Wolmershäuser, *Organometallics*, 2003, **22**, 5069-5078.

14. (a) M. A. K. Ahmed, W. R. McWhinnie, *J. Organomet. Chem.*, 1985, **281**, 205-211; (b) J. L. Dutton, C. D. Martin, M. J. Sgro, N. D. Jones, P. J. Ragogna, *Inorg. Chem.*, 2009, 48, 3239-3247.

15. T. S. Lobana, W. R. McWhinnie, *Indian. J. Chem. Sect. A*, 1992, **31**, 460-462.

16. P. Pyykkö, M. Atsumi, *Chem. Eur. J.*, 2009, **15**, 186-197.

17. S. Alvarez, *Dalton Trans.*, 2013, **42**, 8617-8636.

18. M. J. Frisch, G. W. Trucks, H. B. Schlegel, G. E. Scuseria, M. A. Robb, J. R. Cheeseman, G. Scalmani, V. Barone, B. Mennucci, G. A. Petersson, H. Nakatsuji, M. Caricato, X. Li, H. P. Hratchian, A. F. Izmaylov, J. Bloino, G. Zheng, J. L. Sonnenberg, M. Hada, M. Ehara, K. Toyoto, R. Fukuda, J. Hasegawa, M. Ishida, T. Nakajima, Y. Honda, O. Kitao, H. Nakai, T. Vreven, J. A. Montgomery Jr., J. E. Peralta, F. Ogliaro, M. Bearpark, J. J. Heyd, E. Brothers, K. N. Kudin, V. N. Staroverov, R. Kobayashi, J. Normand, K. Raghavachari, A. Rendell, J. C. Burant, S. S. Iyengar, J. Tomasi, M. Cossi, N. Rega, J. M. Millam, M. Klene, J. E. Knox, J. B. Cross, V. Bakken, C. Adamo, J. Jaramillo, R. Gomperts, R. E. Stratmann, O. Yazyev, A. J. Austin, R. Cammi, C. Pomelli, J. W. Ochterski, R. L. Martin, K. Morokuma, V. G. Zakrzewski, G. A. Voth, P. Salvador, J. J. Dannenberg, S. Dapprich, A. D. Daniels, O. Farkas, J. B. Foresman, J. V. Ortiz, J. Cioslowski and D. J. Fox, Gaussian 09, Revision A.02, Gaussian, Inc., Wallingford CT, **2009**.

19. (a) J. P. Perdew, Y. Wang, *Phys. Rev. B*, 1992, **23**, 13244-13249; (b) A. D. Becke, *J. Chem. Phys.*, 1993, **98**, 5648-5652.

20. J. M. L. Martin, A. Sundermann, *J. Chem. Phys.*, 2001, **114**, 3408-3420.

21. G. A. Petersson, M. A. Al-Laham, *J. Chem. Phys.*, 1991, **94**, 6081-6090.

22. E. D. Glendening, J. K. Badenhoop, A. E. Reed, J. E. Carpenter, J. A. Bohmann, C. M. Morales, C. R. Landis, F. Weinhold, Theoretical Chemistry Institute, University of Wisconsin, Madison, NBO 6.0, **2013**.

23. V. Rani, M. Boda, S. Raju, G. N. Patwari, H. B. Singh, R. J. Butcher, *Dalton Trans.*, 2018, **47**, 9114-9127.

24. (a) T.-P. Lin, I.-S. Ke, F. P. Gabbaï, *Angew. Chem. Int. Ed.*, 2012, *51*, 4985-4988; *Angew. Chem.*, 2012, **124**, 5069-5072; (b) Y.-H. Lo, F. P. Gabbaï, *Angew. Chem. Int. Ed.*, 2019, **58**, 10194-10197; *Angew. Chem.*, 2019, **131**, 10300-10303.

25. F. Biegler-König, J. Schönbohm, *J. Comput. Chem.*, 2002, **23**, 1489-1494.

26. P. S. V. Kumar, V. Raghavendra, V. Subramanian, *J. Chem. Sci.*, 2016, **128**, 1527-1536.

27.   T. A. Hamor, N. Al-Salim, A. A. West, W. R. McWhinnie, *J. Organomet. Chem*., 1986, **310**, C5-C6.

28.   (a) G. M. Sheldrick, *Acta Crystallogr, Sect A: Found. Crystallogr*., 2008, **64**, 112-122; (b) G. Sheldrick, *Acta Crystallogr., Sect. A: Cryst. Struct. Commun*., 2015, **71**, 3-8; (c) G. Sheldrick, *Acta Crystallogr., Sect. C: Fundam. Crystallogr*., 2015, **71**, 3-8.

29.   T. Lu, F. Chen, *J. Comput. Chem*., 2012, **33**, 580-592.

6.6 Supplementary Data

Table 6.1 Refinement details for the X-ray structures of **6.4-6.6, 6.8**

| Compound	6.4a	6.4b	6.5	6.6	6.8
Formula	$C_{11}H_8Cl_3NTe$	$C_{11}H_8Cl_3NTe$	$C_{23}H_{20}Cl_4N_2O_2Te_2$	$C_{11}H_{13}NO_4Te$	$C_{24}H_{24}N_2O_7Te_2$
Crystal System	Monoclinic	Orthorhombic	Monoclinic	Triclinic	Monoclinic
Space group	*P21/n*	*P2₁2₁2₁*	*I2/a*	*P-1*	*P2/c*
T/K	100(2)	100(2)	100(2)	100(2)	100(2)
a [Å]	6.8410(3)	6.8250(2)	17.756(4)	7.4274(5)	11.5515(4)
b [Å]	12.7707(6)	8.4104(3)	8.602(3)	8.7073(4)	10.5679(3)
c [Å]	14.5049(7)	22.4903(8)	35.078(5)	9.5745(6)	21.3676(6)
α [°]	90	90	90	89.309(4)	90
β [°]	97.292(4)	90	99.697(19)	74.711(5)	104.168(3)
γ [°]	90	90	90	83.026(4)	90
V [A³]	1256.98(10)	1290.98(9)	5281(2)	592.74(6)	2529.11(14)
Z	4	4	8	2	4
ρ_{cal}g/cm³	2.051	1.997	1.895	1.966	1.858
μ/mm⁻¹	2.974	2.896	2.638	2.512	2.353
GOF	1.063	1.027	1.168	1.060	1.023
2θ range (deg)	5.662- 49.996	5.172-49.988	4.712- 49.998	4.412-62.238	3.932-62.15
Refs collected	11664	8593	56157	3377	20319
Unique/observed	2200	2259	4644	3377	7298
Parameters	145	145	311	189	318
R_{int}	0.0535	0.0645	0.0608	0.0510	0.0600
R_1, wR2[I>2σ(I)]	0.0329, 0.0592	0.0354, 0.0653	0.0345, 0.0712	0.0311, 0.0707	0.0490, 0.1139
R_1, wR2[I>2σ(I)]	0.0438, 0.0652	0.0403, 0.0683	0.0362, 0.0723	0.0380, 0.0732	0.0699, 0.1265

(a) (b)
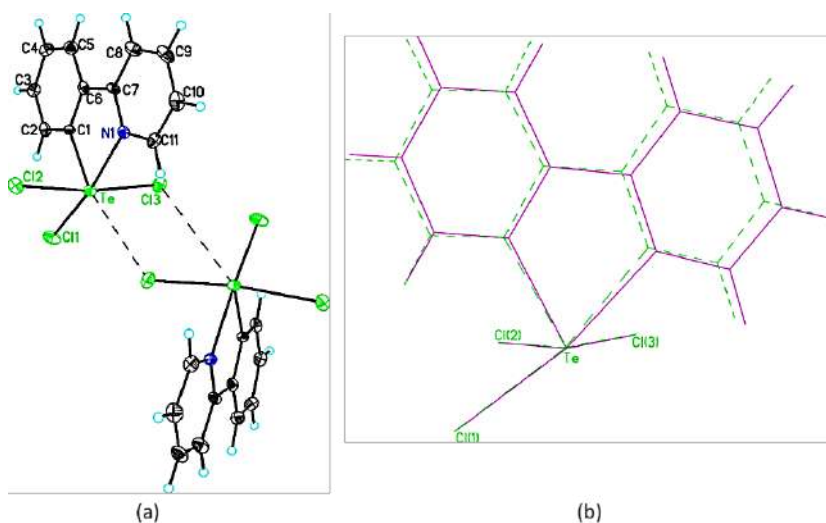
Fig. 6.5 Molecular structures of (a) **6.4b**, thermal ellipsoids are set at the 50% probability level. Selected bond distances and bond angles [Å, °]: C1-Te 2.105 (7), N1-Te 2.286 (6), Cl1-Te 2.455 (2), Cl2-Te 2.504 (2), Cl3-Te 2.515 (2), N1-Te-C1 76.0 (3), N1-Te-Cl1 169.1 (2), N1-Te-Cl2 89.1 (2), N1-Te-Cl3 85.7 (2); (b) Superimposition of the crystallization arrangement of **6.4a** and **6.4b**.
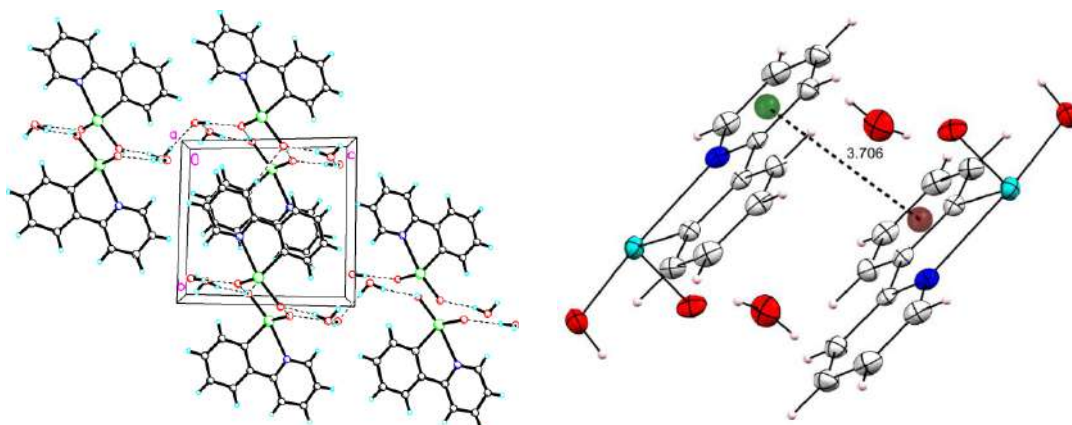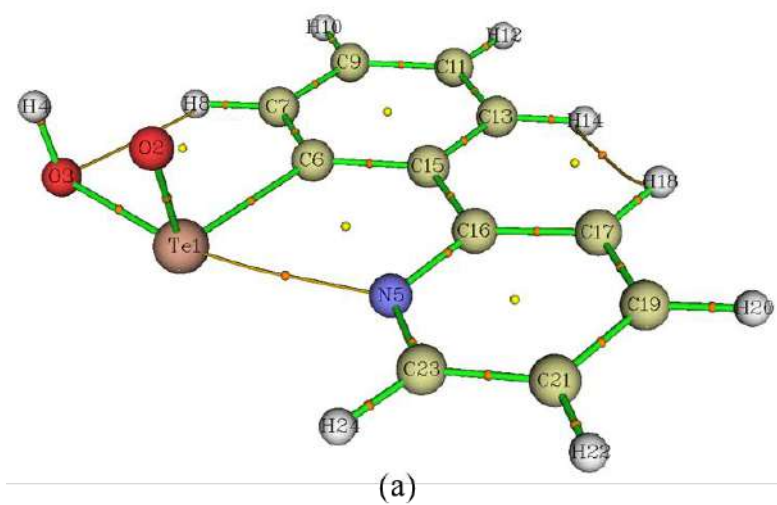

Fig 6.6 Packing diagram of **6.6**.

(a)

Fig 6.7 Atoms in molecule (AIM) bond topology of **6.6**.

Table 6.2 Topological parameters for N-Te bcp of compound **6.6**.

$\rho(r)$	$\nabla^2\rho(r)$	$V(r)$	$G(r)$	$H(r)$	$H/\rho(r)$	$|V(r)/G(r)|$
0.0460	0.0897	-0.0302	0.0227	-0.0075	-0.1630	1.3303

(a)   (b)
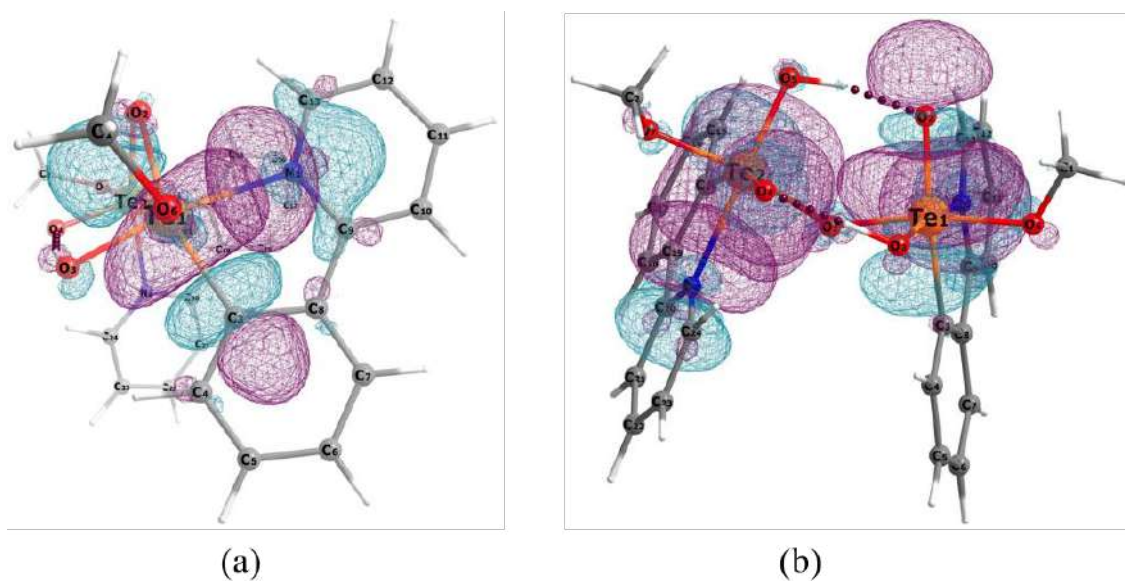
Fig 6.8 Natural bond orbital (NBO) plot of **6.8** showing (a) $lp(N) \rightarrow \sigma^*(Te-C)$, stabilization energy, $\Delta E = 21.59$ kcal/mol; (b) $lp(N) \rightarrow \sigma^*(Te=O)$, stabilization energy, $\Delta E = 20.39$ kcal/mol.
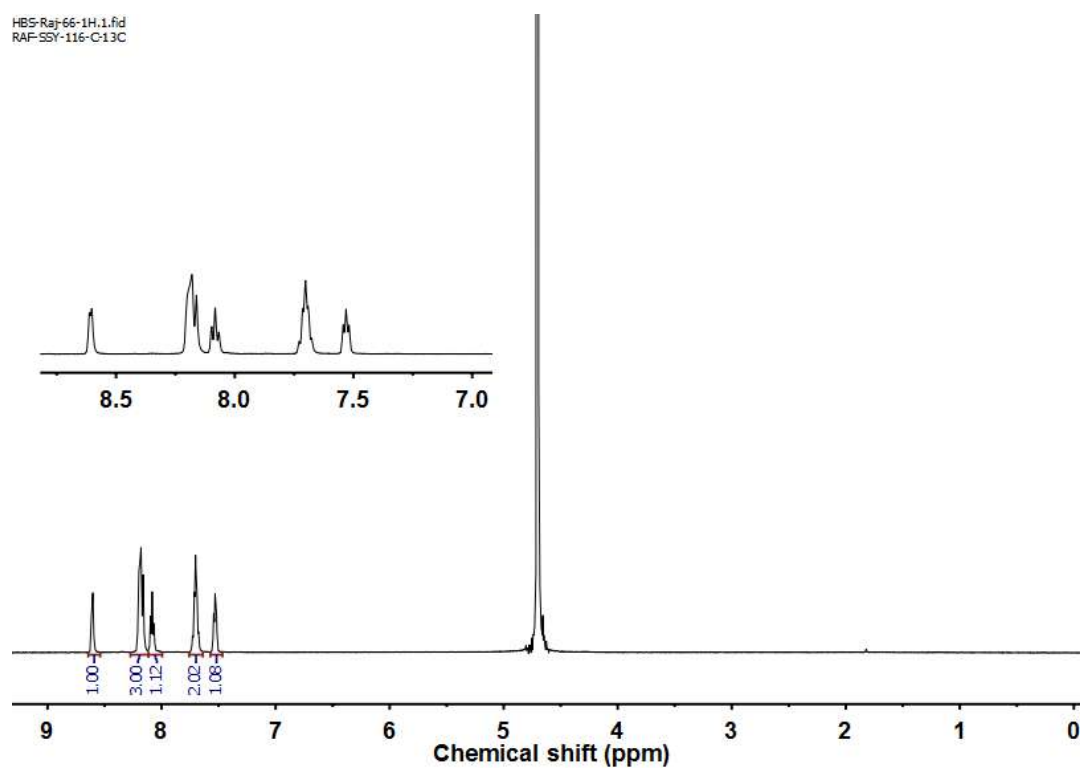
6.7 Representative Spectra

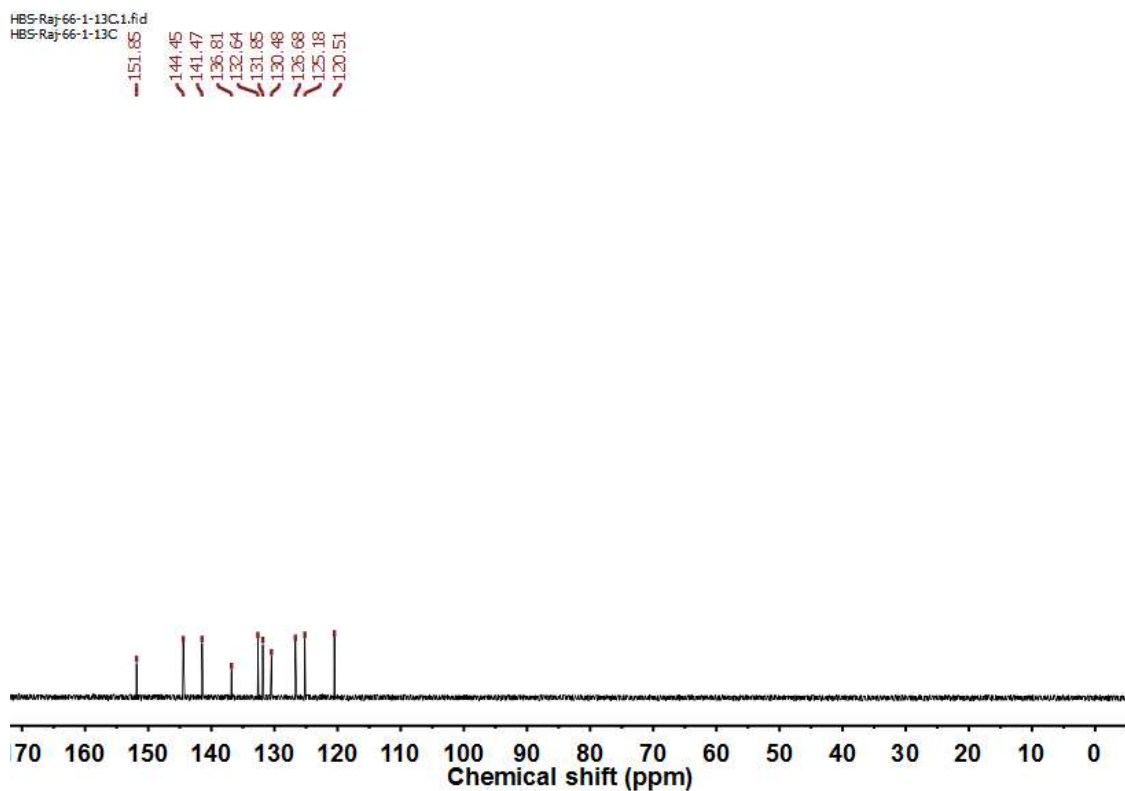**Fig 6.9** ^{1}H NMR Spectrum of **6.6**. Inset showing expanded aromatic region.

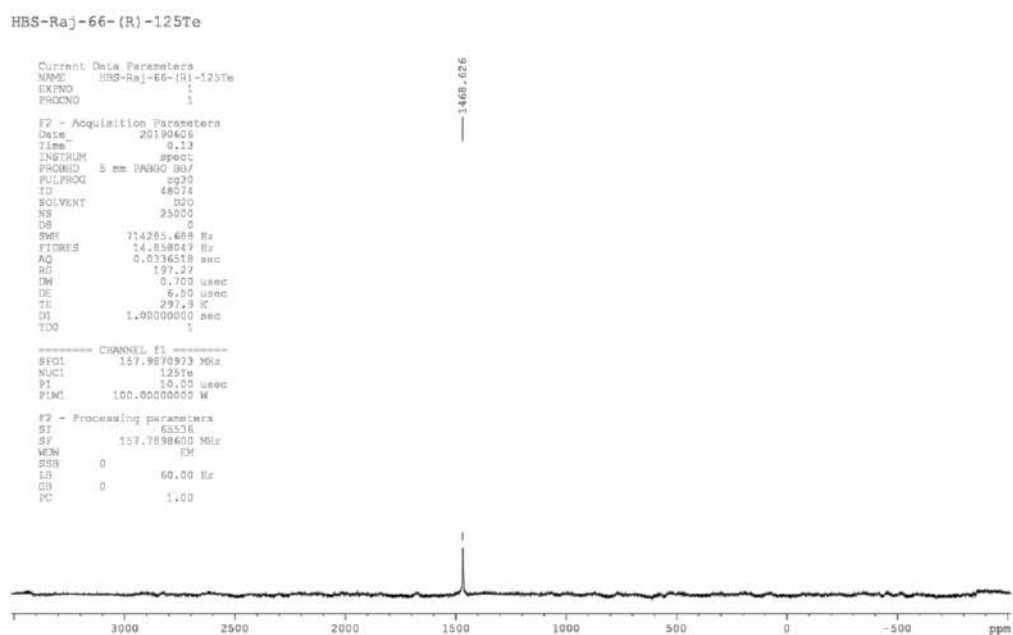**Fig 6.10** ^{13}C NMR Spectrum of **6.6**.

HBS-Raj-66-(R)-125Te

Current Data Parameters
NAME   HBS-Raj-66-(R)-125Te
EXPNO   1
PROCNO   1

F2 - Acquisition Parameters
Date_   20190606
Time_   0.13
INSTRUM   spect
PROBHD   5 mm PABBO BB/
PULPROG   zg30
TD   48074
SOLVENT   D2O
NS   25000
DS   0
SWH   714285.688 Hz
FIDRES   14.858047 Hz
AQ   0.0336518 sec
RG   197.27
DW   0.700 usec
DE   6.50 usec
TE   297.9 K
D1   1.00000000 sec
TD0   1

=========== CHANNEL f1 ===========
SFO1   157.9870973 MHz
NUC1   125Te
P1   10.00 usec
P1W1   100.00000000 W

F2 - Processing parameters
SI   65536
SF   157.7898600 MHz
WDW   EM
SSB   0
LB   60.00 Hz
GB   0
PC   1.00

1468.626

Fig 6.11 ^{125}Te NMR Spectrum of **6.6**.

Fig 6.12 High Resolution ESI-mass spectra (positive mode) of **6.6**. (experimental spectra is depicted in black, simulated pattern is depicted in blue)
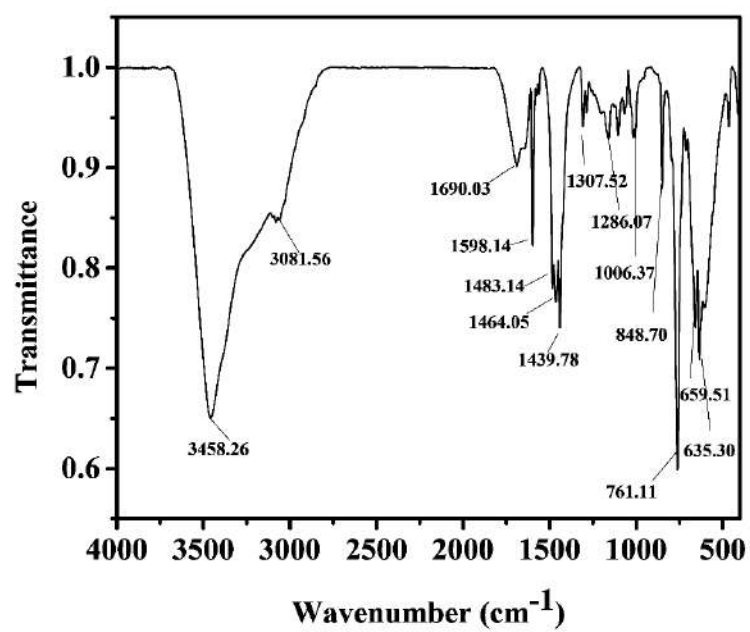
Fig 6.13 FT-IR spectrum (KBr pellet) of **6.6**.

Appendix 2

Isolation of Homoleptic Dicationic Tellurium and Monocationic Bismuth Analogues of Non-N-Heterocyclic Carbene (Non-NHC) Derivatives

7.1 Introduction

Inspired by the extraordinary success of N-heterocyclic carbenes (NHCs), **7.1a** in metal-based chemistry, significant research has been carried out in last few decades to isolate and explore the reactivity of isovalent analogues of NHCs within *p*-block elements, collectively known as main-group NHC analogues (Chart 7.1).[1] The interesting molecular structures, versatile electronic properties and reactivity associated with the main-group NHC analogues have offered abundant opportunities in main-group and coordination chemistry.[1] Compared to the group 14 and15 NHC analogues of period 5, *i.e.*, **7.1b-7.1d**, the isolation of group 16 NHC analogues is very challenging, as the corresponding Te^{4+} cations are expected to be ambivalent in nature, *i.e.*, being highly electrophilic and possessing a lone pair of electron at the same time.[2a] In a groundbreaking report, Ragogna and co-workers have utilized the strong σ-donating ability of the N-atoms of the diazabutadiene α-diimine ligand motifs for the isolation of the Te analogues of NHC derivatives **7.1e**.[2b]
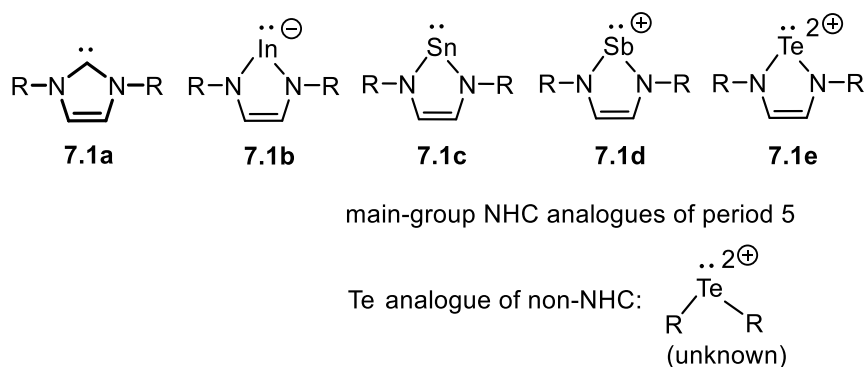

Chart 7.1 NHC (**7.1a**) and other main-group NHC analogues of period 5 (**7.1b-7.1e**).

In the case of NHCs, while the steric properties can be easily fine-tuned by changing the substituents on the N-atoms or by changing the size of the ring, the choices of modifying the electronic properties are limited.[4] In this context, significant research has been undertaken lately to understand and explore the chemistry of "non-NHC" derivatives comprising backbone other than imidazol-2-ylidenes. From the seminal work by Bertrand and co-workers, it is perceived that the non-NHC frameworks can exhibit promising electronic features and wide structural varieties which extend their applications in various fields of contemporary chemistry.[4] Among the main group non-NHC analogues of group 14-16, reports on the heavier main-group

analogues of group 15 and 16 non-NHC derivative are still scarce even though the chemistry of group 14 analogues is well studied.[5] Very recently, Beckmann and co-workers have reported the first examples of heavier group 15 analogues (Bi, Sb) of non-NHC derivatives namely, the bismuthenium ion $[(2,6\text{-}Mes_2C_6H_3)_2Bi][BAr_4]$ and the stibenium ion $[(2,6\text{-}Mes_2C_6H_3)_2Sb][B(C_6F_5)]$ [where Mes = $2,4,6\text{-}Me_3C_6H_2$, Ar = $3,5\text{-}(CF_3)_2C_6H_3$] stabilized by bulky *meta*-terphenyl substituents and weakly coordinating anions.[2a] The corresponding group 16 congeners have not been reported. It is worth-mentioning that in recent times, various cationic organotellurium and organobismuth compounds have received enormous attention because of their fascinating photoluminescence properties and promising applications in photocatalysis.[5]

Srivastava *et al.,*[6a] and Beckmann and co-workers[6b] have independently utilized Intramolecular Chalcogen Bonding (IChB) approach for the isolation of diorganoiodotelluronium(IV) cations. We envisaged that the metathesis reaction of these diorganoiodotelluronium(IV) cations with silver salts with non-coordinating anions might lead to the isolation of hitherto unknown Te analogues of non-NHC derivatives. Accordingly, iodobis[2-(phenylazo)phenyl-*C,N′*]tellureniumtriiodide[6a] was treated with silver perchlorate in acetonitrile/methanol. However, the reaction did not afford the desired diorganotellurenium(IV) dication. We thought that by utilizing stronger IChB interactions, the isolation of desired diorganotellurenium(IV) dication could be achieved. In this context, we planned to use $[(ppy)_2TeI].I_3$, [**7.3**].I_3 [where ppy = 2-(2′-pyridyl)phenyl] as the precursor. It is worth mentioning that by using a tellurium trichloride derivative of the same substrate, *i.e.*, ppyTeCl$_3$, we have recently succeeded in the isolation of the first example of monomeric organotellurinic acid, wherein the lone pair of N-atom of the pyridylphenyl ring strongly participated with the Te center.[7] Herein, by metathesis reaction of [**7.3**].I_3 with silver salts (AgClO$_4$ and AgOTf, Tf = O_2SCF_3), we report the first examples of stable, homoleptic dicationic tellurium analogues of 'non-NHC' derivatives namely $[(ppy)_2Te].2ClO_4$, [**7.4**].$2ClO_4$ and $[(ppy)_2Te].2OTf$, [**7.5**].$2OTf$.

7.2 Results and Discussion

Precursor [**7.3**].I_3 was synthesized by the oxidative addition of iodine with diorganotelluride (ppy)$_2$Te, **7.2**.[8] When [**7.3**].I_3 was treated with an excess (*ca.* 5 equiv.) of AgClO$_4$/AgOTf in acetonitrile solution at ambient temperature, the reaction resulting in the precipitation of silver iodide as an off-white solid. The precipitate was filtered off and the

resultant filtrate, on slow evaporation at ambient temperature afforded stable, white crystalline solids of [**7.4**].2ClO$_4$/[**7.5**].2OTf in *ca.* 90% yield (Scheme 7.1). The ^{1}H and ^{13}C NMR spectra of [**7.4**].2ClO$_4$ and [**7.5**].2OTf confirmed the purity of the compounds with characteristic signals and consistent integration values for the 2-(2′-pyridyl)phenyl moiety. Minute but perceptible changes in chemical shifts were observed for [**7.4**].2ClO$_4$ and [**7.5**].2OTf in comparison to the precursor [**7.3**].I$_3$. In the ^{125}Te NMR spectra, [**7.4**].2ClO$_4$ and [**7.5**].2OTf showed single resonances at δ = 1107 ppm and 1114 ppm, respectively. While these chemical shift values are close to that of precursor [**7.3**].I$_3$ (δ = 1100 ppm), but are significantly upfield shifted in comparison to Te^{IV} NHC analogue, **7.1e** reported by Ragogna and co-workers (δ = 1736 ppm), as in the latter Te center was directly bonded to two N-atoms.[2b]
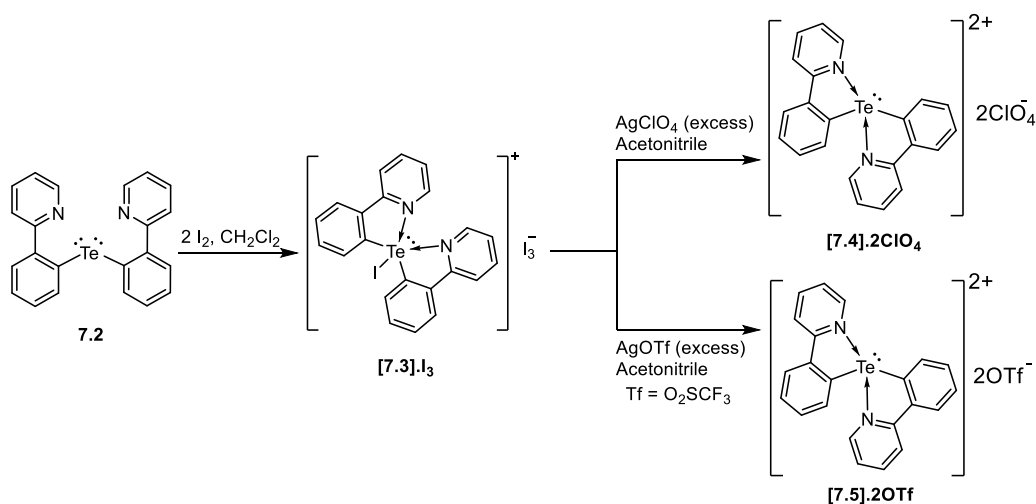
Scheme 7.1 Synthesis of dicationic tellurium analogues of non-NHC derivatives, [**7.4**].2ClO$_4$ and [**7.5**].2OTf.

The molecular structure of [**7.3**].I$_3$ is represented in Figure 7.1. Defined by a C$_2$N$_2$I donor set, the geometry around the Te(IV) center is distorted trigonal bipyramidal, wherein the iodine and N1 atoms occupy the axial positions and the C11, C12 and N2 atoms occupy the equatorial positions. Compound [**7.3**].I$_3$ exhibits significantly stronger N···Te IChB interactions, as evident from the corresponding N···Te distances of 2.295(5) and 2.636(5) Å, which are considerably shorter in comparison to that observed in similar iodotellurium(IV) cations, namely, [(C$_6$H$_5$NNC$_6$H$_4$)$_2$TeI].I$_3$ [2.481(11) and 2.756(13) Å; 2.476(13) and 2.796(28) Å] and [(8-Me$_2$NC$_{10}$H$_6$)$_2$TeI].I$_3$ [2.743(7) and 3.20(1) Å].[6] The Te-I bond distance [2.9158(5) Å] and ∡C-

Te-C [95.2(1)°] in [**7.3**].I_3 are in good agreement with that in [$(C_6H_5NNC_6H_4)_2$TeI].I_3 [2.782 (12)/2.778(15); 97.4(5)/95.5(6)°] and [$(8\text{-}Me_2NC_{10}H_6)_2$TeI].$I_3$ [2.780(2) Å; 96.7(3)°].[6]
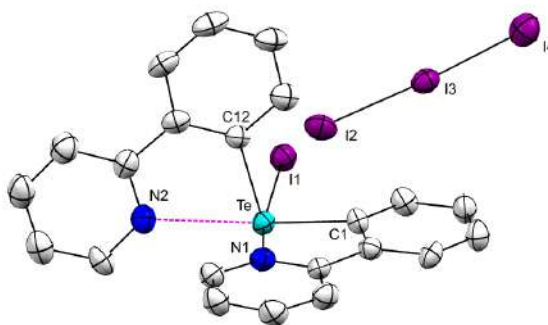

Figure 7.1 Molecular structure of [**7.3**].I_3; thermal ellipsoids are set at the 50% probability level. Selected bond distances and angles [Å, °]: C1-Te 2.134(5), C12-Te 2.141(5), N1···Te 2.295(5), N2···Te 2.636(5), I1-Te 2.9158(5), I2-I3 2.9736(7), I3-I4 2.8779(7), C1-Te-C12 97.2(2), N1···Te···N2 85.1(2), N1···Te-I1 167.7(1), N2···Te-I1 102.3(1), C1-Te-I1 95.2(1), C12-Te-I1 87.3(1), I2-I3-I4 177.06(2).

The molecular structures of [**7.4**].$2ClO_4$ and [**7.5**].2OTf are significantly similar, hence the structure of only [**7.4**].$2ClO_4$ is described here {Figure 7.2a; for the molecular structure of [**7.5**].2OTf see Fig. 7.8}. The spatial arrangement of the Te(IV) center is distorted square pyramidal considering the lone pair of Te and N···Te IChB interactions into account. The donor set C_2N_2 makes a spirocyclic arrangement around the Te center with a C1-Te-C12 bond angle of 92.68(9)°, while both N atoms make a *transoid* angle of 162.83(7)°. In the Te^{IV} NHC analogue **7.1e**, the corresponding N-Te-N angle is significantly larger with an angle of 172.8(2)°.[2b] The interesting feature in the structure of [**7.4**].$2ClO_4$ is the N···Te IChB interactions, which make five membered $TeNC_3$ rings with N···Te distances of 2.224(2) Å and 2.229(2) Å. These distances are significantly shorter than those observed in the precursor [**7.3**].I_3 [2.295(5) and 2.636(5) Å, *vide supra*]. The C-N-Te bond angles are of 114.8(1)° and 115.1(1)°. Both the perchlorate anions are involved in weak interactions with the Te center with distances lying in the range 3.021(2)-3.115(2) Å and these distances are well within the sum of the van der Waals radii of Te and O atom [$\Sigma\ r_{vdw}$ (O, Te) = 3.49 Å].[9]

To shed light on the electronic structure of a Te^{IV} cation, and to understand the role of the N-atoms of the 2-(2´-pyridyl)phenyl on the stability of the synthesized compounds, DFT calculations were carried out using Gaussian 0.9 (Rev A.02) program[10] (functional: B3PW91;[11] mixed basis set: Te: SDB-cc-pVTZ;[12] C/H/N/O: 6-31G**[13]; Bi:cc-pVTZ-PP[14]). After a geometry optimization starting from the crystal coordinates, natural bond orbital (NBO) calculations were performed for cation [**7.4**]$^+$.[15] The NBO analysis treats each N-Te interaction in [**7.4**]$^+$ as an lp(N)→p(Te) donor-acceptor interaction [Figure 7.2b]. A stabilization energy of ~122 kcal/mole of each N→Te interaction inferred that they contributed significantly to the overall stability of the compound. The strong N→Te IChB in [**7.4**]$^+$ was further validated by electron localization function (ELF) calculation, wherein a continuum of elevated ELF values was observed along the N→Te vectors [Figure 7.2c].[16]
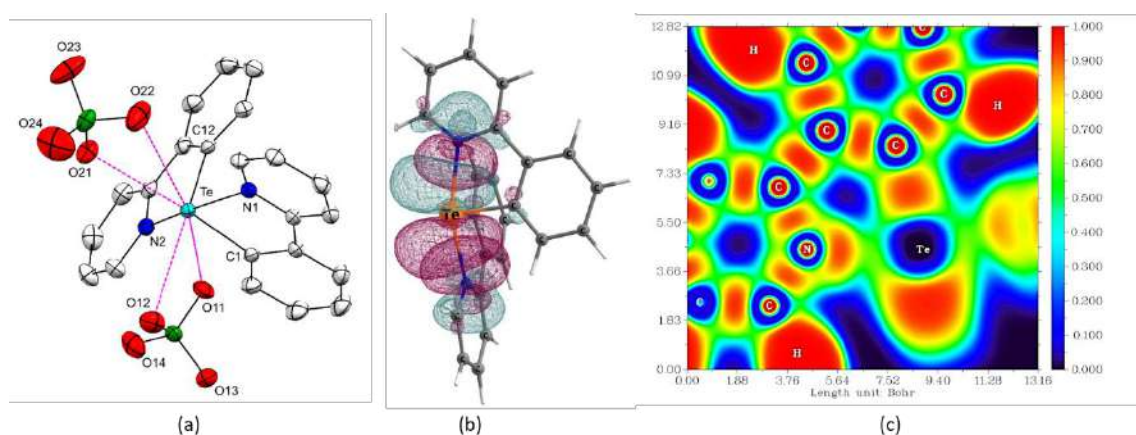
Figure 7.2 (a) Molecular structure of [**7.4**].2ClO$_4$; thermal ellipsoids are drawn at 50% probability level. Selected bond distances and angles [Å, °]: C1-Te 2.116(2), C12-Te 2.117(2), N1···Te 2.224(2), N2···Te 2.229(2), C1-Te-C12 92.68(9), C1-Te···N 77.04(8), C12-Te···N 77.37(8), N1···Te···N2 162.83(7). (b) Natural bond orbital (NBO) plot showing the lp(N)→p(Te) interaction, stabilization energy, ΔE = 122.5, 122.5 kcal/mol. (c) Electron localization function (ELF) for [**7.4**]$^+$ drawing in the plane containing N, Te and C atoms.

To probe the effect of N→Te IChB interactions on the Te(IV) center in [**7.4**]$^+$, electrostatic surface potential (ESP)[17] was calculated for [**7.4**]$^+$ and for a model compound wherein the pyridyl rings were rotated away from the Te center in such a way that no IChB was observed between the N and Te atoms. The ESP of the model compound showed a broad region of

depleted electron density, known as σ-hole region, antipodal to the C-Te bond [Figure 7.3a]. It is worth mentioning that in case of group 14-16 compounds, along the extension of a covalent bond, a highly directional and localized region of depleted electron density (positive electrostatic potential) is observed, due to the anisotropic distribution of electron density and is known as a σ-hole.[18] These σ-holes are responsible for various non-covalent interactions, such as chalcogen bonding (ChB), pnictogen bonding (PnB) and tetrel bonding (TrB) to name a few. The significant diminution of the original σ-hole in compound [**7.4**]$^+$ after N→Te IChB [Figure 7.3b] unambiguously established the direct involvement of the σ-hole in chalcogen bonding with the lone pair of the nitrogen atom. To understand the nature of interaction between the N and Te atom, atoms in molecules (AIM) calculation has been carried out [Figure 7.3c].[19] The analysis of the topological properties of the N···Te bond critical point (bcp) such as, a low electron density, $\rho(r)$ value of 0.129 eÅ^{-3}, Laplacian of electron density, $\nabla^2_{\rho(r)}$ value of -0.018 eÅ^{-3}, a positive kinetic energy density over electron density ratio $[G(r)/\rho(r)]$ of 0.22 a.u. and a total energy density over electron density ratio $[H(r)/\rho(r)]$ of -0.66 a.u. infers a dominant electrostatic interaction between the two atoms. The '-G(r)/V(r)' value of 0.864 further suggests a predominantly ionic character of the N···Te interaction with a significant mixing of covalent character.[20] This is further corroborated by the Natural Population Analysis (NPA) charge of -0.589 for each N atom and 1.785 for the Te atom.
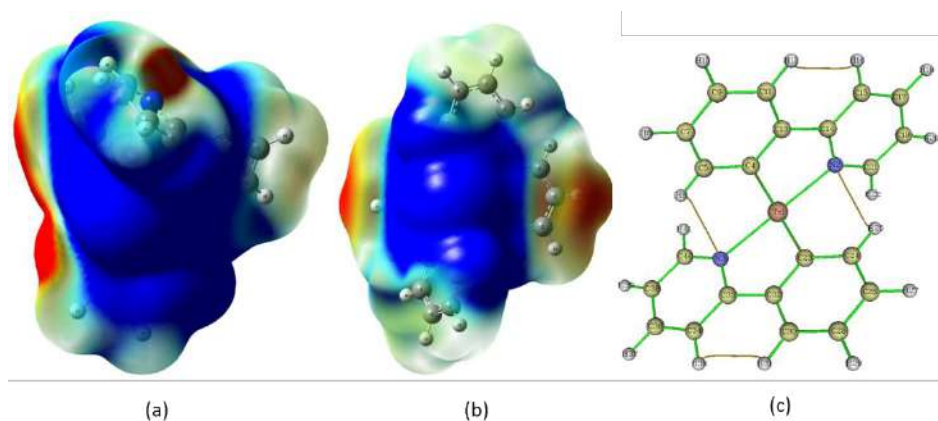

(a) (b) (c)

Figure 7.3 (a) Electrostatic surface potential (ESP) map, $\rho = 0.001$ a.u., showing an enhanced σ-hole region antipodal to C-Te bond in the absence of N→Te IChB interactions. (b) ESP of [**7.4**]$^+$ showing diminution of σ-hole region due to the presence of N→Te IChB interactions. ESPs have

been drawn on the Hirshfeld surface with potential in the range 0.175 a.u. (red)-0.210 a.u. (blue). (c) Atoms in molecule (AIM) bond topology of [**7.4**]$^+$.

In an attempt to synthesize the tricationic species (ppyTe^{3+}), ppyTeCl$_3$,[21] **7.6** was treated with an excess of AgClO$_4$. However, the desired compound [**7.7**].3ClO$_4$ was not stable and the adventitious hydrolysis resulted in the formation of ditelluroxonium bis(perchlorate) [ppyTe(μ-O)]$_2$.2ClO$_4$, [**7.8**].2ClO$_4$ (Scheme 7.2). The ditelluroxonium cation [**7.8**].2ClO$_4$ shows ^{125}Te NMR resonance at 1413 ppm.
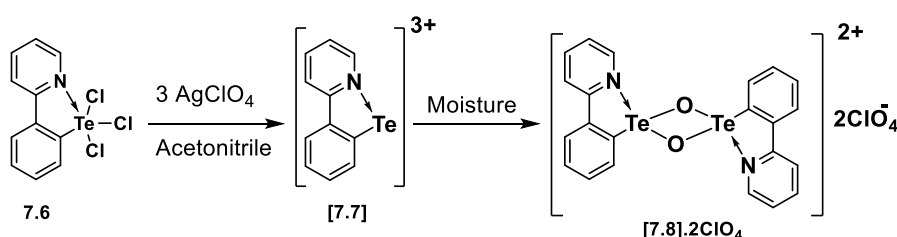
Scheme 7.2 Isolation of [**7.8**].2ClO$_4$ by the attempted synthesis of [**7.7**].3ClO$_4$.

The molecular structure of [**7.8**].2ClO$_4$ is presented in Figure 7.4, which reveals a dimeric structure with crystallographically imposed center of inversion. Each Te(IV) center is coordinated to one ppy ligand in *trans* orientation with respect to the other and forms a Te$_2$O$_2$ core with μ_2-bridging oxygen atoms. The N$\cdots$Te distance of 2.279(9) Å is significantly longer than in [**7.4**].2ClO$_4$ [2.224(2) Å], but shorter that in [**7.3**].I$_3$ [2.295(5) Å]. The Te-O distances of 1.917(8) and 2.068(8) Å are in agreement with similar reported dimeric compounds, namely [Te(2,6-(Me$_2$NCH$_2$)(μ-O)]$_2$.2ClO$_4$ [1.987(4) and 1.996(4) Å] and [Te(6-Ph$_2$P(O)-Ace-5-) (μ-O)]$_2$.2OTf [1.920(3)-2.070(3) Å, Ace = acenaphthyl].[22] The non-bonding distance between the two Te centers is 3.080(1) Å is significantly shorter than the sum of the van der Waal radii [Σ r_{vdw} (Te, Te) = 3.98 Å].[9]
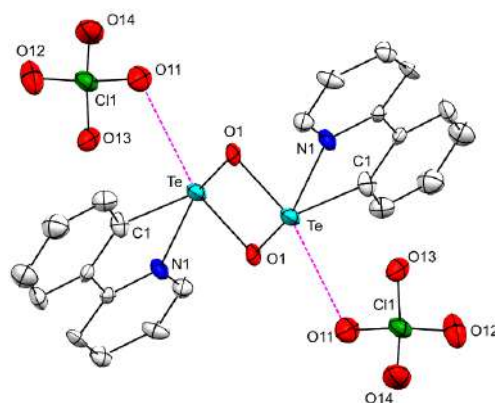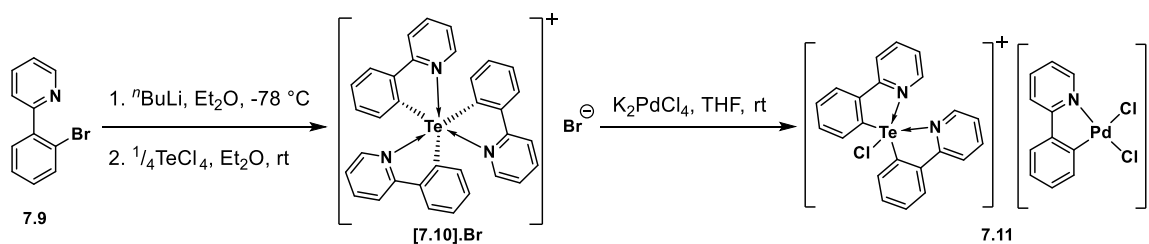
Figure 7.4 Molecular structure of [**7.8**].2ClO₄; thermal ellipsoids are set at the 50% probability level. Selected bond distances and angles [Å, °] C-Te 2.11(1), N···Te 2.279(9), O1-Te 1.917(8), O2-Te 2.068(8), O11···Te 2.784(9), C-Te···N 76.0(4), O1-Te-O2 78.8(3), Te-O-Te 101.2(3).

To compare the structural parameters of the diorganodications [**7.4**].2ClO₄ and [**7.5**].2OTf with the corresponding monocation, (ppy)₃Te⁺ and to explore the coordination ability of the Te center, ppyBr, **7.9**[23] was treated with *ⁿ*BuLi followed by TeCl₄ to afford [(ppy)₃Te].Br, [**7.10**].Br (Scheme 7.3). Compound [**7.10**].Br showed ¹²⁵Te NMR resonance at 867 ppm, which is consistent with the value observed for similar reported triorganotelluronium(IV) cation namely, triphenyltelluronium chloride (773 ppm) and tris(8-quinolinyl)telluronium chloride (669 ppm).[24] Interestingly, when [**7.10**].Br was treated with K₂PdCl₄, a reverse transmetallation was observed resulting in the formation of the Pdᴵᴵ complex of chlorotelluronium cation, namely [(ppy)₂TeCl].[(ppy)PdCl₂], **7.11**. In the absence of any other possible explanation, the stronger N···Te IChB in [**7.10**].Br could be held responsible for the reverse transmetallation in contrast to

the Gabbaï and co-workers' report, wherein tris(8-quinolinyl) telluronium chloride on reaction with a Pd(II) precursor resulted in the formation 1:1 palladated complex with the telluronium ion acting as a σ-acceptor ligand.[24b] In the ¹²⁵Te NMR spectrum, **7.11** showed single resonance at 1309 ppm.

Scheme 7.3 Synthesis of Pd(II) complex of chlorotelluronium cation, **7.11**.

In the molecular structure of [**7.10**].Br [Figure 7.5a], the distortion from regular octahedron is less [∡N-Te-C$_{(trans)}$ 163.4(3)-165.7(3)°] in comparison to that of the related compound, tris(8-quinolinyl)telluronium chloride [∡N-Te-C$_{(trans)}$ 146.7(2)-147.8(2)°].[24b] Again, The N⋯Te IChB distances are significantly shorter [2.680(8)-2.689(7) Å] in comparison to tris(8-quinolinyl)telluronium chloride [2.950(5)-2.988(6) Å]. In the molecular structure of **7.11** [Figure 7.5b], the cationic entity, the halide site is mixed Cl/Br with occupancies of 0.908(8):0.092(8). Hence, the structure is described with respect to the Cl$^-$ ligand. The spatial arrangement around the Te^{IV} center is similar to that of iodotelluronium cation, [**7.3**].I$_3$. In particular, The C-Te distances [2.15(1), 2.14(1) Å] and N⋯Te distances [2.291(9), 2.67(1) Å] in **7.11** are in good agreement with that observed in [**7.3**].I$_3$. The ∡C-Te-C [94.7(4)°] in **7.11** is slightly smaller than in [**7.3**].I$_3$ [97.2(2)°]. In the anionic entity, the geometry around the Pd^{II} center is essentially square planar. The bond lengths and associated bond angles of the ppy and Cl ligands with the Pd^{II} center are in good agreement with the value observed in similar related dichlorido Pd(II) complexes.[25] Interestingly, an unsupported cation-anion interaction exhibited between the Te^{IV} and Pd^{II} centers with a distance of 3.738(1) Å which is shorter than the sum of van der Waals distances of the two atoms [Σ r_{vdw} (Te, Pd) = 4.14 Å].[9]
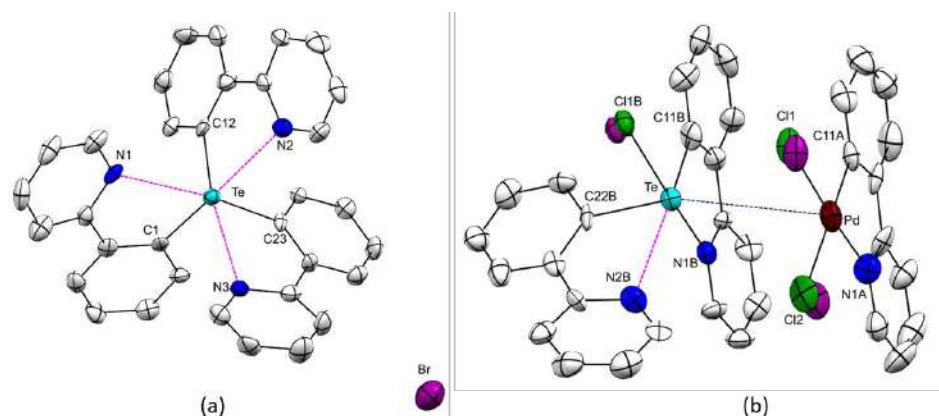
Figure 7.5 Molecular structure of (a) [**7.10**].Br and (b) **7.11**; thermal ellipsoids are set at the 50% probability level. Selected bond distances and angles [Å, °]: For [**7.10**].Br, C1-Te 2.152(9), C12-Te 2.13(1), C23-Te 2.152(7), N1···Te 2.688(7), N2···Te 2.680(8), N3···Te 2.647(8), C1-Te···N1 70.1(3), C12-Te···N2 70.4(3), C23-Te···N3 70.7(3), C1-Te···N2 164.3(3), C12-Te···N3 165.7(3), C23-Te···N1 163.4(3); For **7.11**, C11A-Pd 2.02(1), C11B-Te 2.14(1), C22B-Te 2.15(1), N1A-Pd 2.03(1), N1B···Te 2.291(9), N2B···Te 2.67(1), Pd-Cl1 2.37(1), Pd-Cl2 2.49(2), Te-Cl1B 2.57(1), Pd···Te 3.738(1), N1A-Pd-C11A 81.5(4), N1A-Pd-C12 96.1(5), N1A-Pd-Cl1 173.2(5), C11A-Pd-Cl2 176.7(5), N1B-Te-C11B 76.6(4), N2B-Te-C22B 70.5(4), N1B-Te-Cl1B 167.3(4), N2B-Te-Cl1B 104.1(3). In the cationic entity, the halide site is mixed Cl/Br with occupancies of 0.908(8) (for Cl1B):0.092(8) (for Br1B). In the anionic entity, the halide sites are mixed Cl/Br with occupancies 0.874(9) (for Cl1):0.126(9) (for Br1) and 0.781(9) (for Cl2):0.219(9) (for Br2).

To see the generality of the 'ppy' group on stabilizing other main group non-NHC analogues and to further explore the unique intramolecular interaction ability of the N-atom of the ppy group, we went on to synthesize (ppy)$_2$BiCl, which was planned to be used for the metathesis reaction in a subsequent step to generate a cationic species. Interestingly, when **7.9** was treated with ^{n}BuLi followed by addition of BiCl$_3$, a facile auto-ionization took place, resulting in the formation of diorganobismuthenium chloride, [(ppy)$_2$Bi^{III}].Cl, [**7.12**].Cl (Scheme 7.4). [**7.12**]$^+$ is only the second example of bismuthenium ion reported so far after the Beckmann and co-workers' donor free bismuthenium ion, [(2,6-Mes$_2$C$_6$H$_3$)$_2$Bi][BAr$_4$] [where Mes = 2,4,6-Me$_3$C$_6$H$_2$, Ar = 3,5-(CF$_3$)$_2$C$_6$H$_3$] stabilized by bulky aryl substituents.[2a]
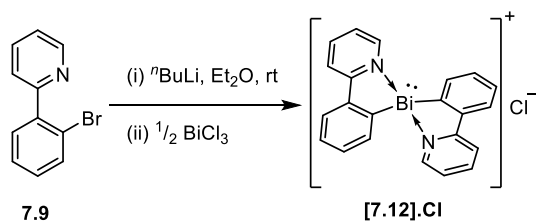
Scheme 7.4 Synthesis of the diorganobismuthenium chloride [**7.12**].Cl.

An examination of the crystal structure of [**7.12**].Cl indicates that, similar to [**7.4**].2ClO$_4$ and [**7.5**].2OTf, the coordination geometry of the Bi(III) center is distorted square pyramidal taking the lone pair of Bi and N$\cdots$Bi intramolecular interactions into account [Figure 7.6a]. The Bi(III) ion sits on a crystallographically imposed center of inversion, containing two ppy groups in *trans* arrangement. The N$\cdots$Bi distance of 2.467(5) Å is well within the sum of the van der Waals radii of the two elements [Σ r_{vdw} (N, Bi) = 4.24 Å],[9] indicating the presence of strong N$\cdots$Bi intramolecular interactions. ∡C-Bi-C angle of 92.1(3)° is significantly smaller than that observed in [(2,6-Mes$_2$C$_6$H$_3$)$_2$Bi][BAr$_4$] [116.69(9)°] [where Mes = 2,4,6-Me$_3$C$_6$H$_2$, Ar = 3,5-(CF$_3$)$_2$C$_6$H$_3$].[2] The NBO analysis indicates strong lp(N)$\rightarrow$$p$(Bi) donor-acceptor interaction in [**7.12**]$^+$, wherein each interaction contributes to the stability of the compound by ΔE = 60.12 kcal/mol [Figure 7.6b]. The ELF study on [**7.12**]$^+$ lends further support to the N$\rightarrow$Bi interaction, which shows a considerable degree of electron sharing between the N and Bi atoms [Figure 6(c)]. Noteworthingly, while comparing with the ELF of [**7.4**].2ClO$_4$ [Figure 7.2c], the sharing of electron between N and the element center in [**7.12**].Cl is less, which might be attributed to the differences in the size of Te^{IV} and Bi^{III} cations. This is further corroborated by the corresponding N$\rightarrow$Te distance in [**7.4**].2ClO$_4$ [2.224(2), 2.229(2) Å] and N$\rightarrow$Bi distance in [**7.12**].Cl [2.467(5) Å] (*vide supra*).
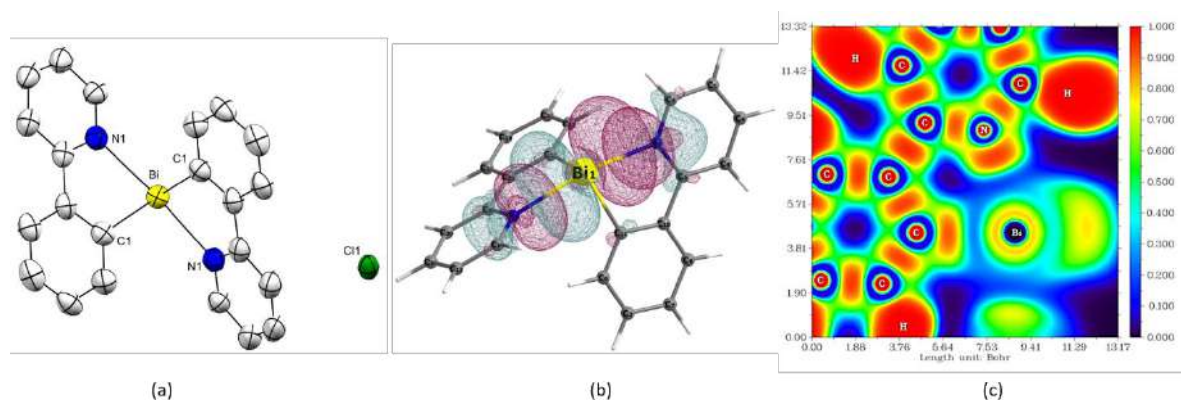
(a)   (b)   (c)

Figure 7.6 (a) Molecular structure of [**7.12**].Cl; thermal ellipsoids are drawn at 50% probability level. Selected bond distances and angles [Å, °]: C1-Bi 2.292(6), N1···Bi 2.467(5), C1-Bi-C1′ 92.1(3), N1···Bi···N1′ 149.5(2), N1···Bi-C1 71.65(19). (b) Natural bond orbital (NBO) plot of [**7.12**]$^+$ showing the lp(N)→p(Bi) interaction, stabilization energy, ΔE = 60.12 kcal/mol for each N→Bi interaction. (c) ELF for [**7.12**]$^+$ drawing in the plane containing N, Bi and C atoms.

The ESP studies indicate a significant reduction in the σ-hole region due to the presence of N→Bi interaction [Figure 7.7b] in comparison to the model compound, wherein in absence of N→Bi interaction a large σ-hole region antipodal to the C-Bi bond is observed [Figure 7.7a]. The analysis of the topological properties of the N→Bi bcp indicates a predominant electrostatic interaction between the two atoms, as suggested by a low electron density, ρ(r) value of 0.059 eÅ^{-3}, a slightly positive Laplacian of electron density, ∇^2ρ(r) value of 0.159 eÅ^{-3}, a positive kinetic energy density over electron density ratio [G(r)/ρ(r)] of 0.800 a.u. and a total energy density over electron density ratio [H(r)/ρ(r)] of -0.125 a.u., a value close to 0 [Figure 7.7c]. The predominant electrostatic nature of the N→Bi interaction is further corroborated by '-G(r)/V(r)' value of 0.07.
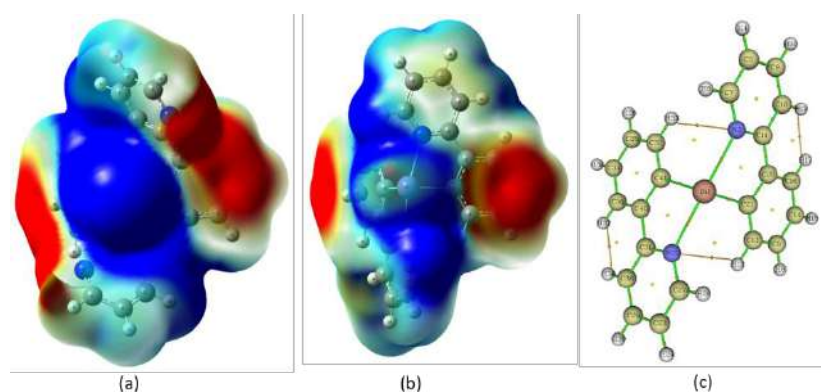
Figure 7.7 (a) ESP map, ρ = 0.001 a.u., showing enhanced σ-hole antipodal to C-Bi bond in absence of N→Bi intramolecular interactions. (b) ESP of [**7.12**]$^+$ showing diminution of σ-hole region due to the presence of N→Bi intramolecular interactions. ESPs have been drawn on the Hirshfeld surface with potential in the range 0.08 a.u. (red)-0.115 a.u. (blue). (c) AIM bond topology of [**7.12**]$^+$.

7.3 Conclusions

In conclusion, we have succeeded in isolating the first examples of robust, IChB stabilized Te analogues of non-NHC derivatives by metathesis reaction of diorganohalotelluronium(IV) cations with AgClO$_4$/AgOTf. This novel series of compounds fill the missing link in the period 5 main-group analogues of non-NHC derivatives. The stability of the dicationic Te^{IV} non-NHC derivatives was achieved by exposing the σ-hole around the Te center to the N-lone pair of a rigid and planar pyridylphenyl ring. The active participation of the σ-hole with the lone pair of N-atom through electrostatic interaction serves the purpose of attenuating the excessive electrophilicity around the Te^{IV} center, which is generally achieved by the strong σ-donating ability of the two N atoms in NHC derivatives. The generality of the phenylpyridyl ring on the stabilization of other main group non-NHC analogues was further established by synthesizing intramolecular interactions stabilized bismuthenium cation. This is only the second example of this compound class and first one to contain an intramolecularly coordinated substituent. Given the tremendous interest in NHCs and their analogues over the last few decades, this new family of compounds would be of significant interest with respect to their synthetic utility and reactivity.

7.4 Experimental Section

All manipulations were performed under a N_2 atmosphere using standard Schlenk techniques. Solvents were dried by following standard methods. The starting materials and solvents were purchased from commercial sources. (ppy)$_2$Te was synthesized by the reaction of (ppy)HgCl with ppyTeCl$_3$ followed by the treatment with an excess of hydrazine hydrate.[8] (ppy)TeCl$_3$ was synthesized following the reported procedure using (ppy)HgCl and TeCl$_4$.[21] (**Caution**: Organomercury compounds are highly toxic. Perchlorate salt with organic ligands are potentially explosive. Adequate precaution should be taken while handing of such compounds). (ppy)Br was synthesized by the treatment of 2-phenylpyridine with Pd(OAc)$_2$ and NBS.[23] ^{1}H (400 and 500 MHz), ^{13}C (100 and 125 MHz) and ^{125}Te (126 MHz, 158 MHz) NMR spectra were recorded on Bruker AV 400 MHz and Bruker AV 500 MHz spectrometers at 25 °C. Chemical shifts cited were referenced to TMS (^{1}H, ^{13}C) as internal and Me$_2$Te (^{125}Te) as external standard. Electron spray mass spectra (ESI-MS) were performed on a Q-Tof micro (YA-105) mass spectrometer. Elemental analyses were performed on a Carlo Erba Model 1106 elemental analyzer. Infrared spectra were recorded on a Perkin Elmer spectrometer.

Synthesis of compound [7.3].I$_3$

A solution of **7.2**[8] (0.100 g, 0.228 mmol) in dry dichloromethane (15 mL) was cooled to 0 °C. A solution of iodine (0.115 g, 0.456 mmol) in carbon tetrachloride (15 mL) was added dropwise to it. After stirring at 0 °C for 1h, the reaction mixture was filtered off and the solvent was removed under vacuum to get a dark red solid of [**7.3**].I$_3$. Red colored crystals of [**7.3**].I$_3$ suitable for single-crystal diffraction analysis were obtained by slow evaporation of a chloroform solution of [**7.3**].I$_3$ at room temperature.

Yield 0.176 g (82 %); m.p. 192-194 °C; ^{1}H NMR (500 MHz, DMSO-d_6) δ 9.26 (d, J = 5.6 Hz, 2H), 8.70 (d, J = 8.3 Hz, 2H), 8.57 (d, J = 7.9 Hz, 2H), 8.40 (d, J = 7.8 Hz, 2H), 8.26 (t, J = 7.8 Hz, 2H), 7.69 – 7.55 (m, 6H); ^{13}C NMR (500 MHz, DMSO-d_6) δ 153.66, 143.61, 139.66, 134.21, 132.06, 130.99, 130.95, 127.30, 127.01, 123.67, 122.09; ^{125}Te NMR (126 MHz, DMSO-d_6) δ 1100; FT-IR (neat, cm^{-1}) 3051 (w), 1589 (m), 1481 (m), 1459 (w), 1437 (m), 1418 (m), 1301 (m), 1283 (m), 1259 (w), 1156 (m), 1103 (w), 1063 (vw), 1015 (m), 793 (w), 752 (s), 658 (vw), 642 (m), 627 (m); MS(ESI$^+$), m/z Calcd for {**7.3**-I}$^+$ (C$_{22}$H$_{16}$N$_2$Te): 438.05, Found: 438.07; Anal. Calc. for C$_{22}$H$_{16}$I$_4$N$_2$Te: C, 28.00, H, 1.71, N, 2.97; Found C, 28.13, H, 1.67, N, 3.09.

Synthesis of [7.4].2ClO₄ and [7.5].2OTf

To a solution of [**7.3**].I₃ (0.040 g, 0.042 mmol) in acetonitrile (15 mL) was added silver salt [AgClO₄ (0.044 g, 0.211 mmol) for [**7.4**].2ClO₄; AgOTf (0.054 g, 0.211 mmol) for [**7.5**].2OTf]. The reaction mixture was stirred at room temperature for 2 h. This resulted in an off-white precipitate. The precipitate was filtered off. The resulting filtrate on slow evaporation afforded colorless crystalline solids of [**7.4**].2ClO₄ and [**7.5**].2OTf.

[7.4].2ClO₄ : Yield 0.023 g (88%); m.p. >300 °C; ^{1}H NMR (500 MHz, DMSO-d_6) δ 8.58 – 8.54 (m, 2H), 8.13 (dd, J = 11.8, 7.8 Hz, 4H), 7.97 (t, J = 7.0 Hz, 2H), 7.65 – 7.61 (m, 2H), 7.49 (dd, J = 10.8, 5.8 Hz, 2H), 7.42 (ddd, J = 15.0, 10.3, 4.3 Hz, 4H).; ^{13}C NMR (125 MHz, DMSO-d_6) δ 156.57, 150.35, 148.53, 141.95, 139.05, 138.48, 129.94, 128.79, 127.81, 124.10, 121.66; ^{125}Te NMR (126 MHz, DMSO-d_6) δ 1107; FT-IR (neat, cm^{-1}) 3064 (vw), 2922 (vw), 1606 (m), 1486 (w), 1463 (w), 1443 (w), 1309 (w), 1293 (vw), 1139 (s), 1112 (s), 1089 (s), 761 (m), 739 (w), 634 (m), 626 (m); MS(ESI$^+$), m/z Calcd for {[**7.4**]ClO₄+H}$^+$ (C$_{22}$H$_{17}$ClN$_2$O$_4$Te): 537.97; Found: 537.98; Anal. Calc. for C$_{22}$H$_{16}$Cl$_2$N$_2$O$_8$Te: C, 41.62; H, 2.54; N, 4.41; Found C, 41.87; H, 2.22; N, 4.56.

[7.5].2OTf : Yield 0.028 g (90%); m.p. >300 °C; ^{1}H NMR (500 MHz, DMSO-d_6) δ 8.59 – 8.55 (m, 2H), 8.15 – 8.08 (m, 4H), 7.98 – 7.93 (m, 2H), 7.64 (dd, J = 7.1, 1.2 Hz, 2H), 7.51 – 7.47 (m, 2H), 7.46 – 7.38 (m, 4H); ^{13}C NMR (125 MHz, DMSO-d_6) δ 156.56, 150.35, 148.54, 141.95, 139.03, 138.49, 129.93, 128.79, 127.80, 124.09, 121.64; ^{125}Te NMR (126 MHz, DMSO-d_6) δ 1114; FT-IR (neat, cm^{-1}) 3054 (m), 3027 (m), 1600 (s), 1590 (s), 1483 (m), 1463 (m), 1438 (m), 1424 (m), 1306 (m), 1288 (m), 1261 (vw), 1171 (w), 1158 (w), 1105 (w), 1017 (m), 887 (w), 797 (w), 759 (s), 736 (m), 628 (m), 465 (m); MS(ESI$^+$), m/z Calcd for {[**7.5**]OTf+H}$^+$ (C$_{23}$H$_{17}$F$_3$N$_2$O$_3$STe): 587.99; Found: 587.96; Anal. Calc. for C$_{24}$H$_{16}$F$_6$N$_2$O$_6$S$_2$Te: C, 39.27; H, 2.20; N, 3.82; Found C, 39.41; H, 2.17; N, 4.16.

Synthesis of compound [7.8].2ClO₄

To a solution of **7.6**[21] (0.200 g, 0.514 mmol) in acetonitrile (15 mL) was added AgClO₄ (0.319 g, 1.542 mmol). The reaction mixture was stirred at room temperature for 2 h. This resulted in an off-white precipitate. The precipitate was filtered off. The resulting filtrate on slow evaporation at room temperature afforded a colorless crystalline solid of [**7.8**].2ClO₄.

Yield: 0.304 g (74 %); m.p. >300 °C; ^{1}H NMR (500 MHz, DMSO-d_6) δ 8.57 (d, J = 4.1 Hz, 2H), 8.12 (dd, J = 11.0, 8.0 Hz, 4H), 7.96 (td, J = 7.8, 1.6 Hz, 2H), 7.64 (d, J = 6.9 Hz, 2H), 7.49 (dd, J = 6.8, 5.1 Hz, 2H), 7.46 – 7.38 (m, 4H); ^{13}C NMR (125 MHz, DMSO-d_6) 156.02, 149.80, 147.99, 141.40, 138.48, 137.94, 129.39, 128.24, 127.25, 123.54, 121.09; ^{125}Te NMR (157 MHz, DMSO-d_6) δ 1413; FT-IR (neat, cm^{-1}) 3077 (vw), 2918 (vw), 1603 (w), 1444 (s), 1308 (vw), 1141 (s), 1089 (s), 1053 (s), 914 (vw), 876 (m), 764 (m), 736 (w), 654 (w), 632 (m), 622 (m), 539 (vw), 498 (w); MS(ESI$^+$), m/z Calcd for {[**7.8**]ClO$_4$}$^+$ (C$_{22}$H$_{16}$ClN$_2$O$_6$Te$_2$): 696.86, Found: 696.89; Anal. Calc. for C$_{22}$H$_{16}$Cl$_2$N$_2$O$_{10}$Te$_2$: C, 33.26, H, 2.03, N, 3.53; Found C, 33.07, H, 1.93, N, 3.71.

Synthesis of compound [7.10].Br

A stirred solution of **7.9**[23] (0.150 g, 0.643 mmol) in dry Et$_2$O (25 mL) was treated dropwise with 1.6 M solution of n-BuLi in hexane (0.482 mL, 0.772 mmol) at -78 °C for 30 min. An Et$_2$O (20 mL) solution of TeCl$_4$ (0.043 g, 0.160 mmol) was added to the reaction mixture at -78 °C. The reaction mixture was stirred for 14 h at room temperature. After completion of the reaction, the solvent was removed under vacuum to get a light yellow solid, which is the mixture of [**7.10**].Br and (ppy)$_2$Te. Dichloromethane (20 mL) was added to the solid and the resulting reaction mixture was filtered through celite. The filtrate was concentrated under vacuum, washed with Et$_2$O (3 × 15 mL) which removed (ppy)$_2$Te and afforded the analytically pure solid of [**7.10**].Br. Light yellow crystals of [**7.10**].Br.2CHCl$_3$ suitable for single-crystal diffraction analysis were obtained by slow diffusion of hexane in to CHCl$_3$ solution of [**7.10**].Br.

Yield: 0.284 g (66 %); m.p. 156 °C; ^{1}H NMR (500 MHz, C$_6$D$_6$) δ 8.80 (dd, J = 7.9, 1.0 Hz, 3H), 8.41 (ddd, J = 4.9, 1.6, 0.9 Hz, 3H), 7.46 (dd, J = 7.8, 1.3 Hz, 3H), 7.27 (d, J = 8.2 Hz, 3H), 7.05 – 6.98 (m, 6H), 6.84 (td, J = 8.0, 1.4 Hz, 3H), 6.54 (ddd, J = 7.4, 4.9, 0.9 Hz, 3H); ^{13}C NMR (125 MHz, C$_6$D$_6$) δ 156.81, 146.48, 141.35, 139.59, 137.07, 130.35, 127.53, 127.38, 122.52, 120.72, 112.75; ^{125}Te NMR (157 MHz, CDCl$_3$) δ 867; FT-IR (neat, cm^{-1}) 3051 (m), 1589 (s), 1476 (m), 1464 (m), 1434 (s), 1300 (m), 1157 (m), 1098 (m), 1071 (w), 1015 (w), 999 (m), 895 (w), 797 (m), 757 (s), 627 (m), 590 (w); MS(ESI$^+$), m/z Calcd for [**7.10**]$^+$ (C$_{33}$H$_{24}$N$_3$Te): 592.11, Found: 592.10; Anal. Calc. for C$_{33}$H$_{24}$BrN$_3$Te: C, 59.15, H, 3.61, N, 6.27; Found C, 58.97, H, 3.54, N, 6.39.

Synthesis of compound 7.11

To a THF solution of [**7.10**].Br (0.075 g, 0.118 mmol), was added a THF solution of K_2PdCl_4 (0.036 g, 0.112 mmol) at room temperature. The reaction mixture was stirred for 12 h. The solvent was removed under vacuum to get a yellow solid. The solid was washed with $CHCl_3$ (3 × 15 mL) and Et_2O (3 × 15 mL) to afford the analytically pure solid of **7.11**. Yellow crystals of **7.11** suitable for single-crystal diffraction analysis were obtained by slow diffusion of benzene into a DMSO solution of **7.11** at room temperature.

Yield: 0.073 g (82 %), m.p. 191 °C; ^{1}H NMR (400 MHz, DMSO-d_6) δ 9.27 (d, J = 5.6 Hz, 1H), 8.70 (d, J = 8.3 Hz, 1H), 8.60 – 8.54 (m, 2H), 8.40 (d, J = 8.0 Hz, 1H), 8.30 – 8.22 (m, 1H), 8.14 (dd, J = 12.7, 4.9 Hz, 2H), 8.00 – 7.94 (m, 1H), 7.69 – 7.56 (m, 4H), 7.50 (ddd, J = 7.4, 4.8, 1.0 Hz, 1H), 7.43 (dtd, J = 16.6, 7.3, 1.5 Hz, 2H); ^{13}C NMR (400 MHz, DMSO-d_6) 156.49, 154.16, 148.38, 144.11, 141.95, 140.17, 139.03, 138.35, 134.71, 132.55, 131.45, 129.93, 128.72, 127.80, 127.74, 127.51, 124.17, 124.09, 122.60, 121.55; ^{125}Te NMR (400 MHz, DMSO-d_6) 1309; FT-IR (neat, cm^{-1}) 3061 (w), 2922 (s), 2852 (s), 1600 (m), 1578 (m), 1485 (w), 1466 (vw), 1439 (w), 1422 (w), 1304 (w), 1288 (w), 1273 (w), 1156 (w), 1017 (w), 790 (w), 757 (s), 739 (m), 661 (vw), 630 (w); MS(ESI$^+$), m/z Calcd for [**7.11**-{(ppy)PdCl$_2$}]$^+$ ($C_{22}H_{16}ClN_2Te$): 473.01, Found: 473.03.

Synthesis of [7.12].Cl

A stirred solution of **7.9**[23] (0.100 g, 0.429 mmol) in dry Et_2O (20 mL) was treated dropwise with 1.6 M solution of *n*-BuLi in hexane (0.322 mL, 0.515 mmol) at -78 °C for 30 min. BiCl$_3$ (0.067 g, 0.212 mmol) was added to the reaction mixture and was stirred for 8 h. After completion of the reaction, the solvent was removed under vacuum to get a white solid. Dichloromethane (20 mL) was added to the solid and the resulting reaction mixture was filtered through celite. The filtrate was concentrated under vacuum to afford the analytically pure solid of [**7.12**].Cl. Colorless crystals of [**7.12**].Cl suitable for single-crystal diffraction analysis were obtained by slow evaporation of a methanol solution of [**7.12**].Cl at room temperature.

Yield 0.169 g (71%); m.p. >300 °C; ^{1}H NMR (500 MHz, DMSO-d_6) δ 8.99 (d, J = 4.7 Hz, 2H), 8.43 (d, J = 7.6 Hz, 2H), 8.38 (d, J = 8.2 Hz, 2H), 8.25 (t, J = 7.3 Hz, 2H), 7.90 (d, J = 7.2 Hz, 2H), 7.73 – 7.69 (m, 2H), 7.52 (dt, J = 22.9, 7.0 Hz, 4H); ^{13}C NMR (125 MHz, DMSO-d_6) δ

186.96, 161.65, 149.07, 145.28, 141.13, 138.19, 133.70, 130.15, 128.64, 124.67, 122.94; FT-IR (neat, cm^{-1}) 3051 (m), 3013 (m), 1625 (vw), 1594 (m), 1479 (m), 1420 (m), 1277 (vw), 1246 (vw), 1153 (w), 1102 (w), 1014 (m), 1000 (w), 902 (vw), 846 (vw), 805 (w), 761 (s), 737 (m), 729 (m), 635 (w), 553 (w); MS(ESI$^+$), m/z Calcd for [**7.12**]$^+$ (C$_{22}$H$_{16}$BiN$_2$): 517.11; Found: 517.13; Anal. Calc. for C$_{22}$H$_{16}$BiClN$_2$: C, 47.80; H, 2.92; N, 5.07; Found C, 47.56; H, 2.87; N, 5.26.

7.5 References

(1) (a) Herrmann, W. A.; Denk, M.; Behm, J.; Scherer, W.; Klingan, F.-R.; Bock, H.; Solouki, B.; Wagner, M. *Angew. Chem. Int. Ed. Engl.* **1992**, *31*, 1485-1488; *Angew. Chem.* **1992**, *104*, 1489-1492. (b) Denk, M.; Lennon, R.; Hayashi, R.; West, R.; Belyakov, A. V.; Verne, H. P.; Haaland, A.; Wagner, M.; Metzler, N. *J. Am. Chem. Soc.* **1994**, *116*, 2691-2692. (c) Carmalt, C. J.; Lomeli, V.; McBurnett, B. G.; Cowley, A. H. *Chem. Commun.* **1997**, 2095-2096. (d) Schmidt, E. S.; Jockisch, A.; Schmidbaur, H. A. *J. Am. Chem. Soc.* **1999**, *121*, 9758-9759. (e) Baker, R. J.; Jones, C.; Platts, J. A. *J. Am. Chem. Soc.* **2003**, *125*, 10534-10535. (f) Yoo, H.; Carroll, P. J.; Berry, D. H. *J. Am. Chem. Soc.* **2006**, *128*, 6038-6039. (g) Segawa, Y.; Yamashita, M.; Nozaki, K. *Science* **2006**, *314*, 113-115. (h) Dutton, J. L.; Tuonone, H. M.; Jennings, M. C.; Ragogna, P. J. *J. Am. Chem. Soc.* **2006**, *128*, 12624-12625. (i) Rupar, P. A.; Staroverov, V. N.; Ragogna, P. J.; Baines, K. M. *J. Am. Chem. Soc.* **2007**, *129*, 15138-15139. (j) Chivers, T.; Konu, J. Ligand-Stabilized Chalcogen Dications. *Angew. Chem. Int. Ed. Engl.* **2009**, *48*, 3025-3027; *Angew. Chem.* **2009**, *121*, 3069-3071. (k) Segawa, Y.; Yamashita, M.; Nozaki, K. *J. Am. Chem. Soc.* **2009**, *131*, 9201-9203. (l) Tulchinsky, Y.; Iron, M. A.; Botoshansky, M.; Gandelman, M. *Nat. Chem.* **2011**, *3*, 525-531. (m) Heims, F.; Pfaff, F. F.; Abram, S.-L.; Farquhar, E. R.; Bruschi, M.; Greco, C.; Ray, K. *J. Am. Chem. Soc.* **2014**, *136*, 582-585.

(2) (a) Olaru, M.; Duvinage, D.; Lork, E.; Mebs, S.; Beckmann, J. *Angew. Chem. Int. Ed. Engl.* **2018**, *57*, 10080-10084; *Angew. Chem.* **2018**, *130*, 10237-10241. (b) Dutton, J. L.; Ragogna, P. J. *Chem. - Eur. J.* **2010**, *16*, 12454-12461.

(3) (a) Buron, C.; Gornitzka, H.; Romanenko, V.; Bertrand, G. *Science* **2000**, *288*, 834-836. (b) Solé, S.; Gornitzka, H.; Schoeller, W. W.; Bourissou, D.; Bertrand, G. *Science* **2001**,

292, 1901-1903. (c) Merceron-Saffon, N.; Baceiredo, A.; Gornitzka, H.; Bertrand, G. *Science* **2003**, *301*, 1223-1225. (d) Canac, Y.; Soleilhavoup, M.; Conejero, S.; Bertrand, G. *J. Organomet. Chem*. **2004**, *689*, 3857-3865. (e) Melaimi, M.; Soleilhavoup, M.; Bertrand, G. *Angew. Chem. Int. Ed. Engl.* **2010**, *49*, 8810-8849; *Angew. Chem.* **2010**, *122*, 8992-9032, and references therein. (f) Melaimi, M.; Jazzar, R.; Soleilhavoup, M.; Bertrand, G. *Angew. Chem. Int. Ed. Engl.* **2017**, *56*, 10046-10068; *Angew. Chem.* **2017**, *129*, 10180-10203, and references therein.

(4) (a) Kira, M.; Ishida, S.; Iwamoto, T.; Kabuto, C. *J. Am. Chem. Soc*. **1999**, *121*, 9722-9723. (b) Kim, K.-C.; Reed, C. A.; Elliott, D. W.; Mueller, L. J.; Tham, F.; Lin, L.; Lambert, J. B. *Science* **2002**, *297*, 825-827. (c) Lambert, J. B.; Lin, L.; Keinan, S.; Müller, T. *J. Am. Chem. Soc*. **2003**, *125*, 6022-6023. (d) Mizuhata, Y.; Sasamori, T.; Tokitoh, N. *Chem. Rev.* **2009**, *109*, 3479-3511. (e) Ghadwal, R. S.; Roesky, H. W.; Pröpper, K.; Dittrich, B.; Klein, S.; Frenking, G. *Angew. Chem. Int. Ed*. *Engl.* **2011**, *50*, 5374-5378; *Angew. Chem.* **2011**, *123*, 5486-5490.

(5) (a) Ohshita, J.; Matsui, S.; Yamamoto, R.; Mizumo, T.; Ooyama, Y.; Harima, Y.; Murafuji, T.; Tao, K.; Kuramochi, Y.; Kaikoh, T.; Higashimura, H. *Organometallics* **2010**, *29*, 3239-3241. (b) He, G.; Delgado, W. T.; Schatz, D. J.; Merten, C.; Mohammadpour, A.; Mayr, L.; Ferguson, M. J.; McDonald, R.; Brown, A.; Shankar, K.; Rivard, E. *Angew. Chem. Int. Ed. Engl.* **2014**, *53*, 4587-4591; *Angew. Chem.* **2014***, 126,* 4675-4679. (c) Toma, O.; Allain, M.; Meinardi, F.; Forni, A.; Botta, C.; Mercier, N. *Angew. Chem. Int. Ed. Engl.* **2016**, *55*, 7998-8002; *Angew. Chem.* **2016**, *128*, 8130-8134. (d) Parke, S. M.; Hupf, E.; Matharu, G. K.; de Aguiar, I.; Xu, L.; Yu, H.; Boone, M. P.; de Souza, G. L. C.; McDonald, R.; Ferguson, M. J.; He, G.; Brown, A.; Rivard, E. *Angew. Chem. Int. Ed. Engl.* **2018**, *57*, 14841-14846; *Angew. Chem.* **2018**, *130*, 15057-15062. (e) Rettig, I. D.; Van, J.; Brauer, J. B.; Luo, W.; McCormick, T. M. *Dalton Trans*., **2019**, *48*, 5665-5673. (f) Hupf, E.; Tsuchiya, Y.; Moffat, W.; Xu, L.; Hirai, M.; Zhou, Y.; Ferguson, M. J.; McDonald, R.; Murai, T.; He, G.; Rivard, E. *Inorg. Chem*. **2019**, *58*, 13323-13336. (g) Clark, J. L.; Hill, J. E.; Rettig, I. D.; Beres, J. J.; Ziniuk, R.; Ohulchanskyy, T. Y.; McCormick, T. M.; Detty, M. R. *Organometallics* **2019**, *38*, 2431-2442.

(6) (a) Srivastava, K.; Shah, P.; Singh, H. B.; Butcher, R. J. *Organometallics* **2011**, *30*, 534-546. (b) Beckmann, J.; Bolsinger, J.; Duthie, A.; Finke, P. *Dalton Trans.* **2013**, *42*, 12193-12202.

(7) Deka, R.; Sarkar, A.; Butcher, R. J.; Junk, P. C.; Turner, D. R.; Deacon, G. B.; Singh, H. B. *Dalton Trans.* 2020, DOI: 10.1039/C9DT04013G.

(8) Al-Salim, N.; West, A. A.; McWhinnie, W. R.; Hamor, T. A. *J. Chem. Soc., Dalton Trans.* **1988**, 2363-2371.

(9) Alvarez, S. A. *Dalton Trans.* **2013**, *42*, 8617-8636.

(10) Frisch, M. J.; Trucks, G. W.; Schlegel, H. B.; Scuseria, G. E.; Robb, M. A.; Cheeseman, J. R.; Scalmani, G.; Barone, V.; Mennucci, B.; Petersson, G. A.; Nakatsuji, H.; Caricato, M.; Li, X.; Hratchian, H. P.; Izmaylov, A. F.; Bloino, J.; Zheng, G.; Sonnenberg, J. L.; Hada, M.; Ehara, M.; Toyoto, K.; Fukuda, R.; Hasegawa, J.; Ishida, M.; Nakajima, T.; Honda, Y.; Kitao, O.; Nakai, H.; Vreven, T.; Montgomery, J. A., Jr.; Peralta, J. E.; Ogliaro, F.; Bearpark, M.; Heyd, J. J.; Brothers, E.; Kudin, K. N.; Staroverov, V. N.; Kobayashi, R.; Normand, J.; Raghavachari, K.; Rendell, A.; Burant, J. C.; Iyengar, S. S.; Tomasi, J.; Cossi, M.; Rega, N.; Millam, J. M.; Klene, M.; Knox, J. E.; Cross, J. B.; Bakken, V.; Adamo, C.; Jaramillo, J.; Gomperts, R.; Stratmann, R. E.; Yazyev, O.; Austin, A. J.; Cammi, R.; Pomelli, C.; Ochterski, J. W.; Martin, R. L.; Morokuma, K.; Zakrzewski, V. G.; Voth, G. A.; Salvador, P.; Dannenberg, J. J.; Dapprich, S.; Daniels, A. D.; Farkas, O.; Foresman, J. B.; Ortiz, J. V.; Cioslowski, J.; Fox, D. J. *Gaussian 09*, revision A.02; Gaussian, Inc.: Wallingford, CT, **2009**.

(11) (a) Perdew, J. P.; Wang, Y. *Phys. Rev. B* **1992**, *23*, 13244-13249. (b) Becke, A. D. *J. Chem. Phys.* **1993**, *98*, 5648-5652.

(12) Martin, J. M. L.; Sundermann, A. *J. Chem. Phys.* **2001**, *114*, 3408-3420.

(13) Pettersson, G. A.; Al-Laham, M. A. *J. Chem. Phys.* **1991**, *94*, 6081-6090.

(14) Pettersson, K. A. *J. Chem. Phys.* **2003**, *119*, 11113-11123.

(15) E. D. Glendening, J. K. Badenhoop, A. E. Reed, J. E. Carpenter, J. A. Bohmann, C. M. Morales, C. R. Landis, F. Weinhold, Theoretical Chemistry Institute, University of Wisconsin, Madison, NBO 6.0, **2013**.

(16) Becke, A. D. *J. Chem. Phys.* **1990**, *92*, 5397-5403.

(17) Murray, J. S.; Paulsen, K.; Politzer, P. *Proc.-Indian Acad. Sci.*, *Chem. Sci.* **1994**, *106*, 267-275.

(18) (a) Clark, T.; Hennemann, M.; Murray, J. S.; Politzer, P. *J. Mol. Model* **2007**, *13*, 291-296. (b) Politzer, P.; Murray, J. S. *ChemPhysChem* **2013**, *14*, 278-294. (c) Clark, T. *WIREs Comput. Mol. Sci.* **2013**, *3*, 13-20. (d) Bauzá, A.; Quiñonero, D.; Deyá, P. M.; Frontera, A. *CrystEngComm* **2013**, *15*, 3137-3144. (e) Lim, J. Y. C.; Beer, P. D. *Chem* **2018**, *4*, 731-783.

(19) Biegler-König, F.; Schönbohm, J. *J. Comput. Chem.* **2002**, *23*, 1489-1494.

(20) Kumar, P. S. V.; Raghavendra, V.; Subramanian, V. *J. Chem. Sci.* **2016**, *128*, 1527-1536.

(21) Lobana, T. S.; McWhinnie, W. R. *Indian. J. Chem. Sect. A* **1992**, *31*, 460-462.

(22) (a) Kobayashi, K.; Sato, S.; Horn, E.; Furukawa, N. *Z. Kristallogr.* **2000**, *215*, 21-22. (b) Hupf, E.; Do, T. G.; Nordheider, A.; Wehrhahn, M.; Camacho, P. S.; Ashbrook, S. E.; Lork, E.; Slawin, A. M. Z.; Mebs, S.; Woollins, J. D.; Beckmann, J. *Organometallics* **2017**, *36*, 1566-1579.

(23) Niedermann, K.; Welch, J. M.; Koller, R.; Cvengroš, J.; Santschi, N.; Battaglia, P.; Togni, *Tetrahedron* **2010**, *66*, 5753-5761.

(24) (a) Jones, C. H. W.; Sharma, R. D. *J. Organomet. Chem.* **1987**, *332*, 115-121. (b) Lin, T.-P.; Gabbaï, F. P. *Angew. Chem. Int. Ed. Engl.* **2013**, *52*, 3864-3868, *Angew. Chem.* **2013**, *125*, 3956-3960.

(25) (a) Maekawa, M.; Munakata, M.; Kitagawa, S.; Nakamura, M. *Anal. Sci.* **1991**, *7*, 521-522. (b) Muranishi, Y.; Wang, Y.; Odoko, M.; Okabe, N. *Acta Cryst.* **2005**, *C61*, m307-m310. (c) Pawlak, T.; Niedzielska, D.; Vícha, J.; Marek R.; Pazderski, L. *J. Organomet. Chem.* **2014**, *759*, 58-66.

(26) G. M. Sheldrick, *SHELXS-97*, *Program for Crystal Structures Solution*; University of Göttingen, **1997**.

(27) G. M. Sheldrick, *SHELXL-97, Program for refinement of Crystal Structures*; University of Göttingen, **1997**.

(28) van der Sluis, P.; Spek, A. L. *Acta Crystallogr, Sect. A: Fundam. Crystallogr.* **1990**, *46*, 194-201.

(29) Lu, T.; Chen, F. Multiwfn: A Multifunctional Wavefunction Analyzer. *J. Comput. Chem.* **2012**, *33*, 580-592.

1 **7.6 Supplementary Data**

2 **Table 7.1** Refinement details for the X-ray structures.

Compound	[7.3].I$_3$	[7.4].2ClO$_4$	[7.5].2OTf	[7.8].2ClO$_4$	[7.10].Br	7.11	[7.12].Cl
Formula	C$_{22}$H$_{16}$I$_4$N$_2$Te	C$_{22}$H$_{16}$Cl$_2$N$_2$O$_8$Te	C$_{24}$H$_{16}$F$_6$N$_2$O$_6$S$_2$Te	C$_{11}$H$_8$ClNO$_5$Te	C$_{35}$H$_{25}$BrCl$_6$N$_3$Te	C$_{36}$H$_{27}$Br$_{0.43}$Cl$_{2.57}$N$_3$PdTe	C$_{22}$H$_{16}$BrClN$_2$
Crystal System	Triclinic	Orthorhombic	Triclinic	Monoclinic	Monoclinic	Monoclinic	Monoclinic
Space group	*P-1*	*Pbca*	*P-1*	*P2$_1$/c*	*P2$_1$/n*	*P2$_1$/c*	*C2/c*
T/K	100(2)	100(2)	100(2)	100(2)	150	100(2)	100(2)
a [Å]	8.1443(6)	16.6878(2)	8.9291(3)	8.7842(11)	14.0963(9)	8.5086(6)	13.5679(6)
b [Å]	10.1239(5)	14.6316(2)	9.1092(3)	7.9053(12)	14.6880(8)	17.9307(18)	12.1082(5)
c [Å]	16.1218(9)	19.0616(4)	18.1349(5)	17.753(3)	18.7881(12)	20.8076(19)	11.7567(5)
α [°]	96.800(4)	90	86.433(2)	90	90	90	90
β [°]	100.455(5)	90	80.450(3)	101.736(15)	110.891(8)	90.160(8)	105.829(4)
γ [°]	103.770(5)	90	64.787(3)	90	90	90	90
V [Å^3]	1251.33(14)	4654.23(14)	1315.95(7)	1207.0(3)	3634.3(4)	3174.5(5)	1858.18(14)
Z	2	8	2	4	4	4	4
ρ$_{calc}$/cm^3	2.504	1.812	1.853	2.186	1.661	1.802	1.976
μ/mm^{-1}	6.135	1.560	1.376	2.701	2.389	2.278	9.640
GOF	1.046	1.039	1.028	0.979	1.038	1.072	1.074
2θ range (deg)	5.214–62.088	4.882–50	4.556–62.382	5.948–50.488	4.48–49.998	4.544–62.028	4.588–62.296
Refs collected	7194	28205	17530	2188	17018	27713	2720
Unique/observed	7194	4095	7570	2188	6394	9197	2720
Parameters	262	316	370	172	415	409	120
R$_{int}$	0.0443	0.0421	0.0499	0.1612	0.0780	0.1738	0.0993
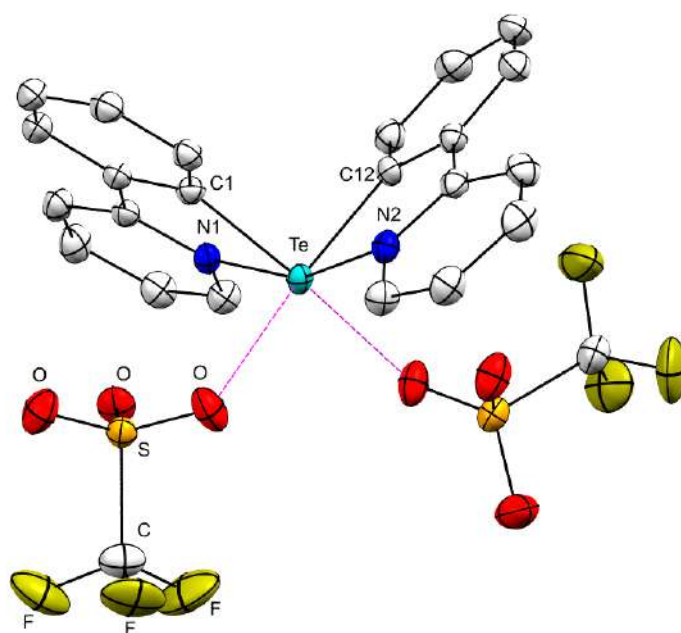
Fig. 7.8 Molecular structure of [**7.5**].2OTf; thermal ellipsoids are set at the 50% probability level. Selected bond distances and angles [Å, °] C1-Te 2.110(2), C12-Te 2.122(2), N1···Te 2.231(2), N2···Te 2.252(2), C1-Te-C12 97.1(1), C1-Te···N 76.83(9), C12-Te···N 77.39(9), N1···Te···N2 160.62(7).
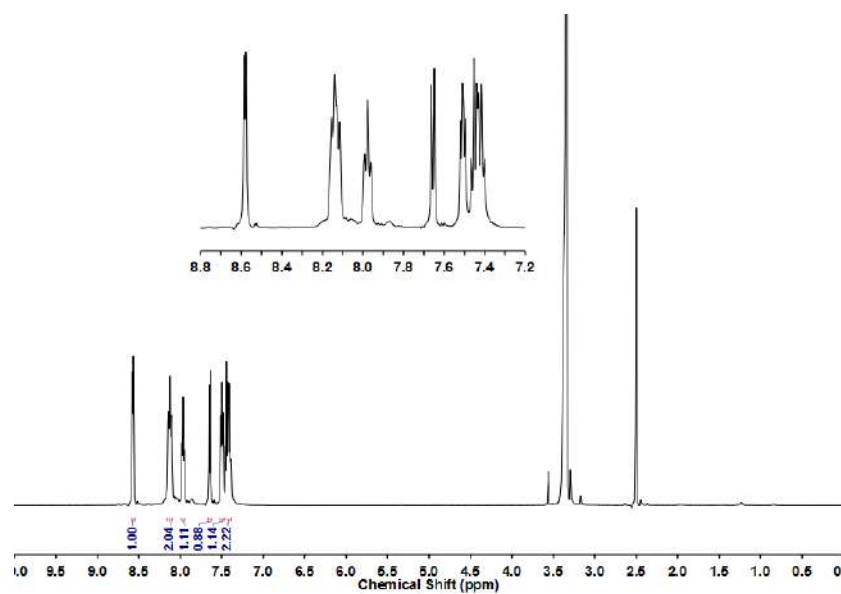
Fig. 7.9 ^{1}H NMR spectrum of **[7.4]**.2ClO$_4$
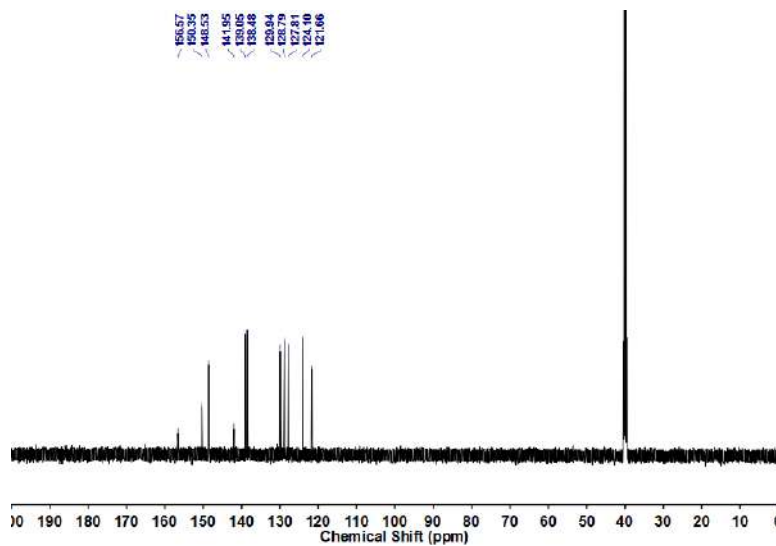
Fig. 7.10 ^{13}C NMR spectrum of **[7.4]**.2ClO$_4$
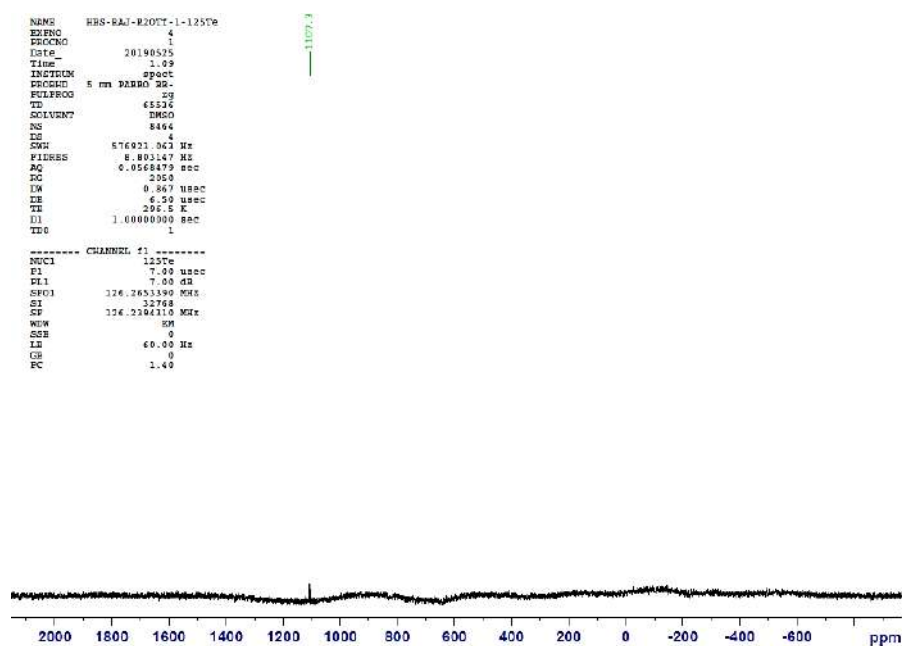
Fig. 7.11 ^{125}Te NMR spectrum of **[7.4]**.2ClO$_4$
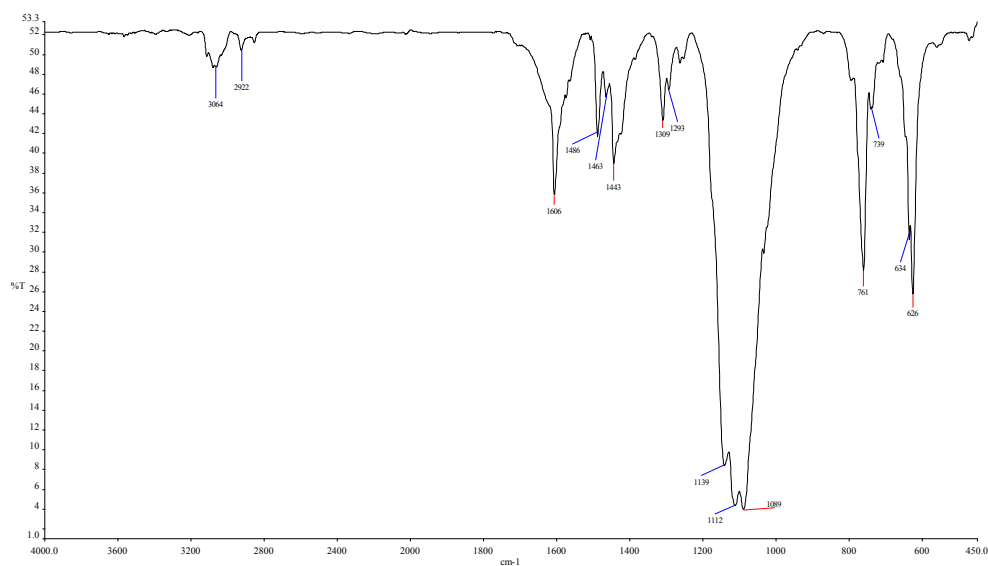
Fig. 7.12 FT-IR spectrum of **[7.4]**.2ClO$_4$
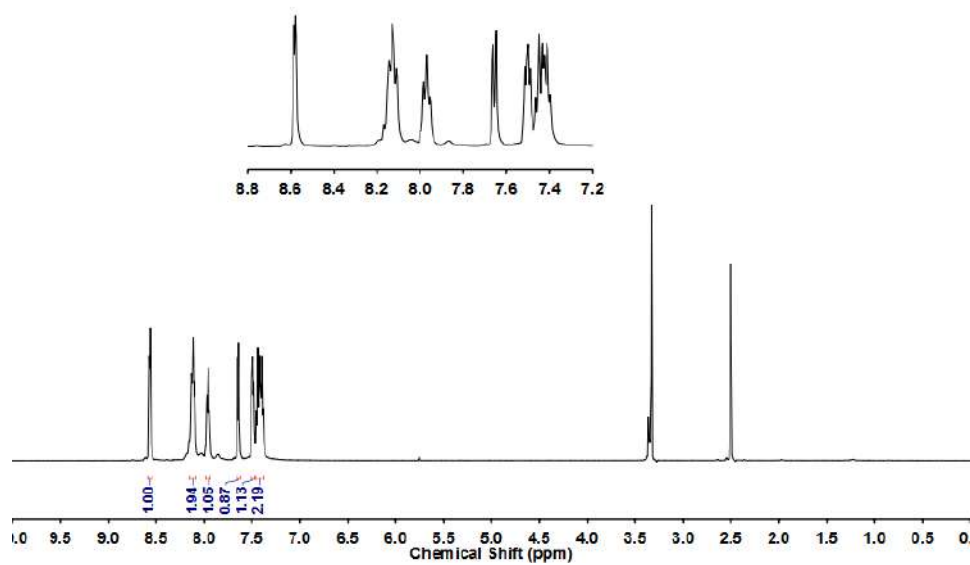
Fig. 7.13 ¹H NMR spectrum of **[7.5]**.2OTf
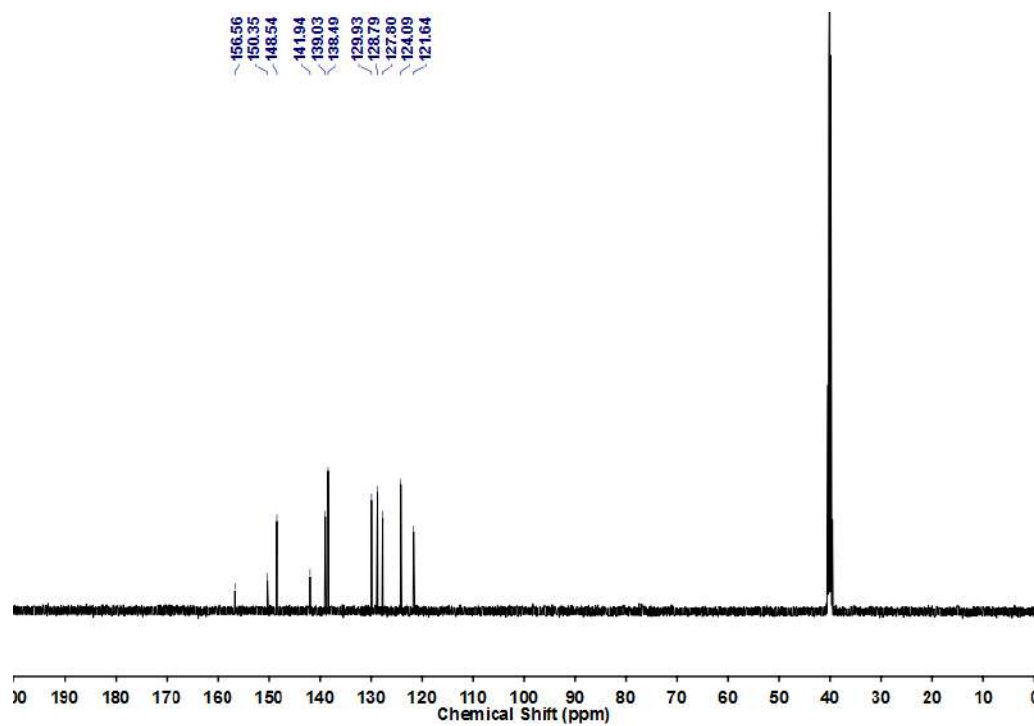
Fig. 7.14 ¹³C NMR spectrum of **[7.5]**.2OTf.
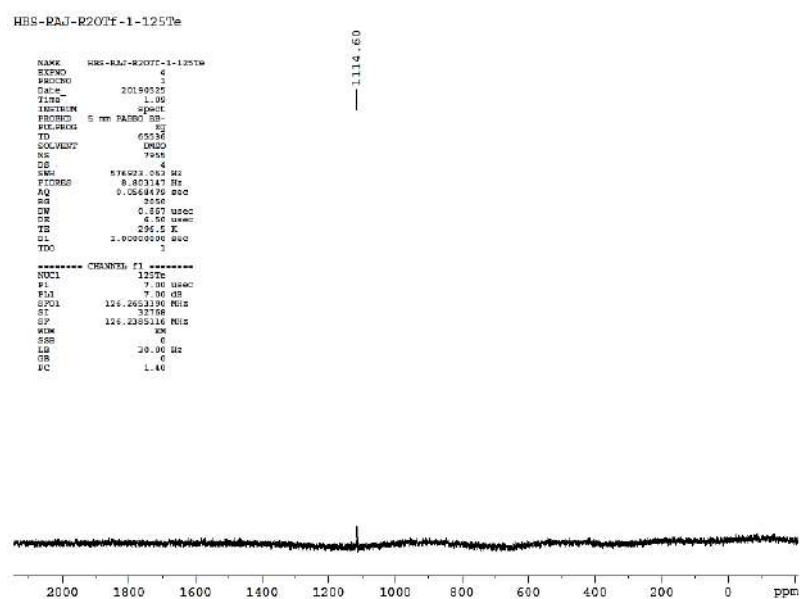
Fig. 7.15 ^{125}Te NMR spectrum of **[7.5]**.2OTf.
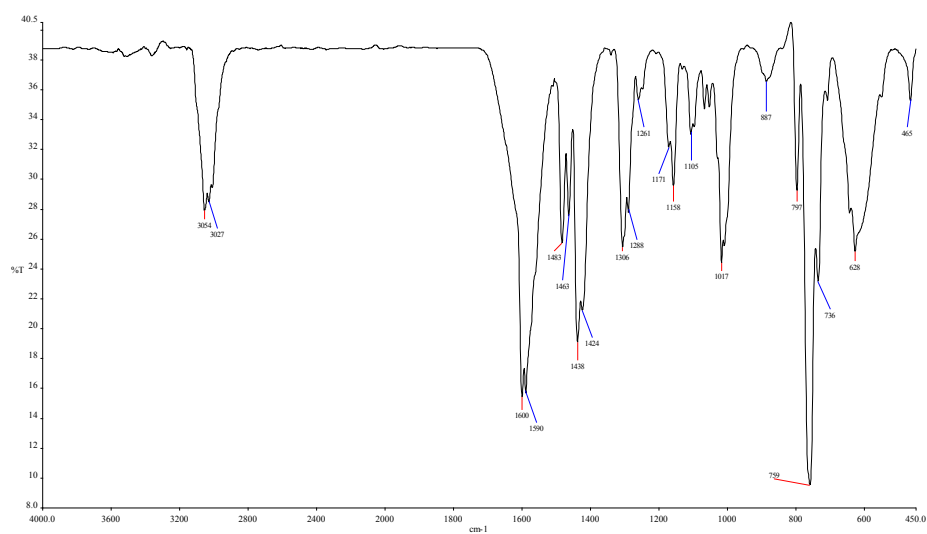
Fig. 7.16 FT-IR spectrum of **[7.5]**.2OTf.
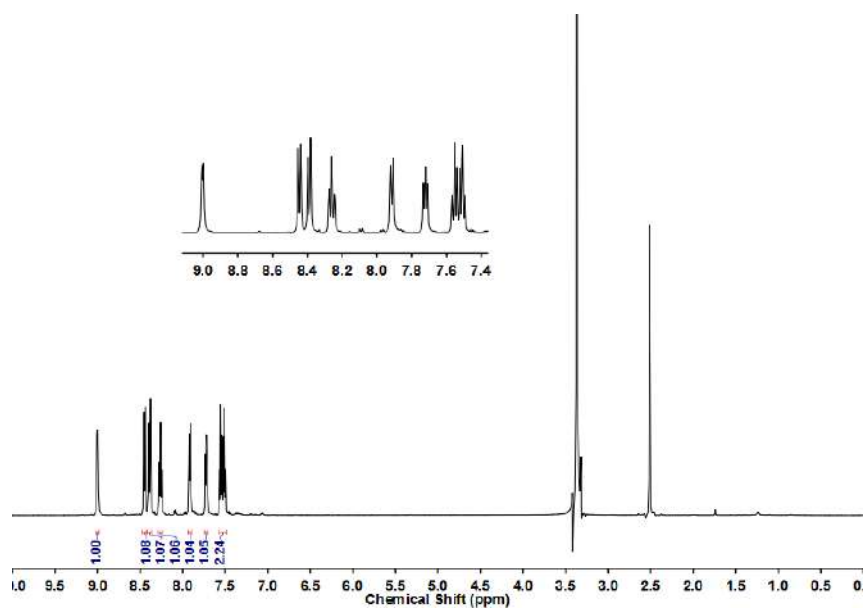
Fig. 7.17 ^{1}H NMR spectrum of **[7.12]**.Cl.
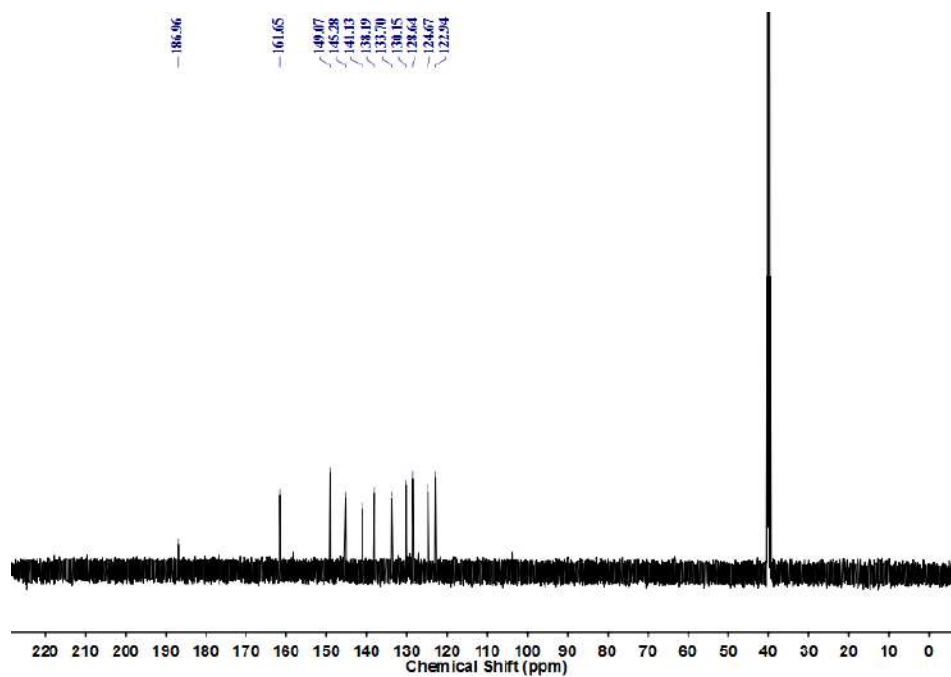
Fig. 7.18 ^{13}C NMR spectrum of **[7.12]**.Cl.
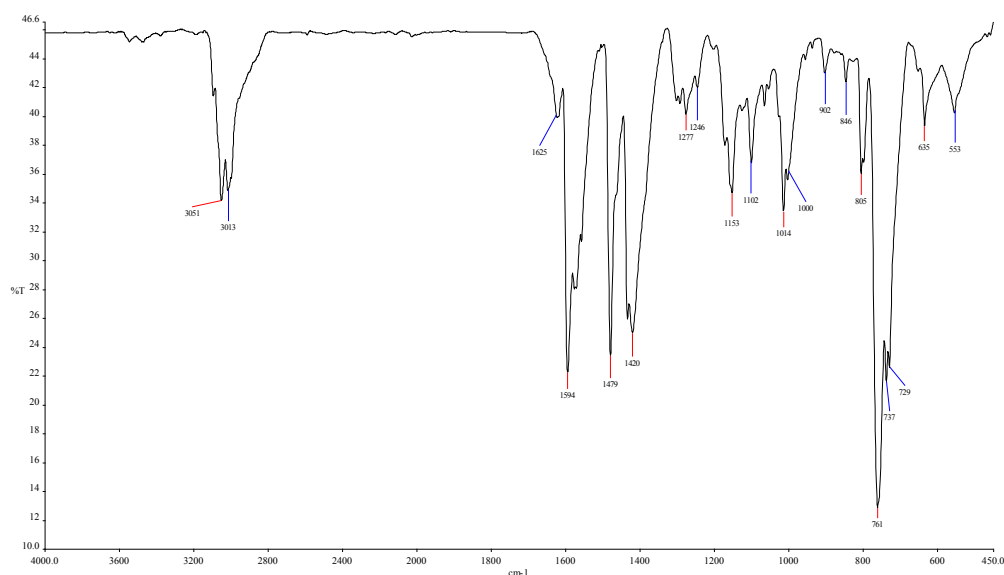
Fig. 7.19 FT-IR spectrum of **[7.12]**.Cl.
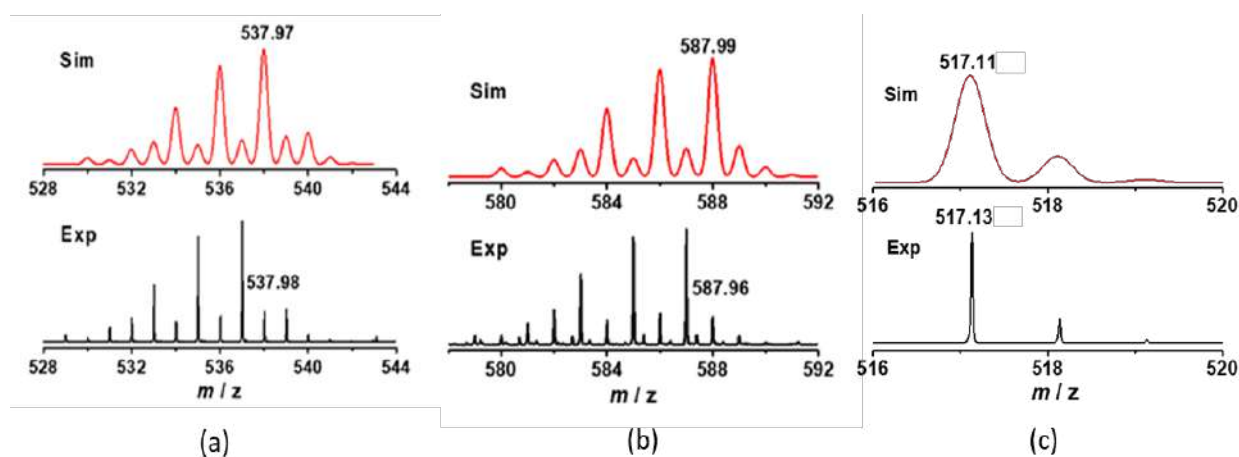
Fig. 7.20 Experimental and simulated ESI (+) mass spectra of (a) {[**7.4**]ClO$_4$+H}$^+$, (b) {[**7.5**]OTf+H}$^+$, (c) [**7.12**]$^+$ (black line, experimental and red line, simulated).

Appendix 3

Exploring the Role of Strong Intramolecular Coordination Ability of 2-(2´-pyridyl)phenyl Group on Main Group Halides: Insights from Synthesis, Structural, and Bonding Analysis

8.1 Introduction

The isolation of monoorgano heavy main group halides (REX$_n$, E = heavy group 13-16 elements, X = halide, n = 1-3) has always been a topic of significant interest with respect to their synthetic aspects, structural diversities, and potential applications.[1-3] These compounds are synthetically challenging as the further substitution of the halide(s) can lead to the higher conglomerates such as di/tri-organo main group halides (R$_m$EX$_n$, m = 1-3, n = 3-1).[1-3] In this context, ligands with one intramolecular coordinating group have gained significant attention for the stabilization of different monomeric, monoorgano main group halides. Ligands with one coordinating group can be (i) aryl groups with *ortho*-substituted pendent arms such as **8.1-8.5,** and (ii) *peri*-substituted pendent arms such as **8.6-8.7** (Chart 8.1).[1-4] These aryl groups make covalent bond to the element center via the C-atom, at the same time the donor atom of the pendant arm makes intramolecular interaction D→E (D = donor atom) with the element center (E), the distance between the two atoms (D and E) being significantly shorter than the sum of their van der Waal radii. This interaction results in the considerable attenuation of the Lewis acidity around the metal center and stabilizes the molecule as monomeric, monoorgano halide species.
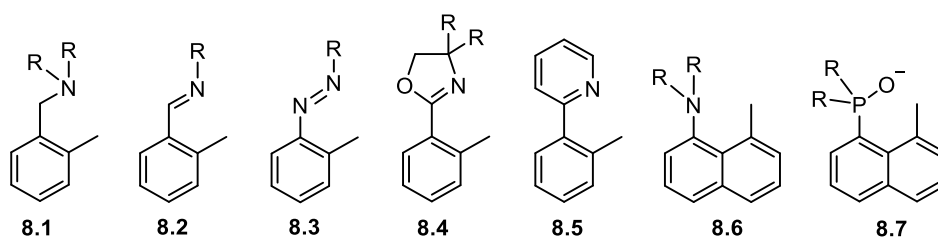

Chart 8.1. Examples of ligands (**8.1-8.7**) with one coordinating pendant arm.

Our group has been actively working on the synthesis of various organotellurium compounds stabilized by a built-in nitrogen coordinating group, such as dioorganotelluride, diorganoditelluride, organotelluroxanes, metal tellurolate complexes, to name a few.[5] Apart from being synthetically important, these intramolecular interaction stabilized organotellurium compounds have gained significant interest with respect to their structural varieties, diverse reactivity, and widespread applications in contemporary chemistry.[5] Recently, using the strong intramolecular coordination ability of the N atom of the 2-(2′-pyridyl)phenyl group (ppy), **8.5**, we have succeeded in the isolation of the novel example of monomeric organotellurinic(IV) acid and Te and Bi analogues of non-N-Heterocyclic Carbene (non-NHC) derivatives.[6,7] The molecular structures of both these classes of compounds reveal that the pyridyl N-atom of the ppy group

makes very strong electrostatic interaction with the element (Te/Bi) center. This observation was further corroborated by Density Functional Theory (DFT) calculations, which suggest that the stability of both monomeric organotellurinic(IV) acid and non-NHC carbenoid derivatives relies on the σ-hole participation of the Te atom with the strong intramolecular coordination ability of the pyridyl N-atom of the ppy group. The extraordinary intramolecular stabilization effect offered by the N atom of the ppy group prompted us to probe its reactivity towards the main group halides. Accordingly, in the current study, we envisaged to make use of the strong coordinating ability of the ppy group to isolate novel main group compounds and explored the transmetallation reaction of ppyHgCl with group 14 and15 halides.

The heavier group 16 monoorgano trihalides of the ppy group, namely $ppyTeCl_3$ and $ppyTeBr_3$ were reported by Mcwhinnie and co-workers by the transmetallation of ppyHgCl with $TeCl_4$ and $TeBr_4$ respectively.[4b,4d] While the report on the molecular structure of $ppyTeBr_3$ dates back to 1988, the structural characterization of $ppyTeCl_3$ remained obscure, until recently, we have reported two polymorphs of $ppyTeCl_3$ [monomeric (monoclinic)/dimeric (orthorhombic)] obtained by the crystallization from methanol and methanol+ethanol mixture separately.[4b,6] Mcwhinnie and co-workers have reported the synthesis of the corresponding monohalide congeners, *i.e.*, ppyTeCl, and ppyTeBr by the reduction of $ppyTeCl_3$ and $ppyTeBr_3$ with $H_2NNH_2.H_2O$.[4b] Although the molecular structures of both ppyTeCl and ppyTeBr were reported earlier, however, they are associated with considerable degree of disorders.[8] Furthermore, the solution state characterizations of both these species are not known in the literature to our knowledge. As such, this article features a comparatively straight forward synthetic approach for ppyTeCl and ppyTeBr and their detailed solution state characterizations. In addition, we have also included the molecular structures of two new polymorphs of ppyTeCl and ppyTeBr with better quality for comparison with that of the reported structures and other main group congeners.

8.2 Results and Discussion

The starting material ppyHgCl, **8.8** was synthesized by the treatment of 2-phenyl pyridine with $Hg(OAc)_2$ (Ac=$OCCH_3$) and LiCl, as reported in the literature.[4b] When **8.8** was treated with ECl_n (E=Sn, n=4; E=Sb, n=3), it underwent transmetallation to afford novel monoorgano main group halides, namely $ppySnCl_3$, **8.9** and $ppySbCl_2$, **8.10** respectively (Scheme 8.1). The reaction of **8.8** with $InCl_3$ was unsuccessful under the identical condition and no transmetallated product was obtained. Interestingly, when **8.8** was treated with $BiCl_3$, the reaction took a different course

and afforded **8.11**, a bismuthenium ion [(ppy)$_2$Bi]$^+$ stabilized by monoorgano bismuth trichloride anion [ppyBiCl$_3$]$^-$. Notably, this is the third example bismuthenium ion, a class of Bi analogue of a non-NHC derivative. Starting from 2-(2-bromophenyl)pyridine (ppyBr), using ^{n}BuLi followed by the addition of BiCl$_3$, we have recently succeeded in isolating the second example of bismuthenium cation, [(ppy)$_2$Bi]$^+$.Cl$^-$ stabilized by the same aryl group (ppy).[7] The formation of [(ppy)$_2$Bi]$^+$ in both these cases might proceed through the intermediacy of ppyBiCl$_2$, which then underwent significant elongation of Bi-Cl bond due to the strong N→Bi interaction to afford the auto-ionized product. The corresponding first example of bismuthenium ion, namely [(2,6-Mes$_2$C$_6$H$_3$)$_2$Bi]$^+$.[BAr$_4$]$^-$ [where Mes = 2,4,6-Me$_3$C$_6$H$_2$, Ar = 3,5-(CF$_3$)$_2$C$_6$H$_3$] was reported by Beckmann and co-workers using sterically bulky *meta*-terphenyl substituents.[9]
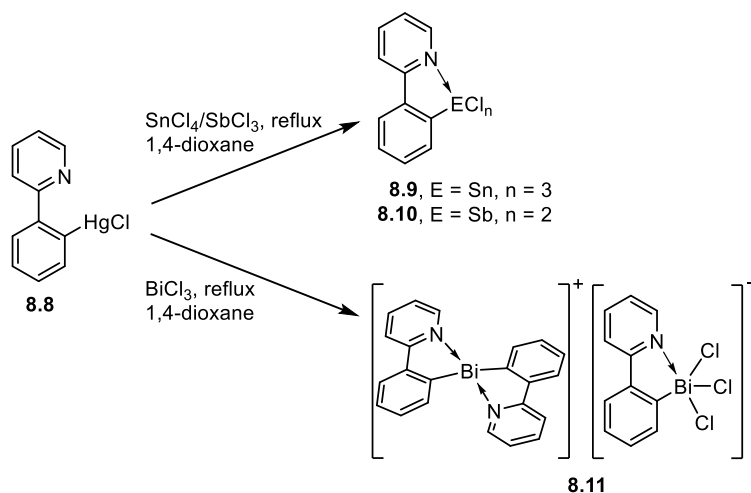

Scheme 8.1. Transmetallation of **8.8** with SnCl$_4$, SbCl$_3$, and BiCl$_3$.

Synthesized compounds **8.9-8.11** are characterized by multinuclear NMR spectroscopy, FTIR spectroscopy, HRMS, and CHN analysis. The ^{1}H and ^{13}C NMR spectra of **8.9-8.11** are consistent with the proposed structures, each showing characteristic signals with consistent integration values for 2-(2′-pyridyl)phenyl moiety. It should be mentioned that the ^{1}H and ^{13}C NMR spectra of **2** which showed resonances at 3.57 and 66.97 ppm respectively, corresponding to dioxane molecule, but this was lost on drying for the microanalysis determination. The ^{119}Sn{^{1}H} NMR spectrum of **8.9** shows a single resonance at δ -440.3 ppm. This value is in good agreement with the value expected for a six-coordinate Sn^{IV} complex.[10]

When ppy$_2$Te$^{[4b]}$ was treated with SO$_2$Cl$_2$ at 0°C, the reaction afforded in the formation of ppyTeCl, **8.12** (Scheme 8.2). It is worth mentioning that the formation of aryltellurium halide, RTeCl (R = alkyl/aryl) from the chlorination of diorganotelluride, R$_2$Te is prevalent in literature

and is believed to take place via the reductive elimination of the *in situ* generated diorganodichloride, R_2TeCl_2.[5g, 11] In a recent study, we have also made a similar observation, wherein the DFT calculation revealed that RTeCl [R = 2,6-$(Me_2NCH_2)_2C_6H_3$] is considerably stable than the corresponding R_2TeCl_2.[11b] The destabilization of R_2TeCl_2 in comparison to RTeCl might be attributed to the formation of Te(IV) species with increased Lewis acidity at the Te(IV) center. In another instance, when $(ppyTe)_2$[12] was treated with Br_2 at 0°C, it resulted in the formation of ppyTeBr, **8.13**. Synthetically, both these reactions are advantageous, as the reported synthesis for **8.12** and **8.13** involve multistep processes, and yields of the reactions were poor than the current procedures.
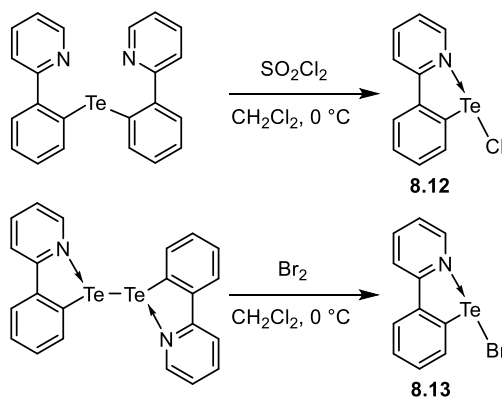
Scheme 8.2. Synthesis of **8.12** and **8.13**.

Similar to **8.9-8.11**, the ^{1}H and ^{13}C NMR spectra of **8.12** and **8.13** exhibit resonances in the aromatic regions with consistent integration values corresponding to the ppy moiety. In the ^{125}Te NMR spectra, compounds **8.12** and **8.13** show single resonance at δ=1318.5 and δ=1274.3 ppm, respectively. Both these chemical shift values are in agreement with the similar reported monohalide with sp^2 N coordinating group, namely 2-(^{t}BuNCH)C_6H_4TeCl (δ=1258.6 ppm), [$C_6H_4(C_5H_8NO)TeCl$] (δ=1202.8 ppm) and [$C_6H_4(C_4H_6NO)TeCl$] (δ=1226 ppm).[13-15]

The identity of the compounds **8.9-8.13** could be further established by Electrospray Ionization Mass Spectrometry. In the mass spectra, taken in the positive ion mode, the molecular/prominent ion peaks at *m*/z 421.90 (Calc. 421.89 [(M-Cl-OH_2)+DMSO]$^+$) (**8.9**), 309.94 (Calc. 309.93 [M-Cl]$^+$) (**8.10**), 517.09 {517.11 Calc. [M-$(ppyBiCl_3)$)]$^+$)} (**8.11**), 283.98 (Calc. 283.97 [M-Cl]$^+$) (**8.12**), 283.98 (Calc. 283.97 [M-Br]$^+$) (**8.13**) substantiated the formation of the respective compounds. It is worth mentioning that the observed patterns in the mass spectra for the compounds were in agreement with the simulated isotopic patterns.

8.3 X-ray crystallographic studies

The identity of the synthesized compounds is unequivocally validated by single-crystal X-ray diffraction study. A comparison of the related bond lengths (Å) and bond angles (°) in **8.9-8.13** are given in Table 8.1, while the crystallographic data and structure refinement parameters are given in Table 8.3. The molecular structure of **8.9** {crystallized as [**8.9**.2(0.5diox)] (diox=1,4-dioxane)} reveals that the geometry around the Sn^{IV} center is distorted octahedral, and its coordination environment is completed by a $CNCl_3O$ donor set [Figure 8.1a]. Of particular interest in the molecular structure of **8.9** is the N→Sn distance of 2.274(2) Å, which is in good agreement with the values observed in related monoorgano tin(IV) trichloride, with sp^2 N-donor arms, such as $Sn[2-C_6H_4C(Ph)=NMe]Cl_3$ [2.284(4) Å][1a] and $Sn(2-C_6H_4N=NPh)Cl_3$ [2.451(3) Å][1f]. Again, the N→Sn bond distance in **8.9** is significantly shorter than that with sp^3 N-donor arms, such as $Sn[2-(Me_2NCH_2)C_6H_4]Cl_3$ [2.380(2) Å, 2.391(3) Å][1c-d], $Sn[2-(Me_2NCH_2)C_6H_4]Cl_3 \cdot DMSO$ [2.393(2) Å][1c]. Sn-Cl1 [2.4243(7) Å] and Sn-Cl3 [2.4217(7) Å], *trans* to N and C respectively are essentially the same indicating a similar *trans* influence for neutral N and anionic C emphasizing the important role of N. The *trans* elongation in **2** is more pronounced in comparison to the similar reported monoorganotin(IV) trichlorides.[1a, c-d, f]. Both the H-atoms of the water molecule are involved in hydrogen bonding with the two dioxane molecules with O2···H and O3···H distances of 1.90(3) Å and 1.97(4) Å respectively. There is no intermolecular contact of significance in the packing diagram of **2**, as two adjacent molecules are oriented in a head-to-tail manner, thereby minimizing the probability for dimerization/aggregation.
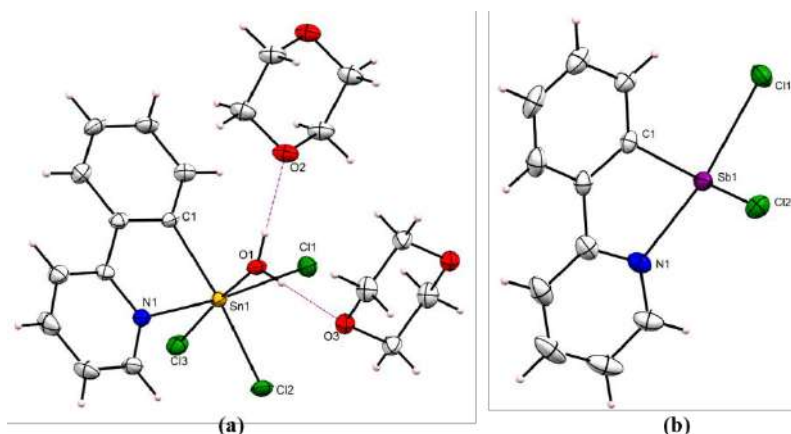
Figure 8.1. Molecular structures of (a) **8.9** and (b) **8.10** plotted with 50% probability displacement ellipsoids.

In the molecular structure of **8.10**, the spatial arrangement of each Sb atom is distorted trigonal bipyramidal taking the lone pair of Sb in to account [Figure 8.1b]. Similar to complex **8.9**, the pyridyl N-atom in compound **8.10** makes strong interaction with N→Sb bond distance of 2.310(4) Å, which is significantly shorter than intramolecularly coordinated similar monoorgano antimony(II) dichloride with sp^2 N-donor arms, such as Sb[o-C_6H_4(CH=NNC_6H_3^{i}Pr-2,6]Cl_2 [2.416(2) Å],[2c] Sb[C_6H_3-2,6-(CH=N-tBu)$_2$]Cl_2 [2.415(2) Å],[2d] Sb[C_6H_3-2,6-(CH=N-2′,6′-$Me_2C_6H_3$)$_2$]Cl_2 [2.401(2) Å][2d] and with sp^3 N-donor arms Sb[8-(Me_2N)$C_{10}H_6$]Cl_2 [2.460(4) Å][2a] and Sb[2-(Me_2NCH$_2$)C_6H_4]Cl_2 [2.407(5) Å],[2b]. The Sb1-Cl1 bond distance [2.634(1) Å] is significantly longer than the Sb1-Cl2 bond distance [2.427(1) Å], which is attributed to the *trans* influence of the pyridyl N atom.

The molecular structure of **8.11** consists of a bismuthenium ion, [(ppy)$_2$Bi(III)]$^+$ as the cationic entity and a monoorgano bismuth(III) trichloride, [ppyBiCl_3]$^-$ as the anionic entity [Figure 8.2]. In the cationic entity of **8.11**, the geometry around the Bi^{III} center is distorted square pyramidal taking the lone pair of Bi into account. The N→Bi distances are 2.416(14) and 2.413(15) Å, which are in good agreement with that observed in [(ppy)$_2$Bi]$^+$·Cl$^-$ [2.467(5) Å].[7] The anionic entity in **8.11**, *i.e.*, [ppyBiCl_3]$^-$, represents a rare example of monoorganobismuth(III) trichloride anion. The geometry around the Bi^{III} center is distorted square pyramidal, where C33 atom occupies the apical position and the pyridyl N-atom and the three Cl-atoms occupy the basal positions The N3→Bi2 distance of 2.45(1) Å is well within the sum of the van der Waals radii of the two elements [Σr_{vdw}

(N, Bi) = 4.24 Å].[16] This distance is considerably shorter in comparison to related monoorgano bismuth(II) chloride with N containing pendant arm(s), such as, Bi[C$_6$H$_3$-2,6-(CH=N-^{t}Bu)$_2$]Cl$_2$ [2.470(7) Å, 2.499(6) Å],[2d] Bi[C$_6$H$_3$-2,6-(CH=N-2′,6′-Me$_2$C$_6$H$_3$)$_2$]Cl$_2$ [2.500(4) Å, 2.522(4) Å],[2d] Bi[2,6-(Me$_2$NCH$_2$)$_2$C$_6$H$_3$]Cl$_2$ [2.561(3) Å, 2.570(4) Å],[3a] Bi[2,6-{MeN(CH$_2$CH$_2$)$_2$NCH$_2$}$_2$C$_6$H$_3$]Cl$_2$ [2.583(5) Å][3b].
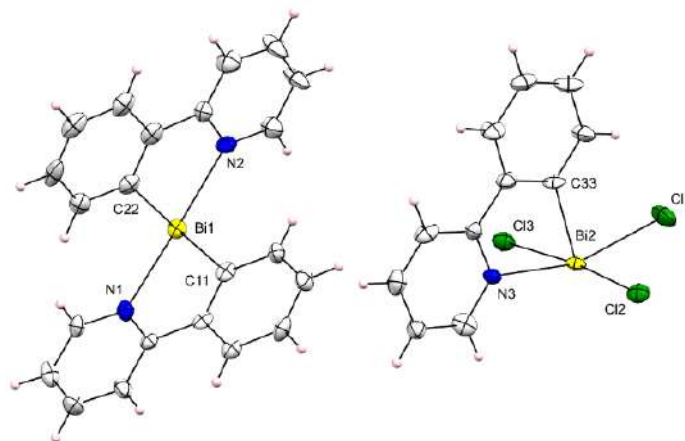
Figure 8.2. Molecular structures of **8.11** plotted with 50% probability displacement ellipsoids.

During the crystallization of **8.12** and **8.13**, we succeeded in isolating two new polymorphs with better quality in comparison to the literature reported structure [Figure 8.3a-8.3b)]. In the reported structures for both **8.12** and **8.13**, a single unit cell consists of six independent molecules with significant disorders. Consequently, the bond lengths and the associated bond angles vary over a wide range.[8] Nevertheless, all the bond parameters for the polymorphs of **8.12** and **8.13** in the present work are in good agreement with their corresponding reported structures. In particular, the N→Te distance [2.228(2) Å] of **8.12** in the present study is considerably longer in comparison to the average N→Te bond distance observed in the earlier reported polymorph [2.205(11) Å] [Figure 8.3a].[8a] However, the N→Te distance in **8.12** is significantly shorter in comparison to that of the corresponding tellurium(IV) trichloride, *i.e*., ppyTeCl$_3$ [2.277(3)/2.286(6) Å]. The molecular structure of **8.13** is isostructural to that of **8.12**, with the chloride ligand in the latter is being changed with the bromide ligand [Figure 8.3b]. The corresponding N→Te bond distance [2.235(11) Å] of **8.13** in the present study is close to that of the average value observed for the reported polymorphs [2.236(11) Å].[8b]
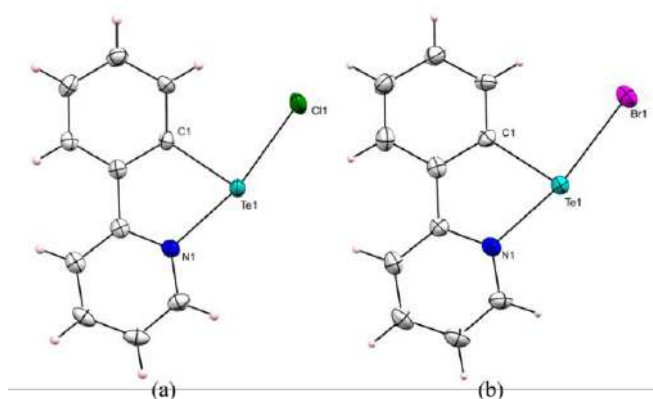
Figure 8.3. Molecular structures of (a) **8.12** and (b) **8.13** plotted with 50% probability displacement ellipsoids.

Table 8.1. A comparison of the relevant bond parameters of the monoorgano element halides.

Bond length (Å)/angle (°)	ppySnCl₃[a]	ppySbCl₂[a]	[ppyBiCl₃]⁻[a]	ppyTeCl[a]	ppyTeCl[b]	ppyTeBr[a]	ppyTeBr[b]
C- E	2.147(2)	2.156(4)	2.26(2)	2.104(2)	2.606(11)$_{avg}$	2.109(5)	2.111(6)$_{avg}$
N→E	2.274(2)	2.310(4)	2.45(1)	2.228(2)	2.205(11)$_{avg}$	2.235(3)	2.236(11)$_{avg}$
E-X1	2.4243(7)	2.634(1)	2.715(5)	2.5748(6)	2.077(7)$_{avg}$	2.7221(5)	2.707(11)$_{avg}$
E-X2	2.3767(7)	2.427(1)	2.696(4)	–	–	–	–
E-X3	2.4217(7)	–	2.744(4)	–	–	–	–
N-E-C	77.44(8)	75.1(1)	71.5(6)	76.30(7)	75.7(5)$_{avg}$	76.6(1)	75.9(5)$_{avg}$
N-E-X$_{trans}$	169.17(6)	165.76(9)	162.0(4)	167.69(4)	168.2(5)$_{avg}$	168.40(9)	169.2(2)$_{avg}$
C-E-X$_{trans}$	165.64(6)	–	–	–	–	–	–
N-E-X$_{cis}$	94.87(6)	86.71(9)	90.0(4) 84.3(4)	–	–	–	–
C-E-X$_{cis}$	98.59(6) 96.69(6)	91.0(1) 91.5(1)	90.5(5) 91.7(5) 89.7(5)	91.44(6)	92.9(4)$_{avg}$	91.9(1)	93.6(5)$_{avg}$
Cl-E-Cl$_{trans}$	–	–	173.4(1)	–	–	–	–

[a]Entries in these columns refer to the crystal structures determined in the present work.

[b]Entries in these columns refer to the crystal structures from the literature (polymorphs).[9]

E = Sn (**8.9**), Sb (**8.10**), Bi (**8.11**), Te (**8.12**, **8.13**); X = Cl (**8.9-8.12**), Br (**8.13**)

8.4 Computation Studies

To understand the nature of bonding in the synthesized compounds **8.9-8.13**, in particular, to probe the role of N→E bond on the stabilization of the compounds, detailed DFT calculations were carried out by using Gaussian 0.9 (Rev A.02) program[17] (functional: B3PW91;[18] mixed basis sets: Sn/Sb/Te: ECP28MDF_VTZ[19a-b], (Pseudopotential ECP28MDF)[19b-c]; Bi: ECP60MDF_VTZ[19a] (Pseudopotential ECP60MDF)[19c]; C/H/N/O/Br/Cl: 6-31G**[19d]). Starting from single-crystal coordinates, compounds **8.9-8.13** were optimized and subsequently subjected to NBO analysis.[20] Examination of the NBO plots reveals that while in all the compounds **8.9-8.13,** the pyridyl nitrogen atom uses its lone pair (*lp*) as donor orbitals, significant disparities were observed among the acceptor orbitals across the series of the compounds [**8.9-8.13**] [Figure 8.4]. In particular, in compound **8.9**, the N→Sn interaction is attributed to two prominent donor-acceptor interactions, namely *lp*(N)→σ*(Sn-C15) [Figure 8.4a] and N(*lp*)→σ*(Sn-Cl2) [Figure 8.4b]. The second-order stabilization energies of 20.83 kcal/mol and 20.87 kcal/mol respectively for both these interactions indicate the significant contribution of N→Sn bond in the overall stability of the molecule. In compound **8.10**, the NBO analysis treats the N→Sb interaction as an *lp*(N)→*p**(Sb) donor-acceptor interaction [Figure 8.4c] with stabilization energy of 44.43 kcal/mol. A similar interaction *i.e.*, *lp*(N)→*p**(Bi) was observed in the anionic entity of **8.11** *i.e.*, [ppyBiCl₃]⁻ with stabilization energy of 41.29 kcal/mol [Figure 8.4d]. It is worth mentioning that the N→Bi interaction in the cationic entity of **8.11**, *i.e.*, [(ppy)₂Bi]⁺ also displays similar *lp*(N)→*p**(Bi) interaction, which is in good agreement with that of the [(ppy)₂Bi]⁺.Cl⁻ reported earlier.[7] Interestingly, in case of tellurium halides, *i.e.*, in **8.12** and **8.13**, the NBO analysis indicates each N→Te interaction as *lp*(N)→σ*(Te-X) donor-acceptor interaction with stabilization energy of 47.06 kcal/mol (for **8.12**) [Figure 8.4e] and 47.72 kcal/mol (for **8.13**) [Figure 8.4f], respectively.
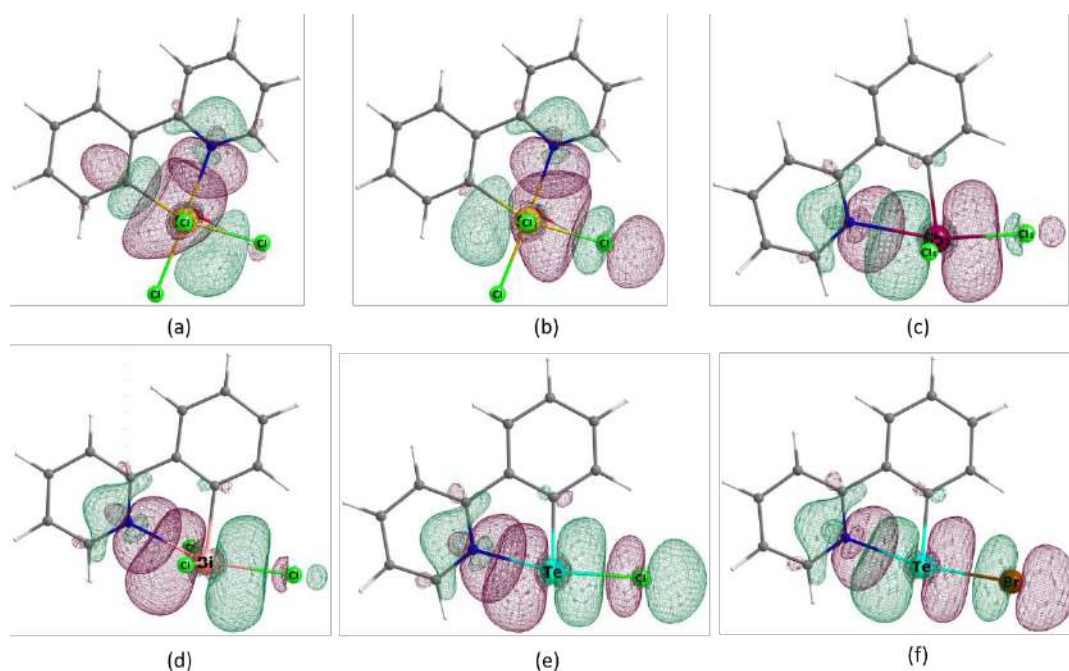
Figure 8.4. The prominent Natural Bond Orbital (NBO) plots of (a-b) **8.9**, (c) **8.10**, (d) **8.11**, (e) **8.12** and (f) **8.13** showing strong N→E (E=Sn, Sb, Bi and Te) interactions.

The presence of N→E interactions in **8.9-8.13** was further validated by electron localization function (ELF) calculation, which is commonly used to map the electron-pair localization in a molecule.[21] A continuum of elevated ELF values along the N→E vectors throughout the series of **8.9-8.13** clearly indicates the strong N→E interactions involved in the respective molecule [Figure 8.5a-8.5e].
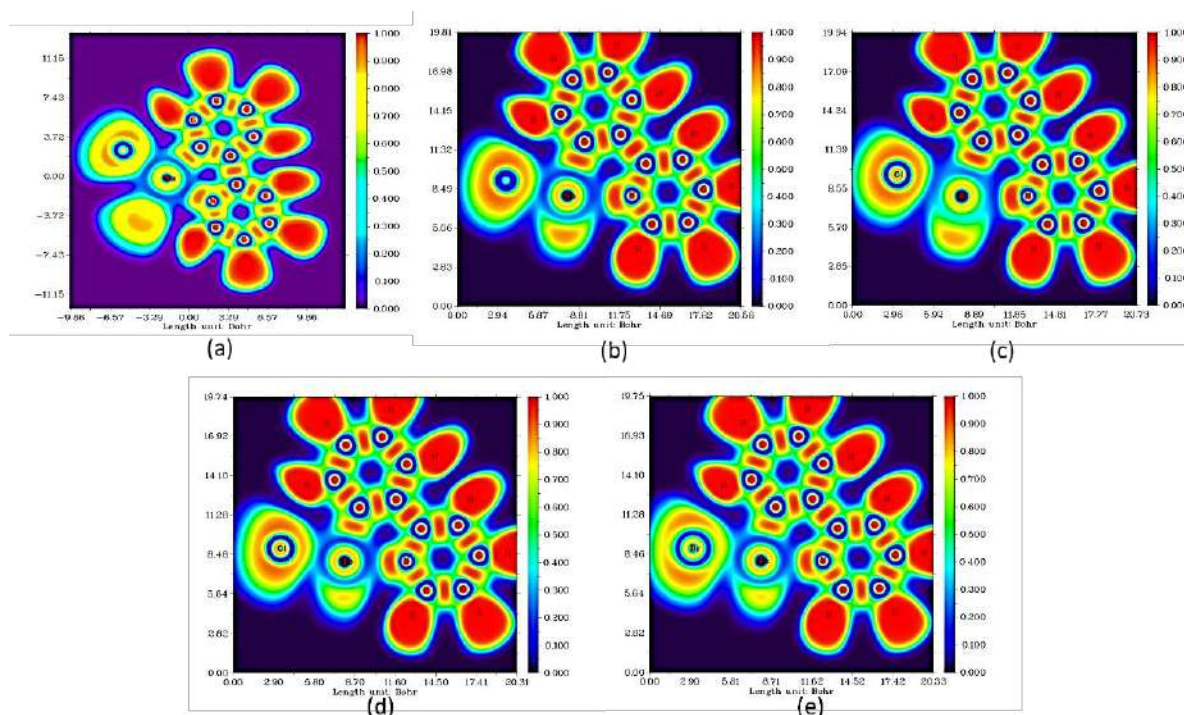
Figure 8.5. Electron localization function (ELF) for (a) **8.9**, (b) **8.10**, (c) **8.11**, (d) **8.12** and (e) **8.13** drawing in the plane containing N, C and E (E=Sn, Sb, Bi and Te) atoms.

To probe the effect of N→E interactions on the stabilization of the synthesized compounds **8.9-8.13**, electrostatic surface potential (ESP) was calculated, which provides insight into the local electron density distribution over the entire molecular surface as a function of electrostatic potential.[22] For comparative purposes, analogous calculations were carried out for the model compounds (denoted by ''' with the parent compounds, *i.e.*, **8.9′-8.13′**) wherein the pyridyl rings were twisted away from the element center in such a way that no N→E was observed. The ESPs of the model compounds, lacking the intramolecular N→E interactions, showed relatively positive ESPs, *i.e.*, regions of depleted electron density (indicated by relative blue coloration), known as σ-hole region around the E center [Figure 8.6a′ (for **8.9′**), 8.6b′ (for **8.10′**), 8.6c′ (for **8.11′**), 8.6d′ (for **8.12′**) and 8.6e′ (**8.13′**)]. The significant diminution of the σ-hole region in the original compounds [Figure 8.6a (for **8.9**), 8.6b (for **8.10**), 8.6c (for **8.11**), 8.6d (for **8.12**) and 8.6e (**13**)] after N→E interactions unambiguously established the direct involvement of the σ-hole bonding to stabilize the N→E donor-acceptor interactions.
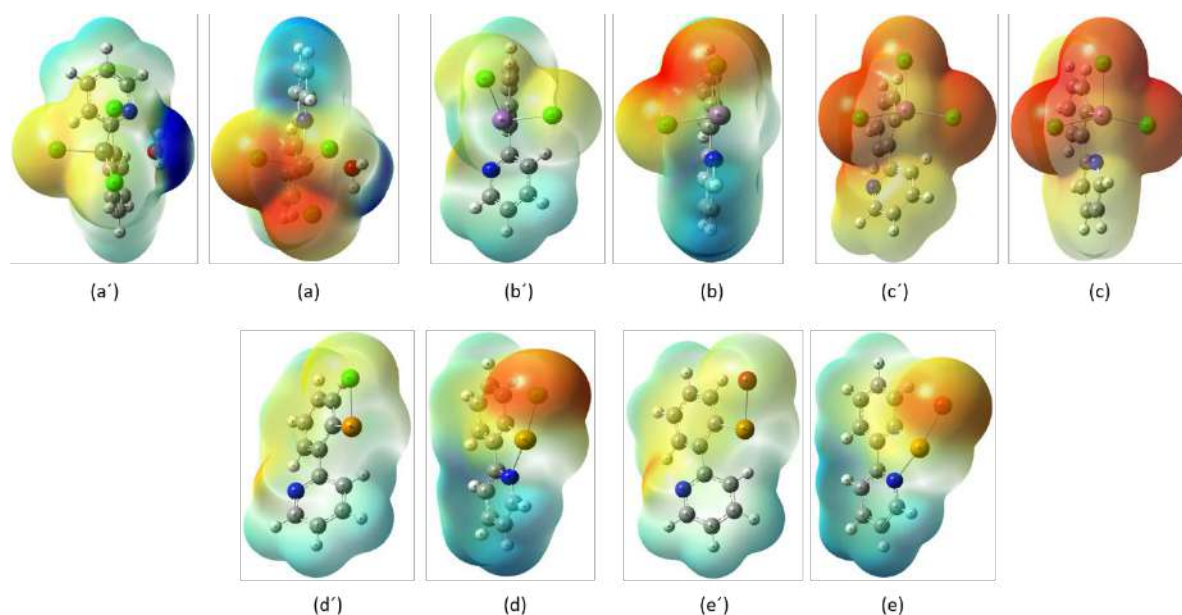
Figure 8.6. Relative Electrostatic Surface Potentials (ESPs) mapped on the 0.001 a.u. electron density surface of the model compounds [a´ (for **8.9´**), b´ (for **8.10´**), c´ (for **8.11´**), d´ (for **8.12´**) and e´ (**8.13´**) lacking the intramolecular coordination from the N-donor group and origin compounds [a (for **8.9**), b (for **8.10**), c (for **8.11**), d (for **8.12**) and e (for **8.13**) with N→E interactions. Blue colour indicates the positive region with less electron density, while the red colour indicates the negative region with high electron density.

To throw light on the nature of N→E interactions in **8.9-8.13**, Atoms in Molecules (AIM) calculations have been carried out.[23] The N→E bond critical points (bcp) for the synthesized monoorgano element halides are mentioned in Table 8.2, and the corresponding electron density plots are shown in Figure 8.7. A close inspection of the topological parameters of the N→E bcps of the synthesized compounds indicates that all these compounds show small electron densities [$\rho(r)$] lying in the range of 0.0446-0.0652 e Å^{-3}, and positive Laplacians values, $\nabla^2\rho(r)$ lying in the range 0.104-0.166 e Å^{-3}. The low $\rho(r)$ values and negative values of total energy density (H) over $\rho(r)$ ratios indicate predominantly ionic or almost negligible covalency of the N→E interactions. While the ionic character of N→E bond is more pronounced in the case of [ppyBiCl$_3$]$^-$ in comparison to that of ppySnCl$_3$ and ppySnCl$_3$, the mixing of covalency was more pronounced in cases of ppyTeCl and ppyTeBr. These ionic/covalent nature of the N→E interactions across the series of synthesized compounds were further corroborated by |V(r)/G(r)| values, which is almost

equal to 1 in case of [ppyBiCl$_3$]$^-$, ~1.2 in case of ppySnCl$_3$ and ppySbCl$_2$, ~1.3 in case of ppyTeCl and ppyTeBr.
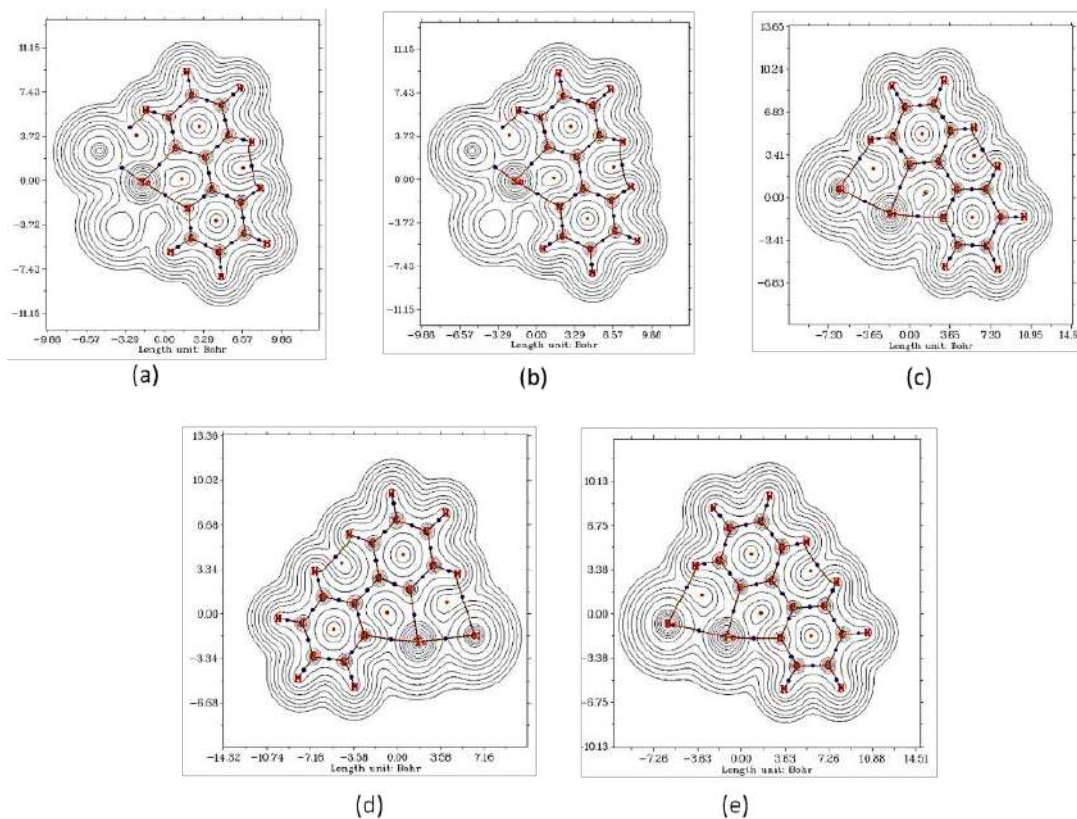

Figure 8.7. Laplacian of electron density [$\nabla^2\rho(r)$] plots for (a) **8.9**, (b) **8.10**, (c) **8.11**, (d) **8.12** and (e) **8.13**.

Table 8.2. N→E Bond critical points for the monoorgano element halides.

	$\rho(r)$	$\nabla^2\rho(r)$	ε	V(r)	G(r)	H(r)	H/$\rho(r)$	|V(r)/G(r)|
ppySnCl$_3$	0.0602	0.166	0.0123	-0.0595	0.0505	-0.009	-0.149	1.178
ppySbCl$_2$	0.0498	0.104	0.0655	-0.0405	0.0333	-0.007	-0.140	1.216
[ppyBiCl$_3$]$^-$	0.0446	0.120	0.0453	-0.0360	0.0330	-0.003	-0.067	1.091
ppyTeCl	0.0663	0.136	0.250	-0.0629	0.0485	-0.014	-0.211	1.297
ppyTeBr	0.0652	0.133	0.243	-0.0607	0.0469	-0.014	-0.214	1.294

8.5 Conclusions

Monoorgano tin trichloride [ppySnCl$_3$, **8.9**] and antimony dichloride [ppySbCl$_2$, **8.10**] have been synthesized by the transmetallation of ppyHgCl with SnCl$_3$ and SbCl$_2$ respectively. The reaction of ppyHgCl with BiCl$_3$ under identical reaction condition results in the formation of diorgano bismuthenium ion stabilized by a monoorgano bismuthenium cation, *i.e.*, {[(ppy)$_2$Bi]$^+$.[ppyBiCl$_3$]$^-$, **8.11**}. The heavier group 16 monohalide, namely ppyTeCl (**8.12**) and ppyTeBr (**8.13**), are synthesized by direct reaction of (ppy)$_2$Te and (ppyTe)$_2$ with SO$_2$Cl$_2$ and Br$_2$ respectively, and their hitherto unknown solution state characterizations are accomplished. The molecular structures of the compounds **8.9-8.13** reveal strong intramolecular interactions between the pyridyl N atoms with the element centers as indicated by the N-E bond distances of 2.274(2) Å [in **8.9**], 2.310(4) Å [in **8.10**], 2.45(1) Å [in **8.11**], 2.228(2) Å [in **8.12**] and 2.235(3) Å [in **8.13**]. The *trans* influences of the N atoms in **8.9-8.10**, **8.12-8.13**, result in the elongation of Te-Cl bonds *trans* to the pyridyl N atoms. The pronounced effects of N→E interactions in the stabilization of **8.9-8.13** are further manifested by DFT calculations, which indicate σ-hole supported N→E donor-acceptor interactions in **8.9-8.13**.

8.6 Experimental Sections:

All reactions were performed with standard Schlenk (nitrogen) techniques. Solvents were dried by following standard methods. The starting materials and solvents were purchased from commercial sources. (ppy)HgCl was synthesized by the reaction of 2-phenylpyridine with Hg(OAC)$_2$ and LiCl.[4] (ppy)$_2$Te was synthesized by the reaction of ppyHgCl with ppyTeCl$_3$ followed by the treatment with an excess of hydrazine hydrate.[4] (ppyTe)$_2$ was synthesized by the treatment of ppyTeBr with an excess of hydrazine hydrate.[10] (**Caution**: organomercury compounds are highly toxic. Adequate precaution should be taken while handling of such compounds). ^{1}H (400 and 500 MHz), ^{13}C (100 and 125 MHz), ^{119}Sn (186 MHz), and ^{125}Te (126 MHz, 158 MHz) NMR spectra were recorded on Bruker AV 400 MHz and Bruker AV 500 MHz spectrometers at 25 °C. Chemical shifts cited were referenced to TMS (^{1}H, ^{13}C) as internal, Me$_2$Te (^{125}Te), and Me$_4$Sn (^{119}Sn) as external standard. Electron spray mass spectra (ESI-MS) were performed on a Q-Tof micro (YA-105) mass spectrometer. Elemental analyses were performed on a Carlo Erba Model 1106 elemental analyzer. Infrared spectra were recorded on a Perkin Elmer spectrometer.

General procedure for synthesis of 8.9-8.11

To a 1,4-dioxane (25 mL) solution of ppyHgCl (0.200 g, 0.513 mmol), element halide (0.134 g, 0.514 mmol of $SnCl_4$ for **8.9**; 0.117 g, 0.513 mmol of $SbCl_3$ for **8.10**; 0.162 g, 0.514 mmol of $BiCl_3$ for **8.11**) was added. The reaction mixture was refluxed for 18h. After cooling at room temperature, the reaction resulted in the precipitaion of white solid. The white solid thus obtained was filterred off, washed with hexane (3 × 15 mL), Et_2O (3 × 15 mL) to afford the analytically pure colourless, crystalline solids of **8.9-8.11**.

8.9.2(0.5diox)**: Yield** 0.158 g (77%); **^{1}H NMR** (400 MHz, DMSO-d_6) δ 9.15 (s, 1H), 8.62 (d, J = 8.1 Hz, 1H), 8.38 (d, J = 7.7 Hz, 1H), 8.33 (t, J = 7.8 Hz, 1H), 7.89 (d, J = 6.7 Hz, 1H), 7.83 – 7.79 (m, 1H), 7.64 (t, J = 7.1 Hz, 1H), 7.58 (t, J = 7.5 Hz, 1H), 3.57 (s, 8H, diox). No signal in ^{1}H from H_2O is detected; **^{13}C NMR** (100 MHz, DMSO-d_6) δ 156.69, 150.44, 148.64, 142.06, 139.14, 138.57, 130.02, 128.88, 127.90, 124.18, 121.75, 66.97 (diox); **FT-IR** (neat, cm^{-1}) 3098(m), 2966(w), 2918(vw), 2898(vw), 2861(m), 1945(vw), 1605(m), 1574(m), 1564(m), 1474(m), 1452(m), 1435(m), 1369(w), 1290(s), 1281(s), 1256(s), 1151(w), 1110(s), 1080(m), 892(s), 870(s), 856(s), 761(s), 737(s), 646(w), 629(w), 617(m); **^{119}Sn{^{1}H} NMR** (186 MHz, DMSO-d_6) δ -440.30; **ESI-MS** (positive mode) m/z = 421.90 (observed) {Calc. 421.89 for [(M-Cl-OH$_2$)+DMSO]$^+$ ($C_{13}H_{14}Cl_2NOSSn$)}; Anal. Calc. for $C_{11}H_{10}Cl_3NOSn$: C, 33.26; H, 2.54; N, 3.53; Found C, 33.08; H, 2.27; N, 3.79 (compound lost the two dioxane molecules of solvation upon drying under vacuum)

8.10: **Yield** 0.154 g (87%); **^{1}H NMR** (400 MHz, DMSO-d_6) δ 8.93 (d, J = 4.8 Hz, 1H), 8.63 (d, J = 7.3 Hz, 1H), 8.49 (d, J = 8.2 Hz, 1H), 8.35 (d, J = 7.0 Hz, 1H), 8.27 (td, J = 8.0, 1.5 Hz, 1H), 7.71 – 7.65 (m, 2H), 7.61 (td, J = 7.5, 1.4 Hz, 1H); **^{13}C NMR** (100 MHz, DMSO-d_6) δ 157.06, 156.28, 146.06, 142.42, 139.11, 134.02, 131.63, 130.26, 126.52, 125.24, 121.27; **FT-IR** (neat, cm^{-1}) 3077(w), 3057 (m), 3027(m), 2003(vw), 1971(vw), 1939(vw), 1862(vw), 1832(vw), 1600(s), 1569(vw), 1556(vw), 1483(s), 1439(s), 1427(s), 1302(m), 1283(m), 1266(w), 1168(w), 1159(w), 1108(vw), 1051(w), 1019(m), 1009(m), 895(vw), 798(w), 763(s), 739(s), 661(vw), 639(m); **ESI-MS** (positive mode) m/z = 309.94 {Calc. 309.93 for [M-Cl]$^+$ ($C_{11}H_8ClNSb$)}; Anal. Calc. for $C_{11}H_8Cl_2NSb$: C, 38.09; H, 2.32; N, 4.04; Found C, 37.87; H, 2.07; N, 4.15.

8.11: Yield 0.371 g (73%); **^{1}H NMR** (400 MHz, DMSO-d_6) δ 8.93 (d, J = 4.7 Hz, 1H), 8.63 (d, J = 7.0 Hz, 1H), 8.57 (dd, J = 4.7, 0.7 Hz, 1H), 8.48 (d, J = 8.2 Hz, 1H), 8.35 (d, J = 7.2 Hz, 1H), 8.27 (td, J = 8.0, 1.5 Hz, 1H), 8.12 (dd, J = 14.5, 4.9 Hz, 1H), 7.97 (td, J = 7.9, 1.8 Hz, 1H), 7.70 – 7.59 (m, 3H), 7.52 – 7.48 (m, 1H), 7.47 – 7.38 (m, 1H); **^{13}C NMR** (100 MHz, DMSO- d_6) δ 157.04, 156.55, 156.29, 150.32, 148.48, 146.06, 142.40, 141.91, 139.13, 139.02, 138.44, 134.03, 131.63, 130.26, 129.89, 128.75, 127.76, 126.51, 125.23, 124.05, 121.62, 121.26; **FT-IR** (neat, cm^{-1}) 3071(w), 3057(w), 3027(w), 2010(vw), 1974(vw), 1942(vw), 1903(vw), 1864(vw), 1828(vw), 1598(m), 1569(m), 1478(m), 1435(m), 1422(m), 1296(m), 1280(m), 1263(w), 1246(w), 1173(w), 1163(w), 1107(w), 1051(vw), 1025(w), 1015(w), 1007(w), 892(vw), 875(vw), 802(w), 760(s), 734(s), 656(vw), 638(w), 626(vw), 549(vw); **ESI-MS** (positive mode) m/z = 517.09 {Calc. 517.11 for [M-(ppyBiCl$_3$)]$^+$ (C$_{22}$H$_{16}$BiN$_2$)}; Anal. Calc. for C$_{33}$H$_{24}$Bi$_2$Cl$_3$N$_3$: C, 40.16; H, 2.45; N, 4.26; Found C, 40.28; H, 2.29; N, 4.56.

General procedure for synthesis of 8.12-8.13

To a CH$_2$Cl$_2$ solution of (ppy)$_2$Te[4b] [0.250 g, 0.573 mmol for **8.12**] or (ppyTe)$_2$[10] [0.250 g, 0.444 mmol for **8.13**] was added SO$_2$Cl$_2$ [0.079 g, 47.305 μL, 0.585 mmol for **8.12**] or Br$_2$ [0.070 g, 22.403 μL, 0.444 mmol for **8.13**] at 0 °C for 8h. The reaction resulted in the immediate precipitation of yellow solids. The solid was then filterred off, washed with hexane (3 × 15 mL), to afford the analytically pure colourless, crystalline solids of **8.12-8.13**.

8.12: Yield 0.131 g (72%); **^{1}H NMR** (400 MHz, CDCl$_3$) δ 8.77 (ddd, J = 5.6, 1.4, 1.0 Hz, 1H), 8.59 (dd, J = 8.1, 0.8 Hz, 1H), 8.23 (d, J = 8.4 Hz, 1H), 8.17 (dd, J = 7.9, 1.3 Hz, 1H), 8.03 – 7.98 (m, 1H), 7.58 (ddd, J = 8.2, 7.2, 1.3 Hz, 1H), 7.49 (ddd, J = 8.3, 7.2, 1.2 Hz, 1H), 7.36 (ddd, J = 7.1, 5.7, 1.1 Hz, 1H); **^{13}C NMR** (100 MHz, CDCl$_3$) δ 154.62, 142.31, 138.42, 133.70, 133.30, 131.67, 131.16, 126.83, 126.20, 122.59, 121.22; **^{125}Te NMR** (126 MHz, CDCl$_3$) δ 1318.5; **FT-IR** (neat, cm^{-1}) 3105(vw), 3057(w), 3027(vw), 1972(vw), 1932(vw), 1866(vw), 1839(vw), 1810(vw), 1603(m), 1584(m), 1568(w), 1479(m), 1461(w), 1439(m), 1427(m), 1319(vw), 1302(vw), 1278(w), 1247(vw), 1169(vw), 1161(vw), 1059(vw), 1049(vw), 1019(w), 998(vw), 956(vw), 883(vw), 788(vw), 753(s), 729(s), 643(vw), 558(vw); **ESI-MS** (positive mode) m/z = 283.98 {Calc. 283.97 for [M-Cl]$^+$ (C$_{11}$H$_8$NTe)}; Anal. Calc. for C$_{11}$H$_8$ClNTe: C, 41.65; H, 2.54; N, 4.42; Found C, 41.18; H, 2.47; N, 4.53.

8.13: Yield 0.141 g (88%); **^{1}H NMR** (500 MHz, CDCl$_3$) δ 8.80 – 8.73 (m, 1H), 8.61 (dt, *J* = 10.7, 5.3 Hz, 1H), 8.25 – 8.20 (m, 1H), 8.14 (dd, *J* = 16.1, 11.2 Hz, 1H), 8.05 – 7.98 (m, 1H), 7.56 (ddd, *J* = 17.7, 9.6, 8.2 Hz, 1H), 7.53 – 7.47 (m, 1H), 7.38 (ddd, *J* = 15.2, 7.8, 2.8 Hz, 1H); **^{13}C NMR** (125 MHz, CDCl$_3$) δ 154.04, 142.34, 138.50, 134.97, 133.79, 131.26, 128.48, 127.08, 126.13, 122.78, 121.14; **^{125}Te NMR** (126 MHz, CDCl$_3$) δ 1274.3; **FT-IR** (neat, cm^{-1}) 3098(vw), 3054(w), 3027(vw), 1603(m), 1584(m), 1568(w), 1547(vw), 1478(m), 1461(w), 1437(m), 1420(m), 1303(w), 1278(m), 1244(vw), 1159(w), 1100(vw), 1058(vw), 1017(w), 954(vw), 866(vw), 744(s), 724(m), 660(vw), 639(w), 549(vw); **ESI-MS** (positive mode) m/z = 283.98 {Calc. 283.97 [M-Br]$^+$ (C$_{11}$H$_8$NTe)}; Anal. Calc. for C$_{11}$H$_8$BrNTe: C, 36.53; H, 2.23; N, 3.87; Found C, 36.39; H, 2.31; N, 3.91.

X-ray Crystallography Data

The diffraction measurements for compounds **8.9-8.13** were performed on a Rigaku Saturn 724 diffractometer using graphite monochromated Mo Kα radiation (λ = 0.7107 Å). The data collection was carried out by standard ω-scan technique and were evaluated and reduced by using *CrystalClear-SM* Expert software. The structures were refined by full-matrix least-square with the anisotropic non-hydrogen atoms and hydrogen atoms with fixed isotropic thermal parameter of 0.07 Å^2 using the SHELXL program.[24]

Computational Methodology

DFT calculations were carried out using Gaussian 0.9 (Rev A.02) program[17] (functional: B3PW91;[18] mixed basis sets: Sn/Sb/Te: ECP28MDF_VTZ[19a-b], (Pseudopotential ECP28MDF)[19b-c]; Bi: ECP60MDF_VTZ[19a] (Pseudopotential ECP60MDF)[19c]; C/H/N/O/Br/Cl: 6-31G**[19d]). Frequency calculations were calculated, and all the structures were detected with minima such that no negative frequencies were observed. The topological analyses were carried out using Multiwfn software.[25]

8.7 References

[1] a) W. Clegg, C. M. J. Grievson, K. Wade, *J. Chem. Soc., Chem. Commun.* **1987**, 969-970; b) S. H. L. Thoonen, B.-J. Deelman, G. van Koten, *J. Organomet. Chem.* **2004**, *689*, 2145-2157; c) R. A. Varga, C. Silvestru, C. Deleanu, *Appl. Organometal. Chem.* **2005**, *19*, 153-160; d) P. Novák, Z. Padělková, I. Císařová, L. Kolářová, A. Růžiĉa, J. Holeĉek, *Appl. Organometal. Chem.* **2006**, *20*, 226-232; e) I. Barbul, R. A. Varga, K. C. Molloy, C. Silvestru, *Dalton Trans.* **2013**, *42*, 15427-15437; f) V. Chandrasekhar, R. K. Metre, S. Biswas, *Organometallics* **2013**, *32*, 3419-3422; g) C. Zeppek, J. Pichler, A. Torvisco, M. Flock, F. Uhlig, *J. Organomet. Chem.* **2013**, *740*, 41-49; h) A. Khan, D. Foucher, *Coord. Chem. Rev.* **2016**, *312*, 41-66; i) S. Thoonen, B.-J. Deelman, G. van Koten, *Chem. Commun.* **2018**, *54*, 739-742; j) N. Rabiee, M. Safarkhani, M. M. Amini, *Rev. Inorg. Chem.* **2019**, *39*, 13-45; k) M. Olaru, S. Krupke, E. Lork, S. Mebs, J. Beckmann, *Dalton Trans.* **2019**, *48*, 5585-5594.

[2] a) C. J. Carmalt, A. H. Cowley, R. D. Culp, R. A. Jones, S. Kamepalli, N. C. Norman, *Inorg. Chem.* **1997**, *36,* 2770-2776; b) L. M. Opris, A. Silvestru, C. Silvestru, H. J. Breunig, E. Lork, *Dalton Trans.* **2003**, 4367-4374; c) L. Dostál, R. Jambor, A. Růžiĉa, P. Šimon, *Eur. J. Inorg. Chem.* **2011**, 2380-2386; d) I. Vránová, R. Jambor, A. Růžiĉa, R. Jirásko, L. Dostál, *Organometallics* **2015**, *34*, 534-541.

[3] a) A. P. Soran, C. Silvestru, H. J. Breunig, G. Balázs, J. C. Green, *Organometallics* **2007**, *26*, 1196-1203; b) A. Soran, H. J. Breunig, V. Lippolis, M. Arca, C. Silvestru, *Dalton Trans.* **2009**, 77-84; c) I. Vránová, M. Alonso, R. Lo, R. Sedlák, R. Jambor, A. Růžiĉa, F. D. Proft, P. Hobza, L. Dostál, *Chem. Eur. J.* **2015**, *21*, 16917-16928.

[4] a) M. A. K. Ahmed, N. I. Al-Salim, W. R. McWhinnie, T. A. Hamor, *J. Organomet. Chem.* **1985**, *281*, 205-211; b) A. A. West, W. R. McWhinnie, T. A. Hamor, *J. Chem. Soc., Dalton Trans.* **1988**, 2363-2371; c) Z. Majeed, W. R. McWhinnie, T. A. Hamor, *J. Organomet. Chem.* **1997**, *549*, 257-262; d) T. S. Lobana, W. R. McWhinnie, *Indian. J. Chem. Sect. A* **1992**, *31*, 460-462.

[5] a) N. Sudha, H. B. Singh, *Coord. Chem. Rev.* **1994**, *135-136*, 469-515; b) R. Kaur, S. C. Menon, H. B. Singh, *Proc. Indian Acad. Sci. (Chem. Sci.)* **1996**, *108*, 159-164; c) G. Mugesh, H. B. Singh, R. J. Butcher, *J. Organomet. Chem.* **1999**, *577*, 243-248; d) G. Mugesh, H. B. Singh, *Acc. Chem. Res.* **2002**, *35*, 226-236; e) S. D. Apte, S. S. Zade, H.

B. Singh, R. J. Butcher, *Organometallics* **2003**, *22*, 5473-5477; f) K. Srivastava, S. Sharma, H. B. Singh, U. P. Singh, R. J. Butcher, *Chem. Commun.* **2010**, *46*, 1130-1132; g) K. Srivastava, P. Shah, H. B. Singh, R. J. Butcher, *Organometallics* **2011**, *30*, 534-546; h) P. Rakesh, H. B. Singh, R. J. Butcher, *Dalton Trans.* **2012**, *41*, 10707-10714; i) K. Srivastava, A. Panda, S. Sharma, H. B. Singh, *J. Organomet. Chem.* **2018**, *861*, 174-206; j) A. Gupta, R. Deka, K. Srivastava, H. B. Singh, R. J. Butcher, *Polyhedron* **2019**, 172, 95-103; k) A. Gupta, R. Deka, A. Sarkar, H. B. Singh, R. J. Butcher, *Dalton Trans.* **2019**, 48, 10979-10985.

[6] R. Deka, A. Sarkar, R. J. Butcher, P. C. Junk, D. R. Turner, G. B. Deacon, H. B. Singh, *Dalton. Trans.* **2019** (**DOI:**10.1039/C9DT04013G).

[7] R. Deka, A. Sarkar, R. J. Butcher, P. C. Junk, D. R. Turner, G. B. Deacon, H. B. Singh, *Organometallics.* **2020**, *39*, 334-343.

[8] a) T. A. Hamor, H. Chen, W. R. McWhinnie, S. L. W. McWhinnie, Z. Majeed, *J. Organomet. Chem.* **1996**, *523*, 53-61; b) M. R. Greaves, T. A. Hamor, B. J. Howlin, T. S. Lobana, S. A. Mbogo, W. R. McWhinnie, D. C. Povey, *J. Organomet. Chem.* **1991**, *420,* 327-335.

[9] M. Olaru, D. Duvinage, E. Lork, S. Mebs, J. Beckmann, *Angew. Chem. Int. Ed.* **2018**, *57*, 10080-10084.

[10] a) J. Otera, *J. Organomet. Chem.* **1981**, *221*, 57-61; b) J. Holeček, M. Nádvorník, K. Handlíř, A. Lyčka, *J. Organomet. Chem.* **1986**, *315*, 299-308; c) R. Schmiedgen, F. Huber, H. Preut, G, Ruisi, R. Barbierit, *Appl. Organomet. Chem.* **199**4, *8*, 397-407; d) A. Tyagi, G. Kedarnath, A. Wadawale, V. K. Jain, M. Kumar, B. Vishwanadh, *RSC Adv.* **2015**, *5*, 62882-62890.

[11] a) I. D. Sadekov, A. A. Maksiinko, A. G. Maslakov, V. I. Minkin, *J. Organomet. Chem.* 1990, 391, 179-188; b) A. Gupta, R. Deka, H. B. Singh, R. J. Butcher, *New J. Chem.* **2019**, 43, 13225-13233.

[12] T. A. Hamor, N. Al-Salim, A. A. West, W. R. McWhinnie, *J. Organomet. Chem.* **1986**, *310,* C5-C6.

[13] M. Hejda, E. Lork, S. Mebs, L. Dostál, J. Beckmann, *Eur. J. Inorg. Chem.* **2017**, 3435-3445.

[14] S. D. Apte, S. S. Zade, H. B. Singh, R. J. Butcher, *Organometallics* **2003**, *22*, 5473-5477.

[15] S. Kumar, H. B. Singh, G. Wolmershäuser, *J. Organomet. Chem.* **2005**, *690*, 3149-3153.

[16] S. Alvarez, *Dalton Trans.* **2013**, *42*, 8617-8636.

[17] M. J. Frisch, G. W. Trucks, H. B. Schlegel, G. E. Scuseria, M. A. Robb, J. R. Cheeseman, G. Scalmani, V. Barone, B. Mennucci, G. A. Petersson, H. Nakatsuji, M. Caricato, X. Li, H. P. Hratchian, A. F. Izmaylov, J. Bloino, G. Zheng, J. L. Sonnenberg, M. Hada, M. Ehara, K. Toyoto, R. Fukuda, J. Hasegawa, M. Ishida, T. Nakajima, Y. Honda, O. Kitao, H. Nakai, T. Vreven, J. A. Montgomery Jr., J. E. Peralta, F. Ogliaro, M. Bearpark, J. J. Heyd, E. Brothers, K. N. Kudin, V. N. Staroverov, R. Kobayashi, J. Normand, K. Raghavachari, A. Rendell, J. C. Burant, S. S. Iyengar, J. Tomasi, M. Cossi, N. Rega, J. M. Millam, M. Klene, J. E. Knox, J. B. Cross, V. Bakken, C. Adamo, J. Jaramillo, R. Gomperts, R. E. Stratmann, O. Yazyev, A. J. Austin, R. Cammi, C. Pomelli, J. W. Ochterski, R. L. Martin, K. Morokuma, V. G. Zakrzewski, G. A. Voth, P. Salvador, J. J. Dannenberg, S. Dapprich, A. D. Daniels, O. Farkas, J. B. Foresman, J. V. Ortiz, J. Cioslowski, D. J. Fox, Gaussian 09, Revision A.02, Gaussian, Inc., Wallingford CT, **2009**.

[18] a) J. P. Perdew, Y. Wang, *Phys. Rev. B* **1992**, *23*, 13244-13249; b) A. D. Becke, *J. Chem. Phys.* **1993**, *98*, 5648-5652.

[19] a) K. A. Peterson, *J. Chem. Phys.* **2003**, *119*, 11099-11112; b) K. A. Peterson, D. Figgen, E. Goll, H. Stoll, M. Dolg, *J. Chem. Phys.* **2003**, *119*, 11113-11123; c) B. Metz, H. Stoll, M. Dolg, *J. Chem. Phys.* **2000**, *113*, 2563-2569; d) G. A. Pettersson, M. A. Al-Laham, *J. Chem. Phys.* **1991**, *94*, 6081-6090.

[20] E. D. Glendening, J. K. Badenhoop, A. E. Reed, J. E. Carpenter, J. A. Bohmann, C. M. Morales, C. R. Landis, F. Weinhold, NBO 6.0, **2013**.

[21] A. D. Becke, *J. Chem. Phys.* **1990**, *92*, 5397-5403.

[22] J. S. Murray; K. Paulsen; P. Politzer, *Proc.-Indian Acad. Sci.* (*Chem. Sci.)* **1994**, *106*, 267-275.

[23] a) F. Biegler-König; J. Schönbohm, *J. Comput. Chem.* **2002**, *23*, 1489-1494; b) P. S. V. Kumar; V. Raghavendra; V. Subramanian, *J. Chem. Sci.* **2016**, *128*, 1527-1536.

[24] a) G. M. Sheldrick, *Acta Cryst.*, **2008**, *A64*, 112-122; b) G. M. Sheldrick, *Acta Cryst.*, **2015**, *C71*, 3-8; c) G. M. Sheldrick, *Acta Cryst.*, **2015**, *A71*, 3-8.

[25] T. Lu, F. Chen, *J. Comput. Chem.* **2012**, *33*, 580-592.

8.8 Supplementary Data

Table 8.3 Refinement details for the X-ray structures.

Compound	9	10	11	12	13
Formula	$C_{15}H_{18}Cl_3NO_3Sn$	$C_{11}H_8Cl_2NSb$	$C_{60}H_{50}Bi_4Cl_6N_6O$	$C_{11}H_8ClNTe$	$C_{11}H_8BrNTe$
Crystal System	Triclinic	Monoclinic	Triclinic	Monoclinic	Triclinic
Space group	*P-1*	*P2₁/n*	*P-1*	*P2₁/n*	*P-1*
T/K	293(2)	100(2)	153(2)	293(2)	100(2)
a [Å]	7.3277(2)	8.5469(2)	10.4514(4)	8.89797(14)	7.0125(3)
b [Å]	10.5412(3)	9.4389(2)	12.0023(7)	7.01569(10)	8.9211(4)
c [Å]	11.6971(2)	14.8647(5)	13.5487(8)	16.7233(3)	10.1544(5)
α [°]	84.565(2)	90	70.233(5)	90	107.133(4)
β [°]	89.436(2)	105.298(3)	82.617(4)	94.1727(14)	98.893(4)
γ [°]	83.637(3)	90	72.969(4)	90	112.807(4)
V [Å³]	893.91(4)	1156.69(6)	1528.46(15)	1041.19(3)	532.91(5)
Z	2	4	1	4	2
$\rho_{calc}g/cm^3$	1.803	1.992	2.164	2.024	2.254
μ/mm^{-1}	1.889	2.810	11.790	3.069	6.497
GOF	1.089	1.035	1.049	1.104	1.089
2θ range (deg)	3.906-49.998	5.166-62.068	4.078-62.348	4.884-49.994	5.378-62.228
Refs collected	9612	11457	28515	13473	12653
Unique/observed	3155	3412	28515	1836	3123
Parameters	216	136	387	127	127
R_{int}	0.0283	0.0307	0.1577	0.0168	0.0381
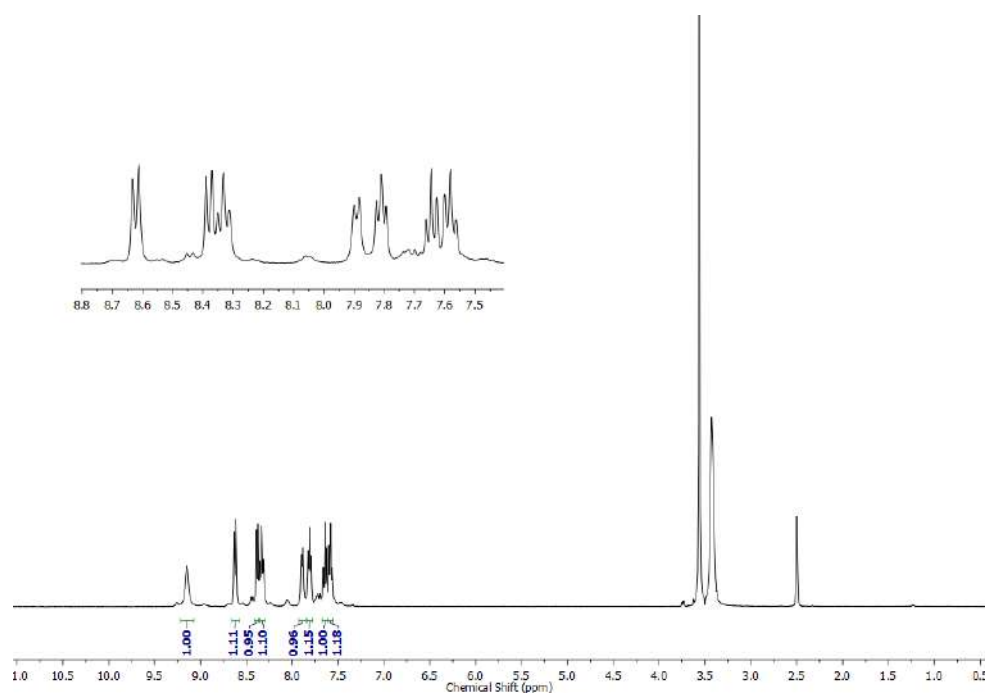
Figure 8.8 ^{1}H NMR spectrum of **8.9**.
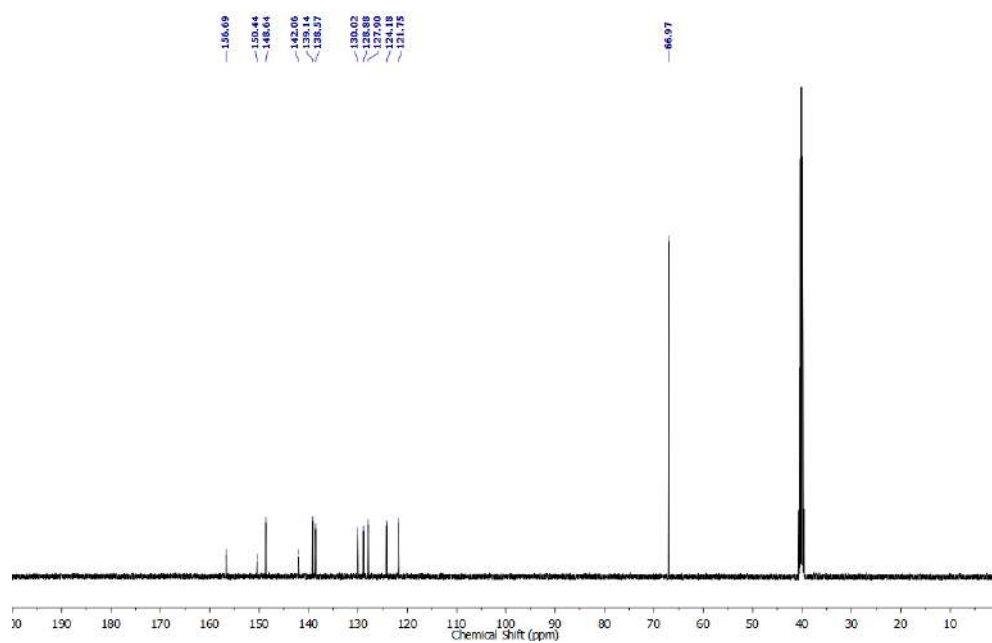
Figure 8.9 ^{13}C NMR spectrum of **8.9**.
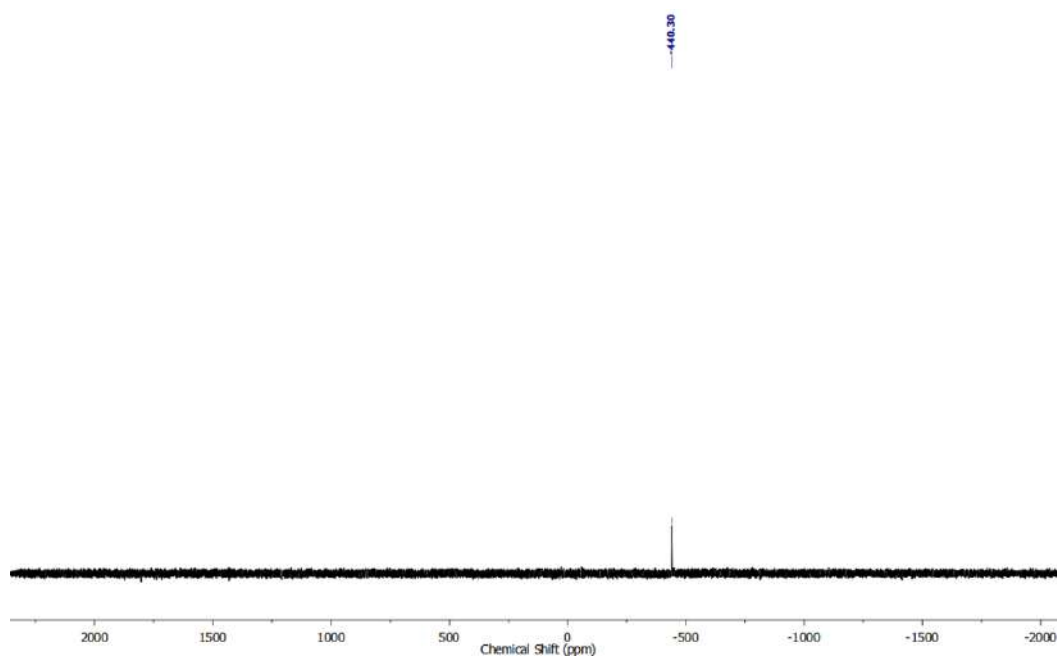
Figure 8.10 ^{125}Te NMR spectrum of **8.9**.
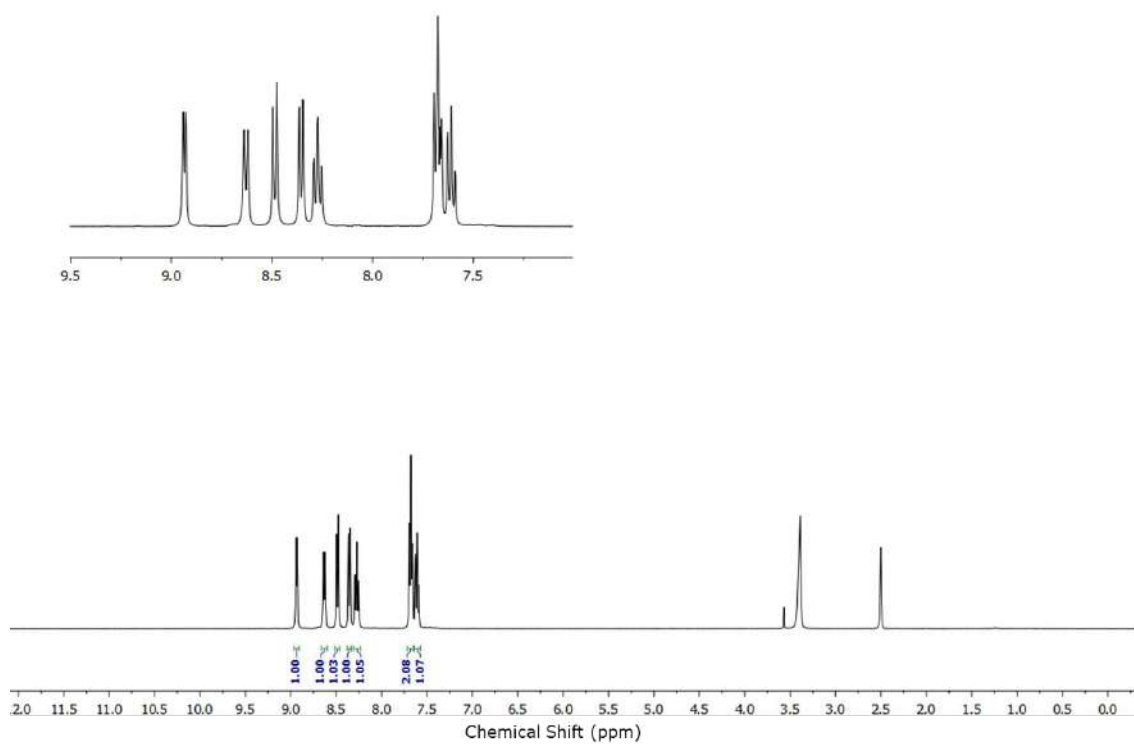
Figure 8.12 ^{1}H NMR spectrum of **8.10**.
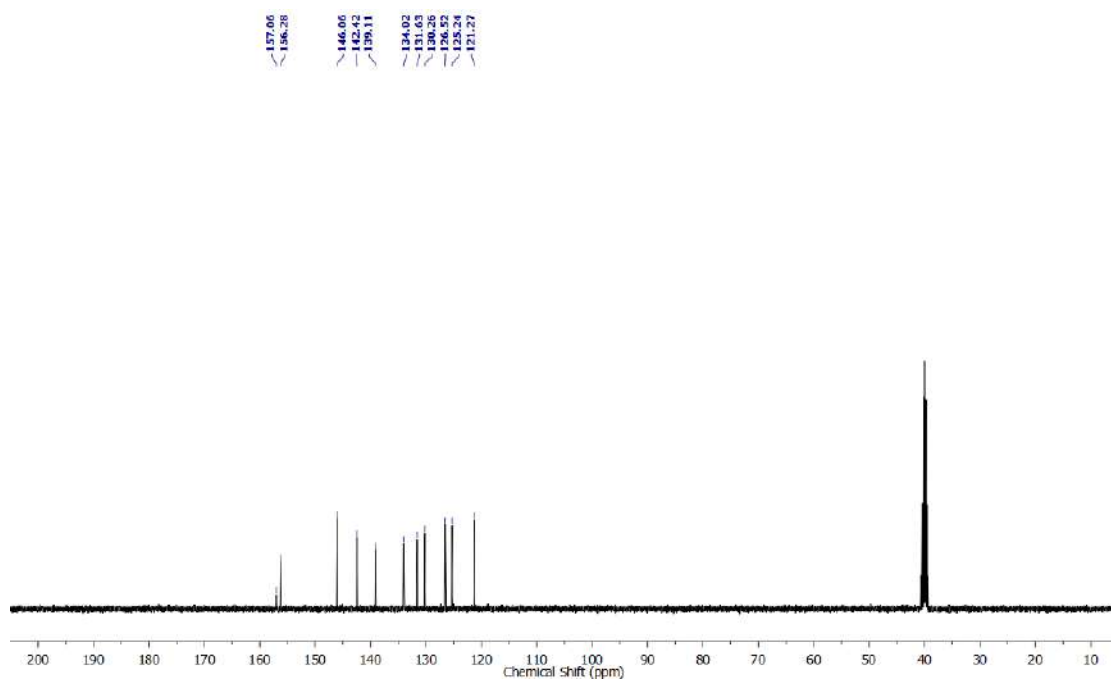
Figure 8.13 ^{13}C NMR spectrum of **8.10**.
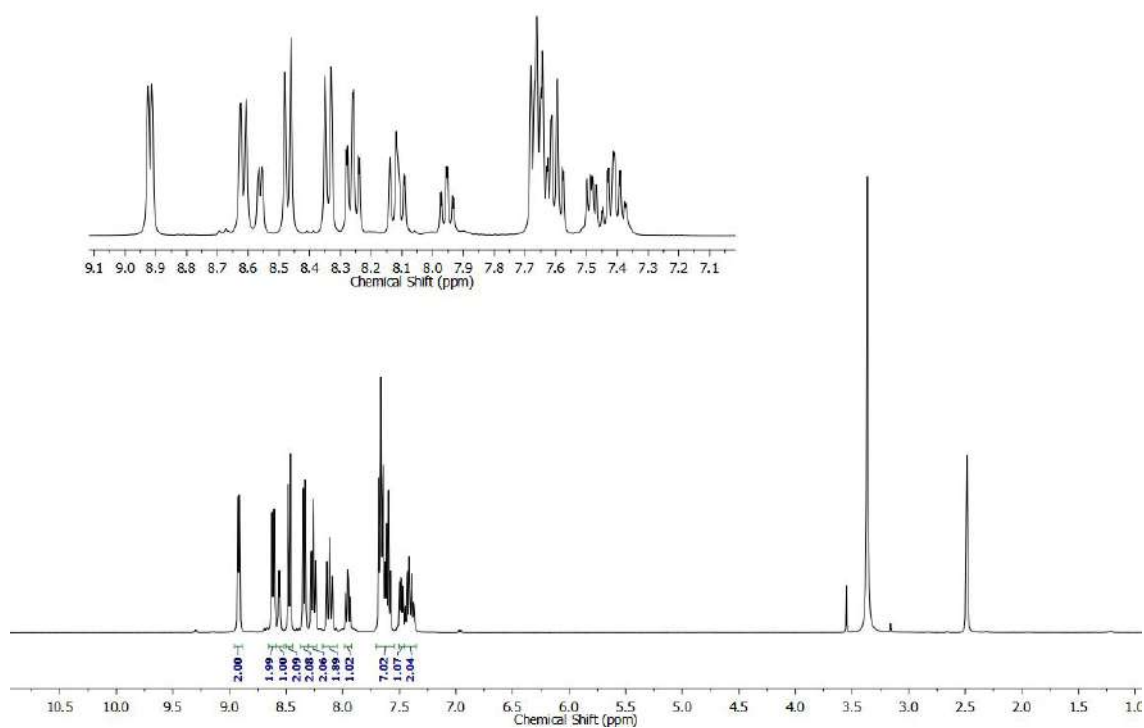
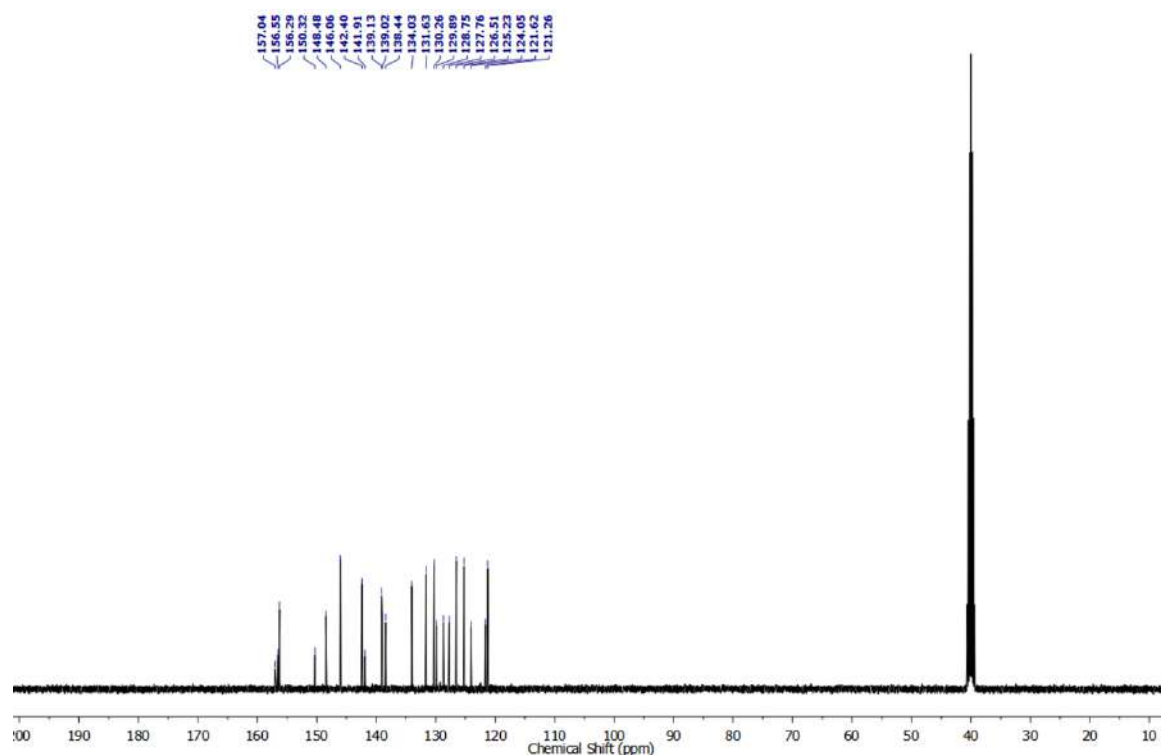**Figure 8.15** ^{1}H NMR spectrum of **8.11**.
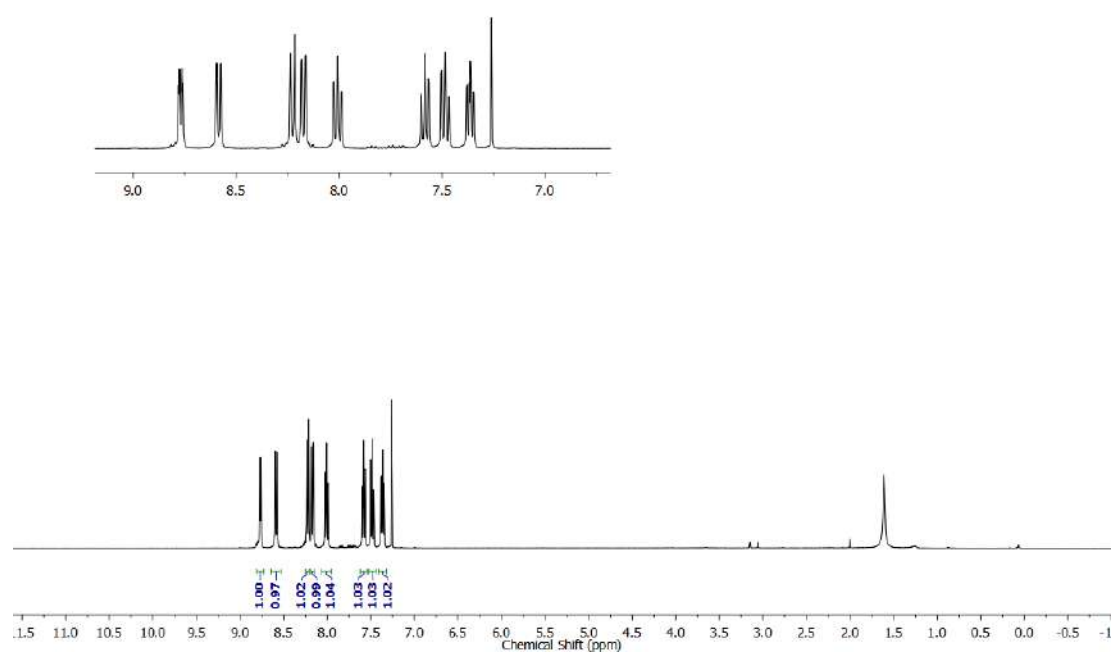
Figure 8.16 ^{13}C NMR spectrum of **8.11**.

Figure 8.18 ^{1}H NMR spectrum of **8.12**.
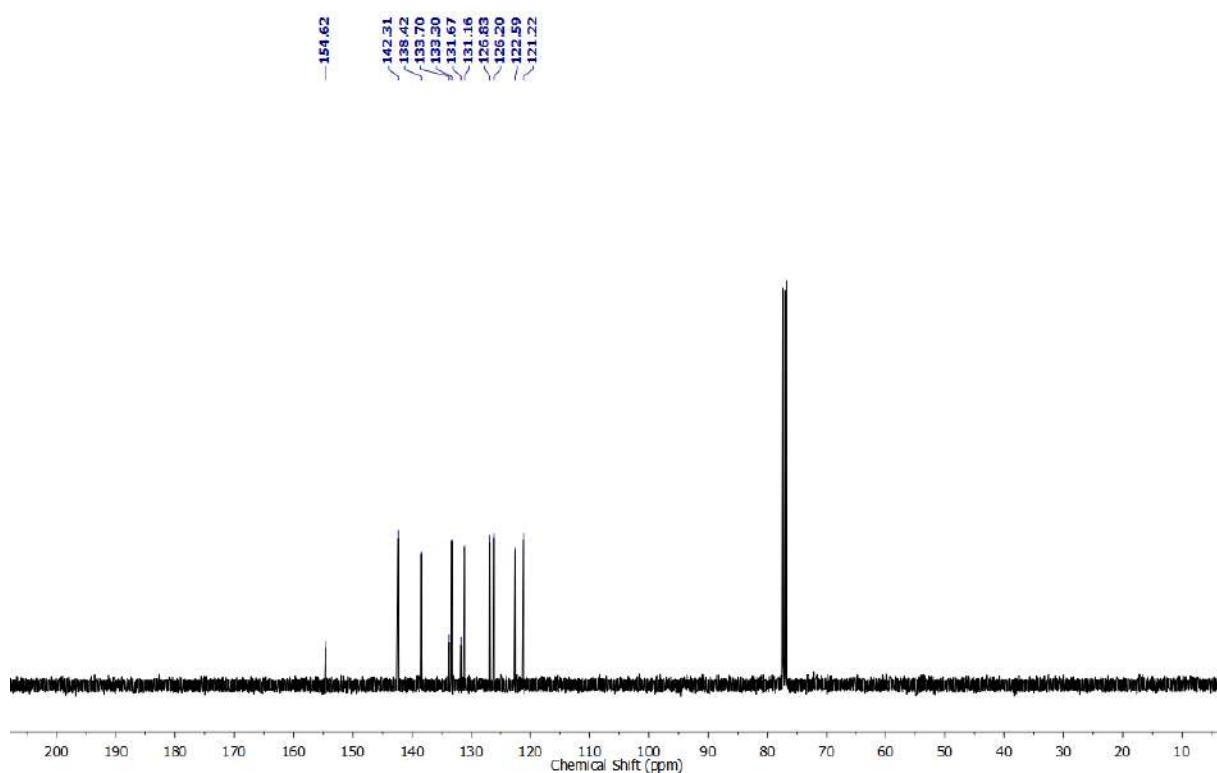
Figure 8.19 ^{13}C NMR spectrum of **8.12**.
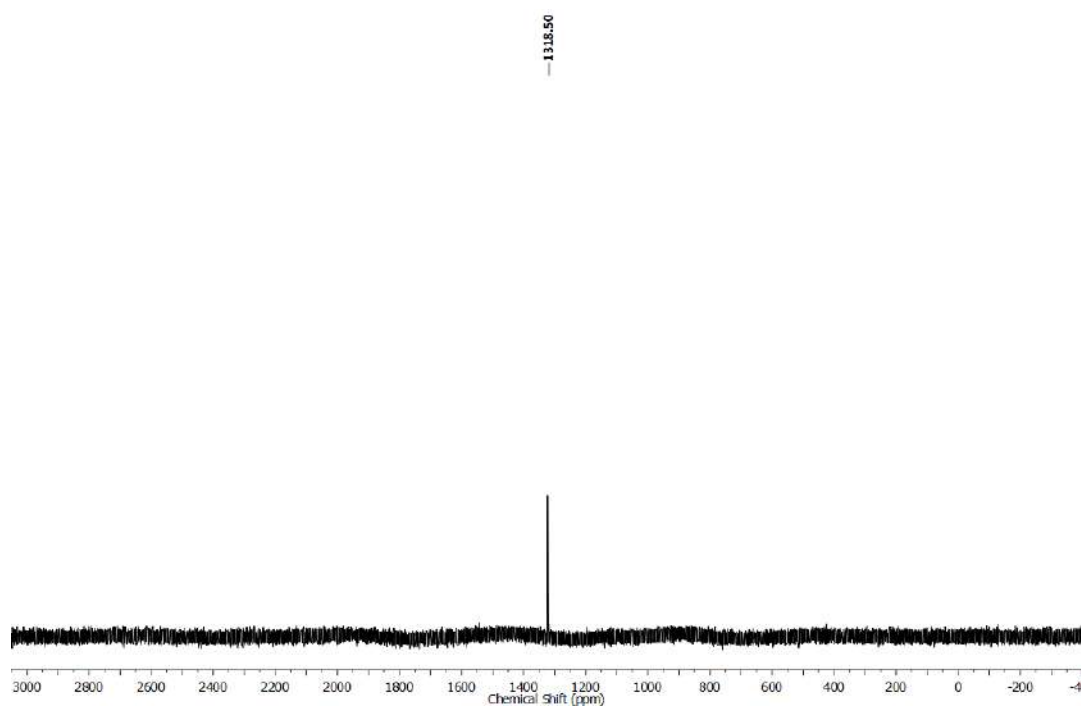
Figure 8.20 ^{125}Te NMR spectrum of **8.12**.
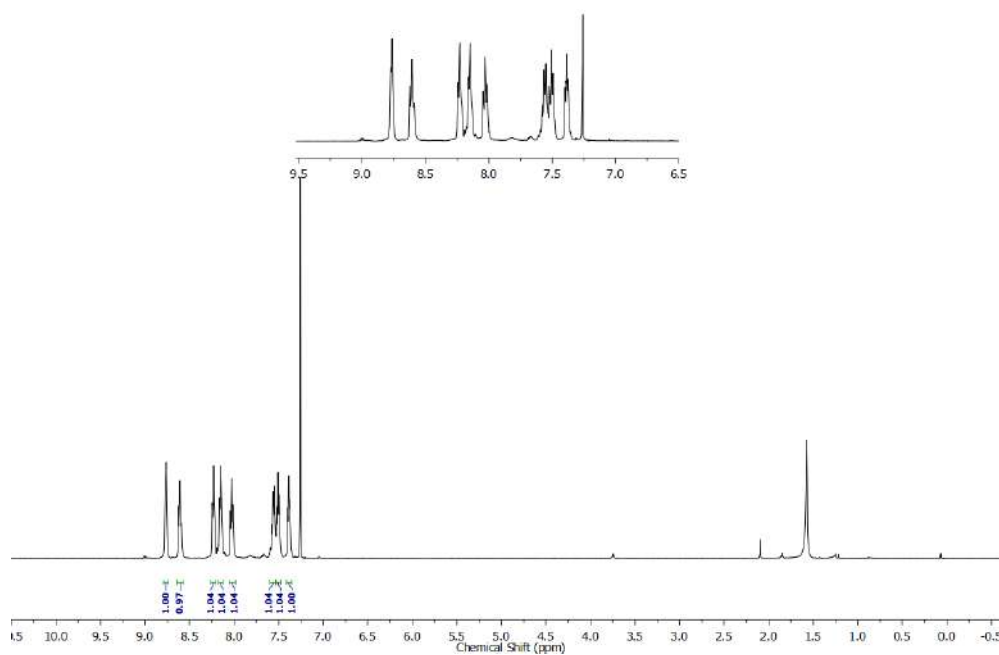
Figure 8.22 ¹H NMR spectrum of **8.13**.
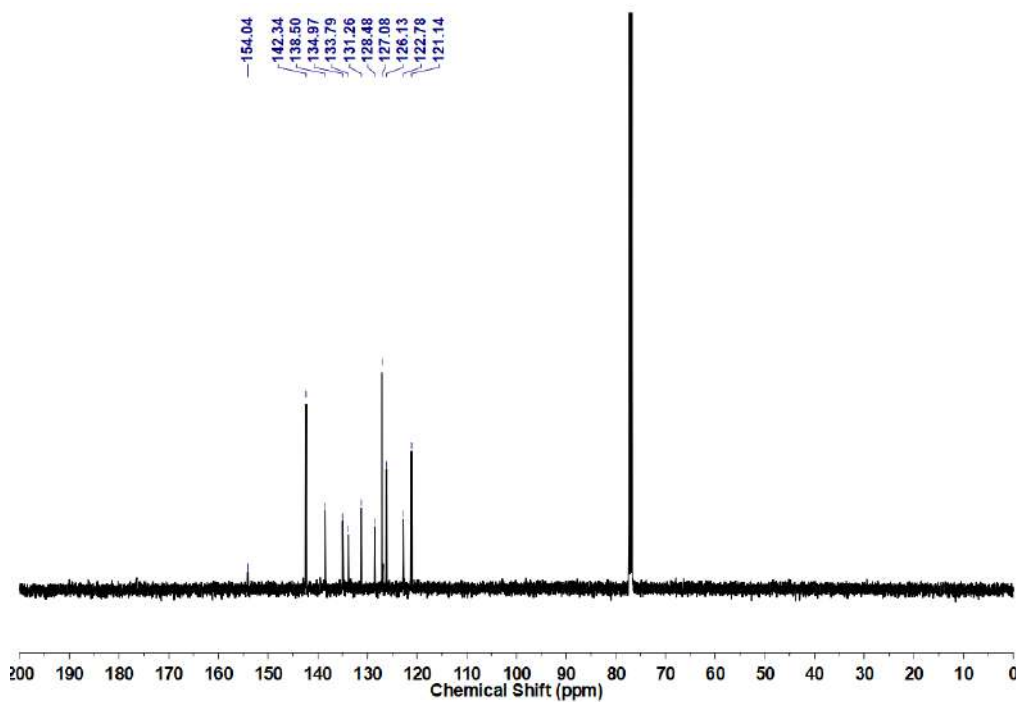
Figure 8.23 ¹³C NMR spectrum of **8.13**.

—1274.36

00 2900 2800 2700 2600 2500 2400 2300 2200 2100 2000 1900 1800 1700 1600 1500 1400 1300 1200 1100 1000 900 800 700 600 500 400 300 200 100 0 -100
Chemical Shift (ppm)
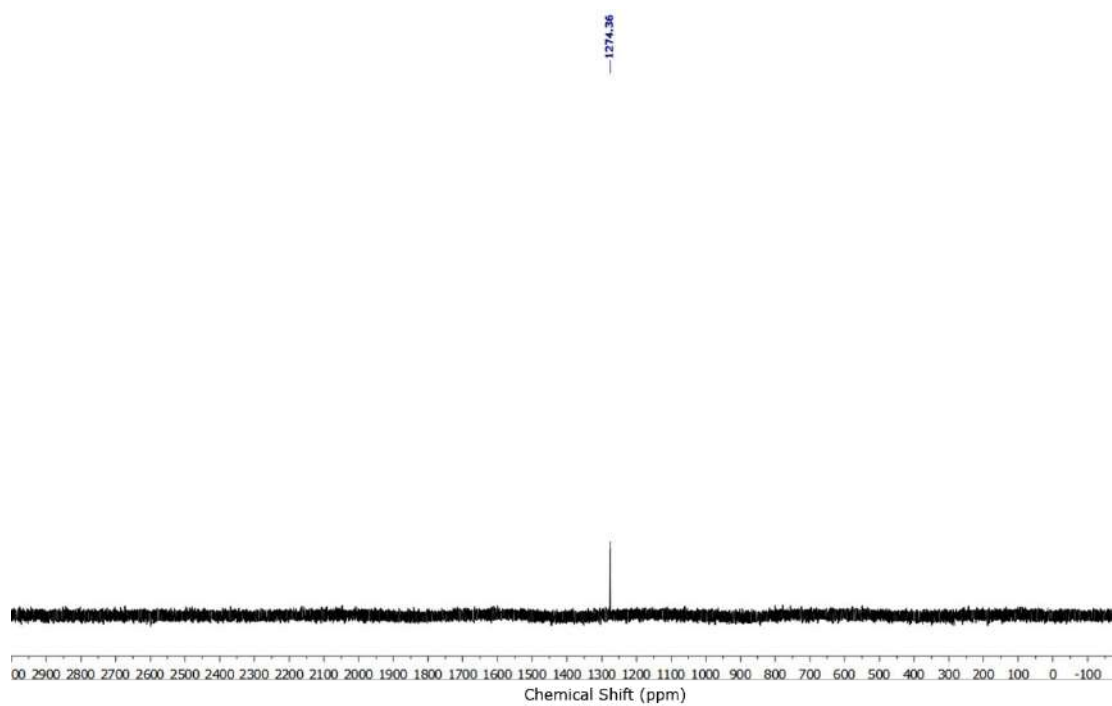
Figure 8.24 [125]Te NMR spectrum of **8.13**.

The lanthanoid metals [La (Z=57)-Lu (Z=71)] are regarded as hard metal centers and subsequently their chemistry has been dominated by hard donor ligands like ethers, amines, amides, *etc*. However, there have been considerable concerns, in recent years, for the preparation of complexes containing soft donor ligands, in particular with those of group 16. This is driven in part not only due to their promising technological interests (such as in magnetism,[1a] optics and electronics[1b-c] *etc*.), but also from inquisitiveness to improve the understanding of such unconventional hard-soft interactions. Most of the studies on lanthanoid chalcogenolates have been focused either on clusters of lanthanoid compounds or on oligomers or polymers of the same,[1d-l] which is attributed to their affinity for high and variable coordination number. Consequently, synthesis of monomeric lanthanoid chalcogenolates is considered to be very challenging.

'Pincer ligands' are a class of ligands consisting of donor atoms which are capable of coordinating in a tridentate manner (preferably meridionally) to the central metal atom, thus, giving rise to the phenomenon of chelation. Chelation makes their structures versatile enough to modify them and provide the dual combination of stability as well as reactivity with metal complexes; both of which are crucial in coordination chemistry. It is precisely the convenience in fine-tuning the ligand backbone as well as the flanking arms, that triggers the development of various palindromic pincers (such as PCP, PNP, CCC, CNC, NNN, NCN, OCO, SPS, SeCSe *etc*.) as well as non-palindromic pincers (such as NNP, PCN *etc*.), which eventually makes them universal ancillary ligands in metal based chemistry.[2] In fact, after the first revolutionary report on organometallic complexes of tridentate PCP ligand by Moulton *et al.*,[2c] the coordination chemistry of pincer ligands has become a privileged avenue which is explored in almost all modern aspects of organometallic chemistry, such as homogenous catalysis,[2d-e] sensing,[2f] molecular recognition,[2g] optoelectronics,[2h] and supramolecular chemistry[2i] to name a few.

Chapter 1:

The introductory chapter gives a general overview of the basic properties and chemistry of rare-earth and chalcogen elements. A brief summary on the synthetic procedures and current perspectives of organolanthanoid chalcogenolate complexes are included. In addition, general aspects of 'redox active multidentate ligands' and 'pincer ligands' are also reviewed in Chapter 1.

Chapter 2:

Chapter 2 describes the facile synthesis of monomeric lanthanoid chalcogenolates by using hybrid, Intramolecular Chalcogen Bonding (IChB)[3] stabilised organochalcogen compounds. In particular, when ditellurides **S1** and **S2** were treated with Ln(0) metals (Yb, Eu), the metals underwent oxidative addition to afford the lanthanoid chalcogenolates, **S3-S8** (**Scheme S1**). Here, the donor atoms from the auxiliary arms, which were initially involved in secondary bonding interactions with chalcogen atoms (D⋯E; D = N, E = Te), acted as chelating arms in the resulting metal complexes. In fact, the Ln⋯N interactions, together with the steric bulk of the ligands, prevented the formation of higher order aggregates and confined the molecules to monomers.
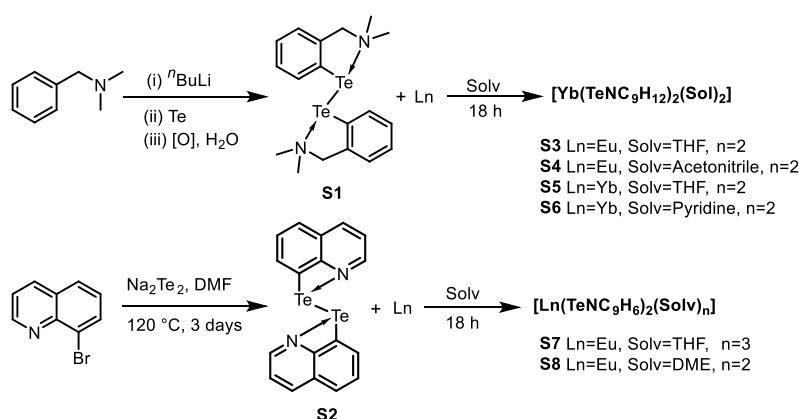
Scheme S1. Synthesis of bis[2-(dimethylamino)methyl)phenyl]ditelluride, **S1** and 8,8'-diquinolyl ditelluride, **S2** and their lanthanoid complexes **S3-S8**.

All the complexes **S3-S8** were authenticated by single crystal X-ray diffraction studies. In complexes **S3-S6**, the six-coordinated lanthanoid metal atom was located on a crystallographically imposed centre of inversion, containing two 2-(dimethylamino)methyl)phenyltellurolate ligands in *trans* arrangement [**Figure S1 (a)**]. Each 2-(dimethylamino)methyl)phenyltellurolate ligand filled two coordination sites, one from the tellurium and the other from the nitrogen atom; both these atoms were involved in the formation of six membered chelating ring to the metal. The rest of the two coordination sites around the divalent metal centre were occupied by two solvent molecules. All the complexes were isostructural where the geometry around the Ln metal centres were octahedral, with the angle Te-Ln-Te1=180°, N-Ln-N1=180° and D-Ln-D1=180° (where D= donor atom of the solvent molecule). Of particular interest are the Ln-Te distances in all

complexes, which were found to be significantly shorter in comparison to the similar reported lanthanoid tellurolate complexes.[4]

Interestingly, in the case of quinoline tellurolate ligand, significant changes in the coordination numbers were observed in the resulting complexes. For instance, in THF, the ligand afforded seven coordinated complex, [Eu(TeNC$_9$H$_6$)$_2$(THF)$_3$] **S7** [**Figure S1 (b)**], whereas in DME it afforded eight coordinated complex [Eu(TeNC$_9$H$_6$)$_2$(DME)$_2$] **S8**. Although, the spatial arrangements of the quinoline tellurolate ligands around the Eu(II) centre were different in **S7** and **S8**, nevertheless, the Eu-Te distances in both complexes were in good agreement with those of **S3-S6**.


(a)   (b)
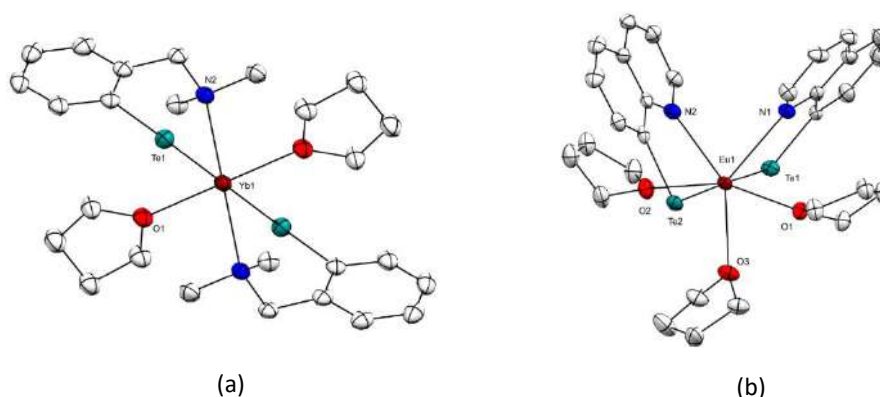
Figure S1. Molecular structures of monomeric lanthanoid chalcogenolates, **(a) S5** and **(b) S7**.

Chapter 3:

In an attempt to synthesize lanthanoid thiolate complexes, it was envisaged to synthesize quinoline thiolate ligand by reacting 8-quinolinesulfonyl chloride with tin dichloride in the presence of hydrochloric acid. The reaction afforded bis(8-sulfanylquinolinium) hexachloridostannate(IV). From literature survey it was perceived that after Edinger's report[5] on the presence of bis(8-sulfanylquinolinium) hexachloridostannate(IV) as an intermediate for the conversion of 8-quinolinesulfonic acid to 8-quinolinethiol, bis(8-sulfanylquinolinium) hexachloridostannate(IV) has been commonly used as a reactive intermediate in various organotin reactions.[6] However, there is no structural characterization of bis(8-sulfanylquinolinium) hexachloridostannate(IV) available in literature. In Chapter 3, the isolation and characterization of bis(8-sulfanylquinolinium) hexachloridostannate(IV) is reported. In addition, some new interesting reaction behaviors of bis(8-sulfanylquinolinium) hexachloridostannate(IV) in different solvents are also included.

The synthesis of bis(8-sulfanylquinolinium) hexachloridostannate(IV), **S10** was accomplished by following the reported procedure wherein 8-quinolinesulfonyl chloride, **S9** (synthesized by reacting quinoline-8-sulfonic acid with phosphorus pentachloride) was treated with tin dichloride in the presence of hydrochloric acid (**Scheme S2**).[5] Interestingly, when bis(8-sulfanylquinolinium) hexachloridostannate(IV) salt was recrystallized from chloroform or dichloromethane, it yielded *cis*-dichloridobis(8-quinolinethiolato) tin(IV), **S11**. When it was recrystallized from methanol, it afforded crystals of 8,8'-dithiodiquinolinium hexachloridostannate(IV), **S12**. The behavior of **S10** in DMSO was also investigated and it was observed that it provided a convenient approach for the synthesis of 8,8'-diquinolyl disulfide, **S13**.
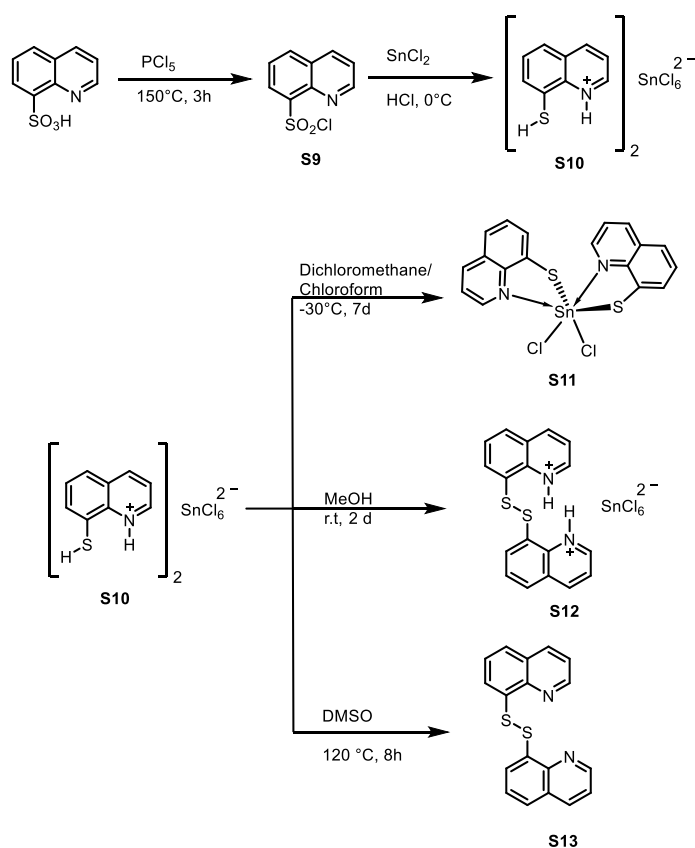
Scheme S2. Synthetic routes to *cis*-dichloridobis(8-quinolinethiolato)tin(IV), **S11** and 8,8'-dithiodiquinolinium hexachloridostannate(IV) derivative, **S12** and 8,8'-diquinolyl disulfide, **S13**.

In the molecular structure of **S10**, two 8-sulfanylquinolinium ions were H-bonded to two *trans*- Cl atoms from SnCl$_6^{2-}$ [**Figure S2 (a)**]. The asymmetric unit contained one 8-sulfanylquinolinium ion and half of a [SnCl$_6^{2-}$] ion with Sn(IV) atom sitting on the edge of the cell. The geometry around

Sn(IV) was distorted octahedral with three different Sn1-Cl bond distances; Sn1-Cl1 2.4115(18) Å, Sn1-Cl2 2.4378(18) Å and the one participating in intermolecular H-bonding with quinolinium ion, Sn1-Cl3 was 2.4330(17) Å. Both the intermolecular H-bonding distances were 2.393 Å. The C-S bond length was observed to be 1.770(8) Å indicating its single bond nature.

During the crystallization of *cis*-dichloridobis(8-quinolinethiolato)tin(IV) **S11**, two polymorphs namely **S11m** and **S11t** were obtained. Complex **S11m** was obtained by evaporation of a saturated dichloromethane solution and it crystallized in monoclinic space group *C2/c*. Whereas complex **S11t** was obtained by evaporation of a chloroform solution and crystallized in triclinic space group *P-1*. The single-crystal X-ray diffraction analyses revealed that the hexacoordinated metal center, Sn(IV) ions in both **S11m** and **S11t** were chelated by two 8-qunolinthiolate anions and coordinated by two chloride ions. The co-ordination environment of Sn(IV) was distorted octahedral with the N-donor atoms as well as the chloride ligands were in *cis* alignment; while the sulfur atoms of the 8-quinolinethiolate anions were *trans* to each other. In both the polymorphs **S11m** and **S11t**, the bond lengths around the metal atom (Sn-N, Sn-Cl) were in the same range and the angular distortions from octahedral geometry at the metal center were similar in both complexes. All the important bond distances, for instance in **S11m** [**Figure S2 (b)**], namely, Sn-S [Sn1-S1=2.4168(4)Å, Sn1-S1´= 2.4169(4) Å], Sn···N [Sn1···N1= 2.2876(15) Å and Sn1···N1´= 2.2875(15) Å] and Sn-Cl [2.4358(5) Å] were in good agreement with similar reported complexes, such as *cis*-dichloridobis(8-quinolinolato)tin(IV)[7] and dibenzylchlorido(8-quinolinethiolato)tin(IV)[8].
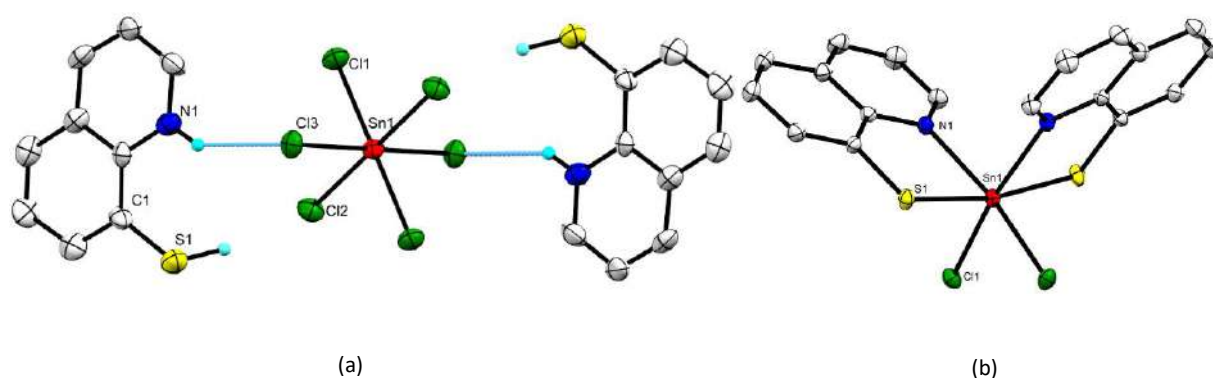

(a)   (b)

Figure S2. Molecular structures of **(a)** bis(8-sulfanylquinolinium) hexachloridostannate(IV), **S10** and **(b)** *cis*-dichloridobis(8-quinolinethiolato)tin(IV), **S11m**.

Chapter 4:

Chapter 4 describes the electronic structural properties of Ru and Os complexes of N,N´-bis(2-pyridyl)benzene-1,2-diamine ligand with the help of structural, electrochemical and DFT analyses. It is worth mentioning that in recent times, N,N´-disubstituted 1,2-diaminobenzenes have gained profound interest from the researchers owing to their expedient applications in various aspects, for example, as a building block for supramolecular arrays,[9a] in synthesizing N-heterocyclic carbene[9b] and its various analogues[9c-e]. Apart from these remarkable applications, N,N´-disubstituted 1,2-diaminobenzenes derivatives are accepted to be one of the preferred choices of ligand for transition metal complexes[10] especially due to its inherent 'redox non-innocence' behavior, a term given by Jørgensen[11] to ligands that consist of variable energetically accessible levels that can actively participate in redox processes giving rise to an apparent ambiguity in oxidation states. The fact that, N,N´-disubstituted 1,2-diaminobenzenes can undergo two successive one-electron oxidation to form *o*-diiminosemiquinone radical (L$^{\cdot-}$) and *o*-diiminoquinone (L^0) respectively as shown in **Figure S3**, thus offers variable oxidation states to the bonded metal atom.
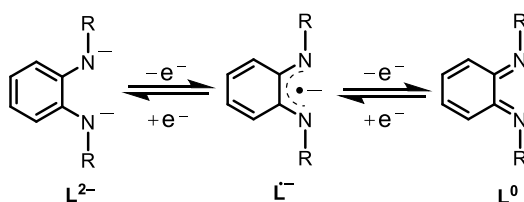

Figure S3. Redox transformations of N,N´-disubstituted 1,2-diaminobenzenes.

From the literature survey it was found that the substituent 'R' in N,N´-disubstituted 1,2-diaminobenzenes has played pivotal role in the redox non-innocence of the ligand, consequently the modification of 'R' could significantly alter the electronic structures of the resulting metal complexes.[12] In this context, Chapter 4 features the syntheses and molecular structures of ruthenium and osmium complex of a relatively less-explored ligand namely, N,N´-bis(2-pyridyl)benzene-1,2-diamine, specially providing a critical insight in to their electronic properties. The electronic structural behavior of the complexes was examined by means of a wide array of analytical techniques (magnetic resonance, UV-Vis-NIR spectroscopy and electrochemistry); comprehensive computational studies were also carried out to provide additional support to the experimental work.

Ligand N,N´-bis(2-pyridyl)benzene-1,2-diamnine, **H₂L** was prepared by following the reported procedure wherein *o*-phenylenediamnine was treated with 2-bromopyridine at 195 °C [**Scheme S3**].[13] The mononuclear complexes [Ru^{III}(acac)₂(L)], (**S14**), [Ru^{II}(Ph-tpy)(L)], (**S15**), and [Os^{II}(bpy)₂(L)](ClO₄), ([**S16**]ClO₄) were synthesized in a single step reactions between **H₂L** and the metal precursors *cis*-Ru^{II}(acac)₂(CH₃CN)₂, Ru^{III}(Ph-tpy)(Cl₃) and *cis*-Os^{II}(bpy)₂Cl₂ respectively in the presence of Et₃N in polar protic solvent medium (*e.g.* ethanol or methanol).
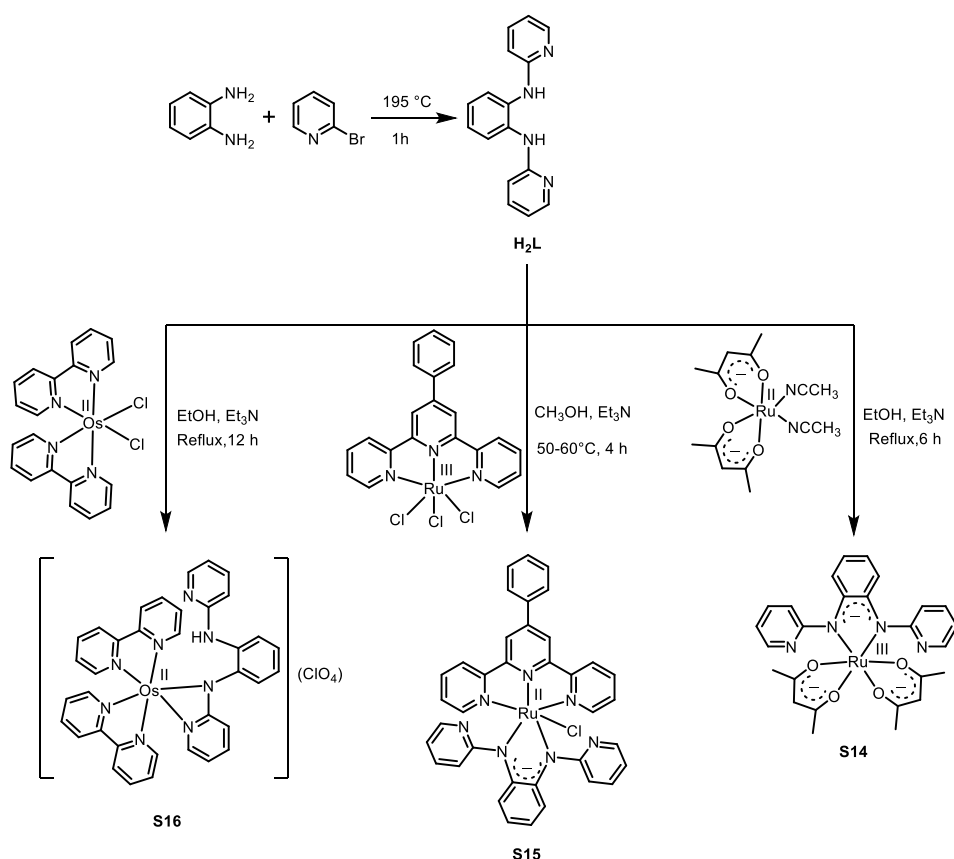
Scheme S3. Synthesis of N,N´-bis(2-pyridyl)benzene-1,2-diamine, **H₂L** and Ru and Os complexes, **S14**-**S16**.

Cyclic voltammetry and differential pulse voltammetric studies in combination with EPR spectroscopy and theoretically calculated Muliken spin density can be used for the unambiguous assignment of the accessible redox states within a molecule. Compounds **S14**-**S16** demonstrated successive oxidation and reduction waves within a potential window of ±2.0 V versus SCE in CH₃CN [**Figure S4 (a)-(c)**]. In particular, the reversible oxidation waves for **S14** at 0.48 V could be ascribed to {M^{II}-Q$^{•-}$}↔{M^{II}-Q$^{•}$} transformation. However, the corresponding anodic shift in

potential for **S15** was not attained in the experimental cyclic voltammetry scale, which might be attributed to the π-acceptor nature of the co-ligand. A reversible, ligand based (71%) oxidation wave [{M^{II}-Q^-}$\leftrightarrow${M^{II}-$Q^{\bullet}$}] was obtained at 0.12 V for [**S16**](ClO_4). Complexes [**S14**] and [**S15**] exhibited mixed metal-ligand (~50%-50%) and solely ligand based (~72%) reduction at -0.81 V and -0.43V respectively. A terpyridine based reduction was also observed in [**S15**] at -0.92 V. Complex [**S16**](ClO_4) displayed bipyridine based reduction (~90%) at -1.21 V. The difference in π-donation capability of Ru and Os along with terpyridine and bipyridine could be held responsible for changes in redox behavior of respective complexes bearing non-innocent *o*-quinonediimine ligand.
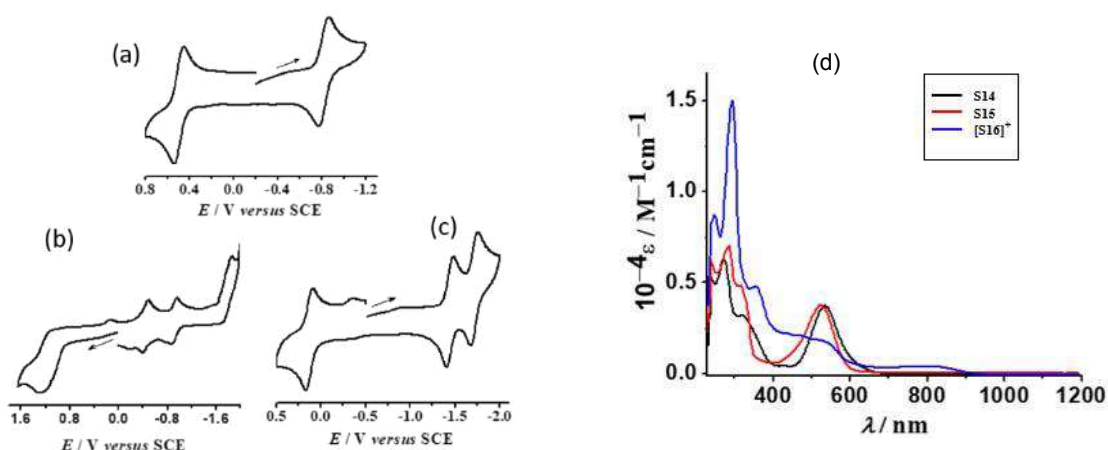

Figure S4. Cyclic and differential pulse voltammograms of (a) **S14** (b) **S15** and (c) [**S16**](ClO_4) in CH_3CN/0.1 M Et_4NClO_4; (d) UV-Vis spectra of complexes **S14** (black), **S15**(red), and [**S16**](ClO_4) (blue) in CH_2Cl_2.

From the UV-Visible study, it was observed that compounds **S14**-**S16** displayed moderately intense transitions at 535 nm, 521 nm and 547 nm respectively [**Figure S4 (d)**], which could be assigned as ligand-to-metal charge transfer (LMCT) involving π-orbitals ($L^{\bullet-}$) of partially reduced ligand to $d\pi$ of metals. While the higher energy bands were assigned to ligand-to-ligand charge transfer (LLCT) transitions. However, slight disparity in position of the spectral bands on moving from **S14** to **S15** to [**S16**](ClO_4) was mainly attributed to the variation in σ-donating (acac) and π-acceptance (terpy and bpy) capabilities of the ancillary ligands.

All three complexes **S14**-**S16** were authenticated by single crystal X-ray diffraction studies. In both **S14** [**Figure S5 (a)**] and **S15** [**Figure S5 (b)**], the geometry around Ru was distorted octahedral. From the bond distances of the ligand backbone to the metal center and their comparison with the similar reported complexes,[14] it could be inferred that in **S14** the ligand was in semiquinone state, *i.e.*, L$^{\bullet-}$ and the free radical was delocalized through C1-N1, C1-C2 and C2-N2 bonds. In complex **S15**, C1-N1 distance resembles to that of a double bond, while C2-N2 corresponds to a single bond. From comparison with the literature,[14c-e] it can be inferred that ligand is in monoionic state, where the negative charge is located on N2 atom. In the molecular structure of **[S16]ClO₄**, the divalent Os ion was coordinated to one nitrogen atom of *o*-phenylenediamnine, one nitrogen atom from the flanking pyridine group and two bipyridyl ancillary ligands. Interestingly, second 'N2<u>H</u>' proton from *o*-phenylenediamnine core did not undergo deprotonation during the reaction and eventually did not participate in coordination with Os metal. The C1-N1 bond distance of 1.43(2) Å indicated the single bond character of the same and hence the best description of **[3.8]** was [Os^{II}(bpy)$_2$(L$^-$)Cl](ClO$_4$), where the negative charge was localized on N1 atom.
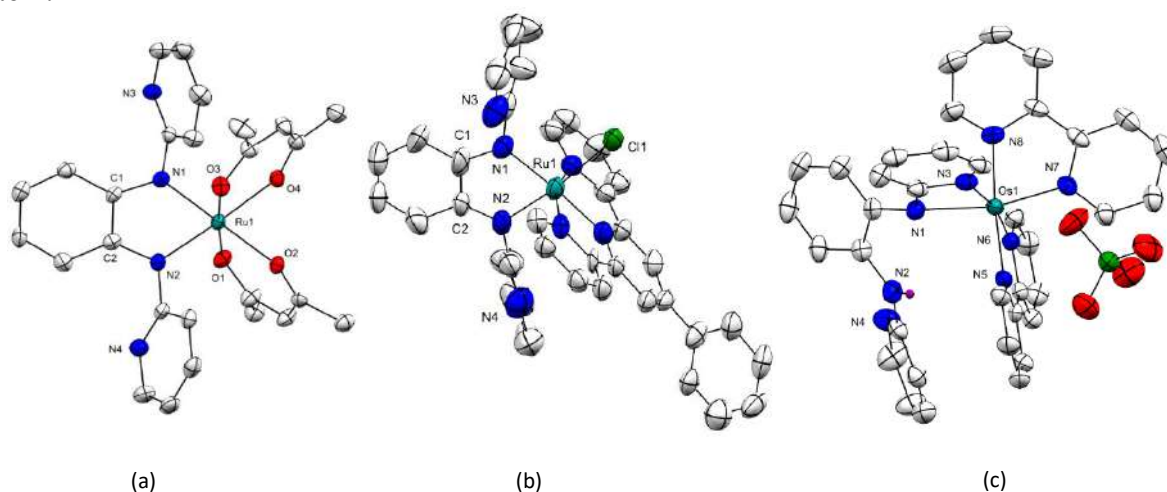

(a) (b) (c)

Figure S5. Molecular structures of **(a) S14** and **(b) S15** and (c) **S16**.

Chapter 5:

Chapter 5 deals with the chemistry of pyrrole based NNN pincer ligands and their complexes. It is worth mentioning that amidst various pincer scaffolds, NNN- pincer ligands based on pyrrole framework have recently drawn significant interest with respect to their interesting structural properties and applications.[15] However, reports on transition metal complexes and group 16

complexes of pyrrole based NNN ligands are rather scarce in literature. In this chapter, syntheses of Se/Te as well as Pd/Pt complexes of NNN-pincer ligands has been included focusing on their bonding properties.

The ligands of present interest, **L^1-L^3** were synthesised by Mannich reaction following the reported procedure[16] wherein pyrrole was treated with formaldehyde and secondary amine (dimethylamine/pyrrolidine/piperidine) (**Scheme S4**). In order to unveil the characteristic of N-Se/Te bond, lithiated ligand $Li[NC_4H_2(CH_2NMe_2)_2-2,5]$ was treated with Te/Se powder followed by aerial oxidation to afford dichalcogenides, **S17-S18**. In another approach, $Li[NC_4H_2(CH_2NMe_2)_2-2,5]$ was treated with Te/Se and then bromobenzene was added to synthesise unsymmetrical monotellurides, **S19-S20**. It is worth mentioning that all these synthesized chalcogenides were not stable under ambient conditions and in common organic solvents, which in turn precluded their detailed characterizations through ^1H NMR spectroscopy. However, the ^{77}Se NMR and ESI-MS of the compounds could be obtained by recording the spectra directly from the reaction aliquots. These substantiated the formation of the compounds.
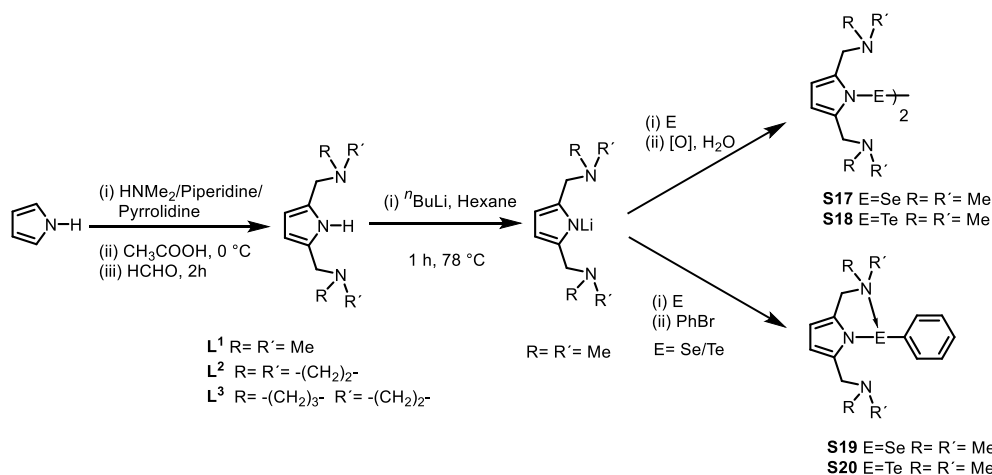
Scheme S4. Synthetic routes for pyrrole based NNN-pincer ligands, **L^1-L^3** and chalcogen compounds **S17-S20**.

When **L^2** was treated with $Pd(COD)Cl_2$ in the presence of trimethylamine, the displacement of COD resulted in the formation of complex **S21** (**Scheme S5**). However, in the case of $Pt(COD)Cl_2$, the chloride ions behaved as leaving groups, giving rise to complexes, **S22-S23**. Interestingly, in both the Pt complexes, the cyclooctadiene moiety experienced a Pt-induced

deprotonation in the position α to one of the double bonds followed by formation of a new double bond via 1,2-shift. This afforded 2,5-cyclooctadienyl ligand. It is worth mentioning that during the isomerisation process, one of the former π-bonded carbon atoms changed its coordination mode to C-Pt σ-bond. In another instance, the lithiated ligand Li[NC$_4$H$_2$(CH$_2$NMe$_2$)$_2$-2,5] on treatment with Pd(COD)Cl$_2$ afforded complex **S24** where an additional coordination of dimethylamine to Pd centre was observed. This might have resulted from decomposition of the starting material.
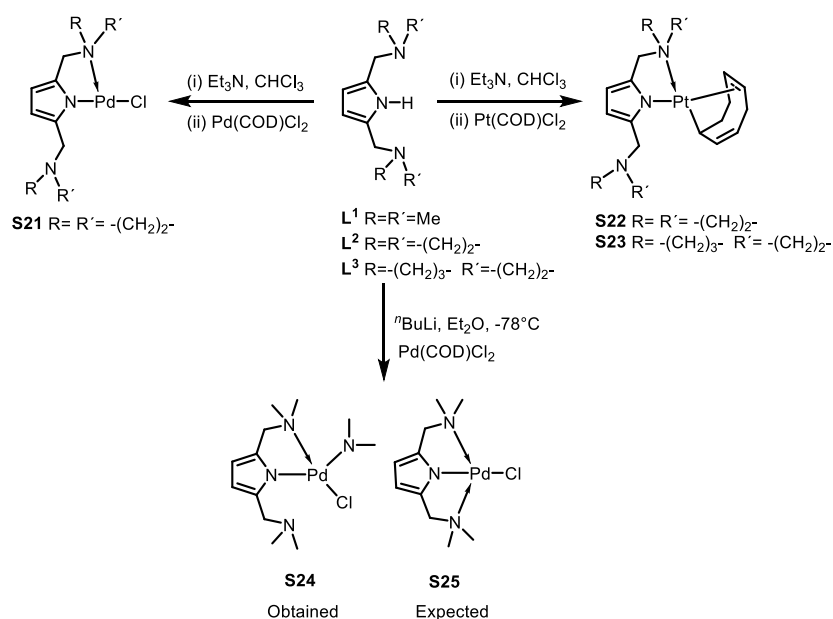
Scheme S5. Synthetic routes for Pd and Pt complexes **S21-S24**.

Complexes **S21-S24** were authenticated by single crystal X-ray diffraction studies [**Figure S6 (a)-(b)**]. To understand the nature of N-Se/Te bond, DFT calculation was carried out for compounds **S17-S20**. From Natural Bond Order (NBO) analysis performed on the optimised structures [**Figure S6 (c)-(d)**], it was observed that in both the compounds **S19** and **S20,** the chalcogen centre contained three bonds, one with phenyl group (Se32-C33), second one with amine group from the side chain (N30-E32) and the third bond was with pyrrole (N1-E32) where N1 gave its lone pair to σ* of E32-C33 bond.
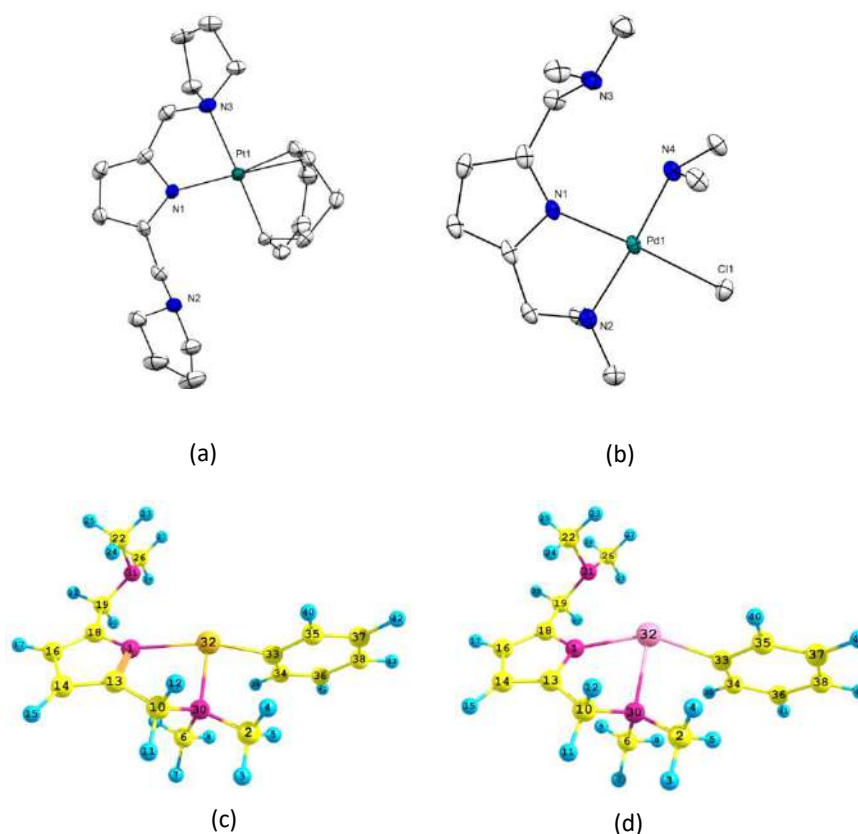
Figure S6. Molecular structures of (a) **S22** and (b) **S24**; optimized structures of (c) **S19** and (d) **S20** on which NBO analysis have been performed.

Reference:

1   (a) Regulacio, M. D.; Bussmann, K.; Lewis, B.; Stoll, S. L. *J. Am. Chem. Soc.*, **2006**, *128*, 11173. (b) Kuriki, K.; Koiki, Y.; Okamoto, Y. *Chem. Rev.* **2002**, *102*, 2347. (c) Kumar, G. A.; Riman, R. E.; Chen, S.; Smith, D.; Ballato, J.; Banerjee, S.; Kornienko, A.; Brennan, J. G. *Appl. Phys. Lett*., **2006**, *88*, 91902. (d) Li, H.-X.; Zhu, Y.-J.; Cheng, M.-L.; Ren, Z.-G.; Lang, J.-P.; Shen, Q. *Coord. Chem. Rev.*, **2006**, *250*, 2059. (e) Kumar, G. A.; Riman, R. E.; Brennan, J. G. *Coord. Chem. Rev.*, **2014**, *273-274*, 111. (f) Boncher, W.; Dalafu, H.; Rosa, N.; Stoll, S. *Coord. Chem. Rev.*, **2015**, *289-290*, 279. (g) Nief, F. *Coord. Chem. Rev*., **1998**, *178-180*, 13. (h) Freedman, D.; Melman, J. H.; Emge, T.J.; Brennan, J.G. *Inorg. Chem.*, **1998**, *37*, 4162. (i) Lissner, F.; T. Schleid, *Z. Anorg. Allg. Chem.* **2004**, *630*, 1741. (j) Lissner, F.; Schleid, T. *Z. Anorg. Allg. Chem*., **2005**, *631*, 1119. (k) Schurz, C. M.; Talmon-Gros, P.; Lissner, F.; Schleid, T. *Solid State Sci.* **2013**, *17*, 140. (l) Lissner, F.; Schleid, T. *Z. Anorg. Allg. Chem*. **1994**, *620*, 2003.

2   (a) Peris, E.; Crabtree, R. H. *Chem. Soc. Rev.*, **2018**, *47*, 1959 and reference therein. (b) The Chemistry of Pincer Compounds; Morales-Morales, D., Jensen, C. M., Eds.; Elsevier; Amsterdam, **2007**. (c) Moulton, C. J.; Shaw, B. L. *J. Chem. Soc., Dalton Trans*. **1976**, 1020. (d) Selander, N.; K. J. Szabó, *Chem. Rev.*, **2011**, *111*, 2048 and reference therein. (e) Gunanathan, C.; Milstein, D. *Chem. Rev.*, **2014**, *114*, 12024.; (f) Albrecht, M.; van Koten, G. *Angew. Chem., Int. Ed.*, **2001**, *40*, 3750. (g) Tu, T.; Fang, W.; Bao, X.; Li, X.; Dötz, K. H. *Angew. Chem., Int. Ed.*, **2011**, *50*, 6601. (h) Prokhorov, A. M.; Hofbeck, T.; Czerwieniec, R.; Suleymanova, A. F.; Kozhevnikov, D. N.; Yersin, H. *J. Am. Chem. Soc.*, **2014**, *136*, 9637. (i) Hall, J. R.; Loeb, S. J.; Shimizu, G. K. H.; Yap, G. P. A. *Angew. Chem., Int. Ed.*, **1998**, *37*, 121.

3   (a) Bleiholder, C.; Werz, D. B.; Kö1ppel, H.; Gleiter, R. *J. Am. Chem. Soc.* **2006**, *128*, 2666. (b) Bleiholder, C.; Gleiter, R.; Werz, D. B.; Kö1ppel, H. *Inorg. Chem.* **2007**, *46*, 2249. (c) Cozzolino, A. F.; Elder, P. J. W.; Vargas-Baca, I. *Coord. Chem. Rev*. **2011**, *255*, 1426. (d) Mukherjee, A. J.; Zade, S. S.; Singh, H. B.; Sunoj, R. B. *Chem. Rev*., **2010**, *110*, 4357. (e) Pascoe, D. J.; Ling, K. B.; S. Cockrof, L. *J. Am. Chem. Soc.* **2017**, *139*, 15160. (f) Selvakumar, K; Singh, H. B. *Chem. Sci.*, **2018**, *9*, 7027.

4   (a) Berg, D. J.; Andersen, R. A.; Zalkin, A. *Organometallics* **1988**, *7*, 1858. (b) Cary, D. R.; Arnold, J. *Inorg. Chem.* **1994**, *33*, 1791. (c) Khasnis, D. V.; Brewer, M.; Lee, J.; T. Emge, J.; Brennan, J.G. *J. Am. Chem. Soc.* **1994**, *116*, 7129. (d) Brewer, M.; Khasnis, D.; Buretea, M.; Berardini, M., Emge, T. J., Brennan, J.C., *Inorg. Chem.* **1994**, *33*, 2743.

5   Edinger, A. *Ber. Dtsch. Chem. Ges.* **1908**, *41*, 937.

6   (a) Banfield, J. *J. Org. Chem.* **1960**, *25*, 300. (b) Corsini, A.; Fernando, Q.; Freiser, H. *Anal. Chem.* **1963**, *35*, 1424. (c) Dalziel, J. A. W.; Kealey, D. *Analyst*. **1964**, *89*, 411. (d) Henkel, G.; Krebs, B.; Schmidt, W. *Angew. Chem. Int. Ed.* **1992**, *31*, 1366.

7   Archer, S. J.; Koch, K. R.; Schmidt, S. *Inorg. Chim. Acta*. **1987**, *126*, 209.

8   Kellö, E.; Vrábel, V.; Lyčka, A.; Sivý, J. *Acta Cryst*. **1993**, *C49*, 1943.

9   (a) Bensemann, I.; Gdaniec, M.; Łakomecka, K.; Milewska, M. J.; Połoński, T. *Org. Biomol. Chem*., **2003**, *1*, 1425. (b) Wang, H.; Xia, Y.; Lv, S.; Xu, J.; Sun, Z.; *Tetrahedron Lett.* **2013**, *54*, 2124. (c) Ould, D. M. C.; Rigby, A. C.; Wilkins, L. C.; Adams, S. J.; Platts, J. A., Pope, S. J. A.; Richards, E.; Melen, R. L. *Organometallics*, **2018**, *37*, 712. (d) Krupski, S.; Pöttgen, R.; Schellenberg, I.; Hahn, F. E. *Dalton Trans*., **2014**, *43*, 173. (e)Weber, L.; Kahlert, J.; Böhling,

L.; Brockhinke, A.; Stammler, H-G.; Neumann, B.; Harder, R. A.; Low, P. J.; Fox, M. A. *Dalton Trans.,***2013**, *42*, 2266.

10 (a) Chłopek, K.; Bothe, E.; Neese, F.; Weyhermüller, T.; Wieghardt K., *Inorg. Chem.* **2006**, *45*, 6298. (b) Khusniyarov, M. M.; Weyhermüller, T.; Bill, E.; Wieghardt, K. *Angew. Chem. Int. Ed*. **2008**, *47*, 1228. (c) Blackmore, K. J.; Joseph, N. L.; Ziller, W.; Heyduk, A. F. *J. Am. Chem. Soc.*, **2008**, *130* , 2728. (d) Samanta, S.; Goswami, S. *J. Am. Chem. Soc.*, **2009**, *131* , 924.

11 Jørgensen, C. K. *Coord. Chem. Rev*. **1966**, *1*, 164.

12 (a) Ghosh, P.; Mandal, S.; Chatterjee, I.; Mondal, T. K.; Goswami, S. *Inorg. Chem*. **2015**, *54*, 6235. (b) Durgaprasad, G.; Luna, J. A.; Spielvogel, K. D.; Haas, C.; Shaw, S. K.; Daly, S.R.; *Organometallics* **2017**, *36*, 4020. (c) Chaudhuri, P.; Hess, M.; Müller, J.; Hildenbrand, K.; Bill, E.; Weyhermüller, T.; Wieghardt, K. *J. Am. Chem. Soc.* **1999,** *121,* 9599.

13 Gdaniec, M.; Bensemann, I.; Połoński, T. *ActaCryst*., **2004**, *C60*, o215.

14 (a) van der Meer, M.; Manck, S.; Sobottka, S.; Plebst, S.; Sarkar, B. *Organometallics*, **2015**, *34*, 5393. (b) Das, A.; Ghosh, P.; Plebs, S.; Schwederski, B.; Mobin S. M.; Kaim, W.; Lahiri, G. K. *Inorg. Chem.*, **2015**, *54*, 3376. (c) Bhattacharya, S.; Gupta, P.; Basuli, F.; Pierpont, C. G. *Inorg. Chem*. **2002**, *41*, 5810. (d) Ferrando-Miguel, G.; Wu, P.; Huffman, J. C.; Caulton, K. G. *New J. Chem.*, **2005**, *29*, 193. (e) Baya, M.; Esteruelas, M. A.; Oñate, E.; *Organometallics* **2011**, *30*, 4404.

15 (a) Huang, J.-H.; Kuo, P. -C.; Lee, G. -H.; Peng, S. –M.; *J. Chin. Chem. Soc.,* **2000,** *47,* 1191. (b) Kuo, P. -C.; Huang, J.-H.; Hung, C. –H.; Lee, G. -H.; Peng, S. –M. *Eur. J. Inorg. Chem.* **2003**, 1440. (c) Banerjee, S.; Shi, Y.; Cao, C.; Odom, A. L. *J. Organomet. Chem.* **2005**, *690*, 5066. (d) Maaß, C.; Andrada, D. M.; Mata, R. A.; Herbst-Irmer, R., Stalke, D. *Inorg. Chem.* **2013**, *52*, 9539. (e) Vránová, I.; Jambor, R.; Růžička, A.; Hoffmann, A.; Herres-Pawlis, S.; Dostál, L. *Dalton Trans*., **2015**, *44*, 395.

16 Kim, I. T.; Elsenbaumer, R. L., *Tetrahedron Lett.*, **1998**, *39*, 1087.

List of Publications

1. Venkateshwaran, K.; Prasad, P. R.; **Deka, R**.; Raju, S.; Singh, H. B.; Butcher, R. J. "**Contrasting Reactivity of 2-Chloro-1-formyl-3-hydroxymethylenecyclohexene and its Schiff Bases towards Disodium Diselenide: Isolation of Selenospirocycles versus Azapentalenes**" *Asian J. Org. Chem.* **2019**, *8*, 128-137.

2. Yadav, S.; **Deka, R**.; Singh, H. B. "**Recent Developments in the Chemistry of NHC-Based Selones: Syntheses, Applications and Reactivity**" *Chemistry Letters* **2019**, *48*, 65-79.

3. Venkateshwaran, K.; **Deka, R**.; Raju, S.; Singh, H. B.; Butcher, R. J. "**Synthesis of Hypervalent Organoselenium Compounds Stabilized by Intramolecular Coordination: Crystal Structures of 6-Phenyl-6,7-dihydro-5H-2,3-dioxa-2aλ^4 selenacyclopenta[hi]indene and 5-Phenyl-5,6-dihydro-4H-benzo[c][1,2]oxaselenole-7-carbaldehyde**" *Acta Cryst.* **2019**, *C75*, 70-76.

4. Yadav, S.; **Deka, R**.; Singh, H. B.; Raju, S.; Butcher, R. J. "**Synthesis of N-Heterocyclic Nitrenium (NHN) Ions and Related Donor Systems: Coordination with d^{10}-Metal Ions**" *Inorg. Chim. Acta* **2019**, *488*, 269-277.

5. Gupta, A.; **Deka, R**.; Singh, H. B.; Raju, S.; Butcher, R. J. "**Synthesis of Intramolecularly Coordinated Heteroleptic Diorganotellurides and Diorganotelluroxides: Isolation of a Monomeric Diorganotelluroxide [{2,6-(Me$_2$NCH$_2$)$_2$C$_6$H$_3$}$_2$TeO] and Diorganohydroxytelluronium Chloride [{2,6-(Me$_2$NCH$_2$)$_2$C$_6$H$_3$}$_2$Te(OH)]Cl**" *J. Organomet. Chem.* **2019**, *894*, 10-17.

6. Gupta, A.; **Deka, R**.; Srivastava, K.; Singh, H. B.; Butcher, R. J. "**Synthesis of Pd(II) Complexes of Unsymmetrical, Hybrid Selenoether and Telluroether Ligands: Isolation of Tellura-Palladacycles by Fine Tuning of Intramolecular Chalcogen Bonding in Hybrid Telluroether Ligands**" *Polyhedron.* **2019**, *172*, 95-103.

7. Gupta, A.; **Deka, R**.; Sarkar, A.; Singh, H. B.; Butcher, R. J. "**Oxidation Behavior of Intramolecularly Coordinated Unsymmetrical Diorganotellurides: Isolation of Novel Tetraorganoditelluronic Acids, [RR′Te(μ-O)(OH)$_2$]$_2$**" *Dalton Trans.* **2019**, *48*, 10979-10985.

8. Gupta, A.; **Deka, R.**; Sarkar, A.; Singh, H. B.; Butcher, R. J. "**Reactivity of Bis[{2,6-(dimethylamino)methyl}phenyl]telluride with Pd(II) and Hg(II): Isolation of the First Pd(II) Complex of an Organotellurenium Cation as a Ligand**" *New J. Chem.* **2019**, *43*, 13225-13233.

9. Gupta, A.; **Deka, R.**; Singh, H. B.; Butcher, R. J. "**Structural Characterization of the Derivatives of Bis[{2,6-(dimethylamino)-2 methyl}phenyl]selenide with Pd(II) and Hg(II)**" *Acta Cryst. C* **2020** (*Under revision*).

10. **Deka, R.**; Butcher, R. J.; Junk, P. C.; Turner, D. R.; Deacon, G. B.; Singh, H. B. **An Insight into the Redox Activity of Ru and Os complexes of the N, N´-Bis(2-pyridyl)benzene-1,2-diamine ligand: Structural, Electrochemical and Electronic Structure Analysis by Density Functional Theory Calculations**" *Inorg. Chim. Acta.*, **2020**, *499*, 119193.

11. **Deka, R.**; Sarkar, A.; Singh, H. B.; Butcher, R. J.; Junk, P. C.; Turner, D. R.; Deacon, G. B. "**Isolation of the Novel Examples of Homoleptic Dicationic Tellurium and Monocationic Bismuth Analogues of Non-N-Heterocyclic Carbene (Non-NHC) Derivatives**" *Organometallics*, **2020**, *39*, 334-343.

12. **Deka, R.**; Sarkar, A.; Singh, H. B.; Butcher, R. J.; Junk, P. C.; Turner, D. R.; Deacon, G. B. "**Isolation of the Novel Example of a Monomeric Organotellurinic Acid**" *Dalton Trans.*, **2020**, *49*, 1173-1180.

13. **Deka, R.**; Sarkar, A.; Singh, H. B.; Butcher, R. J.; Junk, P. C.; Turner, D. R.; Deacon, G. B. "**Synthesis, Characterization and Theoretical Studies of cis-Dichloridobis(8-quinolinethiolato)tin(IV) and Bis(8-sulfanylquinolinium) hexachloridostannate(IV) Derivatives**" *Aust. J. Chem.*, **2020** (*Under minor revision*).

14. **Deka, R.**; Sarkar, A.; Singh, H. B.; Butcher, R. J.; Junk, P. C.; Turner, D. R.; Deacon, G. B. "**Exploring the Role of Strong Intramolecular Coordination Ability of 2-(2´-pyridyl)phenyl Group in Heavy Main Group Halides: Insights from Synthesis, Structural, and Bonding Analyses**" *Eur. J. Inorg. Chem.* **2020** (*Under revision*)

15. <u>Deka, R</u>. Guo, Z.; Singh, H. B.; Turner, D.; Junk, P. C.; Deacon, G. B. "**Facile Synthesis of Monomeric Lanthanide Chalcogenolates from 2-(dimethylamino)methyl)phenyltellurolate and Quinoline-8-tellurolate Ligands: Theoretical Studies on Lanthanoid-Chalcogen Bond**" (*Manuscript Under Preparation*)

16. <u>Deka, R</u>.; Turner, D.; Junk, P. C.; Deacon, G. B; Singh, H. B. "**Synthesis of Pd (II) P(II) Complexes of Pyrrole Based NNN-Pincer Ligands: Pt-induced C−H Activation of Cyclooctadiene**" (*Manuscript Under Preparation*)

My words seem to fall short to explain my sense of gratitude to the people who supported in one way or other during this wonderful journey of my research career. It is indeed a pleasant task to express my thanks to all, without whose support, guidance and critical suggestions this journey wouldn't have been possible.

To commence with, I express my special appreciation and deepest gratitude to my research supervisors, Prof. H. B. Singh (IITB), Prof. Glen B. Deacon (Monash University) and Dr. David turner (Monash University) for their careful guidance and supervision throughout my PhD tenure. I am extremely grateful to them for their constant encouragement and moral support at each and every step of my research work. It is, in fact, Glen's zeal for perfection and passion towards science will always motivate me to do more. A very special thanks to Prof. Peter Junk (James Cook University) for his invaluable advice and feedback on my research while I was at Monash. I would also like to offer my earnest gratitude to my research progress committee (RPC) member, Prof. R. Murugavel for invaluably constructive criticism and suggestions toward improving my work.

With great appreciation I would like to acknowledge the Monash University staff, IITB-Monash Academy staff and Chemistry department staff (IITB) not only for their prompt support but also for kind care.

I owe a great deal of appreciation to my Monash colleagues Zhifang, Nurul, Owen, Ruchika and Khansa for their support, generous care and the homely feeling that I received at Monash. I will always cherish the moment spent with Zhifang and Nurul. I would like to offer my special thanks to Dr. Rory Kelly for training me handling of air-sensitive chemistry at Monash. My sincere thanks go to Dave's lab members (Jamie, Steph, Adrian and Nick) for their generous help.

I sincerely admire the contribution of all the lab-mates from IITB for extending their unstinted support, timely motivation, sympathetic attitude and unfailing help during the course of my PhD. My thanks go to my seniors (Shikha Di, Varsha Di, Satheesh Anna, Venkatesh Prasad, Saravanan Anna, Aravindhan, Ehsaan Bhaiya) and my juniors (Ram, Shakti, Abhishek, Badal, Manish, Sanjana, Dipto, Aniruddh) for maintaining a pleasant lab environment. I would like to specially mention the name of Sangeeta and Anand Bhaiya for their unbound support and love during last five years. I extend my thanks to Arup for his sincere help for the computational studies of my compounds.

I am indebted to my all IITB friends for providing a stimulating and fun filled environment. My thanks go in particular to Asif, Sanjib, Sudip, Suman, Uttam, Pallabita, Pragya, Soumya, Mursaleen, Nishikant Bhaiya for their infallible love and company. It was their love that raised me up again and again whenever I got weary. Special mention goes to Asif and Suman for their timely help during my thesis writing.